Fall 2018

Monitoring and Evaluating the Influences of Class V Injection Wells on Urban Karst Hydrology

James Adam Shelley
Western Kentucky University, adam.shelley@wku.edu

MODELING AND EVALUATING THE INFLUENCES OF CLASS V INJECTION WELLS ON URBAN KARST HYDROLOGY

A Thesis
Presented to
The Faculty of the Department of Geography and Geology
Western Kentucky University
Bowling Green, Kentucky

In Partial Fulfillment
Of the Requirements for the Degree
Master of Science

By
James Adam Shelley

December 2018

MODELING AND EVALUATING THE INFLUENCES OF CLASS V INJECTION WELLS ON URBAN KARST HYDROLOGY

Date Recommended 11/9/18

Jason Polk, Director of Thesis

Nicholas Crawford

Nicholas Crawford

Leslie North

Matt Powell

Cheryl O. Davis 11/19/18

Dean, Graduate School Date

Dedication

This work is dedicated to the hungry, the foolish.

Acknowledgements

I would like to thank the following entities and people for funding, advising, and assisting me with my research:

Kentucky Water Resources Research Institute | Geological Society of America | Western Kentucky University | City of Bowling Green, Department of Public Works | Dr. Jason Polk | Dr. Leslie North | Dr. Nicholas Crawford | Matt Powell | Caleb Koostra | James Graham | Amber Woods | Summer Abston | Chad Doughty | Taylor Berzins | Kyle Bearden | Rachel Kaiser | Fernando Hernandez | Travis Brummett.

CONTENTS

LIST OF FIGURES

LIST OF EQUATIONS

MODELING AND EVALUATING THE INFLUENCES OF CLASS V INJECTION WELLS ON URBAN KARST HYDROLOGY

James Shelley December 2018 187 Pages

Directed by: Jason Polk, Nicholas Crawford, Leslie North, and Matt Powell

Department of Geography and Geology Western Kentucky University

The response of a karst aquifer to storm events is often faster and more severe than that of a non-karst aquifer. This distinction is often problematic for planners and municipalities, because karst flooding does not typically occur along perennial water courses; thus, traditional flood management strategies are usually ineffective. The City of Bowling Green (CoBG), Kentucky is a representative example of an area plagued by karst flooding. The CoBG, is an urban karst area (UKA), that uses Class V Injection Wells to lessen the severity of flooding. The overall effectiveness, siting, and flooding impact of Injection Wells in UKA's is lacking; their influence on groundwater is evident from decades of recurring problems in the form of flooding and groundwater contamination. This research examined Class V Injection Wells in the CoBG to determine how Injection Well siting, design, and performance influence urban karst hydrology. The study used high-resolution monitoring, as well as hydrologic modeling, to evaluate Injection Well and spring responses during storm and baseflow conditions. In evaluating the properties of the karst aquifer and the influences from the surrounding environment, a relationship was established between precipitation events, the drainage capacity of the Injection Wells, and the underlying karst system. Ultimately, the results from this research could be used to make sound data-driven policy recommendations and to inform stormwater management in UKAs.

Chapter 1: Introduction

Floods are one of the most common and economically impactful natural hazards that occur in the United States (FEMA 2012). The National Flood Insurance Program (NFIP) estimates that the average total per year for flood insurance claims from 2003 to 2012 was approximately four billion dollars (NFIP 2016). In addition to these reactive expenses, the United States (U.S.) government spends billions of dollars each year to respond, assess, and mitigate geohazards. Flooding in karst environments does not represent a large portion of the aforementioned flood cost, but it does cause significant monetary damage (Milanovic 2014). Nevertheless, most damages resulting from karst flooding could be assuaged or circumvented with the promulgation of reasonable, practical regulations and the implementation of proper flood controls. The importance of sustainable management in karst environments cannot be overstated, given that more than 20% of the world's land surface is underlain by karst geology (Williams 1993; White et al. 1995; Veni et al. 2002). In most environments, flooding is a function of the precipitation infiltration/runoff relationship. Likewise, flooding in a karst environment is the result of a similar relationship but is influenced by many more variables; to adequately characterize flooding in a karst terrain, it is necessary to understand how subsurface fluid flow in a heterogeneous medium responds to surface influences.

The majority of urban karst areas (UKAs) are prone to groundwater flooding due the high permeability and diffusivity of the underlying aquifer (Parise and Gunn 2007). Unfortunately, very few studies examine the influence of subsurface activity on surface

flooding in karst areas (Crawford 1982; Crawford and Feeney 1987; Bonacci et al. 2006; Zhou 2007). Additionally, there are relatively few studies, which have examined urban karst flooding through a modeling approach (Fleury 2013). Evidence supporting the previous statement is affirmed through examining the City of Bowling Green's (CoBG) history of flooding and urban karst issues.

The CoBG is one of the most extensively studied karst environments in the United States (Crawford 1987; Kemmerly 1993; Nedvidek 2014); however, there are very few studies in the area that attempt to quantitatively evaluate flooding mechanisms based on aquifer properties and urban development. The CoBG is a representative example of the hydrological problems that can plague karst environments. The CoBG is arguably the largest city in the United States built entirely upon a sinkhole plain (Crawford 1987). Over the last thirty years, the CoBG population has almost doubled, and the land area has grown by approximately 16 kilometers (Nedvidek 2014). During this period, stormwater quantity management has not significantly changed and the CoBG still uses many of the same flood controls, which primarily include Class V Injection Wells. Neglecting several studies by Crawford (1982, 1987, 1988) that identified that the overuse and poor siting of Injection Wells may be contributing to localized flooding and sinkhole collapse within the City. Furthermore, sustainable development necessitates proactive management, and without an understanding of the system, it is impossible to maintain the health of the environment during urban expansion; therefore, it is important to model system behavior and evaluate the development criteria to understand the impacts and influences of urbanization on karst hydrology.

The primary objective of this research was to examine Class V Injection Wells in the CoBG to determine how Injection Well siting, design, and performance influence urban karst hydrology. The results presented herein improve flood hazard mapping in karst terrains and enable the creation of a methodology for adequate design and siting procedures for Class V Injection Wells in UKAs. In addition, the completion of the primary objective provides answers to the following research questions:

- How can high-resolution monitoring and modeling the response of Class V Injection Wells, and the primary drainage basin outlet to which they flow under variable storm conditions, prove to be a reliable method for assessing flood risk in UKAs?
- Are the current guidelines regulating the siting, design, and best management practices for Class V Injection Wells in the CoBG effective at mitigating flood risk for the more probabilistic storm events?
- What siting, design, and maintenance BMP's would be effective at improving the drainage capacity and the longevity of Class V Injection Wells?

The response of a karst aquifer to storm events and surface stream flooding is often faster and more severe than that of a non-karst aquifer (Veni et al. 2002). This accelerated reaction is the result of a highly permeable system that allows stormwater runoff to travel quickly through interconnected subsurface pathways. As with any environment, landuse drastically affects surface stormwater drainage. Urbanization is a primary contributor to flow alteration by increasing the impervious surface cover. Increases in runoff are manageable in non-karst areas because of the feasibility and diversity of stormwater controls. Contrastingly, karst environments are significantly

affected by increases in runoff, because traditional stormwater management strategies are not practicable (Crawford 1989). Stormwater management in a karst area involves the use of the subsurface drainage system. Most urban karst areas lack the suitable topographic gradient for engineered stormwater solutions, such as conveyances to surface water bodies (Crawford and Feeny 1987; Campbell 2005); hence, the alternative to standard techniques normally involves the use of Class V Injection Wells. Throughout Kentucky, Injection Wells (including modified sinkholes) are ubiquitous; they exist in major urban areas, such as Louisville, Lexington, and more than 40% of the counties in the state (Crawford and Groves 1984), as well as nearby areas in Tennessee, Virginia, Georgia and similar karst areas. Flood control with Class V Injection Wells is useful, if properly sited (Campbell 2005); however, when using Class V Injection Wells in a karst area, inherent problems exist. Commonly, Injection Wells do not perform their intended function, because of the lack of hydraulic testing and geophysical site investigation before drilling the well. The result is that drainage capacities are exceeded and backflooding occurs (Crawford 1982). Typically, backflooding occurs because of a clogged conduit due to high sediment and debris loads that are transported through the injection feature, or the feature being overwhelmed due to exceeding its flow tolerance, which is often unknown until it occurs. Unfortunately, planners and governments do not often fully recognize the flood potential associated with karst landscapes, because traditional procedures and guidelines for flood assessment are inadequate for karst areas (Kemmerly 1993). Despite all of the aforementioned concerns, people continue to develop in flood prone karst areas exacerbating preexisting issues.

Class V Injection Wells are meant to alleviate flooding, however, with increased

runoff inflow, it is likely they may actually exacerbate the problem. The previous statement draws from two of three contributing factors for karst flooding outlined by Zhou (2007), who proposed that flooding in karst environments is largely the result of a limited capacity of the recharge/infiltration sources and the underlying karst drainage system in conveying large volumes of stormwater. Rapid recharge into the karst aquifer causes groundwater levels to quickly rise and during high-intensity and prolonged storm events the water table can rise above the topographic surface and cause flooding (Bonacci et al. 2006; Bailly-Comte et al. 2008; Gutiérrez et al. 2014). Given that the fluctuation of groundwater levels are contingent on the recharge potential and hydrodynamic responsiveness of the underlying aquifer, this study focused on evaluating the influence of Class V Injection Wells on flooding in UKAs.

Chapter 2: Literature Review

Stormwater Regulations and Policies

The United States federal government has promulgated many laws and regulations to preserve and protect the environment. One of the most effective and transformative approaches to attaining this goal for water quality was the enactment of the Clean Water Act (CWA). In 1972, Congress passed the CWA as a way to reduce point source discharges (Schiff 2014). When trying to establish an enforcement mechanism, the complexity of converting water quality standards into numeric effluent limits for specific point sources made Congress force the Environmental Protection Agency to set effluent limitations based on technological standards (Salzman and Thompson 2003). In conjunction with the enactment of CWA, the National Pollution Discharge Elimination System (NPDES) was created to implement technological-based standards for effluent limitations (EPA 1989). Under the CWA, the NPDES system requires a permit for any person discharging any pollutant (CWA 2002). The creation of the permitting system eventually formed an avenue for states to qualify to issue NPDES permits within their jurisdiction. Currently, approximately three-quarters of the states meet the minimum qualifications for eligibility for the permitting program, and the EPA issues permits for the states that do not qualify (Salzman and Thompson 2003). Overall, the NPDES system is effective in managing point source pollution but lacks a regulatory mechanism for controlling groundwater and non-point source pollution.

Established in 1974, The Safe Drinking Water Act (SDWA) was enacted during one of the most federally active periods for environmental legislation (Cox 1997). The primary objective of the SDWA is to set national minimum standards for drinking water

quality within the United States and establish a regulatory authority for enforcement. Unlike the CWA, the SDWA does provide some protection to underground sources of water. One of the primary ways the SDWA prevents contamination to underground sources of drinking water (USDW) is through the Underground Injection Control (UIC) program. UIC programs regulate injection well procedures, documentation, and management (SDWA 2002). Additionally, the introduction of UIC programs has ushered in amendments to the SDWA, adding another layer of protection for USDWs.

Prior to the federally mandated UIC programs, underground injection of hazardous and non-hazardous wastes into geologic strata was completely unregulated (EPA 2003). The first actual use of UIC began in the 1930s with oil companies. The production of oil was generating large quantities of waste and industries had no way to dispose of it. In response to the issue, the oil companies began using depleted reservoirs to inject the waste generated from the oil production underground (Bonura and Voorhees 2005). Naturally, groundwater contamination became an issue and, by the 1960's, states were concerned about groundwater pollution. Finally, in the early 1970s, the EPA was concerned that facilities were avoiding regulated surface waste treatment, opting for the most convenient method of disposal through Injection Wells (Bonura and Voorhees 2005). The aforementioned fear was accompanied by citizen complaints and water pollution litigation (EPA 2003). At the time, an underground injection was a state's responsibility, but this changed in 1972, when groundwater was granted limited federal protection through the CWA. In the CWA, Congress mandated that for States to participate in the National Pollution Discharge Elimination System (NPDES) permitting program, it was necessary for them to have authority to grant permits to regulate the

"disposal of pollutants into wells" (EPA 2003); however, UIC was not actually regulated until the passage of the SDWA.

The passage of SDWA changed the EPA's policy on underground injection, forcing the agency to form minimum standards to ensure the protection of USDWs (Brasier and Kobelski 1996; Bonura and Voorhees 2005). In 1980, UIC regulations were developed with the goal of protecting USDW from contamination by regulating the "Construction, operation, and closure of Injection Wells" (EPA 2016). Since the inception of the UIC program, over 150 Federal Register Notices have been published to amend, create regulations and guidelines for UIC (EPA 2003). The UIC formation strengthened laws by providing a formal definition for USDW. The EPA defines a USDW in Title 40, Code of Federal Regulations (CFR), § 144.3, as:

"an aquifer or its portion: (a) (1) Which supplies any public water system; or (2) Which contains a sufficient quantity of ground water to supply a public water system; and (i) Currently supplies drinking water for human consumption; or (ii) Contains fewer than 10,000 mg/l total dissolved solids; and (b) Which is not an exempted aquifer"

To effectively enforce the regulation, the UIC program had to develop a definition for an injection well. The EPA formally defines an Injection well in 40 CFR §144.3 as a:

"bored, drilled, or driven shaft whose depth is greater than the largest surface dimension; or, dug hole whose depth is greater than the largest surface dimension; or, an improved sinkhole; or, a subsurface fluid distribution system."

UIC regulations categorize Injection Wells into six separate classes, which have different regulatory requirements and restrictions. Class I wells inject hazardous and non-

hazardous waste into deep geologic formations, whereas Class II wells inject the byproducts of oil and gas production (EPA 2016). Contrastingly, Class III Injection Wells are primarily used for solution mining, and Class IV was used to dispose of radioactive waste, but have since been banned (EPA 2016). Class V Injection Wells are used for injecting non-hazardous fluids to the subsurface. Additionally, Class V Injection Wells are traditionally wells that do not meet the definitions established in the SDWA for Classes I, II, III, IV (EPA 2003). For the purposes of this study, only Class V Injection Wells will be further discussed.

Class V Injection Wells

The Class V designation encompasses over 23 different categories that range from sophisticated injection features to gravity driven removal systems (EPA 2016). Legally, Class V Injection Wells are defined in 40 CFR § 144.80 as: "Injection wells not included in Class I, II, III, IV or VI. Typically, Class V wells are shallow wells used to place a variety of fluids directly below the land surface." Additionally, the EPA subdivides Class V Injection Wells in 40 CFR § 144.81, but for the scope of this literature review, only wells defined in 40 CFR §144.81 subpart (4), (5), and (6) are discussed:

(4) Drainage wells used to drain surface fluids, primarily storm runoff, into a subsurface formation;

(5) Dry wells used for the injection of wastes into a subsurface formation;

(6) Recharge wells used to replenish the water in an aquifer.

The primary function of the above-mentioned wells is to drain stormwater runoff. Stormwater drainage wells are used extensively throughout the United States to alleviate flooding problems that result from impervious surfaces (EPA 1999). In fact, in 1999 the United States Environmental Protection Agency estimated that 686,000 exist within the

United States; however, the EPA released a more modified approximation in 2002, estimating that there are only 650,000 Class V wells. The latest estimation is based on state inventories and a predictive model created by the EPA. Class V Injection Wells used for stormwater drainage are typically low-tech systems that depend on gravity to drain fluids directly into or above a USDW.

Numerous designs for Class V wells exist, but the most common are dug wells, bored wells, and improved sinkholes. All of the well configurations function identically by draining fluids to the subsurface through passive infiltration; relying solely on gravity (EPA 1999). The construction design of a Class V injection well provides little to no pretreatment to the water being injected into the subsurface (Figure 2.1). Pretreatment of stormwater runoff for Class V Injection Wells is not a regulatory requirement under the UIC program. Currently, the Legislative framework governing Class V Injection Wells declares that the wells are "Authorized by Rule," meaning that the owner/operator of the injection well is not required to obtain a permit as long as the proprietor/operator complies with the following rules of submitting basic inventory information about the injection feature to the appropriate permitting authority and operating the wells in a way that does not endanger a USDW (EPA 2016). A more formal explanation of "Authorized by Rule" is given in 40 CFR § 144.82 - § 144.84. The lack of water quality treatment is alarming, especially in a karst environment where groundwater contaminants can be transported long distances rapidly. Moreover, the risk of contamination is intensified when improper siting techniques are used or non-existent. Not only does inadequate injection well siting have an effect on the contamination of groundwater, but it can also cause flooding issues in karst areas (Crawford 1981); furthermore, the current regulatory

framework (Authorized by Rule) takes a lax approach to protection of the fragile karst aquifer by deferring responsibility to well owner. It has been shown that Class V Injection Wells are contributors to groundwater pollution (EPA 1999; Nedvidek 2014); yet, no major revisions or addendums have been made to adjust the current system.

Figure 2.1: Class V Injection Well Design (Created by Author).

Although numerous studies examine the influence of Class V injection wells on water quality, no major studies have been done to assess the efficiency of Class V injection wells as stormwater controls in the context of flood management. Failure in management may be attributed to a lack in the fundamental conceptualization of karst hydrology by land managers.

Karst Hydrology

Karst environments are unique terrains where the primary landscape development mechanism is the dissolution of soluble surface and subsurface rock formations, rather than mechanical processes (Ford and Williams 2007). Karst landscapes are predominantly formed in carbonate and evaporite rock formations, creating unique hydrological and morphological structures (Gutiérrez et al. 2014). Surface water runoff interacts with the CO_2 present in the soil as the water enters the subsurface. The CO_2 dissolves into the meteoric water, lowering the pH, thereby, increasing acidity and dissolution potential (Gutiérrez et. al. 2014). The result of the dissolution process leads to the development of sinkholes, caves, subterranean water bodies, and various other features that are a byproduct of the slow geochemical process of rock dissolution (Veni et. al. 2002) (Figure 2.2).

A karst aquifer is very complex, due to its highly heterogeneous structure and varying permeability. The structure creates the potential for multiple inputs and outputs into the aquifer. In a karst landscape, runoff enters the system through the vadose, or unsaturated, zone (Palmer 2007). The vadose zone of a karst aquifer is the area below the land surface and above the potentiometric water level and serves as the transmission pathway to the deeper parts of

the aquifer (Williams 1983). Water is only temporarily stored in the unsaturated zone, until new infiltration occurs, displacing the capillary water downward to the saturated zone (Palmer 2007). The upper portion of the saturated zone makes up the potentiometric surface, and the lower part consists of water-filled conduits that feed the system. As runoff is recharged to the saturated zone, hydraulic head increases and flushes water

through conduits to a point of resurgence, which is typically at an outlet spring for the groundwater basin. It is important to note that, as recharge enters the karst system, fluctuations occur in the potentiometric surface.

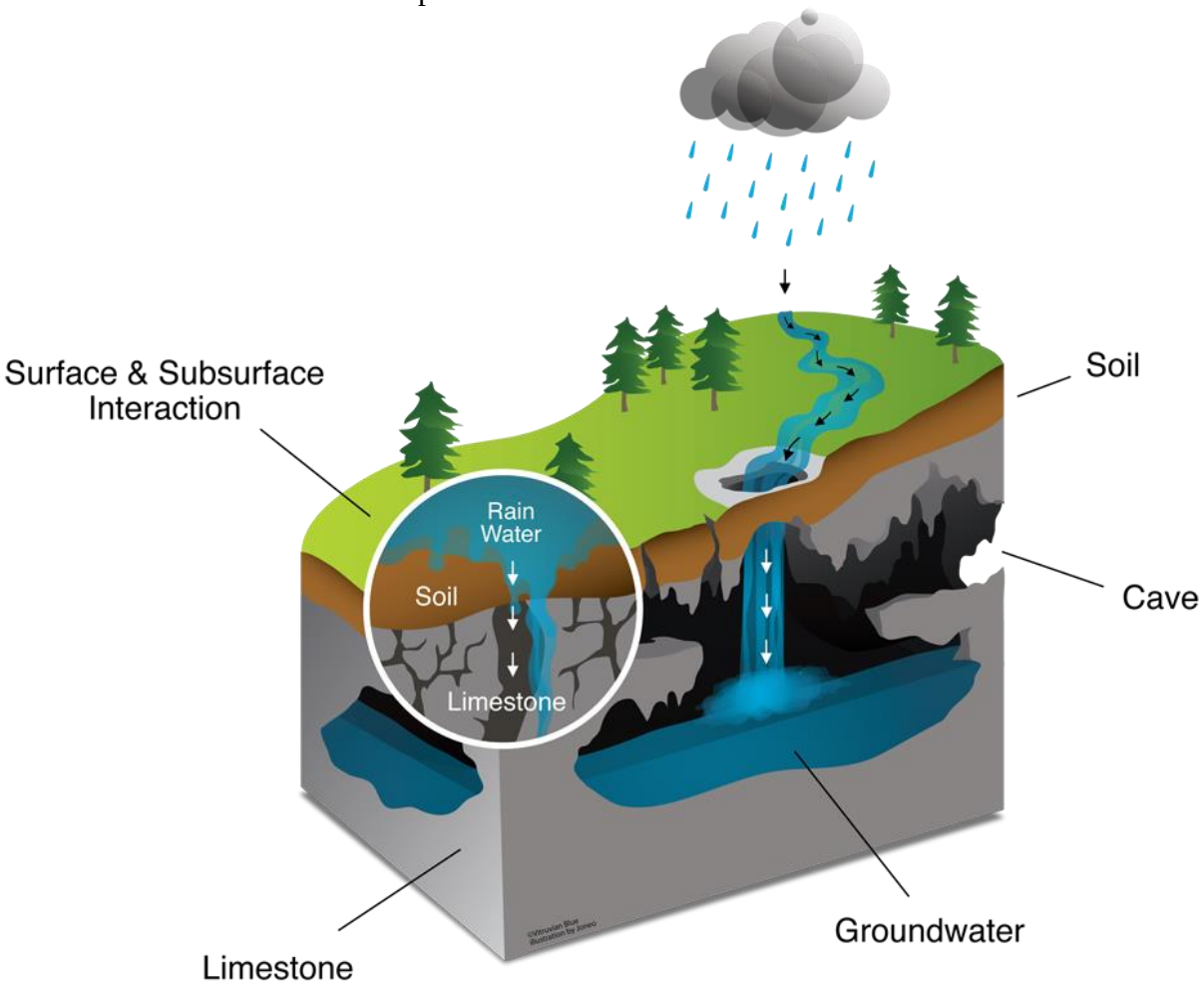

Figure 2.2: Karst Conceptual Model (Jonathan Oglesby 2014).

Recharge sources can originate from within the karst area (autogenic) or from external sources that differ geologically (allogenic) (Goldscheider et. al. 2007). Typically, autogenic recharge water has a diffuse flow rate, whereas, allogenic recharge, by contrast, is often infiltrated through swallow holes or sinkholes and has a much more variable rate of flow (Goldscheider et. al. 2007). Moreover, multiple points of recharge from allogenic sources can complicate water budget calculations and modeling efforts. Internally, the

heterogeneous configuration of a karst aquifer can be broken down into three unique categories based on the triple porosity model. Porosity is the deterministic factor for fluid flow and storage within the karst aquifer. Recharge water enters the aquifer from surface runoff and flows downgradient through the least resistance, anisotropic pathways consisting of matrix, fracture, and conduit porosity; White (2002, 89) defines the three different flows systems as:

> *"(a) Matrix permeability: The intergranular permeability of the unfractured bedrock.*
>
> *(b) Fracture permeability: Mechanical joints, joint swarms and bedding plane partings, all of these possibly enlarged by solution.*
>
> *(c) Conduit permeability: Pipe-like openings with apertures ranging from 1 cm to a few tens of meters."*

Porosity directly affects permeability and hydraulic conductivity of the rock system, and each stage of the porosity model represents a storage capacity, which is paramount for flood applications. The culmination of the aforementioned properties makes characterizing the karst aquifer a tough process, because the inherent heterogeneity creates different hydraulic processes and properties throughout the system.

Flow through the karst aquifer is influenced by the properties listed above, but myriad other factors also contribute to the understanding of groundwater velocities. For most groundwater modeling applications, it is necessary to estimate hydraulic parameters, such as hydraulic conductivity (K) and transmissivity (T). Estimating these hydraulic properties is important, because flow mechanics can be better understood when these characteristics are ascertained. Hydraulic conductivity in the karst system lacks a physical importance, because it represents the proportionality constant in Darcy's Law, which was derived in intergranular porous media under laminar flow conditions (Kresic 2007). The

multiple porosity systems cause shifts in flow regimes from laminar to turbulent, thus preventing Darcian mechanics from being used directly to determine flow (Hao et. al. 2007); however, in the situation where an aquifer is dominated by primary porosity, Darcy's law (Equation 1) can be applied, where

$$Q = K\left(\frac{\Delta H}{L}\right)A_{Total} \quad \text{(Eq. 1)}$$

$\frac{\Delta H}{L}$, represents the hydraulic gradient and A_{total} corresponds to the cross-sectional area (Kresic 2007; Palmer 2007).

In situations where flow is turbulent, transmissivity can provide useful information, because it represents the horizontal flow rate of fluid. Another useful characteristic that determines fluid flow in a karst aquifer is effective porosity. Since porosity directly influences hydraulic conductivity and permeability, it is correct to suggest the effect is tremendous on groundwater velocities (Kresic 2007). Kresic (2007) defines effective porosity as the volume of the interconnected pore spaces that can be flushed as a result of changes in hydraulic head. Furthermore, effective porosity dictates groundwater flow through primary porosity and is an important component in understanding the heterogeneity of the system. In reiterating, it is necessary for any application trying to capture the nature of a karst aquifer to realize that the system is dynamic and highly variable. Different antecedent conditions, and locations within the aquifer could illicit unpredictable responses. Unlike non-karst areas, karst areas have high infiltration rates and overland and surface flows rarely occur (Bonacci 2015). In most circumstances, the aquifer quickly saturates during precipitation events, which contributes to rapid groundwater fluctuations and potentially surface flooding (Milanović 2014). Understanding that in karst landscapes, surface water and groundwater exist as a

unified dynamic system is critical in effective stormwater and flood management.

Urban Karst Flood Management

Seldom are development practices that reduce karst flooding considered, despite the fact that the causes of karst flooding are known, and possible preventative measures and controls exist. One of the most classic examples of continuing practices that fail to acknowledge the unpredictable nature of karst groundwater flow is continued development in areas that have historically been affected by flooding (Parise 2003). It is suggested in the literature that the frequency and severity of karst flood events throughout the world continue to increase in response to land use changes and urban development (Crawford 1989; Kemmerly 1993; Parise 2003; Zhou 2007; Zheng and Qi 2011; Gutiérrez et al. 2014). Furthermore, it is purported that aggressive development in hazardous areas and inadequate infrastructure design alters the volume of water entering the karst system, thereby changing the responsiveness to storm events and causing short duration, high-intensity flood hydrographs (Gutiérrez et al. 2014). In 2002, the United States Geological Survey (USGS), conducted a study in Murfreesboro, Tennessee to examine the hydrologic response of sinkholes to major storm events and found that land use planning and infrastructure design in rapidly expanding UKAs are often slowly developed or poorly carried out, because karst features are not delineated or well understood. Reccurring management failures arise from the refusal to acknowledge that traditional stormwater management strategies are not effective in karst environments and require non-traditional approaches (Kemmerly 1993; Fischer 1999; Hart 2006; Fleury 2009). Proactive legislation and regulation for urban development in karst areas does exist, but often at very limited capacity.

A study by Hart (2006), presents current regulations for urban development within sinkholes and sinkhole watersheds in some cities in the southeastern United States. The study reveals that the primary course of action is the use of zoning ordinances that prohibit development within the 100-year floodplain (Hart 2006). As an additional protection, Knoxville, Tennessee, and Lexington, Kentucky do not allow development within sinkhole watersheds, unless it can be shown that post-construction flood levels will not increase as a result of development (City of Lexington 1985; City of Knoxville 2004). Another method employed by municipalities is the use of minimum setbacks as a tool to restrict increased stormwater inflow into sinkholes. The minimum setback technique is applied widely throughout Florida, Georgia, and Tennessee (Fleury 2009).

As an example, the CoBG has three primary techniques for managing karst flooding: the utilization of storm drains to divert stormwater short distances into a retention basin, sinkhole, or a surface water course; retention basins to collect major flood pulses; and an established sinkhole floodplain. The storm sewers are only slightly effective at conveying runoff to karst features. Typically, the conveyance reaches capacity quickly during short duration, high-intensity storm events and allows stormwater to pond in the streets. Retention basins in the CoBG do not achieve their intended function, because drainage wells are often installed inside the basins.

The suggested sinkhole floodplain is established at the 100-year flood contour. This designation based on work by Daugherty (1976) in determining that sinkhole floodplains should be based on a three-hour, 100-year precipitation event, which assumes no outflow from the sink. Kemmerly (1981) and Crawford (1987) suggest that this designation is effective for retention and potential flood elevations, but it is subject to

fluctuations due to urbanization.

All established flood contours are based on Intensity-Duration-Frequency (IDF) curves generated by Daugherty (1976). The same curves generated in 1976 are still in use for storm water design. This presents a problem given that the curves produced in 1976 use 1961 United States Weather Bureau data (Figure 2.3).

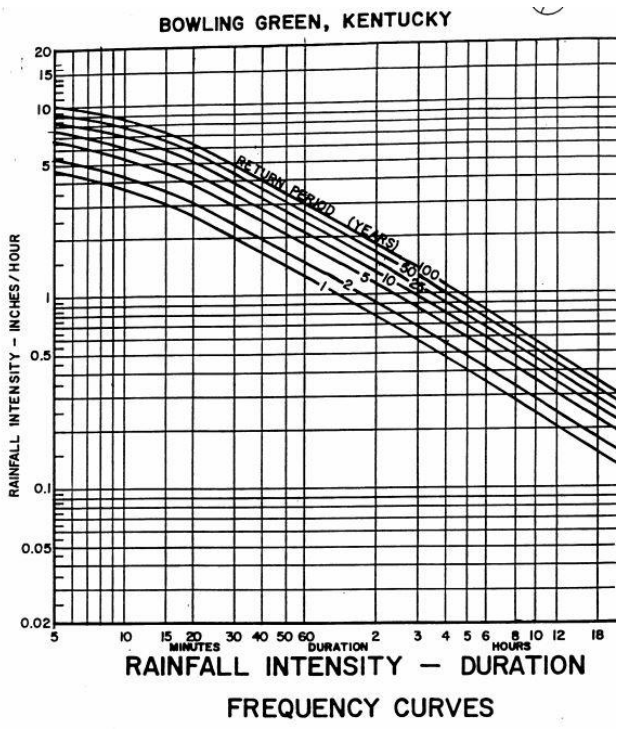

Figure 2.3: CoBG IDF curves circa 1976 (Daugherty 1976).

Moreover, the curves are outdated and may not accurately portray actual rainfall accumulation values, when considering the influence of urban expansion and changing climatic conditions (Pielke et al. 2011). Using Figure 2.3, it can be determined that the three-hour, 100-year event corresponds to about 4 in (101.6 mm) of runoff. Flood easements for the CoBG are based on this value and restrict any development below one foot above the flood line contour (Matheeny 1984). Crawford (1987) suggests that these strategies were successful in the 1980s; however, even then drainage systems did not

have the outlet capacities to drain the large volumes of runoff in the area.

The failure of these management strategies became apparent following the 2010 precipitation event that caused historic flooding across central and western Kentucky and Tennessee. During the event, the Kentucky Mesonet recorded the highest intensity rainfall for the state in Bowling Green, Kentucky (Durkee et al. 2012). The precipitation event on May 1-2 produced 10 in (approximately 258 mm), with a rainfall intensity of 2 in/hour (50.8 mm/hour) for the CoBG (Durkee et al. 2012). Precipitation Frequency Estimates for many south-central Kentucky counties had recurrence intervals as high as 200 years, causing four fatalities and more than two billion dollars in property damage. These disastrous events are very rare and extremely hard to prepare for but do give reason to reevaluate flood design and control strategies. It should be noted, when reviewing the literature, the last study to thoroughly examine flooding in the CoBG was completed by Crawford et al. (1987); moreover, no study has assessed the current status of the system. Crawford's work in the CoBG served as problem identification and solutions through established conceptual, causal relationships, but never offered an applied modeling approach for proactive mitigation. Given land use changes, and urbanization over the past decades, the CoBG's stormwater management strategies need to be evaluated. The re-evaluation is important as the city continues to urbanize. Furthermore, significant efforts could be made to plan and mitigate future flood events.

All of the ordinances discussed above are proactive in nature and do not provide solutions to stormwater issues that predate the zoning restrictions. Although proactive litigation is important, it is possible that focus on future issues is misdirecting attention away from obvious solutions to current problems. One of the easiest and often

overlooked solutions to karst flooding is the maintenance of stormwater controls and karst features. Class V Injection wells are a preferred method of removing stormwater for flood reduction in karst areas (Dinger and Rebmann 1986), but they are prone to clogging and often become obstructed; thus, being unable to perform their intended function. Similarly, sinkholes incur the same issues and, once they are clogged, contribute greatly to flooding (Zhou 2007). Moreover, proper maintenance and BMPs must be implemented in order to manage flooding in karst environments effectively. Proper flood management is important in all karst environments, and most damages from karst related hazards are easily avoided, but practical measures are frequently ignored (University of Kentucky 2012). For example, approximately 55% of Kentucky is underlain by karst geology (Currens 2012) and, despite all of the ordinances and regulations in place to protect citizens and karst resources, damages from sinkhole collapse, flooding, and water contamination still cost the state economy $20 million annually (Dinger et al. 2007). The Kentucky Geological Survey (KGS) reports that a majority of the property loss in the area is the result of building in unsuitable karst areas that do not have insurance coverage (Currens 2012). The incidents mentioned above could be mitigated through the use of informed policy, if the influences of karst hydrology on flooding are better understood (Gutiérrez et al. 2014).

Urban Karst Flooding

Numerous studies document the effects of urbanization on karst hydrologic processes (Crawford 1982; Crawford and Groves 1984; Zhou 2007; Toran et al. 2009). In urban environments, the primary catalyst that alters surface drainage is the increase in impervious land area. The reduction of infiltration leads to a direct increase in overland

flow resulting in higher runoff volumes. Decreased infiltration is problematic for cities that lack adequate surface hydrologic inputs. Typically, sedimentation best management practices are used as methods of stormwater control; otherwise, it is common practice amongst municipalities to direct surface stormwater drainage into nearby water bodies. If surface streams are not readily available, and the use of conventional storm/sewer systems to divert surface stormwater runoff into surface water bodies is not a feasible option, it is commonplace to utilize UICs to divert stormwater runoff into subsurface streams and cavities as a substitute.

The methodology discussed above is predominantly employed in UKAs as a means of flood control (Crawford 1981). Throughout Kentucky, injection wells (including modified sinkholes) are ubiquitous; they exist in major urban areas, such as Louisville, Lexington, and more than 40% of the counties in the state (Crawford and Groves 1984), as well as nearby areas in Tennessee, Virginia, Georgia and other karst environments. Most of aforementioned states have issues with karst flooding, and, in addressing flooding concerns, employ similar approaches to stormwater management.

The occurrence of flooding in karst environments is a common natural hazard causing significant economic destruction. In karst areas, surface stormwater runoff infiltrates rapidly into the carbonate aquifer and flooding occurs once the aquifer reaches full saturation and does not have the capacity to store and transmit surface stormwater runoff (Zhou 2007). In response to subsurface infiltration during storm events; groundwater levels rise to topographic surface generating floods (Price et al. 2000; Gutiérrez et al. 2014). Changes in groundwater level are contingent on the aquifers recharge capabilities and hydrodynamic reaction (Gutiérrez et al. 2014). There are

various types of karst flooding; Zhou (2007) categorizes them into three basic types; recharge, flow, and discharge related sinkhole flooding. In some instances, places may experience combinations of these flooding types. Furthermore, the solution for karst flooding is contingent on the identification of the kind. Additionally, urban expansion exacerbates flooding issues by altering drainage patterns, thus, understanding the karst system is essential. Sinkhole flooding is a common geohazard in karst landscapes and, although it is not typically life threatening, it is known to cause significant economic damage to property owners. Kemmerly (1993) notes that the flood risk associated with sinkhole flooding is not widely recognized by urban planners, or local, state, and federal governments, because flooding often does not occur along perennial watercourses. The lack of karst flood management strategies becomes evident when examining FEMA's guidance and procedures for flood risk mapping because no document exist that detail a flood risk assessment process for karst environments. The inherently dynamic complexities of multiple inputs and interconnected flow paths in a karst system make it difficult to assess flood risk adequately. Complicating issues further, the system will respond differently based on antecedent conditions. Unfortunately, the influence of karst groundwater flow on surface flooding is not thoroughly understood and necessitates improvements in how stormwater runoff is handled based on an improved understanding (Gutiérrez et al. 2014).

Throughout the 1970s and 80s, work was done extensively in the CoBG to understand the local karst system better and to provide practical solutions to sinkhole flooding. Crawford (1984) proposes three leading causes for sinkhole flooding: 1) inflow volumes exceed outflow capacities, 2) transmission of stormwater through conduit and

cave systems are exceeded, forcing storage into nearby sinkholes, and 3) a rising water table causes a backflooding effect. Similarly, these primary causes of sinkhole flooding are supported in other studies (Bonacci et al. 2006; Zhou 2007; Maréchal et al. 2008), but they represent a more quantitative approach to characterizing karst flooding and focus primarily on flash flooding, with the exception of Zhou (2007). Crawford (1982) found that, in some instances, transient springs may transmit water from outside of the drainage divide. The numerous causes of sinkhole flooding creates difficulties in urban floodwater management. Typically, in a non-karstic, fluvial setting, a system of storm sewers is used to convey stormwater to a nearby surface water body; however, karst environments lack adequate surface hydrology and gradients necessary to use conventional storm sewer methods; therefore, to effectively manage flooding, it is necessary to understand the responses of the hydrodynamic components (flow regimes) within the karst system in relation to precipitation events (Worthington 1999; White 2002; Gutiérrez et al. 2014). One approach to facilitate understanding of the influence of karst groundwater fluctuations on surface flooding is through the use of modeling; however, due to the inherent complexities of the karst system, mathematical models simulating groundwater flow are limited to so-called "black box" models. In most flow modeling applications, the study only focuses on inputs (recharge sources) and outputs (springs); ignoring the transmission in between (Quinlan et al. 1991; Kovacs and Sauter 2007) moreover, to accurately model karst terrain flooding, it is necessary to capture the local spatial variations.

Parameter Estimation Methods and Hydrological Modeling

Understanding the intricacies of a karst aquifer is essential for sustainable

protection and development; however, the uniqueness of each environment, and the heterogeneity within the aquifer makes completely characterizing the system impossible. Furthermore, a full understanding is exchanged for approximation through the use of modeling. Modeling system mechanics requires an understanding of the variables that control system response. Consequently, the only variables that will be discussed within the literature review are those that require parameter estimation and indirect measurement. Methodologies for estimating the following flow parameters will be discussed with brevity: transmissivity, hydraulic conductivity, storativity, conduit geometry discharge, and recharge. Moreover, through characterizing groundwater flow in a karst aquifer, it is possible to determine how the identified variables contribute to extreme hydrological events (i.e. karst flooding).

The first step in modeling a karst aquifer is the conceptualization of subsurface flow. The constituents of the conceptual model are a set of applied differential equations governing flow, system geometry, flow variables, and a set of initial and boundary conditions (Kovács and Sauter 2007). The aforementioned variables are the representation of physical components, such as the interconnected areas of recharge, distribution of porosity, and geologic layers. Collectively, modeling of these elements allows for a depiction of how water enters the aquifer, how it is stored, transmitted, and ultimately discharged from the system (White 1999). An adequate conceptualization will distinguish and subdivide the model into three primary zones; soil, unsaturated/vadose, and saturated/phreatic. Moreover, the division is necessary, because varying flow mechanics control each zone. After flow within the aquifer is conceptualized and mathematically defined, it is possible to simulate system response through the use of

different modeling approaches.

Once the conceptual model is constructed, it is possible to use parameter estimates and collected data as inputs into a deterministic or statistical mathematical model. After the basis of the mathematical model is generated, it can then be determined if analytical or numerical methods must be employed. Mathematical modeling approaches are generally broken down into two distinctive categories: global models and distributed models (Kovács and Sauter 2007). Global models, often referred to as lumped parameter models, result from inputs derived from the mathematical analysis of time series hydrographs and ostensibly mirror the overall response and function of the karst aquifer (Kovács and Sauter 2007). These models equate aquifer response as a function of recharge and discharge; thus, parameter estimates for variables controlling these factors have to be generated. Unfortunately, time-series analyses are typically considered "black box" modeling techniques, because they provide little information about the physical properties of the system (Kovács and Sauter 2007); however, numerical and

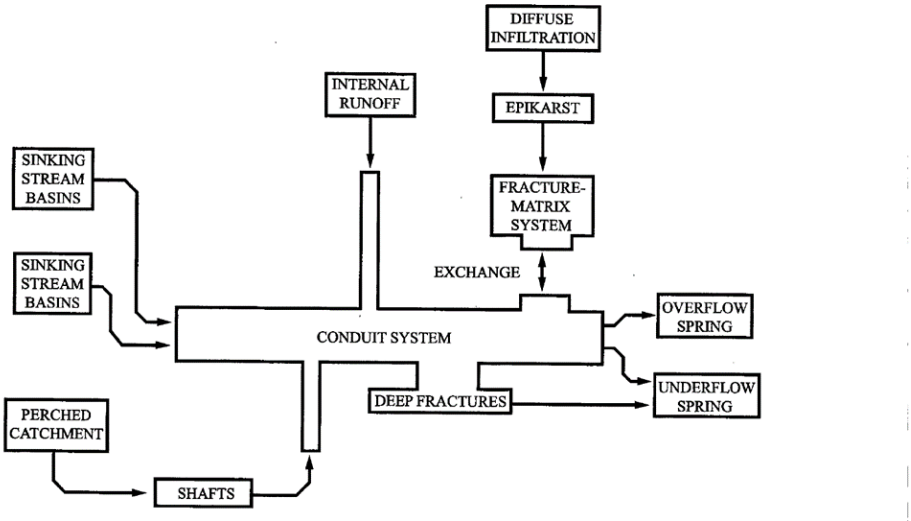

Figure 2.4: Conceptual model for a carbonate aquifer (White 1999)

analytical hydrographs analysis techniques have been developed to aid in ascertaining

these unknown physical properties (Atkinson 1977; Shevenell 1999; Powers and Shevenell 2000; Kovács and Perrochet 2014; Kovács et al. 2015). Regardless, global models fail to take into account the spatial variation of hydraulic parameters throughout the aquifer, because they only examine input and output; thus, localized areas within aquifer are ignored; failing to account for discrepancies between recharge and discharge. Contrastingly, distributed models account for temporal and spatial variations in the hydraulic properties and boundary conditions of the aquifer (Kovács and Sauter 2007).

Distributed models account for the spatial heterogeneity of the system, because they consider the aquifer as a collection of distinct homogenous subunits; therefore, distributed models necessitate the use of specific information on system porosity, hydraulic parameters and recharge inputs (Kovács and Sauter 2007). Given that a distributed model subdivides the aquifer into homogenous units, discretization methods must be employed. The most commonly used discretization methods are the Finite Difference Method (FDM) and the Finite Element Method (FEM) (Faust and Mercer 1980). The above-mentioned methods are used to numerically approximate the partial differential equations that govern fluid flow through the replacement of continuous variables for discrete variables defined at grid blocks or nodes (Faust and Mercer 1980). It is important to note when using a numerical model that limitations and sources of error are accounted for, because all numerical models are based on a set of simplifying assumptions and are limited by the amount and accuracy of the input data. Regardless, each approach has disadvantages and advantages, but distributed models are ideal for flood modeling in karst environments, because they take a holistic approach to the characterization of the subsurface to surface interactions (Liu 2005). Unfortunately, only

a small number of studies have tried the use of groundwater flow models as a tool for predictive surface flood modeling in karst environments, (e.g., Maréchal et al. 2007; Bailly-Comte 2012; Lacobellis 2013); thus, research in this area is greatly needed.

Soft Computing Techniques – Artificial Neural Networks

The complex, data intensive, and time-consuming nature of physical modeling often presents problems for hydrological research (Mohanty et al. 2009; Trichakis et al. 2010; Kong-A-Siou et al. 2011a). Over the past two decades significant progress has been made using artificial neural networks (ANNs) to identify the highly non-linear functions involved in rainfall-runoff relationships (Maier and Dandy 2000; Coppola et al. 2005; Kong-A-Siou et al. 2014). ANNs are biologically inspired computational intelligence models that serve as structures for learning algorithms to process data (Shanmuganathan and Sandhya 2016). Basically, an ANN, like any other model, takes in one or multiple inputs and processes the data then returns an output. The neural network consists of interconnected nodes that are organized into multiple layers. Each node and respective layer within the network are connected through a system of weights that correspond to a real valued number. Data enters the system through the input layer (predictors), which is then communicated to a specified number of hidden layers where the data processing occurs via an activation function. Figure 2.5 is an illustrated conceptualization of an ANN.

Given the inherent complexity of heterogeneous karst aquifers, it is reasonable to assume that it would be extremely difficult to fully capture the physical conditions within the system with a high degree of accuracy. Physically based models use discretization techniques to simplify the partial differential equations that govern fluid flow, thus, to

satisfy the model; a tremendous amount of data regarding hydraulic and geometric properties are needed.

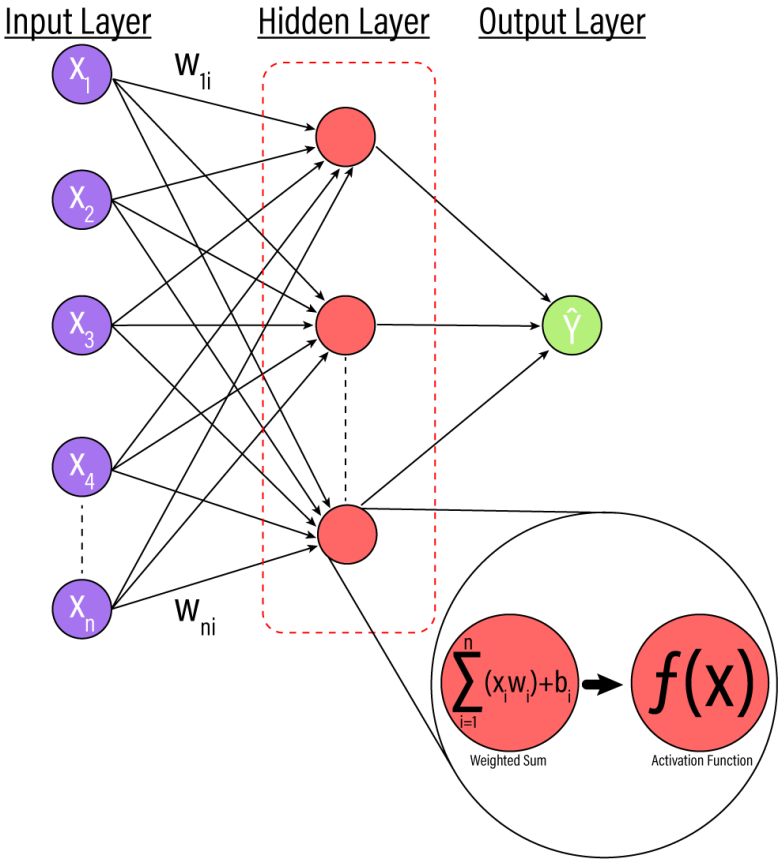

Figure 2.5: Conceptual Model for a Multilayer Perceptron Neural Network Model (Created by author).

Physically based models use discretization techniques to simplify the partial differential equations that govern fluid flow, thus, to satisfy the model; a tremendous amount of data regarding hydraulic and geometric properties are needed. The heterogeneity of a karst environment, coupled with "Black Box" problem makes it nearly impossible to correctly represent the system mathematically. Typically, a fully functional physical model necessitates numerous strict underlying assumptions, which compromises the validity and scalability of the model. Since ANNs do require the modeler to explicitly define mathematical expressions for physical functions, they are ideal for hydrologic modeling in karst environments.

Although the use of ANNs has proliferated the hydrological sciences discipline, they have only recently been applied in the sub-discipline of karst hydrology (Kong-A-Siou et al. 2014). However, literature involving the application of ANN modeling using high-resolution data is scant. Most of the studies in karst environments operate in data resolutions that are on a daily, weekly, or monthly time scale (Trichankis et al. 2010; Kong-A-Siou et al. 2011a, Kong-A-Siou et al. 2014). Due to the limited research with high-resolution data, it is important to reassess input selection determinations, preprocessing, data aggregation techniques, and optimization algorithms to ensure that overfitting does not occur and that the analyses produce meaningful results as dataset size increases.

Case Study: The City of Bowling Green

The City of Bowling Green is a primary example of the hydrological problems that result from rapid urban expansion in a karst environment. The CoBG is located on a sinkhole plain and, as a result, severe stormwater issues arise from its complex karst hydrology. The CoBG, like several UKAs, uses Class V injection wells for stormwater control to reduce the severity of flooding. The karst system is utilized extensively in the CoBG for stormwater control by injecting fluids directly into subsurface voids, cave systems, and solutionally enlarged joints and bedding planes. In the CoBG, the use of injection wells has gone mostly unregulated for decades, with over 2,000 wells installed since the 1960's to promote drainage and allow urbanization and development to occur without causing additional flooding problems (Crawford 1989, 2001; Bowling Green Public Works 2016). In the early 1980's, several studies were performed for the U.S. Environmental Protection Agency (EPA) to determine the nature and extent of the

hydrogeological problems that result from developing on a karst landscape. The studies concluded that, due to improper siting, maintenance, and design of Class V injection wells, they did not alleviate flooding (Crawford 1982). Moreover, the research suggests that the current techniques employed at the time contributed to sinkhole collapse and groundwater contamination (Crawford 1982).

Despite all efforts to characterize the issues surrounding injection wells, little has been done in the last 30 years to assess the current condition of the system and the overall design of drainage wells has not changed, despite the recurring issues. To further complicate the problem, the CoBG's landscape has experienced dramatic changes concerning increased urbanization. Additionally, the population has almost doubled, and the number of drainage wells has more than tripled (Kambesis et al. 2006; Kambesis et al. 2010, Census Bureau 2010).

The CoBG has always had serious flooding issues and is primarily affected by recharge-related and flow-related flooding. As a result, numerous studies were conducted in the past to fully characterize system mechanics and find a permanent solution for flood control (Booker 1978; Daugherty and Trautwein 1980; Crawford 1981; Crawford 1982; Crawford and Groves 1984; Crawford and Feeney 1987). Unfortunately, problems still exist and, even as recently as 2010, the area experienced a catastrophic flood, due to surcharging karst features and wells as the groundwater table rose in response to heavy rains over a short period. In this case, the injection wells contributed to flooding, in part due to their allowing the stormwater to infiltrate quickly, then, conversely, allowing groundwater to easily return to the surface as the water table rose from the aquifer becoming saturated.

In response to the aforementioned research and related studies, the planning commission for the CoBG imposed new regulations to lessen the severity of flooding. The new rules and standards promulgated by the CoBG are structured on three guidelines: prevent property damage using practical regulations, utilize the karst system as a discharge point for storm water, and not interfering with economic development (Matheney 1984). The primary flood control strategies employed within the CoBG are the use of retention basins, establishing the sinkhole at the 100-year flood contour, and drilling Class V Injection Wells (Crawford and Feeney 1987). These strategies alleviated a significant portion of the flooding issues at the time, but urban expansion has outpaced infrastructure development significantly increasing the amount of impervious surface; therefore, the karst system can no longer support the use of the same strategies. There are no guidelines established for the siting of Class V Injection Wells, and, as a consequence, the wells do not drain efficiently, because the intercepted cavity or solutionally-enlarged joint or bedding plane cannot drain runoff volumes (Crawford 1982). Additionally, flood retention basins in the CoBG are ineffective by design, because Injection Wells are commonly placed in the basin. The purpose of retention basins is to retain water for slow infiltration, but injection wells channel stormwater directly into the subsurface rapidly. The design allows high sediment loads into the underground drainage system limiting flow and exacerbating localized flooding (Crawford and Groves 1984).

Unfortunately, due to improper record keeping and weak regulatory enforcement, the CoBG's Injection Well database is outdated, and problems continue to arise with flooding, runoff blockages, well surcharging, and illicit discharges into wells. As a

requirement of the UIC program, owners installing a new Class V Injection Well must complete and file an application containing basic inventory information about the injection feature; however, when comparing the current EPA UIC database against the CoBG Department of Public Works' database, significant discrepancies exist. The federal UIC program has catalogued 524 Class V Injection Wells within the CoBG, but the CoBG's GIS database contains 801 wells (Figure 2.7). This gap increases substantially when the literature on the topic is reviewed. Crawford (1984), in partnership with the EPA, inventoried 444 in CoBG. Disagreement in the number of wells that exist has perpetuated in the literature and various reports over the years. Two decades after the original study done by Crawford (1984), Campbell (2005) estimated the number of Class V Injection Wells to be around 1,000 at the time; nevertheless, the actual number is seemingly unknown. Presently, 2,347 potential Injection Well locations have been mapped based off historical records (Figure 2.7), but additional inventorying and research is needed to fully determine the number of wells in order to study their impact on flood mitigation.

Current Database

Figure 2.6: Class V Injection Well Locations (Source: Created by author).

Potential Injection Well Locations

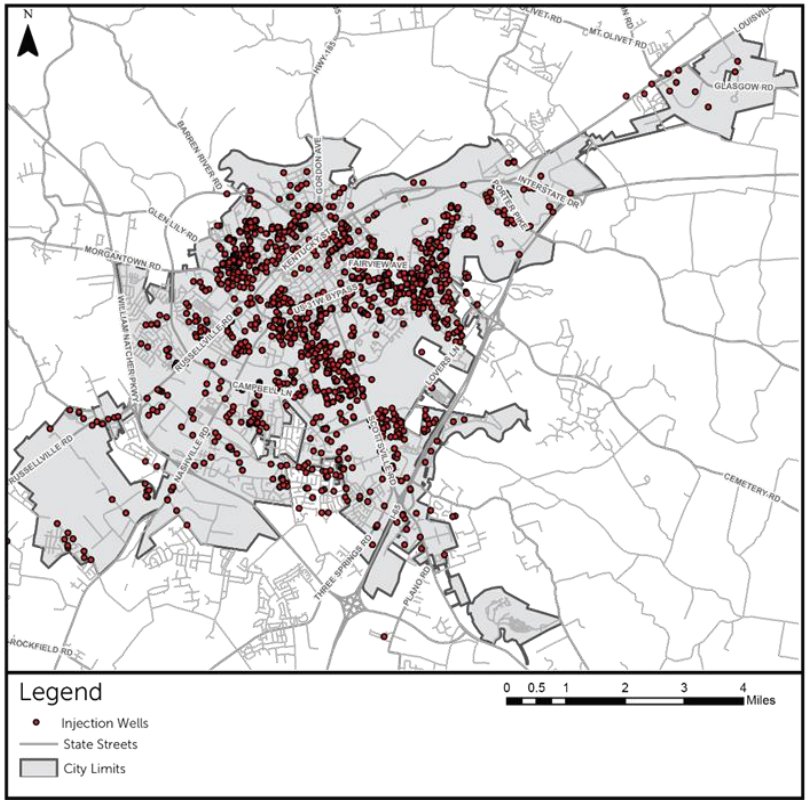

Figure 2.7: Potential Class V Injection Well Locations (Created by Author).

Improper documentation of Injection Wells stems far beyond the CoBG. The EPA's (1999) findings validate the statement above. For the study, the EPA had to develop a model to estimate the number of Injection Wells within each state, because it was believed that the states reporting values were inaccurate; none of the states could produce reliable inventory results (EPA 1999). Similar to the CoBG, most states believe that drainage wells are underreported for many reasons. For most instances, it was found that wells were not reported, because they were located on private property, not improperly identified, lacked coordination between agencies to report them, were grandfathered wells, or were poorly documented (EPA 1999). An incomplete inventory of wells is problematic for numerous reasons. In the context of flooding, an unreliable inventory results in the improper management of injection features. Since well location is unknown, the injection feature cannot be maintained and flood control BMP's cannot be implemented. Failure to implement adequate BMP's could result in a high sediment and debris loads being transported into the conduit and, ultimately, contributing to hydraulic damming by clogging ancillary flow pathways reducing the overall flow capacity. Hydraulic damming would then cause back flooding of the conduit; essentially creating a discharge point from an infiltration source. Although Class V Injection Wells are designed as a stormwater control, studies propose that the wells may contribute to flooding in karst environments (Crawford and Groves 1984; Crawford 1987; Crawford 1989). This assumption is derived from the fact that most municipalities and private companies do not have a procedure for injection well siting, standard design, and have incomplete databases. It is impossible to manage a feature if the location of the feature is unknown. Additionally, siting considerations and criterion are important, because the

effectiveness of a well is contingent on the hydraulic performance of its intersected subsurface feature. Moreover, without proper testing and assessment, the drainage capacity of an injection feature cannot be determined. Another important concept for flooding is the density of injection wells. Injection wells allow water to infiltrate to subsurface more rapidly; thus, as the density of injection wells increases, the volume of infiltration water also increases; therefore, without having locational data on wells, it is possible to attain a high density of features within the same hydrologically connected area and inadvertently increase flooding potential. Most of the aforementioned studies on the CoBG conclude that flooding problems in the CoBG are largely the result of infiltration exceeding the drainage capacity of the system. It is necessary to note these studies primarily focus on sinkhole drainage, not specifically on Class V Injection wells. The prior distinction is important, because, after an exhaustive literature review, no researcher has extensively studied the influence of Class V Injection Wells on karst flooding. This is problematic, because injection wells are frequently used as a mitigation strategy for urban karst flooding.

Municipal Separate Storm Sewer System

One potential factor that may be contributing to the poor documentation and siting of Class V Injection Wells in the CoBG and other UKA's is regulatory overlap and the lack of a regulatory enforcement mechanism. The CoBG's stormwater management strategies are centered on the Phase II requirements of the Municipal Separate Storm Sewer System (MS4) Program. Under the CWA, the EPA developed the MS4 Phase I and II requirements of the NPDES stormwater program as an approach to alleviate the problem of nonpoint source pollution (White and Boswell 2006). Phase I was developed

in 1990 and regulates MS4's in cities and counties whose population exceeds 100,000 and construction sites that are larger than five acres. By 1999, the EPA published the final ruling of the NPDES Phase II requirements for small MS4's located in urbanized areas where the population is less 100,000 and for construction sites ranging from one to five acres (White and Boswell 2006). Both Phases require MS4's designated by the permitting authority to obtain an NPDES permit for their stormwater discharges (Nedvidek 2014). The NPDES formally defines an MS4 in CFR §122.26 (8) as:

> *Municipal separate storm sewer means a conveyance or system of conveyances (including roads with drainage systems, municipal streets, catch basins, curbs, gutters, ditches, man-made channels, or storm drains):*
>
> *(i) Owned or operated by a State, city, town, borough, county, parish, district, association, or other public body (created by or pursuant to State law) having jurisdiction over disposal of sewage, industrial wastes, storm water, or other wastes, including special districts under State law such as a sewer district, flood control district or drainage district, or similar entity, or an Indian tribe or an authorized Indian tribal organization, or a designated and approved management agency under section 208 of the CWA that discharges to waters of the United States;*
>
> *(ii) Designed or used for collecting or conveying storm water;*
>
> *(iii) Which is not a combined sewer; and*
>
> *(iv) Which is not part of a Publicly Owned Treatment Works (POTW) as defined at 40 CFR 122.2.*

Given that this research is being conducted in the CoBG, the study will only detail Phase II requirements; however, the primary difference between the two Phases are the requirements of the water quality regulation. Phase I MS4's are subject to specific water quality standards, whereas, Phase II MS4 permits, by contrast, are regulated under the maximum extent practicable rule (MEP) (White and Boswell 2006). A designated authority within each state outlines and specifies within their NPDES permit the

requirements necessary to ensure the reduction of the discharge of pollutants within the MEP (Olsen 2015). Under the State's issued permit, regulatory authorities require that Phase II MS4's address six minimum control measures (MCM's) in their stormwater program: Public Education and Outreach, Public Participation/Involvement, Illicit Discharge Detection and Elimination, Construction Site Runoff Control, Post-Construction Runoff Control, and Pollution Prevention/Good Housekeeping (EPA 2005).

Currently, the CoBG requires all of its stormwater BMP's to meet a standard of 80% removal of total suspended solids (TSS) prior to discharge, because they have identified sediment as the pollutant of concern (CoBG 2011); however, Class V Injection Wells, one of the primary stormwater BMP's within the City, are not required to meet this standard. Since Class V Injection Wells are regulated under the SDWA through the UIC program, they are not classified as outfalls under the Kentucky Pollutant Discharge Elimination System (KPDES) MS4 program (KPDES 2010). This distinction is necessary, because Class V Injection Wells meet the criterion required to be designated as an outfall under the KPDES MS4 program and have been shown through dye tracing to discharge in Commonwealth waters. The NPDES program regulates MS4 discharges into the Waters of the United States (WOTUS); likewise, the KPDES permitting program controls MS4 discharges into Commonwealth waters. The aforementioned clarification is necessary, because there are differences in the definitions given to WOTUS and Commonwealth waters. Nedvidek (2014) states that the inclusion of wells, springs, and underground waters in the definition given to the Commonwealth waters under KRS 224.01-010(33) should, in theory, bring any stormwater discharges into the karst system under KPDES MS4 purview, which would have a large impact on compliance.

As mentioned earlier, the CoBG primarily uses Class V Injection Wells as a means of flood control; thus, the design of these systems is exclusively focused on water quantity. The lack of pretreatment in Class V Injection Wells has left the karst system receiving the stormwater discharges extremely susceptible to contamination. Moreover, if the KPDES MS4 program were left to regulate the water quality of Class V Injection Well discharges, it would prove to be costly for the CoBG and other UKA's under the permitting authority. The aforementioned scenario also poses a difficult problem for stormwater managers in the CoBG. Due to a large number of Class V Injection Wells within the city, stormwater managers are left with the decision of well closure or the infeasible task of retrofitting each well, which is essentially a choice between flood control and water quality; however, it should be noted that it is possible to reconcile water quantity and quality, through improved siting and design of Class V Injection Well systems. Furthermore, by removing the regulatory overlap between the MS4 program and UIC, it may be possible to clarify "gray areas" of the regulation and eliminate legal loopholes that limit the protection of the karst system. It should be noted that the CoBG stormwater management is aware of these issues and is working diligently on educational campaigns, collaborations, and community outreach programs to combat water quality and quantity issues within the City and this research will aid in that effort.

To conclude, there are significant gaps in the literature concerning flood management in urban karst groundwater systems. Many studies have detailed the conceptual underpinnings behind the influence of subsurface function on surface flooding in karst areas (Crawford 1982; Crawford and Feeney 1987; Bonacci et al. 2006; Zhou 2007), but relatively few have attempted to evaluate the influence of commonly used

flood BMP's on the hydrology of system. When examining karst flooding from the management perspective, most flood controls have been implemented without evaluation. This is especially true for Class V Injection wells. The CoBG has allowed the use of Class V Injection Wells to go unregulated, and despite years of research, the municipality is still unsure about how many wells are within the city limits. Additionally, Crawford (1984) identified several issues with the siting and design of injection wells, but no one has ever attempted no evaluate their effectiveness as stormwater controls or develop a methodology for proper construction and placement. Finally, the groundwater system within the CoBG has been thoroughly researched, but only a few studies (Booker 1978; Crawford and Feeny 1987; Campbell 2005; Cesin and Crawford 2005) have attempted to apply a modeling approach for flood assessment. Additionally, current conditions within the CoBG necessitate the evaluation of the hydraulic performance, construction design, and placement of Class V Injection Wells. In conclusion, the achievement of the needs mentioned above would allow for sustainable development and overall improvements to hazard mitigation strategies and emergency preparedness procedures.

Chapter 3: Study Area

Local Conditions

Located in Warren County, Kentucky, the CoBG spans approximately 36 mi^2 (93 km^2)

of the County and has an average elevation of 492 ft (150 meters) above sea level (Nedvidek 2014). The CoBG is located in the south-central region of Kentucky in between two metropolitan hubs being positioned approximately 59 mi (96 km) north of Nashville, Tennessee and about 119.9 mi (193 km) south of Louisville, Kentucky. According to the United States Census Bureau (2012), the CoBG Metropolitan Area has a population of approximately 60,000 residents, making it the third largest city in the state of Kentucky. The weather in the CoBG is variable, having an average annual temperature of 57.92 °F (14.4 °C), and receiving an average of 49.73 in (1263.39 mm) of rain each year with the majority of the precipitation occurring from March to July (NOAA 2010). The average monthly temperature fluctuates between 78.44 °F (25.8 °C) in the summer and 32.39 °F (0.22 °C) in the winter (NCDC 2005). The area is intensely karstified and contains numerous sinkholes (Crawford 1988). The developed and urban areas of the CoBG continue to expand along the southern and eastern borders, with significant residential and commercial growth (CoBG Planning Commission 2005). Unfortunately, high development expenses and decreasing land availability forces development in flood prone areas, including sinkholes.

The karst landscape of Warren County has been extensively studied; Crawford (1989, 1) stated “more is known about the karst aquifers of Warren County than probably any other karst area in the world.” Knowledge about the karst system has been achieved

through numerous studies, hundreds of dye traces, and thousands of hours of intensive cave exploration and survey. Figure 3.1 (CCKS 2006) is a product of the years of research dedicated to Warren County. The groundwater basins in Figure 3.1 were delineated using dye-tracing data in combination with areas where the potentiometric surface follows a down gradient path opposite of the approximated drainage divide (CCKS 2006). The seven basins identified in Figure 3.1 are the primary groundwater basins for the CoBG. The largest groundwater basin in Figure 3.1 is the Lost River basin. The Lost River karst aquifer basin has been extensively studied and much is understood about the karst system within it (Crawford 1989), but little research has been done in the other groundwater basins.

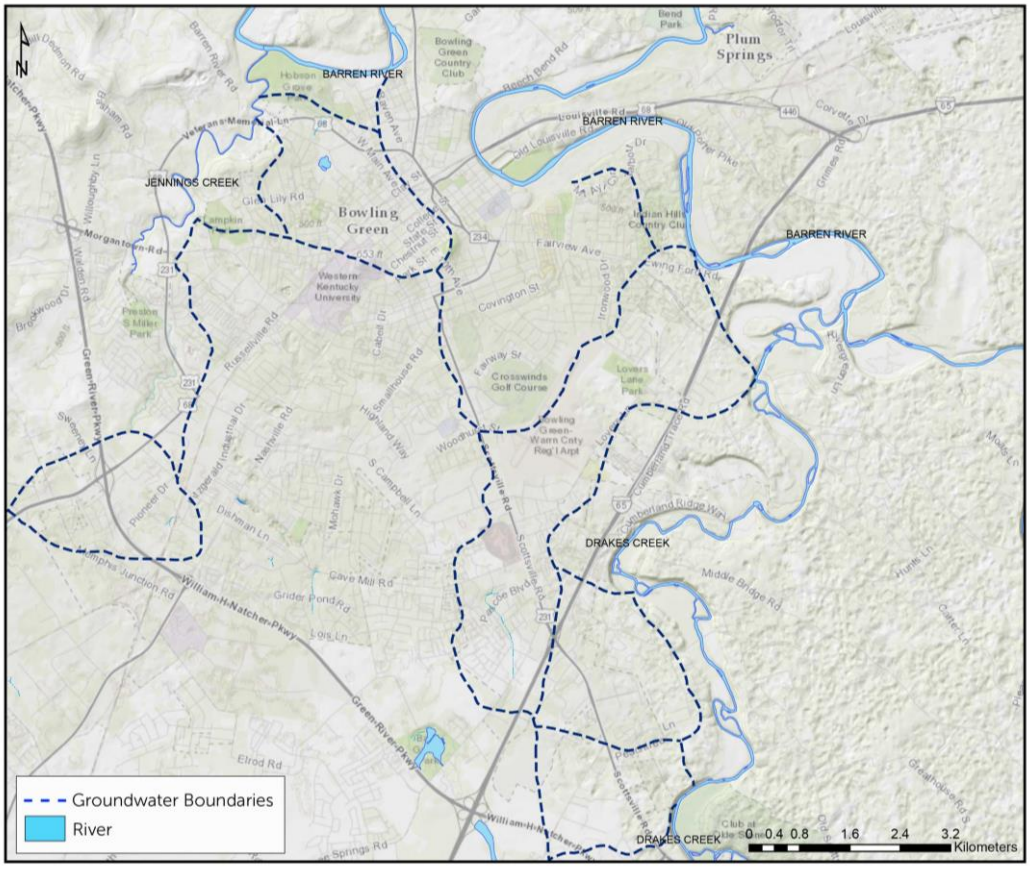

Figure 3.1: Delineated Groundwater Boundaries for Bowling Green, Kentucky (Created by author).

The primary area of focus in this study is a 1.9 mi^2 (5 km^2) delineated groundwater basin in the northwestern portion of city (Figure 3.2). The groundwater basin was chosen because it contains large residential areas prone to flooding, and comparatively, the size of the basin is manageable for data collection and analysis. In addition, there is little documentation suggesting that the site has been thoroughly researched or monitored (Nedvidek 2014). The basin serves as the drainage area for the Bowling Green downtown area. Major subsurface infiltration sources within the basin include 100 Class V Injection Wells (including modified sinkholes), four unmodified sinkholes, and other karst features. Infiltrated stormwater flows down gradient through subsurface pathways, eventually resurging at one of the eight karst springs within the basin. At an elevation 450 ft (137 m) above sea level (asl), New Spring serves as the primary outlet for the groundwater basin. Prior to exiting through the outlet springs, most of the infiltrated stormwater emerges at Limestone Lake, an abandoned limestone quarry. Limestone Lake is located approximately 0.93 mi (1.5 km) away from New Spring, and dye tracing proved that there is a direct hydrological connection between the two systems. New Spring is a perennial spring within the basin that flows on the surface for approximately 820.2 ft (250 m) before sinking back into the subsurface. Dye tracing shows that New Spring flows as sinking stream for about 2952.7 ft (900 m) in a northerly direction, eventually resurging at Hobson Grove Spring, which is a perennial spring that flows into Jennings Creek. Detailed information on the perennial groundwater flow routes, infiltration sources, and potentiometric surface contours are displayed in Figure 3.2. The complex hydrology of the study area basin is a direct result of the underlying karst geology.

Study Area Map (CoBG)

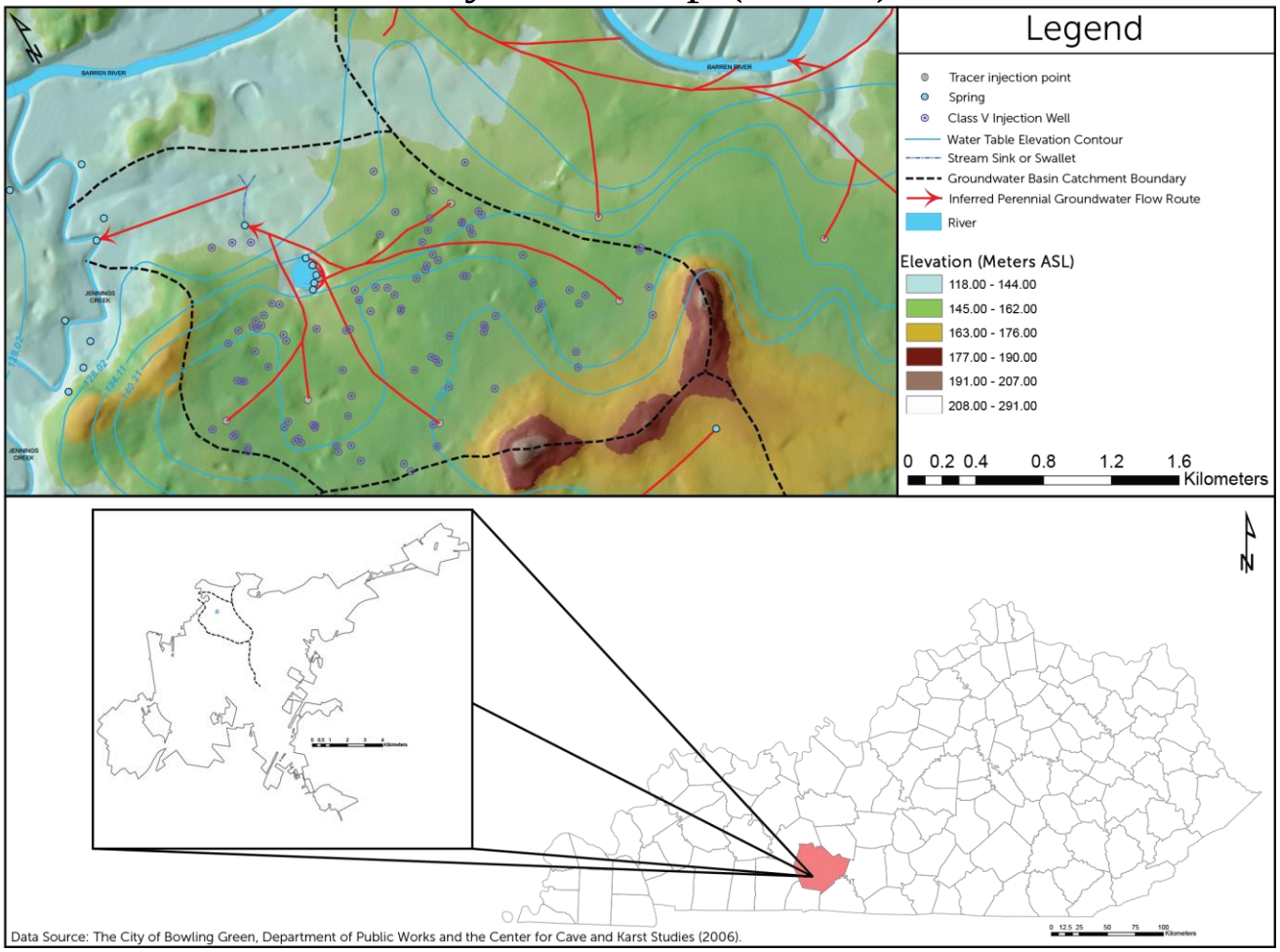

Figure 3.2: Study Area Map: Delineated Basin in Bowling Green, Kentucky (Created by author).

Geology

The CoBG is built atop upper Mississippian Limestones, primarily of the Girkin, Saint (Ste.) Genevieve, and Saint (St.) Louis formations (Crawford et al. 1984) (Figure 3.3). The groundwater basin is almost entirely located in the Ste. Genevieve formation (Figure 3.4). The stratigraphic geological units are comprised of a fine-grained limestone lithology. Each of the previously mentioned stratigraphic layers occurs in varying thicknesses throughout the region and are separated by two distinct chert layers, which are the Corydon Ball chert and Lost River

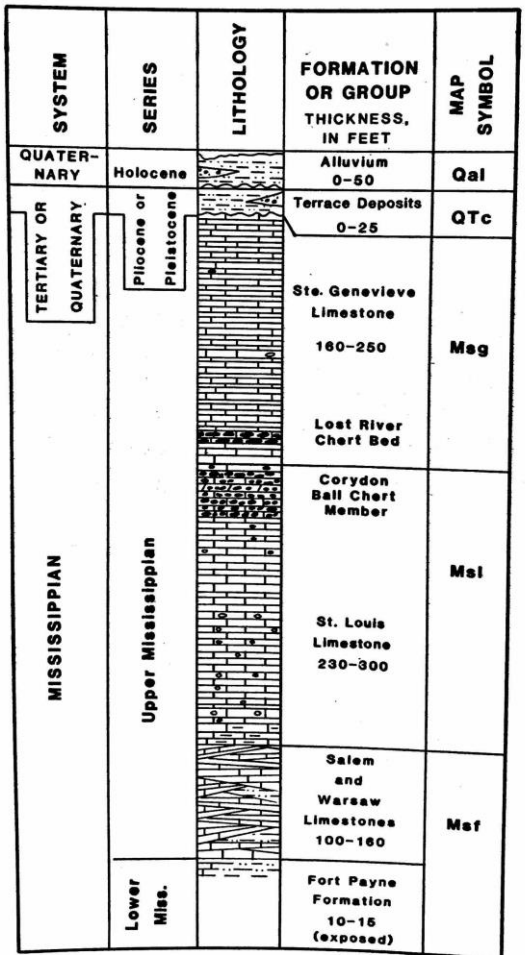

Figure 3.3: Stratigraphic Column for Bowling Green, KY (Crawford 1989).

Study Area Map (Geology)

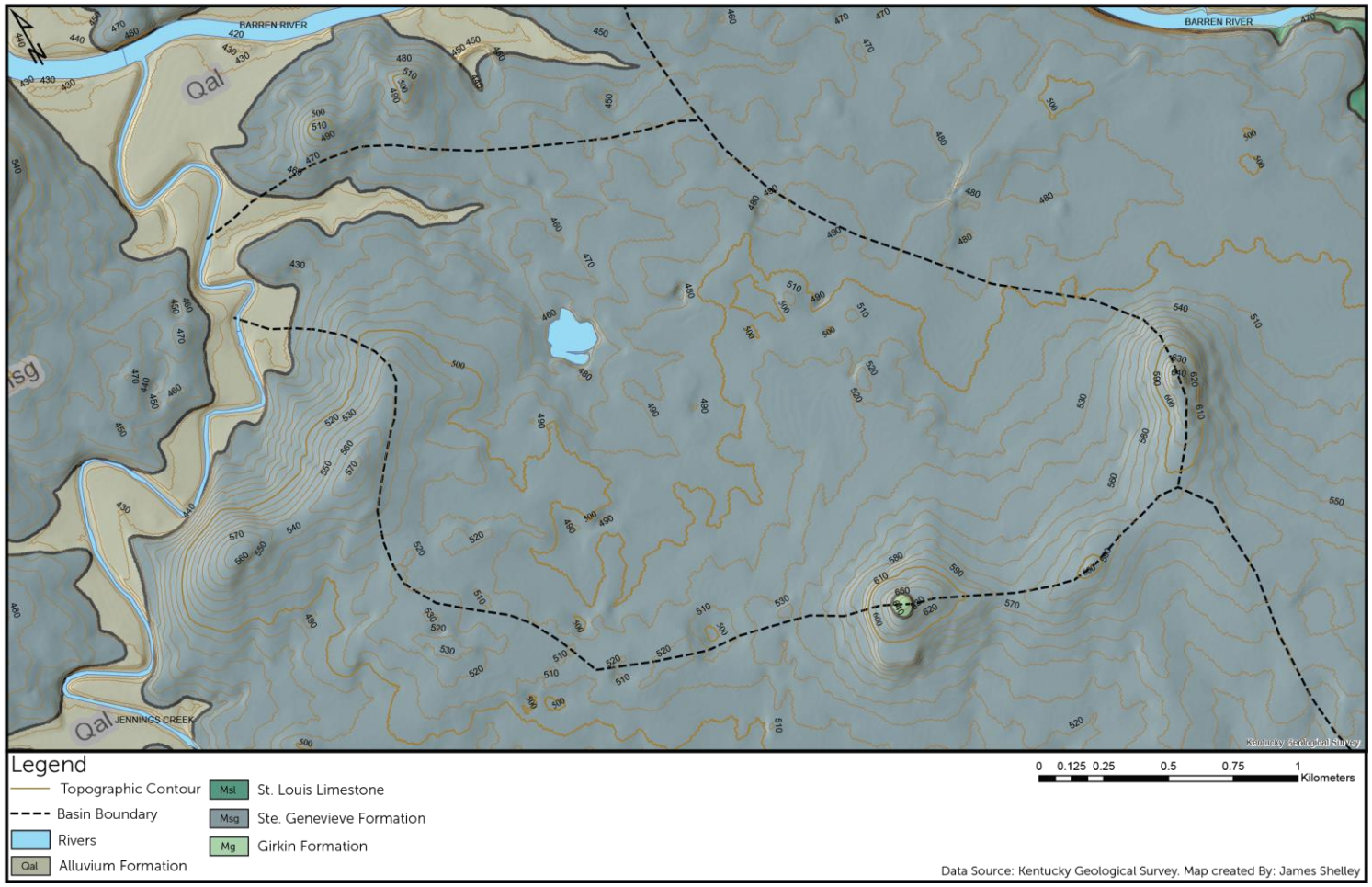

Figure 3.4: Map Showing Geologic Formations within the Study Area Basin (Created by author).

chert (Woodson 1981). As a result, the landscape has a high karst potential and is characterized by thin soils and shallow bedrock depths, with the chert layers providing confining layers in some locations. The carbonate bedrock and local hydrologic conditions are very conducive for the formation of karst features, such as sinkholes, caves, sinking streams, and springs, all of which are abundant in the study area.

Hydrology

Since the City is built on a sinkhole plain, it is almost entirely drained by subsurface streams. The underground streams act as a focal point for the converging groundwater flowing beneath the Pennyroyal sinkhole plain of Warren County, Kentucky (Crawford 1988). Warren County has five major surface streams: the Green River, Barren River, Gasper River, Drakes Creek, and Jennings Creek (Hoffman et al. 1989). For the purposes of this study, only the Barren River and Jennings Creek will be explored in more detail. According to Quinlan and Rowe (1977), most of the drainage from the sinkhole plain terminates at Graham Springs and the Lost River Rise. Graham Springs converges directly with the Barren River, but the Lost River Rise, by contrast, flows into Jennings Creek, which is a tributary of the Barren. The Barren River flows across Warren County in a southeasterly to a northwesterly direction and serves as the eventual discharge point for most of the surface and subsurface streams in the county (Hoffman et al. 1989).

The groundwater basin under study is directly connected to Jennings Creek and, thus, indirectly connected to the Barren. Jennings Creek is predominantly fed by groundwater sources, with the primary flow contributions coming from the Lost River basin and the study area basin (CCKS 2006). Currently, there are two USGS gauging

stations on the Barren River, but none on Jennings Creek. Daily discharge for the Barren River averages around 3451.3 ft^3/s (93.73 m^3/s) (USGS 2016). Most of the CoBG is situated above the floodplain of the Barren River and areas prone to flooding within the city are located in the northwestern section near the confluence of Jennings Creek and the Barren River. Historically, the Barren River is prone to flooding; the river has had eight major flood events with a return period of 50 years or greater occur in the last century (FEMA 1993). Jennings Creek is located near the western border of the city limits and accounts for about 11.58 mi^2 (30 km^2) of the city's drainage area, but does not have a history of flooding (FEMA 1993). FEMA (1993) flood models have shown that if flooding in Jennings Creek were to occur, it would be damaging to some of the areas in the northwestern section of the City. FEMA (1993; 2006) conducted two riverine flood studies for the Warren County area, but little was done to address the localized sinkhole flooding problems. Some of the worst flooding problems in the city occur in small shallow sinkholes within large basins. If unfamiliar with karst landscapes, these shallow depressions are not easily recognized as sinkholes, thus, people often build in flood prone areas (Crawford 1989). The study basin contains many residential areas that have been developed in locations that are at risk of sinkhole flooding. Moreover, the above-mentioned karst flooding continues to be exacerbated by urbanization (Crawford 1989).

Land Conditions

The karst landscape in the CoBG does not allow for much soil development; therefore, much of the land area is characterized by thin soils. As seen in Figure 3.5, it is possible to discern that the soil profile across the basin is widely heterogeneous, but the majority of the subtypes are loams and clays and the basin is dominated by the Fredonia-

Vertrees-Urban and Crider-Urban soil groups (USDA 2004), which are common in urban areas.

Despite the heterogeneity of the soil subtypes, the hydrologic characteristics are more uniform across the basin, with most of the soils falling into the hydrologic soil group C and B. A large portion of the basin belongs group C, which has low hydraulic conductivities. The remainder falls into group B, which are soils with much higher infiltration rates (NEH 2007).

Land cover within the CoBG is primarily developed area (Figure 3.6) with most of the land use being residential. The previously mentioned trends are reflected in the study area (Figure 3.7); however, there is significant industrial and agricultural activity interspersed throughout the basin. The urban area of the CoBG continues to increase along the southern and eastern boundaries, with significant residential and commercial expansion along major highways and secondary roads (FEMA 2006).

High development costs has forced expansion in flood prone areas. Some of the developed area falls within FEMA designated priority grids and the established 100-year floodplain These are based on river flooding and do not take into account the sinkhole flooding in the area; however, development in shallow sinkholes is also occurring and the groundwater basin is heavily urbanized, due of housing development, industrial land modification, and agricultural activities that have drastically increased the amount of impervious surface in the area, in turn altering surface and subsurface drainage. Over the last thirty years, the CoBG population has almost doubled and the land area has grown by approximately 6.178 mi^2 (16 km^2) (CoBG Planning and Zoning 2016). Over this period,

the City made a major transition from an agricultural center to an urban center and will continue to urbanize as it grows and moves towards a metropolitan model.

Study Area Map (Soils)

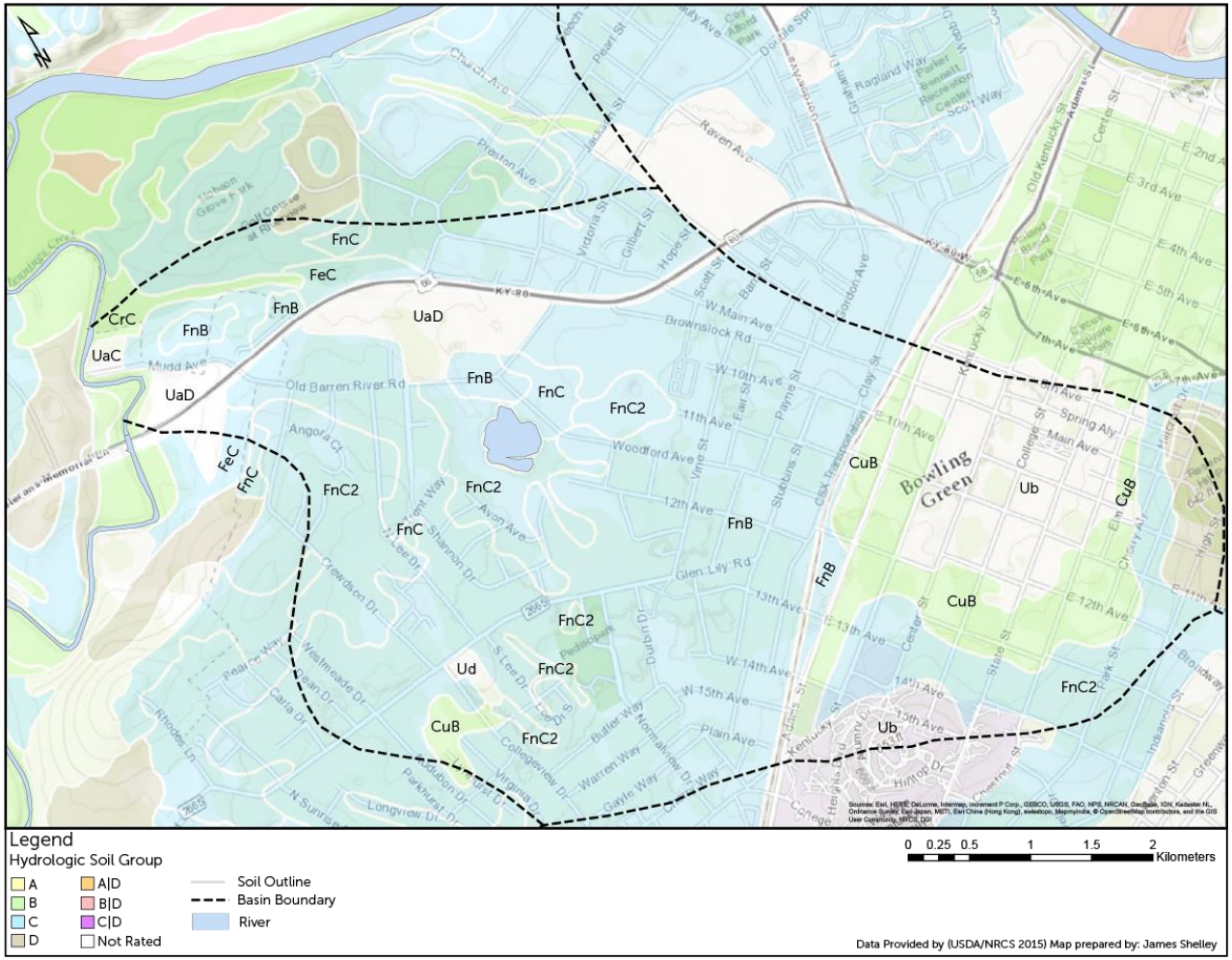

Figure 3.5: Map Showing Soil Groups within the Study Area Basin (Created by author).

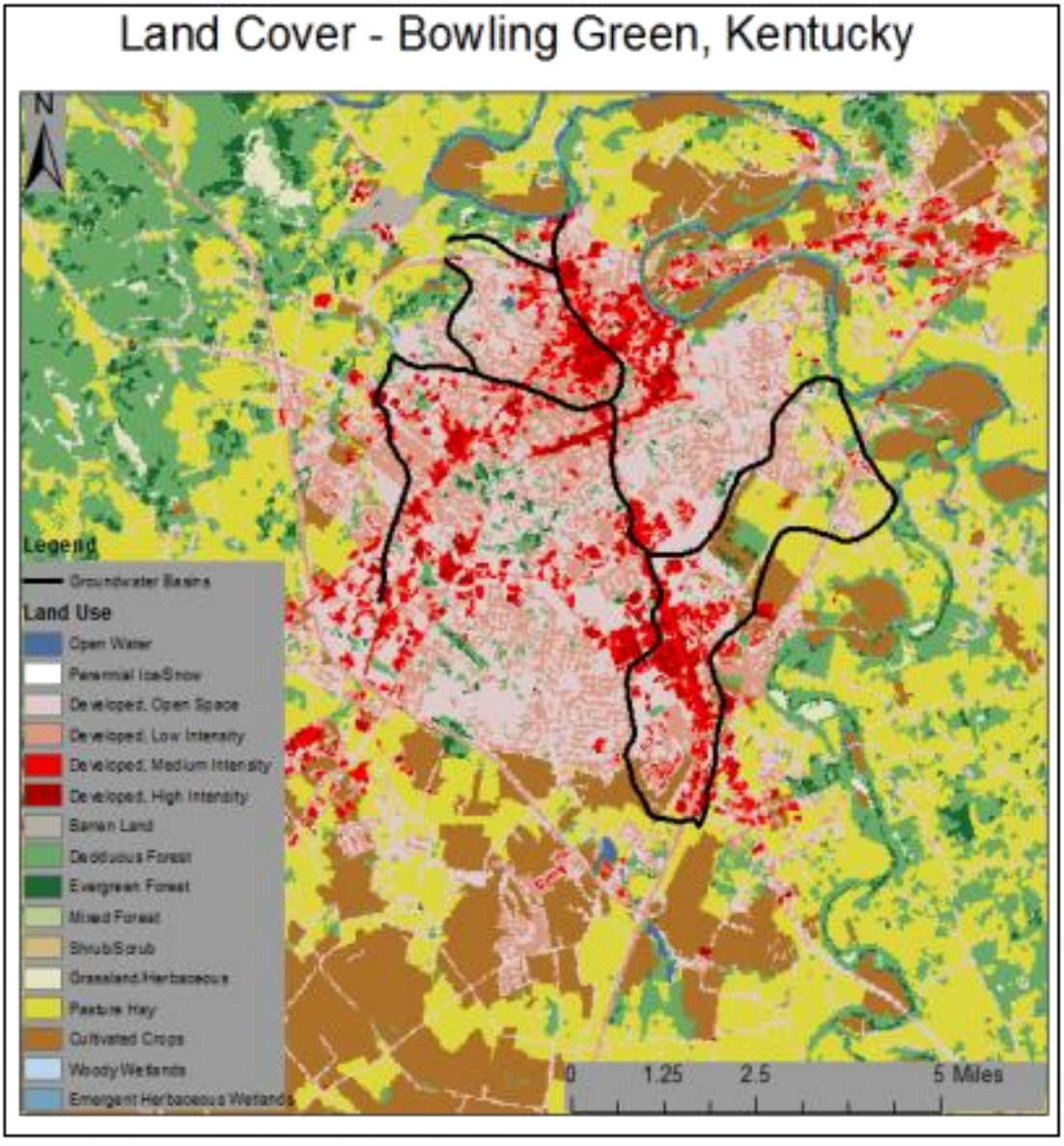

Figure 3.6: Land Cover Map of Bowling Green, Kentucky (Nedvidek 2014)

Study Area Map (Land Use)

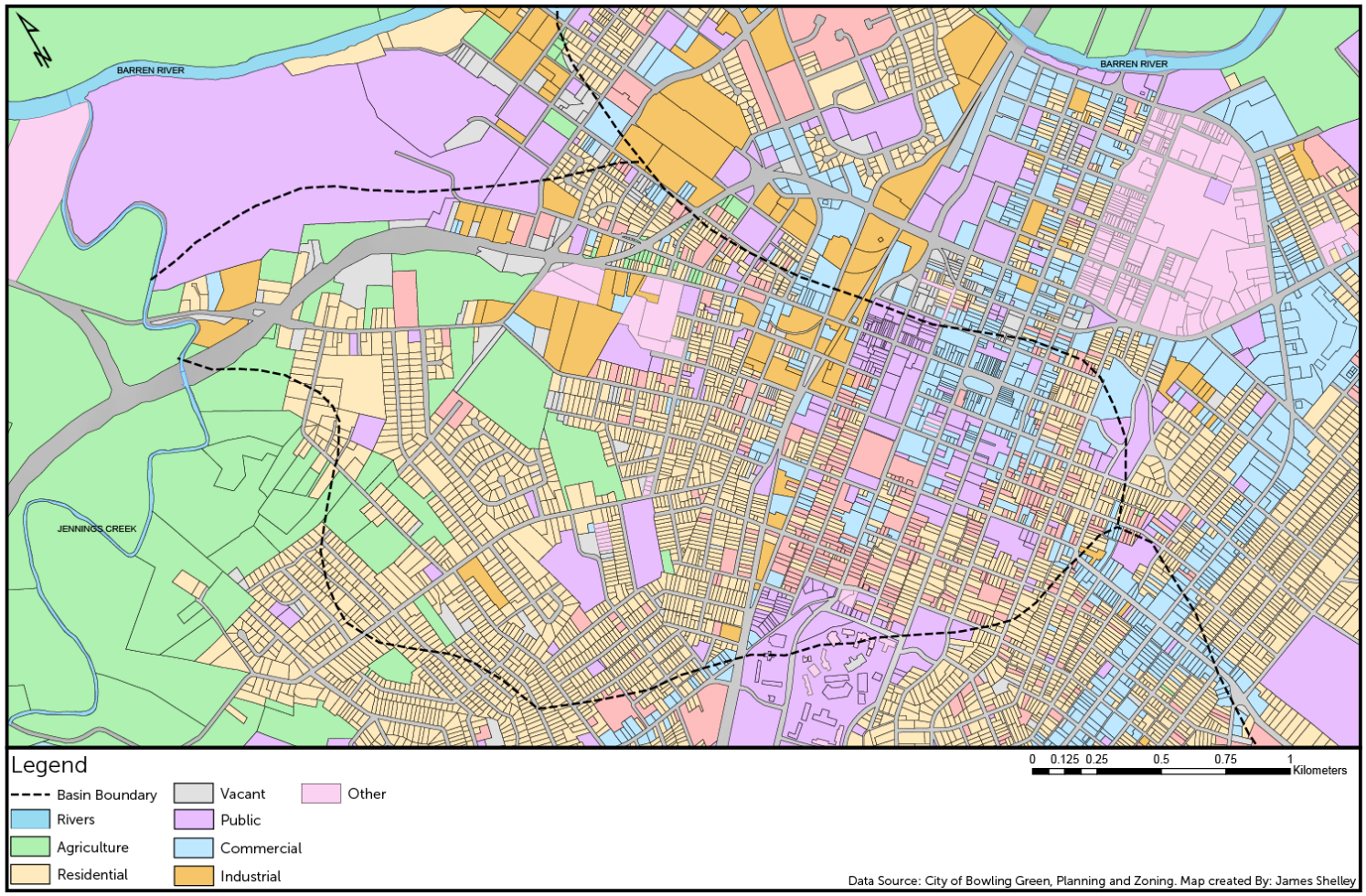

Figure 3.7: Map Showing Land Use within the Study Area Basin (Created by author).

Chapter 4: Methodology

The primary objective of the methodology employed in this research is to evaluate the influence of Class V Injection Wells on urban karst hydrology using surface and subsurface monitoring and modeling techniques. Understanding system influences requires measuring and calculating parameter estimates for weather conditions, surface runoff volumes, and the aquifer's hydraulic properties, as well as Injection Well and spring responses during baseflow conditions and storm events. Through quantifying the hydrodynamic properties of the karst aquifer and the influences from the surrounding environment, it is possible to establish a relationship between precipitation events and the drainage capacity of the Injection Wells and the underlying karst system, as well as explore possible siting issues contributing to the efficiency of the system. The first three sections of the methodology focus on establishing a baseline for current hydrologic conditions. The first portion of the methodology concerns ascertaining properties of the hydrologic inputs and outputs of the study area catchment under seasonal and storm conditions. The inputs to the basin that were calculated, or measured, consist of precipitation, soil infiltration, groundwater recharge, and spring discharge. Measuring these parameters reveals how much water enters the aquifer and how it is stored and transmitted through the system in a defined basin.

The second segment of the methodology is concerned with storm event analysis and performance metrics for monitored Injection Wells. In addition, the second segment details data analytical methods, statistical treatments, and manipulations that were performed on the hydrologic data. Finally, the third section focuses on modeling the potentiometric response to storm events and the methods used to construct an ANN

model to spring discharge prediction, as well as sensitivity analyses and the necessary dataset preparations.

Injection Well Mapping

The study required inventorying all the Class V Injection Wells within the aforementioned 1.9 mi^2 (5 km^2) drainage basin. Prior to conducting the inventory, historical well log data provided by the CoBG was compiled into Microsoft (MS) Excel for preprocessing manipulation. The well logs date back to 1968 and were compiled into a spreadsheet based on the following attributes; postal address, latitude, longitude, date drilled, diameter of the well casing, surface elevation, reported well depth, water level depth, and casing type. The CoBG historical well dataset only contains wells that were drilled by the city. A second dataset containing private well information provided by the EPA UIC program (Region 4) was merged with the CoBG historical dataset using MS Excel. The compiled data was imported into ArcMap for visualization and further processing. In ArcMap, all data were projected using the NAD 1983 State Plane Kentucky South FIPS 1602 projected coordinate system. The first dataset that was added to the map are the data with GPS coordinates. The dataset has 156 well locations with corresponding GPS coordinates. Data with known coordinates were added using the display X and Y feature in ArcMap. Locations that did not have GPS coordinates were geocoded based on postal address attribute field. The City's geocode database only matched 446 locations and the remaining 1,745 locations were geocoded using the United States Census Bureau geocoding database. The geocoded point coordinates were added to the map using the "display X and Y" feature in ArcMap. Once all injection well features were added to the map, they were merged into one shapefile using the "spatial join"

feature.

After a map containing potential injection well locations was constructed, it was necessary to confirm that the wells identified actually exist and the locations of existing wells are accurate. Prior to moving the map document to a field collection platform (Collector for ArcGIS), attribute fields were created in ArcMap for inventory purposes. The following attribute fields were added to the injection well attribute table: date sampled, time sampled, grate type, condition, photos, comments, and a sampled field. The sampled field was prepopulated with "No" so that thematic mapping could be used in the collection software. Moreover, once a location had been sampled and the attribute field had been edited in the collection software to indicate "Yes" the well had been sampled, the color of the point on the map changed from red to green. In order to edit the map in real time, Collector for ArcGIS was used. The ArcMap Document was transferred to ArcGIS Online, so it could be accessed using the Collector for ArcGIS application.

All potential well locations within the basin were groundtruthed. Groundtruthing each well eliminates obstructed wells, provides locational accuracy, and allows for supplemental data collection. At each well, the following attributes were recorded or updated: postal address, latitude, longitude, casing type, the diameter of the well casing, drainage structure dimensions, depth to water, and well condition. Photos and comments were georeferenced to each injection feature. Field data entry in Collector for ArcGIS was completed using a 256 GB, cellular enabled, 9.7-inch iPad Pro with an A9X chip. Well depth at each well was taken using a Heron Dipper-T Well Tape 200 ft (60 m) tape. In total, 100 wells were identified within the delineated groundwater basin.

Site Selection

After inventorying the Class V Injection Wells in the study area catchment, field investigations were conducted to determine which wells have measurable water level depths during baseflow conditions. The inventory identified 100 Class V Injection wells in the groundwater basin. Out of the 100 wells, viable wells without obstruction served as the population from which monitoring sites were selected. Injection wells classified as obstructed are the wells that are clogged with debris and sediment as a result of improper maintenance. Obstructed wells were eliminated from the selection process because they cannot drain effectively and will not accurately portray the responsiveness of the aquifer during storm events. Other features within the unsuitable designation include shallow karst features that have been modified to take stormwater runoff. The shallow karst injection features were eliminated because they remained dry during baseflow conditions. A simple random sampling (SRS) design was used to identify potential injection wells sites for groundwater monitoring and aquifer testing. The SRS design was chosen to eliminate bias, and, because only basic attributes will be collected for the point layer feature during the inventory process, it will not be possible to use a stratified approach. Injection wells were chosen using the sampling design tool in ArcGIS ArcMap. Out of the population, 31 potential monitoring wells were selected (Figure 4.1). A sample size of 31 wells was chosen because it is a statistically representative sample and economically feasible given the funding for the project and logistics of fieldwork to collect the data.

Monitored Injection Wells

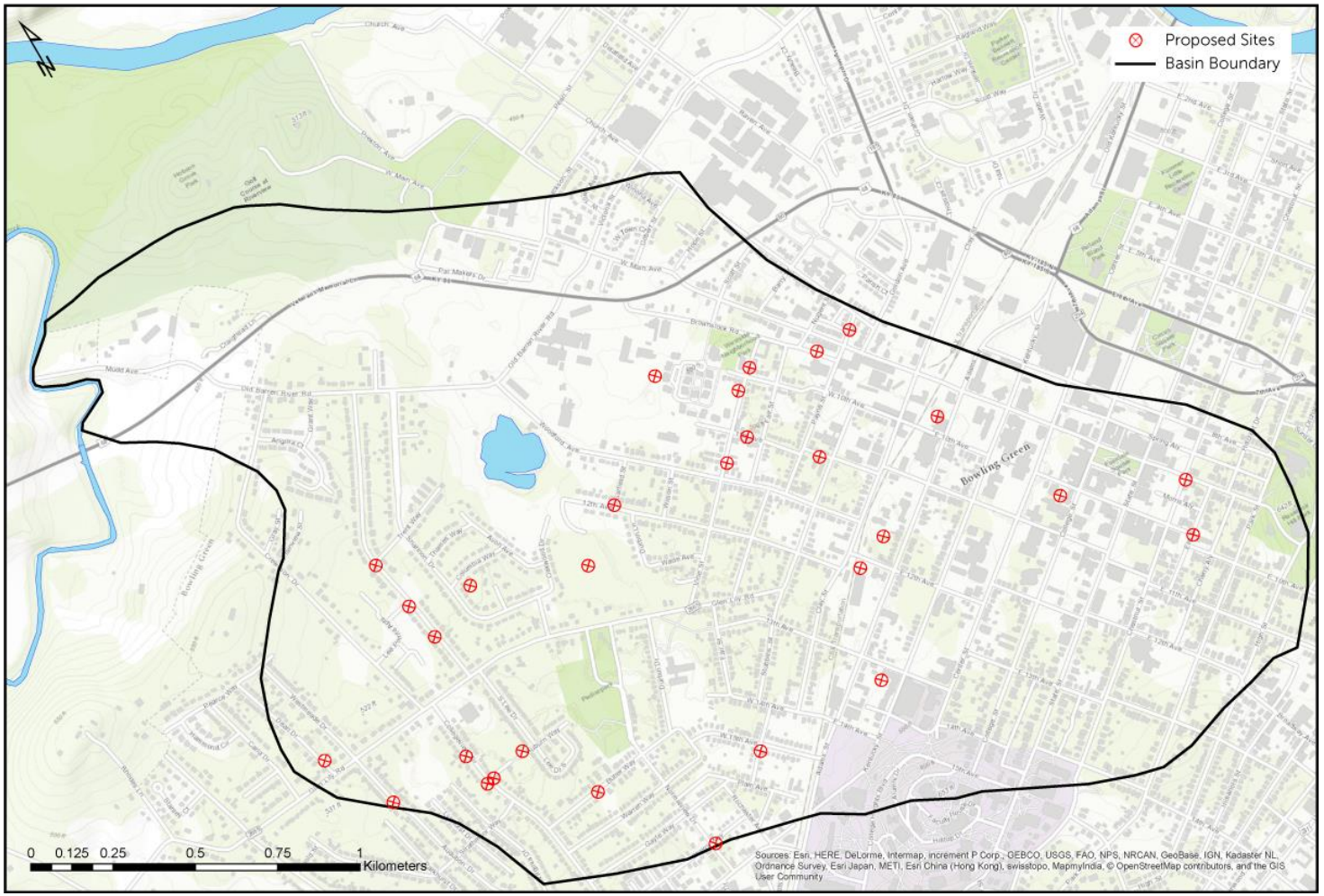

Figure 4.1: Potential Site Selection (Created by author).

High-resolution Monitoring

To adequately assess the aquifer's response to storm events and flood conditions in the study area basin, it was necessary to measure several hydrometeorological parameters. The following input parameters were measured for further data manipulation and analysis: precipitation, temperature, relative humidity, and barometric pressure. All data loggers used in this study recorded data continuously at a one-minute resolution. The data loggers were downloaded and processed on a weekly basis as a precautionary maintenance schedule to prevent data loss. The one-minute resolution was chosen to capture the storm events fully (Lawhon 2014; Nedvidek 2014; Osterhoudt 2014) and to satisfy the sensitivity of the data analysis. A HOBO RX 3000 remote monitoring station was outfitted with several data loggers to monitor weather and soil conditions within the basin continuously. The RX 3000 platform was chosen because it allows multiple data loggers to be linked to one system. Additionally, the monitoring station allows downloading of the data being recorded without disturbance or interruption. A HOBO tipping bucket rain gauge, smart barometric pressure sensor, and U23 Temperature/Relative Humidity data loggers were attached to the monitoring station to measure precipitation, barometric pressure, temperature, and relative humidity. In addition, soil moisture data from the Kentucky Mesonet were used for continuous measurements of the volumetric water content of the soil. The sensors are buried at different depths to capture the variability of the soil profile (Tramblay et al. 2009). Once collected, the data downloaded from the RX 3000 were processed with the HOBOware software and transferred to various other software packages for further processing. The barometric pressure sensors were used to compensate all absolute pressure sensors used

in this study.

Given this study is primarily focused on relating groundwater fluctuations to precipitation, it was necessary to examine how the potentiometric surface responds to storm events. Moreover, since Injection Wells are one of the principal infiltration sources in the basin, they were used to monitor groundwater fluctuations. A non-vented HOBO water level logger was installed inside a PVC stilling well at each Injection Well in the sample population. The data loggers recorded water level fluctuations continuously at one-minute intervals. The data were downloaded weekly and processed using HOBOware software. The water level data were compensated for barometric influences using the barometric pressure data collected with the RX 3000. The barometric compensation was performed in the HOBOware software.

Often, karst flooding is the result of the capacity of the subsurface drainage system, with the primary control being the outlet spring. Furthermore, outlet spring discharge is an essential parameter needed to understand system mechanics during flood events accurately. The delineated groundwater basin has one primary outlet, which is a spring referred to as New Spring. Discharge measurements were made at New Spring using the velocity-area method (Herschy 1997). A Global Water flowmeter was used to measure the velocity of the stream. A stage-discharge rating curve was constructed from the recorded discharge and staff gauge measurements using regression analysis. Specifically, the data were fitted to a power function per USGS methods (Herschy 1997). A HOBO water level data logger was installed in a 5.08 cm (2 in) diameter PVC stilling well with the pressure sensor aligning with the zero datum on the staff gauge. To obtain high-resolution discharge data and match the well data, the water level logger was set up

to measure hydrostatic pressure at one-minute intervals. The generated data were downloaded and processed on a weekly basis. Using HOBOware, the hydrostatic pressure data were compensated for barometric influences using the data collected by the RX-3000. The compensated pressure values were used to calculate water level and converted to discharge using the rating equation, $Q = 8.6678(S)^{3.8212}$, where Q refers to stream discharge, and variable S represents water stage. The power function produced a coefficient of determination of 0.95, which indicates that regression model fits the data strongly. The regression residual plots were examined to determine if data tightly followed the function.

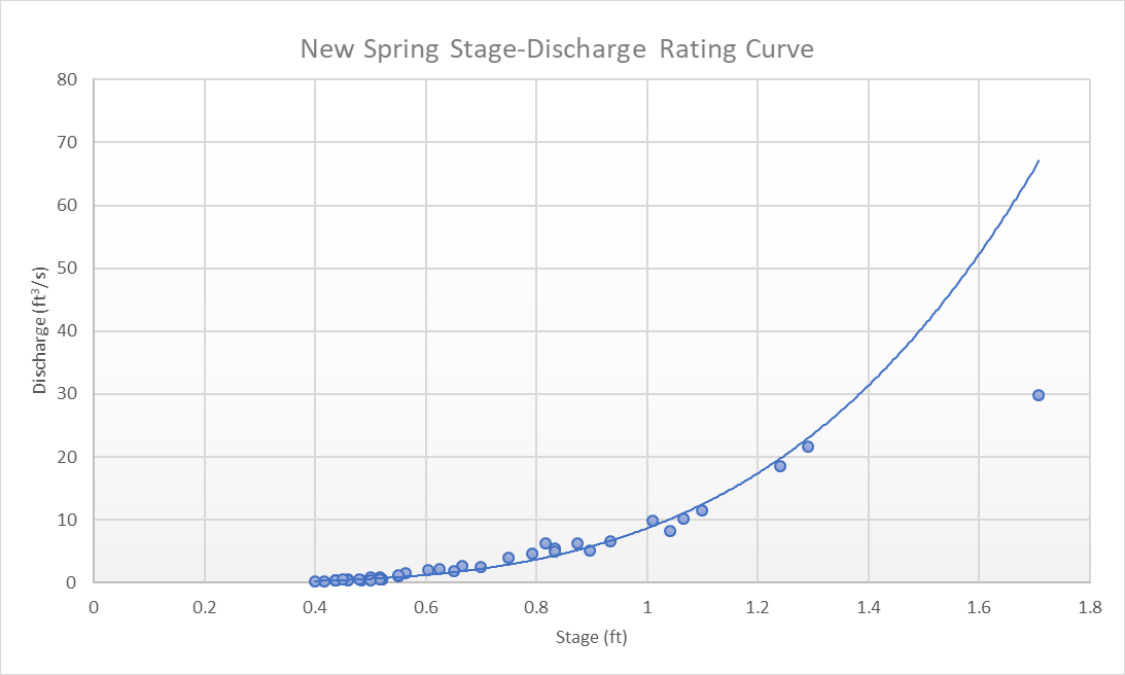

Figure 4.2: New Spring Rating Curve (Created by author).

Water stage was measured at several surface sites that are believed to be hydrologic controls on groundwater level and spring discharge to get a better understanding of basin hydrology. The additional surface water body sites included Limestone Lake, Jennings Creek, and the Barren River.

Water Budgeting

Monthly water budgets were calculated to have a baseline for understanding the basic hydrologic cycle within the New Spring Basin, as well as aquifer drainage properties under storm conditions. The following water balance equation was used and modified as necessary (Gupta 1995):

$$P + Q_{si} + Q_{GI} - E - Q_{SO} - Q_{GO} - \Delta s - n = 0 \qquad \text{(Eq. 2)}$$

where,

P = precipitation
Q_{SI}, Q_{GI} = surface and groundwater inflow
E = evaporation (including transpiration)
Q_{so}, Q_{go} = surface and groundwater outflow
Δs = change of storage
n = discrepancy term

Sub-meter aerial thermal infrared (TIR) imagery was analyzed in ArcGIS to improve the accuracy of the water budget and identify potential losses or gains within the basin through the examination of temperature anomalies. The thermography project area consists of 42,158 flown acres, which completely encompasses the CoBG. Thermal signatures of known karst features were identified in the map and used to evaluate temperature anomalies. Precipitation was measured directly, however, evapotranspiration and infiltration were calculated using the methods described below.

Daily evapotranspiration calculations were made using the Penman-Montieth equation,

and soil infiltration was calculated using the Green and Ampt method to make it possible to create a water balance for the basin.

$$ET_o = \frac{(0.408\Delta)(R_n - G) + \Upsilon\left(\frac{900}{T+273}\right)(u_2)(e_s - e_a)}{\Delta + \Upsilon(1 + 0.34(u_2))} \quad \text{(Eq. 3)}$$

where,

ET_o = Evapotranspiration Rate (mm/day)

T = Mean Air Temperature (°C)

u_2 = Wind Speed (m/s)

R_n = Net Radiation (MJ/m^2)

G = Soil Heat Flux Density (MJ/m^2)

e_s = Saturation Vapor Pressure (kPa)

e_a = Actual Vapor Pressure (kPa)

Δ = Slope of the Vapor Pressure Curve (kPa/°C)

γ = Psychrometric Constant (kPa/°C)

Evapotranspiration was calculated in MS Excel using data collected at the New Spring weather station. Soil infiltration was calculated for each storm event, and the soil's hydraulic and physical properties were determined using the USDA SSURGO database. The soil properties were assigned to a two-dimensional gridded index map covering the study area in the Watershed Modeling Software (WMS) using a Gridded Surface Subsurface Hydrologic Analysis (GSSHA) model for infiltration. Initial moisture content

was pulled from the Kentucky Mesonet station at the Western Kentucky University (WKU) farm.

$$\int_{0}^{F(t)} \frac{F}{F + \psi \Delta \theta} dF \qquad \text{(Eq. 4)}$$

where,

F(t) = Cumulative Depth of Infiltration (L)

K = Hydraulic Conductivity (L/T)

ψ = Wetting Front Suction Head (L)

Θ = Water Content (L)

Precipitation Analysis

Each observed storm event was classified based on generated Frequency Curves (Figures 4.3 and 4.4). The Intensity-Duration-Frequency (IDF) and Depth-Duration Frequency (DDF) curves were created using data from the National Oceanic and Atmospheric Administration's (NOAA) Hydrometeorological Design Studies Center Precipitation Frequency Data Server (HDSC-PFDS). An empirical relationship was used to create the IDF Curves (Chow 1988). The curves were generated using HydroCAD, and Sigmaplot software. Once all recorded storm events were compiled and assigned an IDF/DDF classification, they were given a rank for rainfall intensity and rainfall depth. The two separate ranks were combined and the top twenty storms in terms of intensity and cumulative depth were chosen for further analysis.

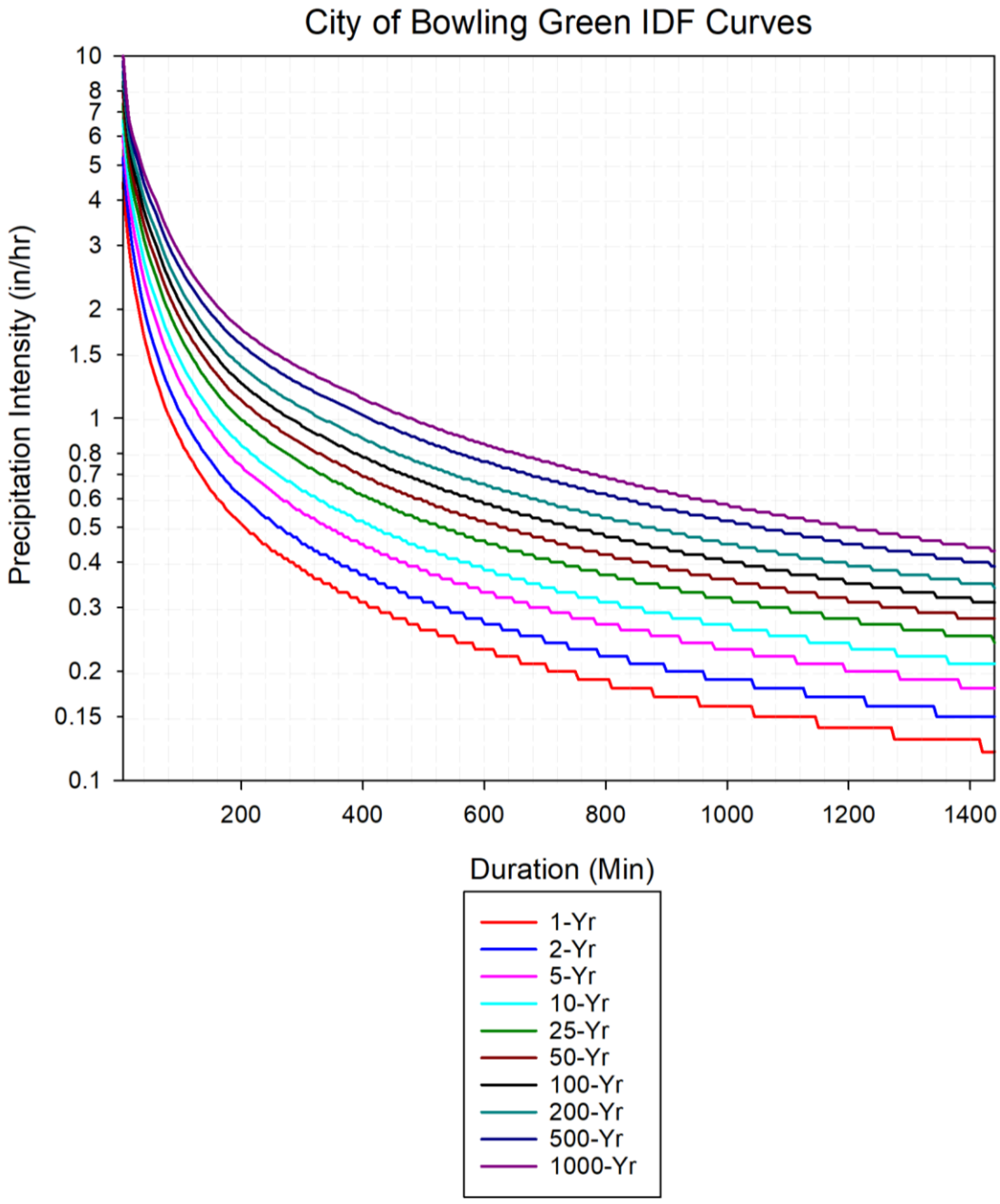

Figure 4.3: Intensity-Duration-Frequency Curves for the City of Bowling Green (Created by Author.)

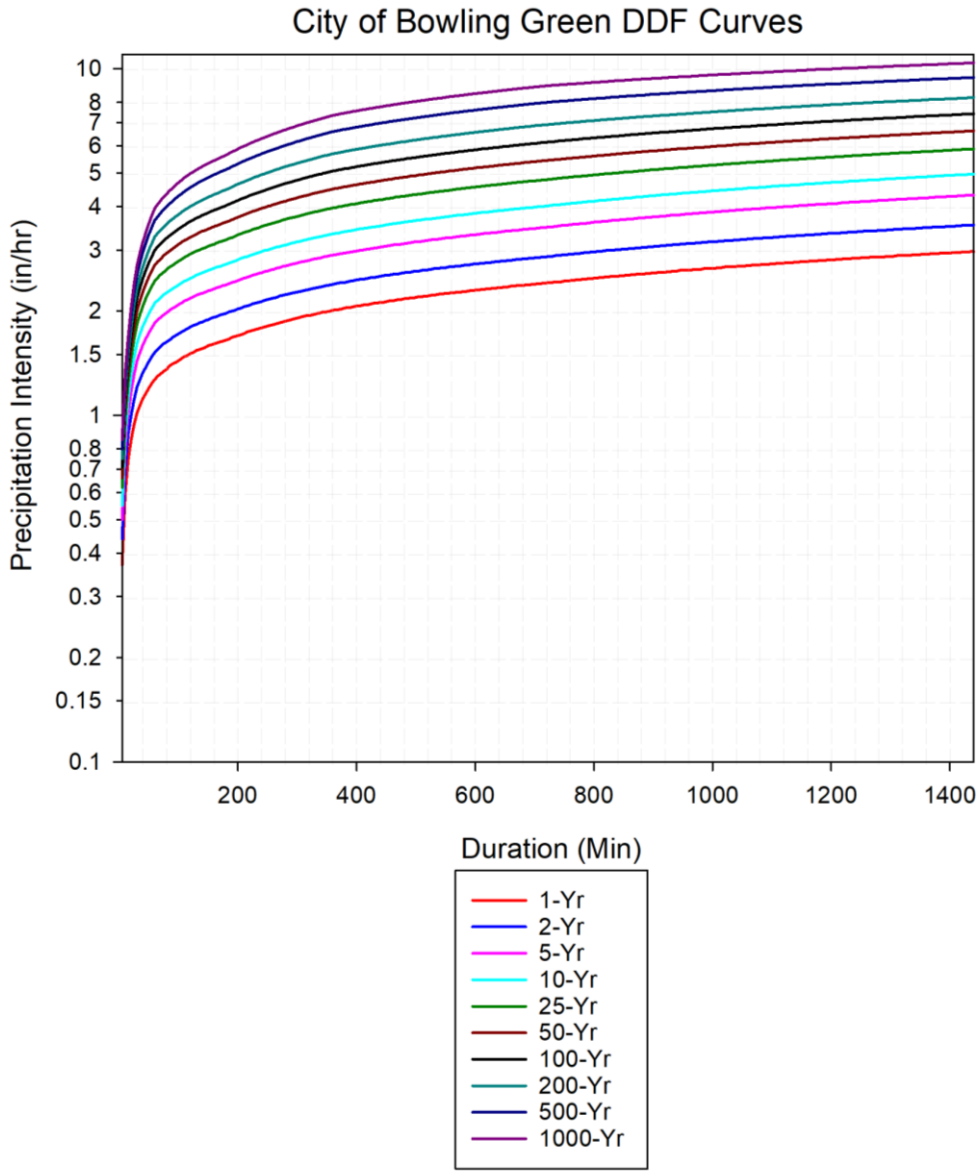

Figure 4.4: Depth-Duration-Frequency Curves for the City of Bowling Green (Created by Author.)

Well Hydrograph Analysis

Once the twenty storm events had been chosen, Well performance metrics could be calculated using the high-resolution monitoring data. Calculated parameters included inflow volume, recession rate, peak inflow rate, and free borehole volume. Analyses were conducted on every monitored well for each chosen storm event. In total, over 600 hydrographs were analyzed, which equates to over 2,400 separate analyses. Due to the constraints imposed by the karst geology, a decision to forgo traditional methods of recharge estimation, such as the Water-Table Fluctuation (WTF) Method, was made and a physical relationship that utilized the high-resolution data to calculate Injection Well Inflow was developed. The main issue that arises when using traditional methods in a fractured rock medium is the variability in hydraulic properties such as conductivity, specific yield, etc. Moreover, the properties of each Injection Well would only reflect local characteristics which are particular to that Well, which would result in large relative differences in estimated recharge between sites (Kovacs et al. 2015).

The equation is adjusted to account for the characteristics and stage data for each monitoring site respectively. Additionally, the equation operates under the assumption of uniform geometry. It is believed that the monitoring resolution adequately captures the well stage changes without producing a significant amount of noise, which ensures accurate estimation of inflow from both surface and subsurface inputs. The accuracy of was validated from field testing and, due to the high resolution of the data, it is believed that the equation adequately captures the flashy nature of the karst system. It would have been possible to modify some sites to measure inflow directly through the use of a weir

or flume, but given that some sites could not be altered, a decision was made to refrain from using that approach. The modification of the drainage system would have provided meaningful insight into what percentage of Injection Well's water level change could be attributed to surface and subsurface sources. The equation developed to calculate Injection Well inflow was:

$$F_n = [n_{t+1} - n_t] \left(\frac{\left(\frac{\pi}{4}\right)(\phi)^2}{t} \right) \quad \text{(Eq. 5)}$$

where,

F_n = Inflow volume at time step t (ft^3)

n = water level at time t (ft)

ϕ = well borehole diameter (ft)

$$CI = \sum_{i=1}^{m} F_n \quad \text{(Eq. 6)}$$

Where,

CI = Cumulative inflow for volume for a recorded storm event

F_n = Inflow volume at time step t (ft^3)

Equation 5 denotes the calculation of the inflow volume for any given time step; thus, cumulative inflow volume for the storm event is calculated through the summation of Fn. The Injection Well inflow volume calculation was started on the time step where the first stage fluctuation occurred and was applied until the well hydrograph entered a recession. Peak inflow rate was determined by returning the maximum inflow volume calculated in MS Excel. Additionally, free borehole volume was calculated by subtracting the depth to water from the surface elevation of the standpipe and using the known radius and pipe length to calculate the volume of a cylinder. Since high-resolution data were utilized, recession rates could be accurately and easily calculated from the data.

$$RR = \frac{\left(Q_{RP} - \left(Q_i\right)\right)}{\Delta t} \qquad \text{(Eq. 7)}$$

where,

RR = Recession Rate (ft/min)

Q_{RP} = Well water stage height at the recession point (ft)

Q_i = Initial water stage prior to storm (ft)

Δt = Duration of recession (min)

Once the Well performance metrics were calculated, basic descriptive statistics were generated from the data for comparative purposes. The four metrics above were chosen because they are believed to characterize the drainage performance of a well adequately. Zhou (2007) states that flooding in karst is primarily attributable to an imbalance between recharge and discharge; moreover that is why inflow volumes and recession rates were calculated. In addition, free borehole volume determines the initial storage capacity of a

Well, and this parameter was used to determine if borehole storage made a difference in the occurrence of flooding. Finally, peak inflow volume was used to see the role that drainage intensity played in Well Exceedances.

Time Series Analysis

Due to the quantity and resolution of the data collected in this study, it was necessary to use time series analysis (TSA) techniques to identify trends obfuscated by the magnitude of the dataset. Also, TSA was used to determine lags and leads in the system, as well as the predictor importance of variables for modeling purposes. The TSA techniques used in this study will be briefly outlined. The primary TSA methods employed in the research are the autocorrelation function (ACF), cross-correlation function (CCF), and the Mann-Kendall trend test.

The heterogeneity of the karst system increases the prevalence of lags and leads between inputs and outputs (Grimmeisen et al. 2016). Lags and leads distort the hydrologic signal and make it difficult to identify causal/non-causal relationships between variables; therefore, to ameliorate interpretation issues, the CCF was used, however, prior to conducting cross-correlation analysis, it was first necessary to ensure that no autocorrelation existed between any of the hydrological series (Machiwal and Jha 2012). The ACF expresses the temporal dependency between values and provides an assessment of the linear correlation between an equidistant successive value series and an identical series with a specified lag (Jenkins and Watts 1968; Machiwal and Jha 2012; Grimmeisen et al. 2016). The ACF is given by the formula below.

$$ACF = \frac{\sum_{t=k+1}^{n-k} \left(X_{t-k} - \bar{X} \right)\left(X_t - \bar{X} \right)}{\sum_{t=1}^{n} \left(X_t - \bar{X} \right)^2} \quad \text{(Eq. 8)}$$

where,

k = Lag; k=1,2,…

X_t = Value of X at row t

$\bar{X}$ = Mean of X

n = Number of observations in the series

The analysis for ACF was conducted in IBM SPSS using the independence model for the standard error quantification and the Anderson test for significance. If the ACF value fell within the upper or lower limit specified by the Anderson Test at α=0.05, the series was not considered random and pre-whitening techniques were utilized to remove the serial correlation. Once the data were checked for serial dependency, the CCF was applied in IBM SPSS to the Injection Well and Surface stream data to establish relationships between variables for modeling and interpretation purposes. The equation for the CCF is displayed below.

$$CCF = \frac{\sum_{t=1}^{n-k} \left(X_t - \bar{X} \right)\left(Y_{t-k} - \bar{Y} \right)}{S_x S_y} \quad \text{(Eq. 9)}$$

where,

k = Lag; k=1,2,…

t = Value of X at row t

$\bar{X}$ = Mean of X

$\bar{Y}$ = Mean of Y

n = Number of observations in the series

$S_x = \sum_{t=1}^{n}(X_t - \bar{X})^2$ - Standard deviation

$S_y = \sum_{t=1}^{n}(Y_t - \bar{Y})^2$ - Standard deviation

After the Cross-Correlation analysis was completed variables that produced strong r^2 values were compiled into a matrix for further analysis. A 15-hour lag time was selected for the CCF, and that determination was made from the observation of empirical trends in Well and Spring Hydrographs. From the correlation matrix, the maximum and minimum CCF and corresponding positive or negative lag was recorded. Conclusions of system influences were drawn from the cross-correlogram. If an asymmetrical cross-correlogram was detected, and CCF exhibited a maximum or minimum for a positive lag, it was concluded that the input signal influenced the output signal (Delbart et al. 2016). The lag time that corresponded to the maxima of the CCF was noted as the mean response time.

Another TSA technique that proved useful in data interpretation was the Mann-Kendall trend test. Given the nonparametric nature of the data collected in this study, it was sometimes difficult to identify the trend direction between two series. The Mann-Kendall trend test is a TSA method that detects monotonic trends within a dataset without

the explicit specification of the trend type (i.e. linear or nonlinear) (Machiwal and Jha 2012). The test was applied in the situation where Injection Wells were considered to share a hydrological connection, particularly in circumstances where the drainage of an upgradient well, in a hydrologically stable period, created a surcharging effect or influenced the stage of a downgradient well. In event of Well-to-Well interconnectivity, the data period that encompassed the surcharging was isolated and the direction of the trend for the influencing and influenced Wells were analyzed and compared. In most cases, trend direction was obvious, but sometimes it was difficult to determine if the upgradient well was still receding at the time of surcharge. The equations used for the Mann-Kendall trend test in MS Excel is outlined below.

$$u_c = \frac{S + m}{\sqrt{V(S)}} \qquad \text{(Eq. 10)}$$

where,

$$s = \sum_{t'=1}^{n-1} \sum_{t=t'+1}^{n} z_k$$

and,

$$V(S) = \frac{1}{18}\left[n(n-1)(2n+5) - \sum_{i=1}^{g} e_i \left(e_i - 1\right)\left(2e_i + 5\right) \right]$$

where,

m = 1 for S < 0

m= -1 for S > 0

g = Number of tied groups

e_i = Number of data in the i^{th} tied group.

If the results of the Mann Kendall corroborated the negative trend of the upgradient Well and the positive trend of the downgradient well, the finding was recorded.

Potentiometric Surface Mapping

To effectively characterize and visualize the response of the aquifer to storm events and seasonal fluctuations, it was necessary to create a potentiometric surface time-series. The time-series data were used to visualize the flooding that occurred after a storm event. It was hoped that the maps could be used to map localized flooding that was overlooked by traditional methods. To create the potentiometric surface, geostatistical tools were used. Potentiometric surfaces were spatially interpolated using the water level data collected in the monitored injection wells through the use of the kriging geostatistical technique. A potentiometric surface map was made for several storm events observed during the monitoring period. The maps were generated on a one-minute time-step until the water receded to baselevel. The GIS ArcMap model (Figure 4.5) shown below was used to simplify the processing time. Although there are many methods to construct a potentiometric surface, the geostatistical technique is chosen because it has been effectively used in karst areas (USGS 2014) and other groundwater mapping projects (Varouchakis et al. 2012; Fisher 2013). An advantage of the kriging model is the ability to estimate the error associated with the interpolated values quantified through kriging standard deviation (Virdee and Kottegoda 1984).

Kriging is an interpolation tool that fits a mathematical function to all points

within a specified area in order to determine an assigned output value. Ordinary kriging was chosen as the interpolation method that was used on the Injection Well data because it assumes that the mean is an unknown constant. Prior to conducting the kriging interpolation, the Injection Well data had to be transformed. The water level data for each respective Well had to be referenced to its surface elevation to have accurate z-values for analysis.

The models were optimized using the Geostatistical Wizard in ArcGIS and in most cases a second order trend removal was necessary. Cross-validation residual charts were checked to ensure that the interpolation models were within a reasonable error range. The kriging formula is given below:

$$\hat{Z}(s_0) = \sum_{i=1}^{n} \lambda Z(s_i) \qquad \text{(Eq. 13)}$$

where,

$Z(s_i)$ = The measured value at the i^{th} location

λ_i = An unknown weight for the measured value at the i^{th} location

s_0 = The prediction location

n = The number of measured values.

Despite the intent to use the interpolated surfaces for flood mapping purposes, a lack of variability in the data meant that the kriging maps were only used for visualization purposes.

One of outcomes of this study was to design a methodology that could be used as

a predictive tool for proactive hazard management and real-time flood warnings. Unfortunately, the development of these systems was beyond the scope of this research, but all of the necessary components have been assembled and tested. Furthermore, full scale implementation would be possible, if the funding was available.

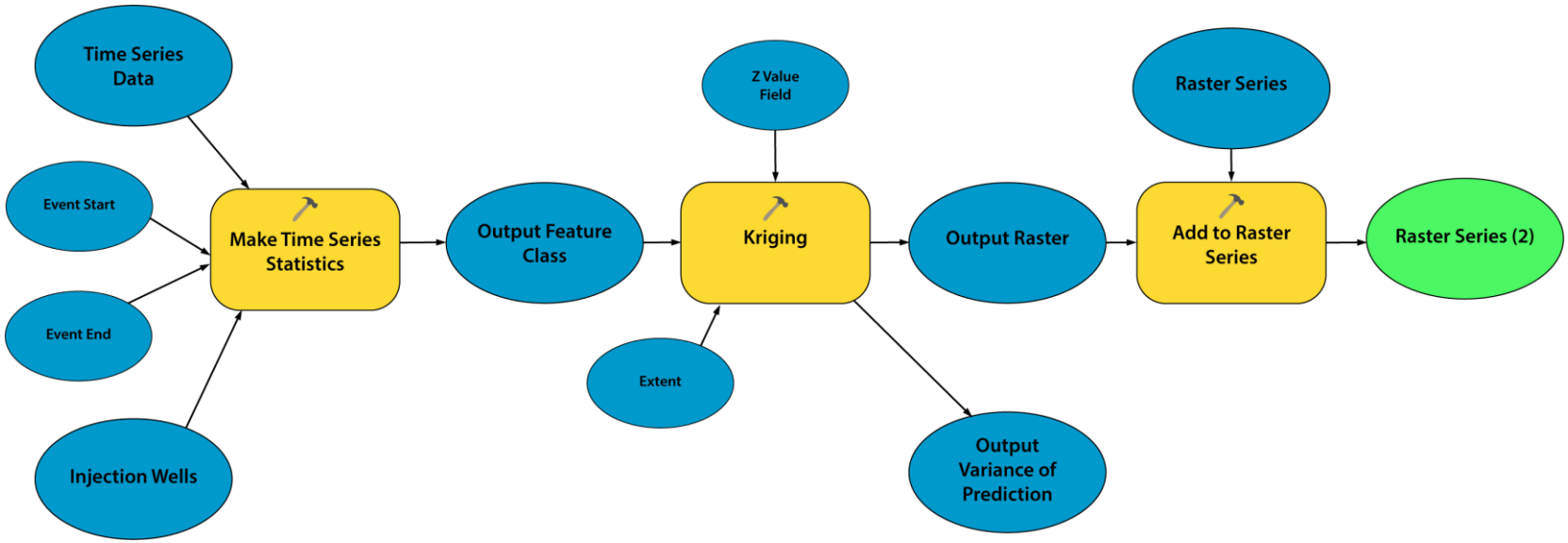

Figure 4.5: Potentiometric Surface Kriging Model (Adapted from Strassberg et al. 2011 by author).

Artificial Neural Networks

Due to time constraints and lack of hydrological information, only one ANN network model was constructed. Most of the studies in karst environments operate in data resolutions that are on a daily, weekly, or monthly time scale (Trichankis et al. 2010; Kong-A-Siou et al. 2011a; Kong-A-Siou et al. 2014). Due to the limited research with high-resolution data, it was important to reassess input selection determinations, preprocessing, data aggregation techniques, and optimization algorithms to ensure that overfitting does not occur and that the analyses produce meaningful results as dataset size increases. This study served as a pilot to evaluate the reliability of models given an extremely large dataset. The ANN model was constructed to predict New Spring stage; therefore, prior to constructing the ANN model, a conceptual model was created.

Every hydrological model, statistical or deterministic, needs to begin with a concept of how the system works, and identify variables that are essential for predicting behavior (Coppola et al. 2005). In this process, the cross-correlation matrices were consulted in conjunction with preexisting knowledge of system behavior to construct a conceptual model. Four inputs were selected for the ANN Model. The chosen inputs consisted of precipitation and water stage for Limestone Lake, Jennings Creek, and the Barren River. All of the variables above were chosen because they were shown through dye trace, TSA, and empirical evidence to share a connection and/or influence New Spring behavior. Once input variables were determined, the data for the selected parameters were compiled and modeled in IBM SPSS Modeler. A multilayer perceptron (MLP) architecture utilizing the Levenberg-Marquardt (LM) optimization algorithm, and sigmoid activation function was selected for the neural network model. The choice

behind the model architecture and training algorithm was driven by the prevalence of the combination in the literature surrounding hydrological neural network modeling. Not only is the combination particularly popular it is also deemed one of the most efficient (Adamowski and Karapataki 2010). Additionally, a trial and error approach was used to evaluate different architectures, activation functions, number of hidden layers, and optimization algorithms. The model had one hidden layer and the dataset was allocated in the following way: 60% training, 25% for testing, and 15% for validation.

Due to the vast amount of data, the techniques outlined in Pitrowski and Napiorkowski (2012) were used to avoid overfitting. After neural network training concluded, the model validation results and simulation were analyzed using root mean squared error (RSME), Mean absolute percentage error (MAPE), and Mean absolute deviation (MAD). Once the error quantification process is completed the next step of the methodology would be to use the error results to calibrate the model. Since the ANN model would be used for hazard mitigation, it would be necessary to update the model weights continually, thus, the process above would need to be repeated. It is believed that if utilized the methodologies outlined above in conjunction with ANN modeling would provide a feasible solution for urban karst flooding prediction and mitigation.

Chapter 5: Results and Discussion

The objective of this study was to better understand the influence of Class V Injection Wells on urban karst hydrology. Ultimately, it is expected that the data collected in this research will be used to make sound data-driven policy recommendations and to inform stormwater management practices surrounding Class V Injection Wells in UKA's. Moreover, it is hoped that CoBG, and other officials and planners in a variety of UKAs, will use the data to better evaluate the current hazard mitigation strategies and emergency preparedness procedures in relation to karst flooding to ensure that high-risk areas are accounted for in their planning and zoning ordinances. The revision of flood zones is crucial because flood risk associated with karst flooding is not widely recognized by urban planners, or local, state, and federal governments since they are not often part of surface perennial watercourses and can be dynamic in nature.

The monitoring period for the study started on October 1, 2017 and ended on April 30, 2018. Over this period, more than 31 million data points were collected and twenty storm events were analyzed using the methodologies described in the previous chapter. Overall, valuable insight concerning the hydrology of the New Spring groundwater basin, as well as localized flooding caused by improper siting, design, and maintenance of Class V Injection Wells, was gained because of this research. Through reviewing the collected and compiled data regarding the siting, design, maintenance, and hydraulic functioning of Injection Wells within the CoBG, it suffices to conclude that the current guidelines and BMP's for Class V Injection Wells in the CoBG are not effective at mitigating flood risk for the more probabilistic storm events. Furthermore, as a result

of poor siting criterion, design flaws, lack of pretreatment sediment controls and scheduled maintenance, it is evident that Class V Injection Wells in the CoBG contribute to water quality issues, Injection Well surcharging, and flash flooding during short duration high-intensity events.

Originally, this project sought to develop a distributed physical model to predict groundwater response to precipitation events, but due to time constraints and lack of essential data, the model development was postponed; however, work is being conducted to develop an Artificial Neural Network (ANN) model that would use the data collected in this project to predict groundwater response to precipitation events. It is believed that using an ANN model would be more cost-effective and accurate at forecasting groundwater levels than a physically based model because of the flexibility and ease of the model architecture; therefore, model development could be easily scaled to a variety of environments. For this research, all preliminary model development will be displayed with the qualification that additional monitoring, analysis, and data for model training are necessary to forecast potentiometric surface fluctuations accurately.

New Spring Basin Hydrology

When trying to adequately characterize the behavior of the karst aquifer in any groundwater basin, it is critical to have accurate boundaries established. The most recent delineation of the New Spring groundwater basin was performed in the 1980s by Dr. Nicholas Crawford (1981, 1984, 1987, 1989). The literature suggests that New Spring serves as the drainage area for downtown Bowling Green, but the primary conveyance for the stormwater routed from the downtown area, “Whiskey Run,” has undergone significant modifications since the last recorded dye trace, which successfully showed a

connection between the two systems (Crawford 1989). The original delineation of the New Spring groundwater basin resulted in an area of 1.9 mi^2 (5km^2), which was based on numerous dye traces, and topographic data. Recently, a dye trace performed by Western Kentucky University Center for Human Geo-Environmental Studies (WKU CHNGES) (Kaiser 2017) failed to replicate the finding mentioned above, but successfully connected Limestone Lake to New Spring. After conducting a thorough hydrologic investigation, it is believed that original delineation significantly overestimates the drainage area for New Spring. The reduction in the drainage area is related to the extensive urban drainage modifications that have occurred since 1989. The drainage alterations have routed the majority of the stormwater runoff within the downtown area outside of the basin. Attempts to correct the original delineation to account for the urban development that has occurred over the last thirty years were made, but without sufficient hydrologic investigations and extensive dye tracing, it is impossible to assert any degree of certainty to the newly delineated boundaries; therefore, all calculations and analyses conducted in this study are based on the assumption that the basin boundaries have not significantly deviated from the original delineation.

A holistic approach for interpretation is necessary when trying to understand the overall hydrology of the basin. Figure 5.1 illustrates that there is a significant discrepancy between inflow, outflow, and storage within the basin.As seen in Figure 5.1, it is evident that discharge accounts for a small fraction of the total water budget calculation. From the water budget, it is possible to ascertain that the outflow only accounts for approximately 35.8% of the inflow for the basin; however, it should be noted that the extremely disproportionate inflow and storage values could be attributed to the faulty

basin delineation. Since the area of basin serves as the basis for the methods used to calculate the cumulative precipitation volume, as well as the soil infiltration and storage volumes, it is obvious that an inaccurate delineation would immensely exaggerate the total volumes Another factor that could impact the overall outflow from the basin is that Limestone Lake is acting as a reservoir for the basin.

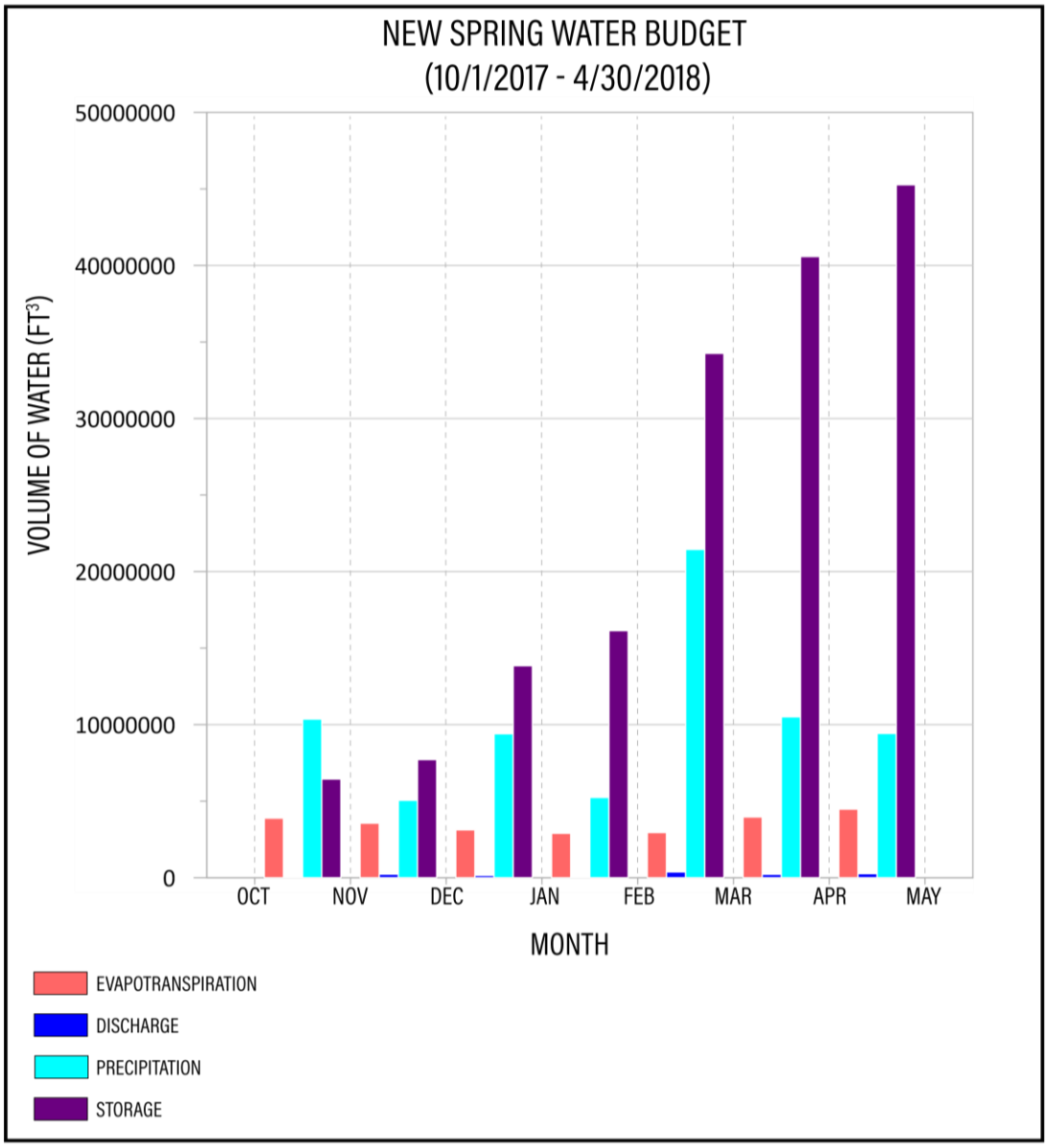

Figure 5.1: Water Budget for the New Spring Groundwater Basin (10/01/2018 – 04/30/2018).

The majority of the stormwater runoff generated within the New Spring Basin during a storm event is first routed to Limestone Lake. In fact, during the most significant storm recorded over the monitoring period on December 22, 2018, Limestone Lake received 14.5% of the cumulative precipitation volume. Additionally, the lake receded to base level after 3.68 days at rate of 0.58 ft/day (0.17 m/day); however, from peak to baseflow, the cumulative discharge of New Spring only accounts for 7.5% of the inflow volume into Limestone Lake. Contrastingly, after 8.47 days New Spring receded to baseflow at a rate of 0.22 ft/day (0.06 m/day). Loss from evapotranspiration is considered to be negligible, because it accounts for less than 1% of the total inflow volume for Limestone Lake. If the basin area is modified to account for the Whiskey Run drainage modification, then the cumulative precipitation volume received by Limestone Lake would increase 5.2 percent; furthermore, the boundary amendment would change the values shown in Figure 5.1, but the magnitude and absolute difference would remain the same. Nevertheless, the area modification cannot reconcile the discrepancy between the amount of water received by Limestone Lake and that discharged by New Spring. It is likely that the water that recedes from Limestone Lake remains in storage within the aquifer. The previous conclusion is asserted, because Limestone Lake is believed to be an expression of the groundwater table. It is also possible that New Spring is not the only outlet for the basin, as it is possible that some springs within the basin have not been identified.

The assumption that Limestone Lake actively recharges the groundwater table is an integral part of the New Spring basin hydrology. The overall groundwater response of the basin is wholly contingent on a set of catchment controls, namely Limestone Lake

and the Barren River. As mentioned earlier, Limestone Lake serves as a temporary reservoir for a significant fraction of the stormwater generated in the basin and, therefore, assists aquifer recharge as well as influencing spring discharge. The Barren River is the ultimate base level control for the basin and, thus, controls outflow and the overall responsiveness of the aquifer. Figure 5.2 shows the hydrologic response of Limestone Lake over the monitoring period. The hydrologic response of the lake mirrors the characteristic behavior of stable karst fed lakes without surface outflow. Over the observed period, the hydrograph displayed little variance. The hydrograph consistently had a gradual rising limb, steady average recession rate of 0.33 ft/day ± 0.04 ft/day (0.10 m/day ± 0.01 m/day), and generally reached peak stage almost a day after the precipitation event. The behavior described above can be attributed to the fact that the lake is isolated within the basin and does not have surface inputs. The majority inflow results from transient springs that are only activated hours after a large storm event. It is possible that the springs carry water from beyond the drainage divide, and as a result, have a slow transfer time. Limestone does receive stormwater from the CoBG's stormwater drainage system, but the inputs for the conveyance only drain a small, localized area.

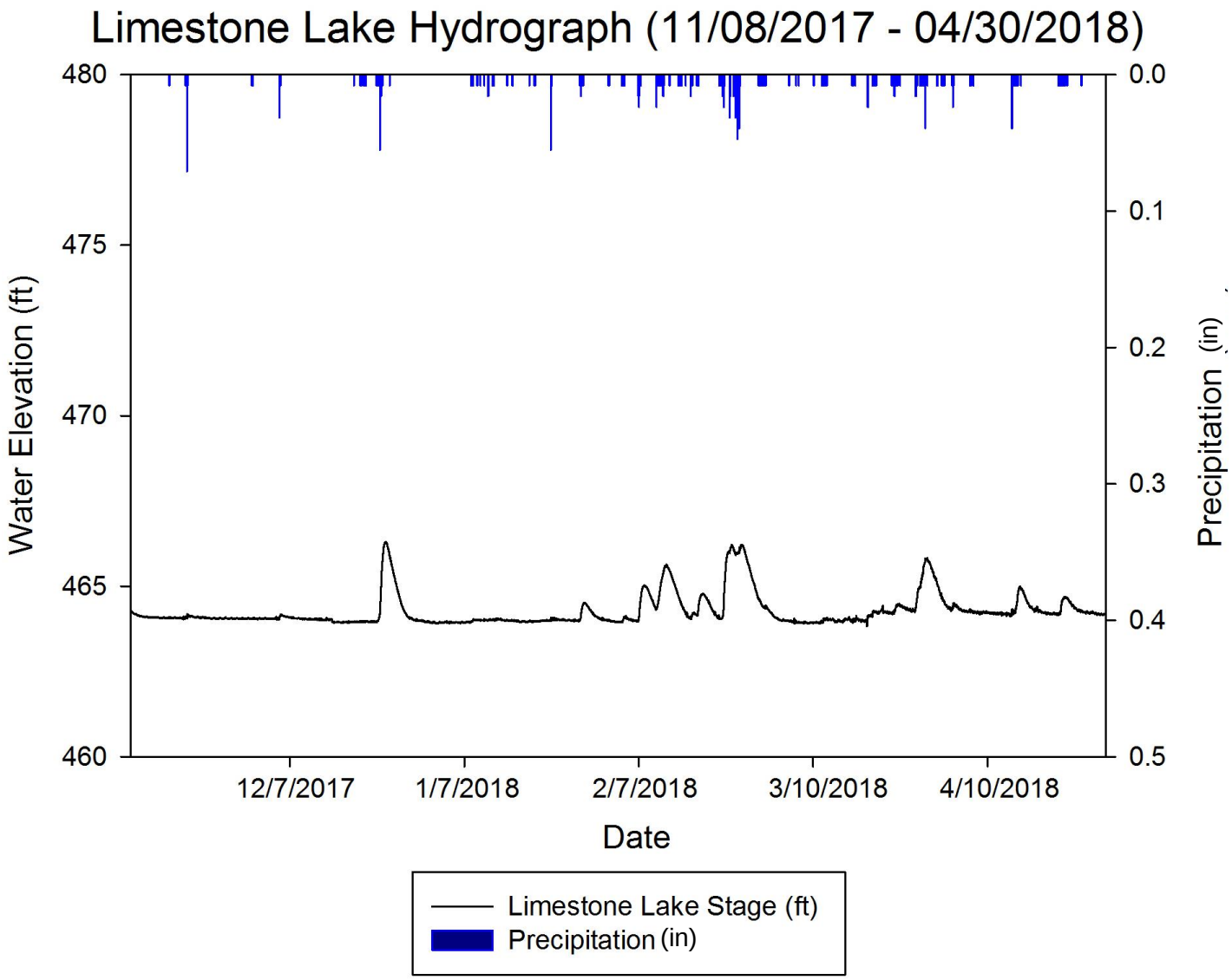

Figure 5.2: Limestone Lake Hydrograph for the Monitoring Period (12/08/2017 – 4/30/2018) (Created by Author).

When the surface water hydrographs are compared against each other, many insightful trends emerge. In general, Figure 5.3, the hydrograph for New Spring, displays a response time that resembles that of the Limestone Lake hydrograph. Contrastingly, New Spring hydrograph reaches peak flow much quicker than Limestone and has a slower recession rate. However, the hydrologic response times and recession rates between the Barren River site and Limestone Lake are similar. The correspondence between the two hydrographs is primarily related to the shared groundwater connection. Evidence supporting the assumption above is shown in the cross-correlation matrix below.

Table 5.1: Cross-Correlation Matrix for New Spring Basin Surface Waterbodies

Cross-Correlation Analysis - New Spring Basin Surface Waterbodies					
		New Spring Water Elevation (ft)	Limestone Lake Water Elevation (ft)	Barren River Water Elevation (ft)	Jennings Creek Water Elevation (ft)
	N	305280	249560	82680	24780
New Spring Water Elevation (ft)	Cross Correlation Coefficient	1	0.828**	0.491**	0.632**
Limestone Lake Water Elevation (ft)	Cross Correlation Coefficient	0.828**	1	0.621**	0.630**
Barren River Water Elevation (ft)	Cross Correlation Coefficient	0.491**	0.621**	1	.0975**
Jennings Creek Water Elevation (ft)	Cross Correlation Coefficient	0.632**	0.632**	0.975**	1
** Correlation is significant at the 0.01 level (2-tailed).					

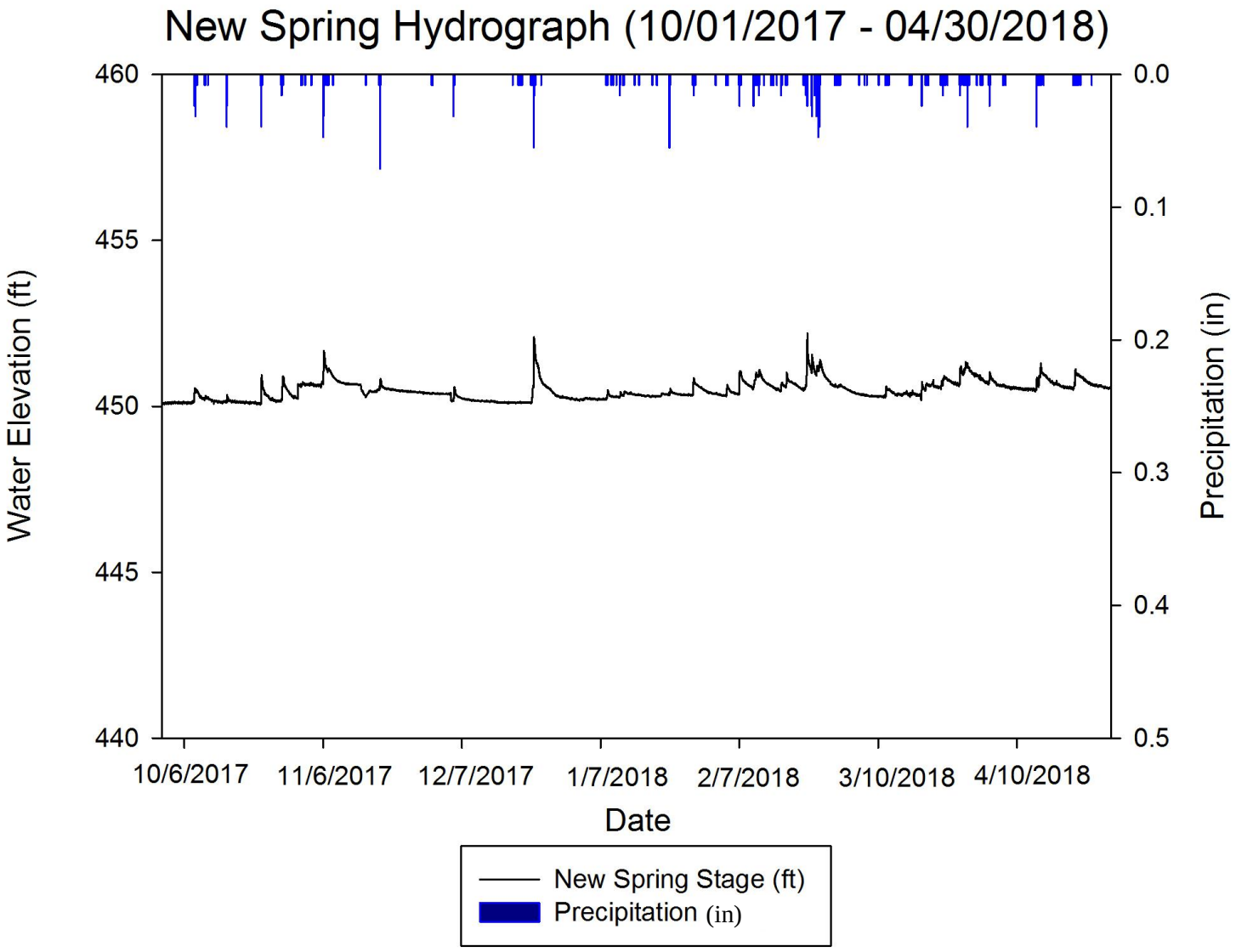

Figure 5.3: New Spring Hydrograph for the Monitoring Period (10/1/2017 – 4/30/2018) (Created by Author).

From Table 5.1, it is possible to gather that there is a statistically significant, moderate-positive relationship between Limestone Lake and the Barren River. It is believed that this relationship would have been shown to be stronger if more data were collected for the Barren River site. Nevertheless, the data bolster the claim of connection. Likewise, it can be drawn from Table 5.1 that most of the variables share a moderate to strong positive relationship, which indicates a shared hydrologic connection, which is a conclusion that has been validated through dye tracing and affirmed again through hydrologic monitoring.

Lags and leads are prevalent in karst hydrology, and it is that delayed response that makes it difficult to come to interpret empirical data. For instance, Limestone Lake leads the Barren River response by approximately six hours, whereas, the Cross-Correlation Function (CCF) for New Spring and Barren is maximized when the hydrologic series is shifted by approximately 15 hours. Aside from examining the correlogram, it is possible to see the lags in the system when Figure 5.2 and 5.3 are compared against Figure 5.4. The stairstep relationship between the variables is more apparent when the hydrographs are configured to storm event resolution (Figure 5.5). The storm event shown in Figure 5.5 occurred on April 15, 2018. The low intensity event had a duration of 12 hours and resulted in 1.13 inches (2.87 cm) of precipitation. Additionally, the event was preceded by another low intensity storm that occurred a day prior and generated 0.45 inches (1.14 cm) of rainfall. From the hydrographs shown in Figure 5.5, New Spring reaches peak discharge then enters recession well before the peak stage of Limestone Lake. Unfortunately, the seven-hour lag time between New Spring and Limestone Lake indicates that connection between the two systems does not

contribute significantly to the discharge at the spring. As Limestone Lake enters its recession, the Jennings Creek and Barren River hydrographs initiate their respective rising limbs; however, Jennings leads Barren by approximately 30 minutes. The trends described above are consistent across the monitoring period. Now that total system behavior has been examined, it is possible to evaluate how the Class V Injection Well influence, and respond to, the systematic hydrologic patterns within the groundwater basin.

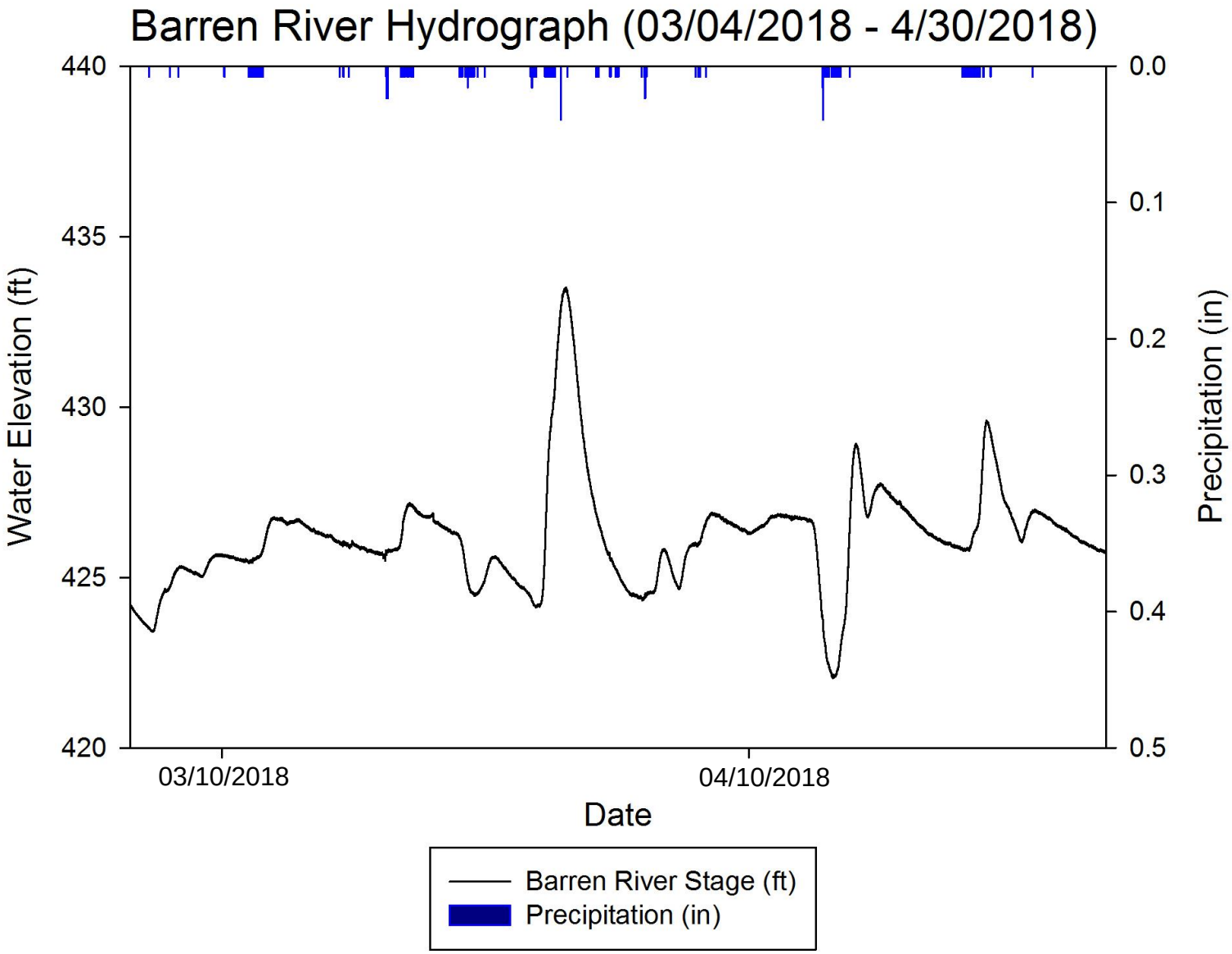

Figure 5.4: Barren River Hydrograph for the Monitoring Period (03/04/2018 – 4/30/2018) (Created by Author).

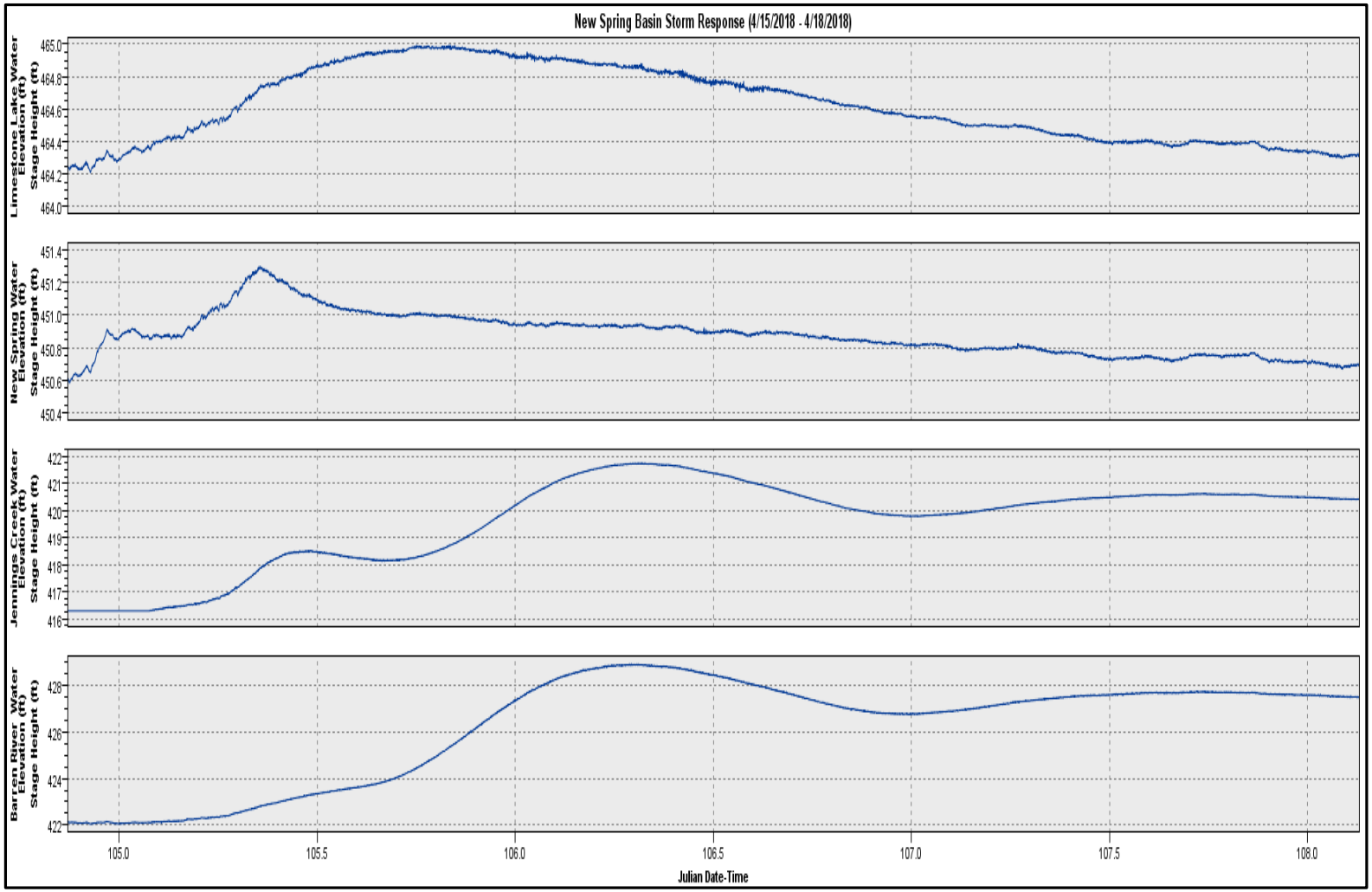

Figure 5.5: New Spring Basin Surface Waterbodies Storm Response (04/15/2018 – 4/18/2018) (Created by Author).

Class V Injection Well Drainage Efficacy

After conducting this study, it is easy to reconcile the idea that it is intuitive that Class V Injection Wells are well suited to function as stormwater controls in UKA's. Despite design flaws and the absence of siting criterion, it seems plausible that initial Wells had an adequate hydraulic performance, as well as a negligible hydrologic impact on the karst system; however, as the City has expanded its urban footprint and haphazardly installed thousands of Wells, there has been a considerable change in flood mitigation efficacy and influence on system behavior. The data and results in this section reflect the current conditions for the Class V Injection Wells in the New Spring groundwater basin, but draw from historical data presented by others (Crawford 1987; Reeder 1989).

Before discussing the results from the hydrograph analysis for the monitored Injection Wells, it is first necessary to address the lack of precipitation variability. The storm events recorded over the monitoring period are not considered extreme in terms of total precipitation or intensity. The most rainfall generated during a single storm event was approximately 2.95 inches (7.49 cm), but the rain was distributed over a 24-hour duration, which diminishes the overall intensity of the storm. Regarding rainfall intensity, the most intense storm measured in at 0.66 in/hour (1.67 cm/hour), but lasted less than an hour, so the potential for rainfall accumulation was reduced. Finally, the highest-ranking storm in terms of intensity and precipitation generation that was documented during the study produced 1.16 inches (2.94 cm) of rain at an intensity of 0.35 inches/hour (0.88 cm/hour). Despite the absence of storm events with chartable return periods, the storms did elicit significant responses in the Injection Wells. Moreover, Injection Well response

is highly variable and wholly dependent on antecedent conditions.

As noted earlier, many of the monitored Injection Wells exceed their grate elevations under low-intensity conditions, which is a result of many different factors. In Figure 5.6, it is shown that 11 of the 30 Wells failed multiple times over the monitoring period.

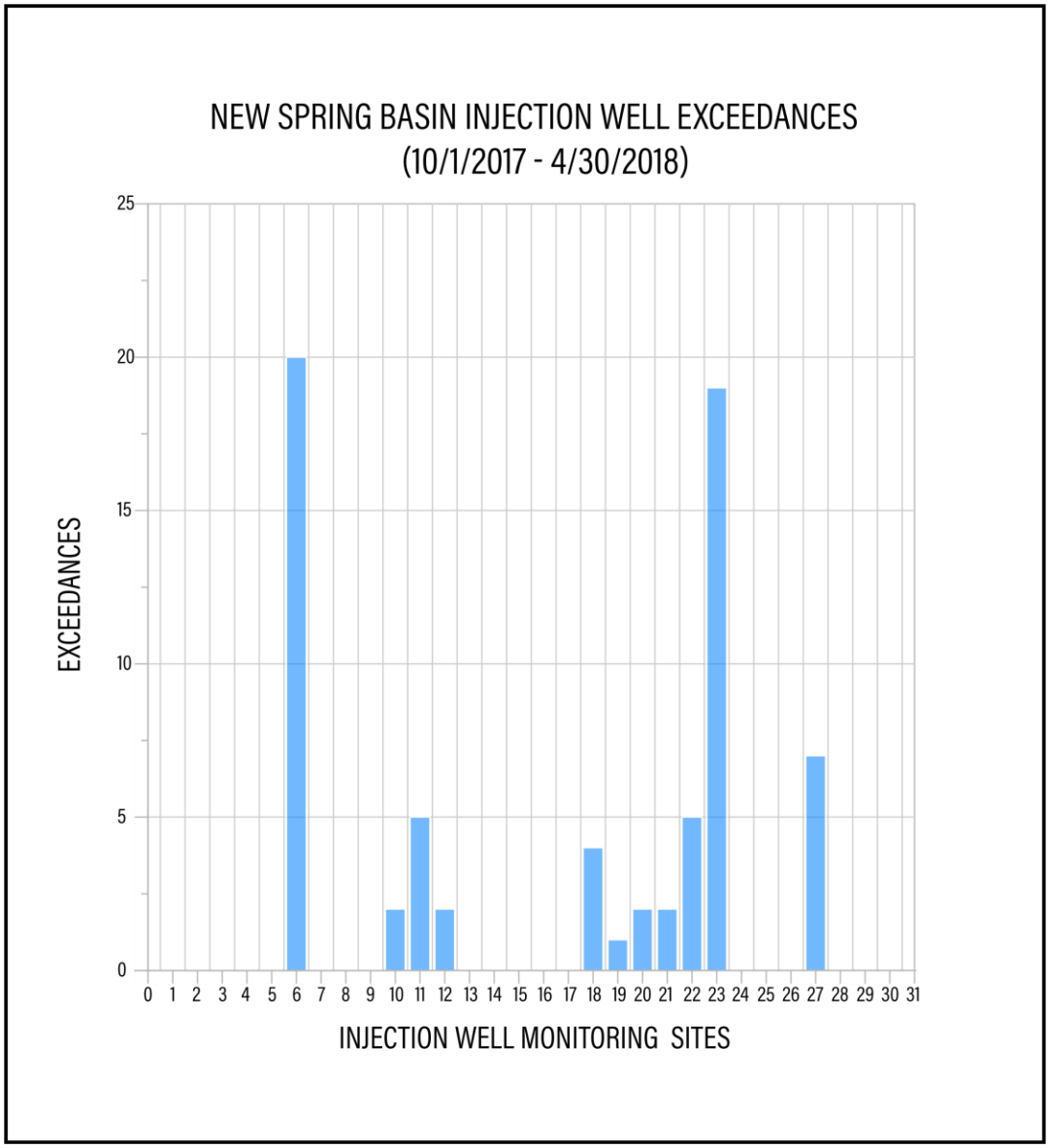

Figure 5.6: New Spring Basin Cumulative Injection Well Exceedances (10/01/2018 – 4/30/2018) (Created by Author).

Given the scope of this research, it is deemed unnecessary to discuss each individual Well in detail, because many of the factors contributing to the success or failure of the Wells overlap. Therefore, three geographically distributed Injection Wells with a high probability of failure were selected for further discussion. Additionally, another subset of Injection Wells that are spatially distributed, perform effective stormwater control, as well as sharing similar hydraulic, design, and siting characteristics with the failure subset, were chosen for analysis. The following Injection Wells were selected for the failure subset: {6, 11, 27}; wells belonging to the success subset are: {5, 26, 29}. To better evaluate the Well's performance, it is best to first understand the underlying patterns and trends within the hydrologic series. Figure 5.7 displays the hydrograph from Injection Well # 6 (IW-6). As Figure 5.6 and 5.7 illustrate, IW-6 exceeded its grate elevation for every storm event analyzed for the monitoring period. The exceedances in Figure 5.7 are primarily a consequence of insufficient borehole storage and rapid infiltration. Most sites include some form of energy dissipation and added soil infiltration prior to routing to the injection feature. In the case of IW-6, rooftop and parking lot runoff are routed directly into the shallow riprap-lined retention basin without sufficient flow reduction.

Hydrograph analyses were performed on all Injection Wells for each storm event. In total, over 600 hydrographs were analyzed. From the Well hydrographs, recession rates were determined. Figure 5.8 displays the recession rate variability for IW-6 and various other Wells within the basin. From the boxplot, it is possible to discern that IW-6 represents a well-drained structure with significant variability. It is believed that IW-6 is connected to a perched system, this is assumed due to the variance in the water temperature. Bonnaci (1987) reports that water temperatures in karst groundwater

typically range from 4.9 °C to 17.8 °C. Bonnaci (1987) also suggests that deviation is possible depending on the location, and proposes a more

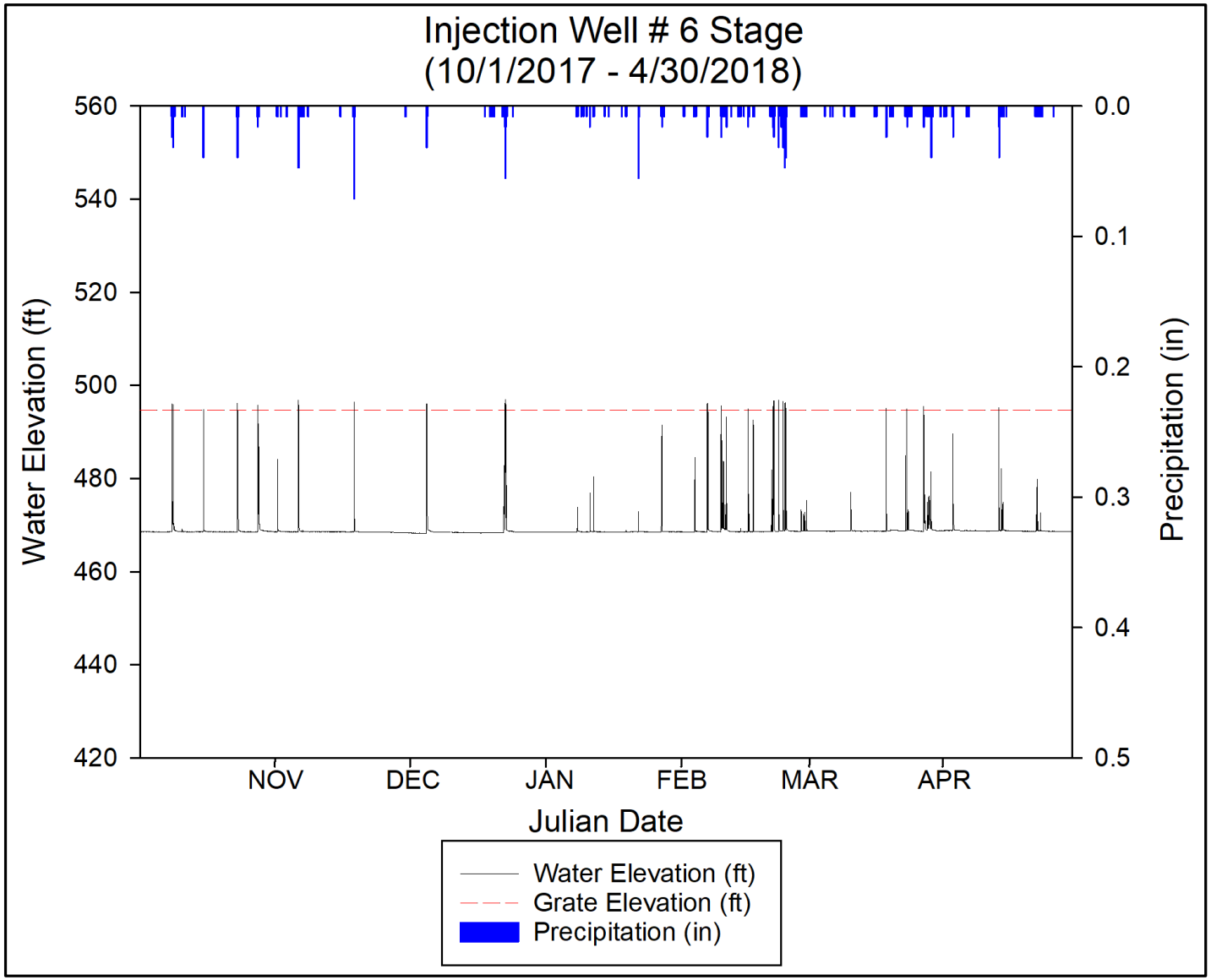

Figure 5.7: Injection Well #6 Hydrograph for the Monitoring Period (10/01/2018 – 4/30/2018) (Created by Author).

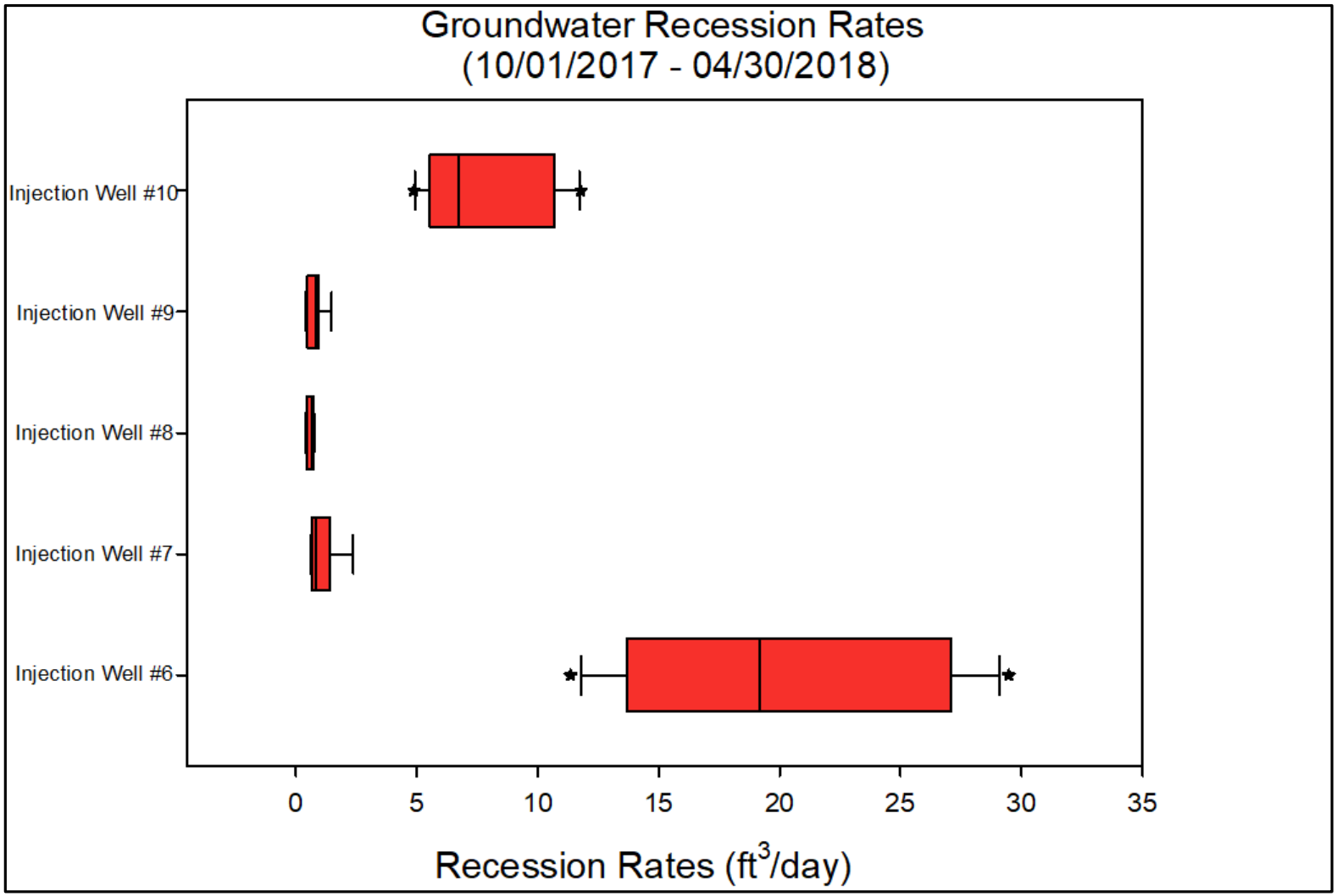

Figure 5.8: Groundwater Recession Rates for Injection Wells 6-10 (10/01/2018 – 4/30/2018) (Created by Author).

conservative range of 4 °C to 20 °C. For this study, a range of 14 °C to 17 °C was determined as the representative range for the regional groundwater temperatures. The temperature range was determined based off a five-year average of real-time, 10-minute resolution water temperature data for known groundwater control in the region. The comparative site, the Lost River Blue Hole, is displayed as a boxplot on Figure 5.9, alongside the water temperature data for IW-6. The temperature variance for IW-6 in Figure 5.9 supports the notion that IW-6 is not directly connected to the water table. Additional reasoning for this assumption can be drawn from the fact that the Well is not shallow, thus, it is not affected by diurnal surface temperature fluctuations. In addition, thermal fluctuations in karst groundwater temperature typically have small amplitudes, often within 1 to 2 °C (Bonnaci 1987).

The shape of the hydrograph shown in Figure 5.7 is indicative of an underdeveloped karst system (Shevenell 1999). Since the hydrograph recession does not contain line segments of varying slopes, it is very likely that IW-6 is dominated by a singular flow regime. Building off the assumption laid out above, it makes sense that the well empties into a perched aquifer, and does not intersect any bedding planes, fractures, or sufficient voids that would allow the Well to drain laterally. The flashy hydraulic behavior of IW-6 indicates that the drainage capacity of the borehole exceeds that of the accepting structure. Water builds up within the borehole until sufficient head is achieved and then the hydrograph can recess at a rate equal to that of the buildup of the rising limb because the water is forced through the opening. Moreover, the well does not have an effective recession rate until an adequate stage has been achieved, which completely diminishes the free borehole volume causing flooding. The hydraulic control mentioned above is one

of the primary reasons that IW-6 is unsuccessful; if the Well had more borehole volume, it would not fail as often. It would also be beneficial if the routed to the structure experienced some detention or additional forms of energy dissipation before entering the basin.

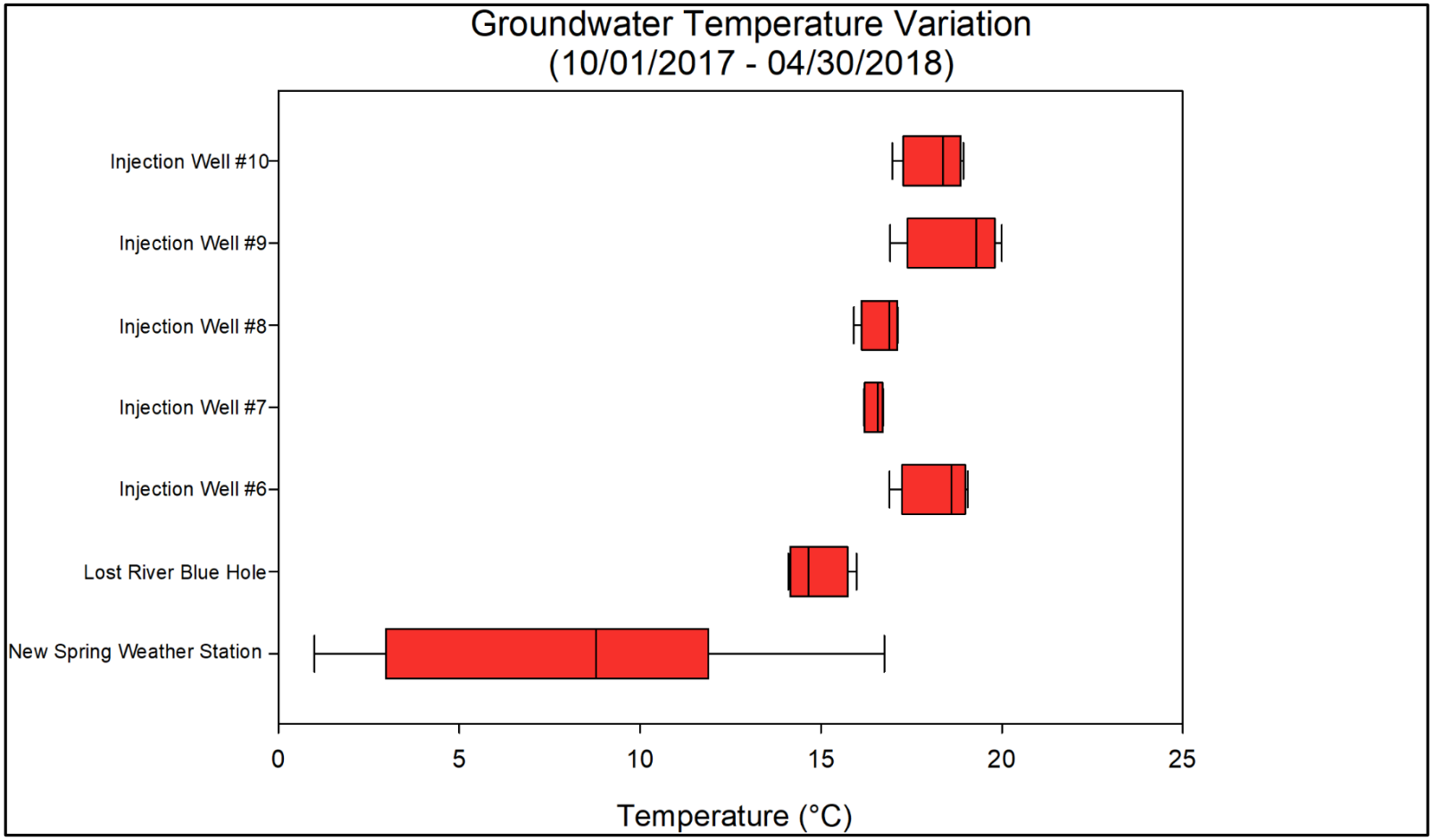

Figure 5.9: Groundwater Temperature Variation for Injection Wells 6-10 (10/01/2018 – 4/30/2018) (Created by Author).

Not all Injection Well failures are the result of poor siting; in fact, the obstruction of the borehole and intersecting karst drainage features with sediment and debris is one of the primary causes of Injection Well failure (Crawford and Groves 1984). Injection Well #11 (IW-11) is a prime example of an Injection Well whose capacity may be lessened due to a flow restriction that is the result of inadequate maintenance. The assumption above is not inherently apparent from looking at Figure 5.10. Based on the hydrograph decomposition methods proposed by Shevenell and Powers (2000), it would be easy to assume that the Well displays the drainage of a developed karst system that encompasses multiple flow regimes. The methods mentioned above would force the conclusion that the hydrograph predominantly reflects a system that consists of small fracture drainage; however, when examining Figures 5.10, 5.11, and 5.12 in conjunction with the Well metadata (e.g., original drill depth, base level stage, etc.), it becomes apparent that IW-11 has undergone significant sedimentation.

Blockages are extremely common with Injections Wells, because of a lack of maintenance. When IW-11 was installed in 1997, the original drill depth was recorded at 98 ft (29.87 m); however, preliminary investigations revealed that there is blockage around 25 ft (7.62 m) and the depth to water is rarely greater than 10 ft (3.04 m). Unfortunately, it is impossible to say why the blockage occurred without collecting downhole footage, but it could potentially be the result of excessive sedimentation, debris clogging, or borehole collapse. Nevertheless, the blockage reduces the amount of free borehole volume and the overall recession rate. Due to the obstruction, it is difficult to confirm connectivity to the groundwater table. In this case, suggesting a disconnection based on the temperature variability shown in

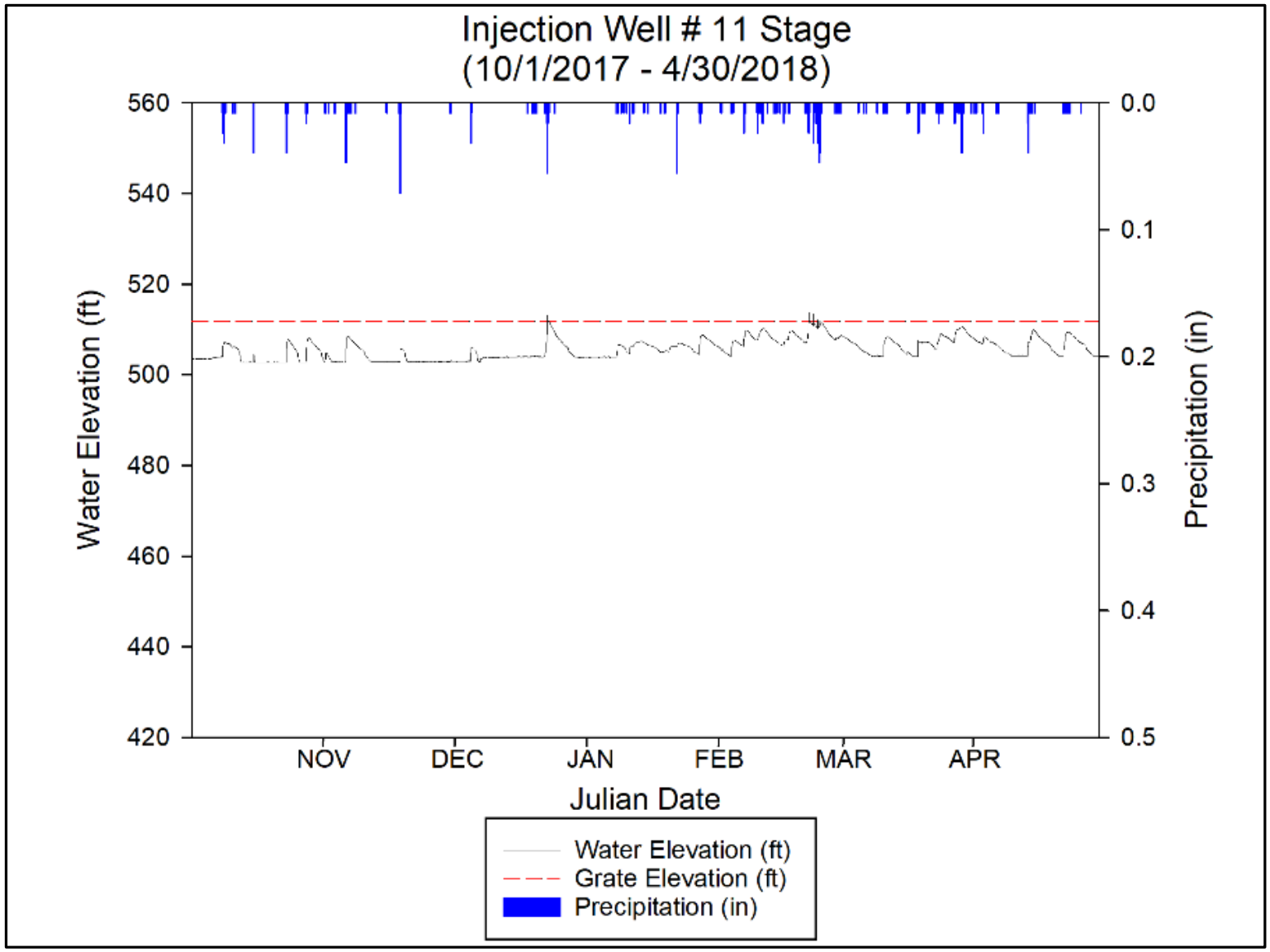

Figure 5.10: Injection Well #11 Hydrograph for the Monitoring Period (10/01/2018 – 4/30/2018) (Created by Author).

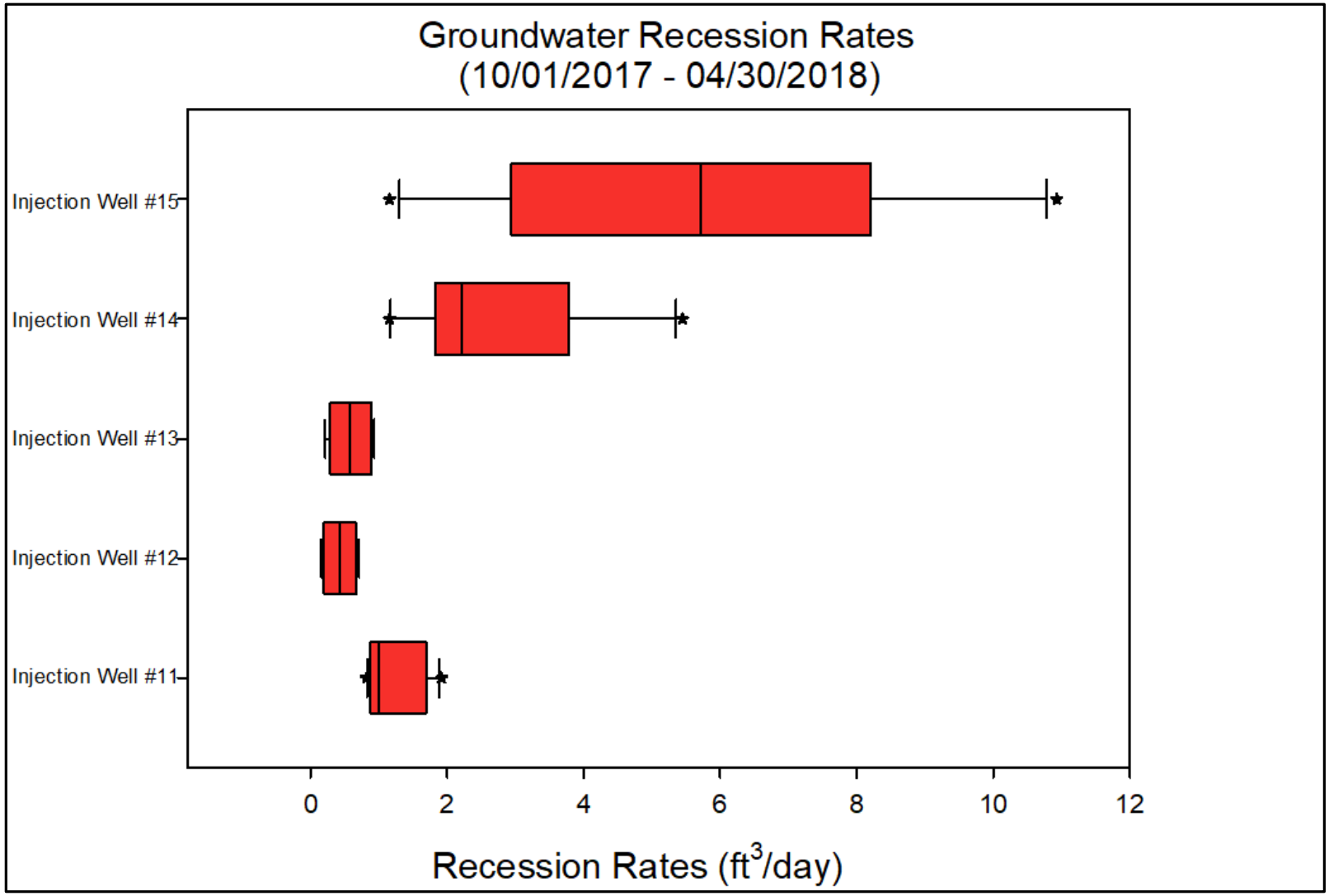

Figure 5.11: Groundwater Recession Rates for Injection Wells 11-15 (10/01/2018 – 4/30/2018) (Created by Author).

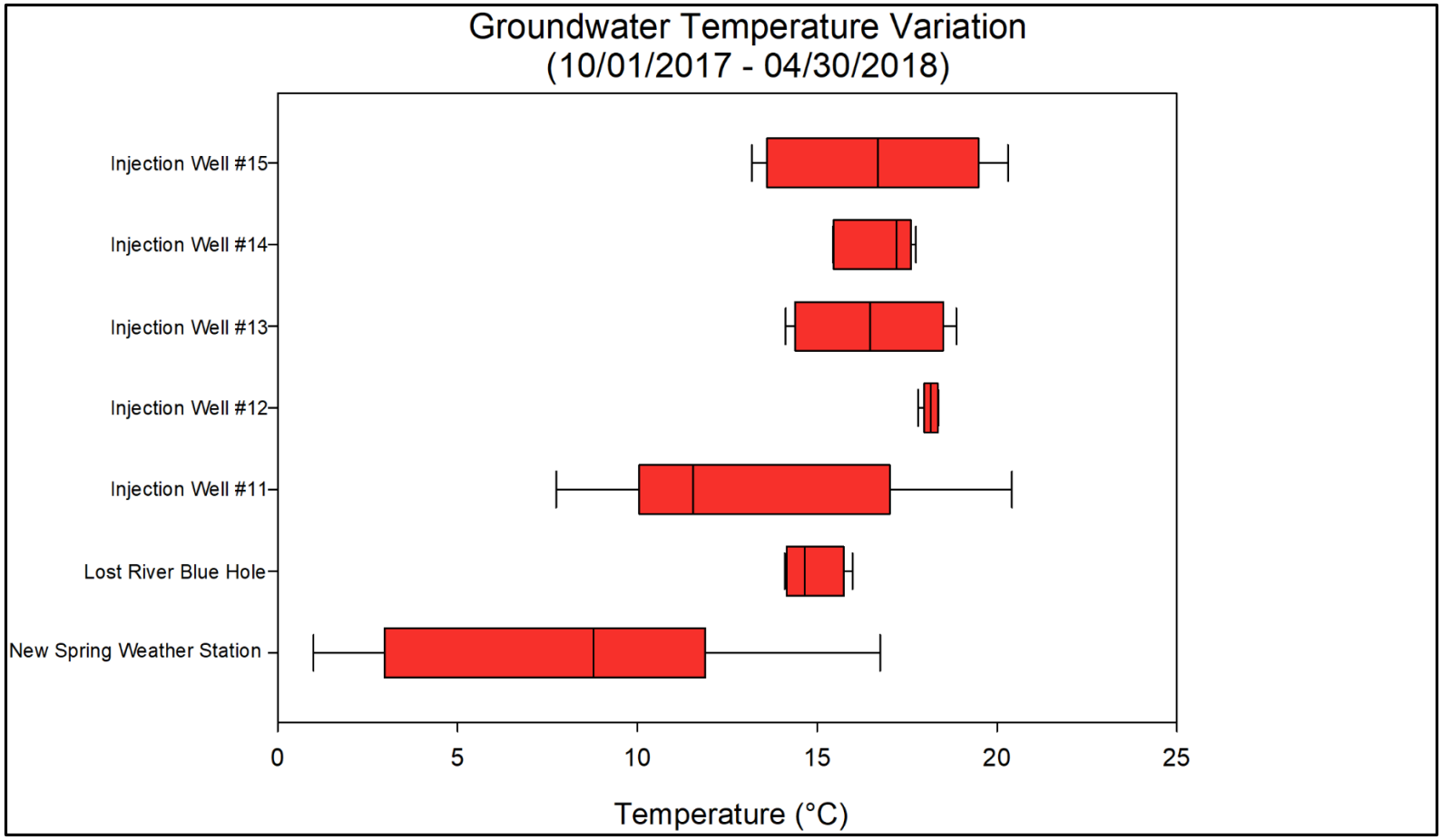

Figure 5.12: Groundwater Temperature Variation for Injection Wells 11-15 (10/01/2018 – 4/30/2018) (Created by Author).

Figure 5.12 would be misleading and faulty, because the blockage causes the water in the borehole to remain perched near the surface vulnerable to diurnal air temperature fluctuations.

The last Well analyzed within the failure subset is Injection Well #27 (IW-27). IW-27 is the only well within the entire failure set that is seemingly connected to the water table. Moreover, the cause of the exceedances experienced by IW-27 is more than likely the result of the underlying karst drainage, rather than poor management practices. The assumption that the Well is connected to the water table is grounded in the same logic used above. It should also be noted that there is a distinct trend in Figure 5.13 that is not present in the other hydrographs shown above, meaning that the base water elevation increases over time. It likely this upward trend is a function of the seasonal fluctuations of the groundwater table, but more data are needed to confirm this assumption. Supporting the belief that IW-27 is a water table well is the fact that average groundwater temperature within the well is in the expected range and experienced little deviation throughout the monitoring period (Figure 5.15). As shown in Figure 5.13, the shape of hydrograph has multiple line segments with varying slopes, which is indicative of a well-developed karst drainage system (Shevenell 1997; Kovacs and Sauter 2007). Additionally, IW-27 has an effective recession rate (Figure 5.14) and almost always has sufficient free borehole storage to accommodate any size storm event.

IW-27 exemplifies the characteristics of an effective Injection Well; thus, it is important to reiterate that exceedances that occurred with IW-27 are more than likely the result of a competition for capacity. Since IW-27 is not obstructed or shallow, and has a direct connection to the water table, it is likely that its drainage capacity is significantly

reduced, due other sources feeding the system to which IW-27 is connected. The reasoning behind the postulation above is related to the variability in IW-27's recession rate.

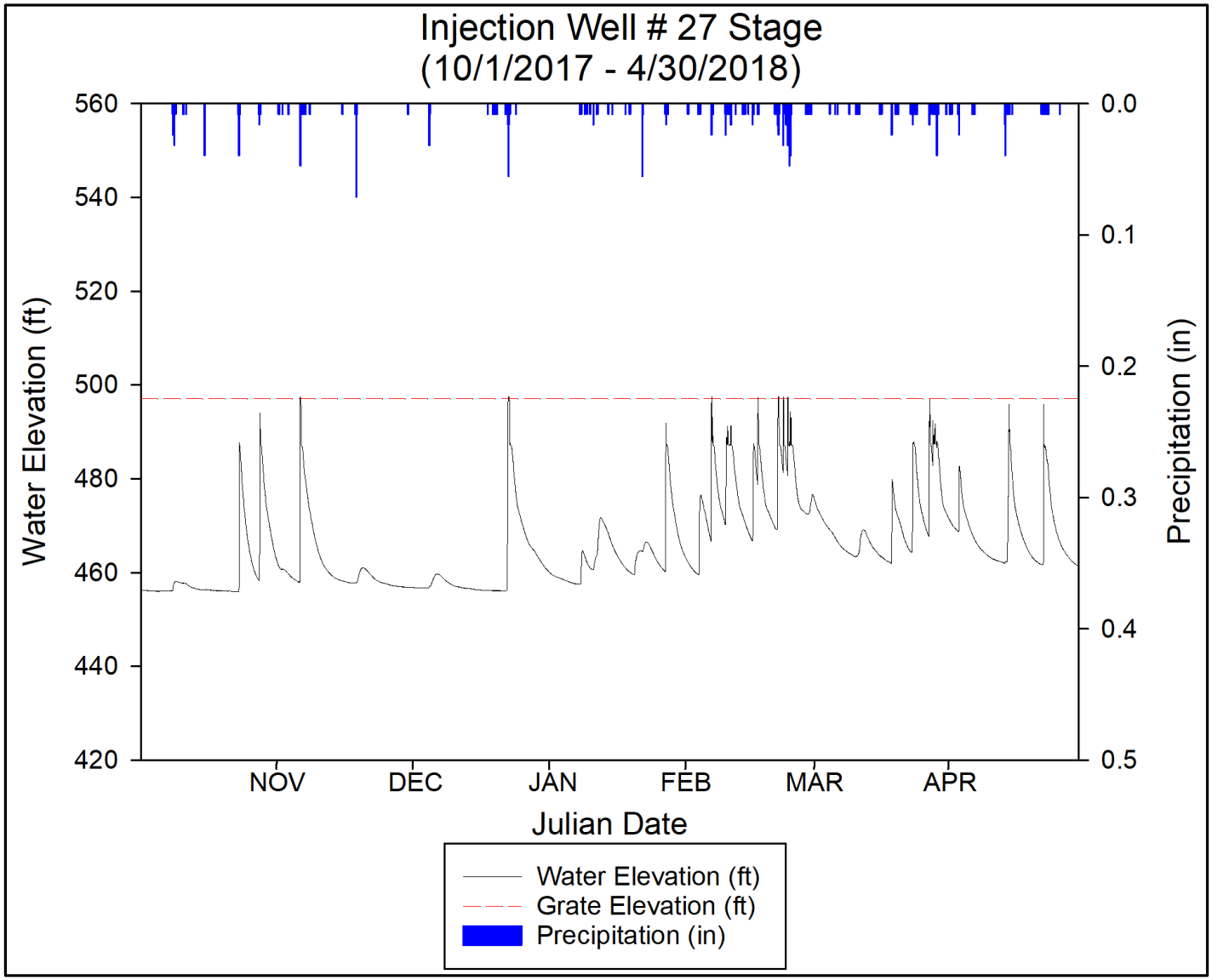

Figure 5.13: Injection Well #27 Hydrograph for the Monitoring Period (10/01/2017 – 4/30/2018) (Created by Author).

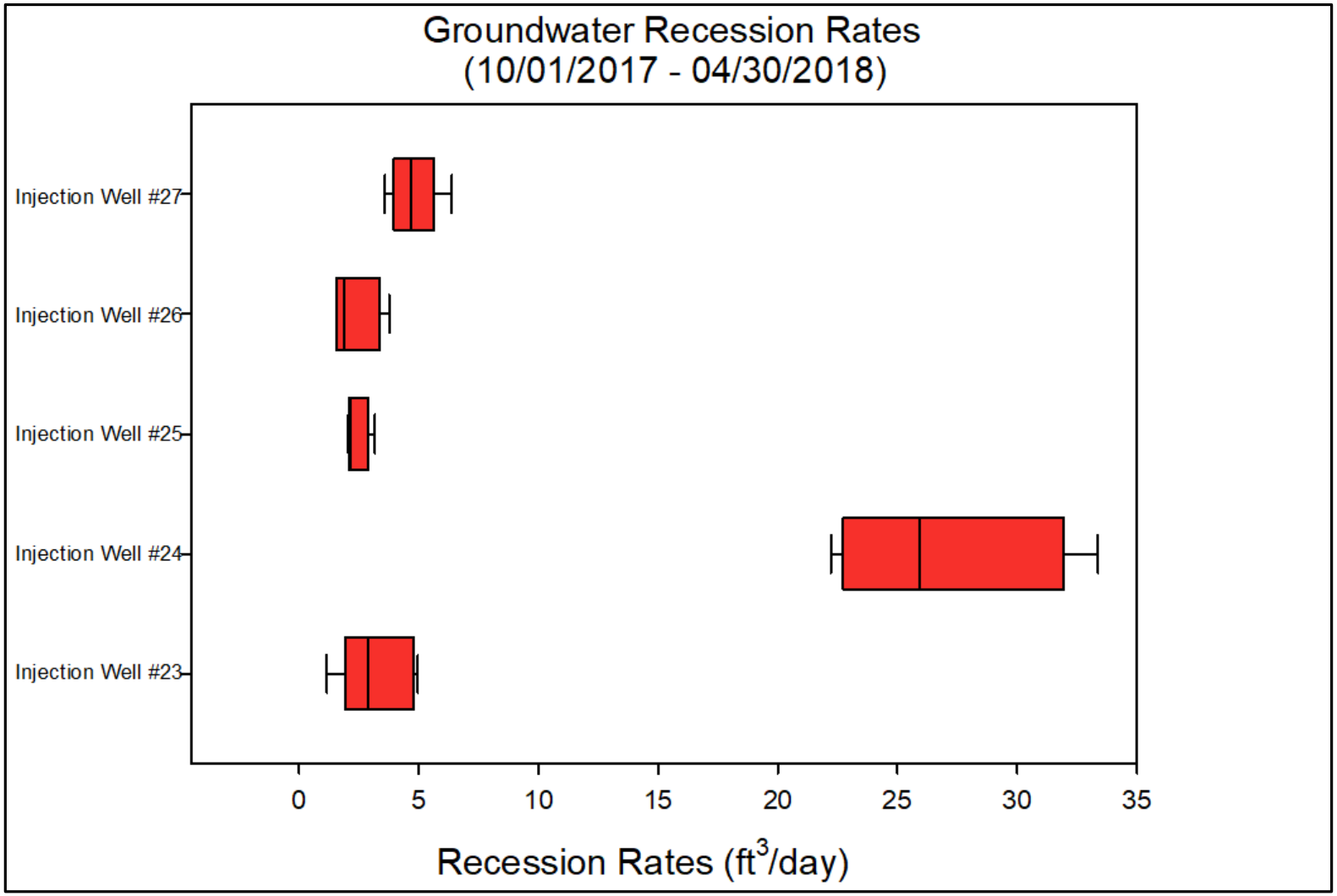

Figure 5.14: Groundwater Recession Rates for Injection Wells 23-27 (10/01/2017 – 4/30/2018) (Created by Author).

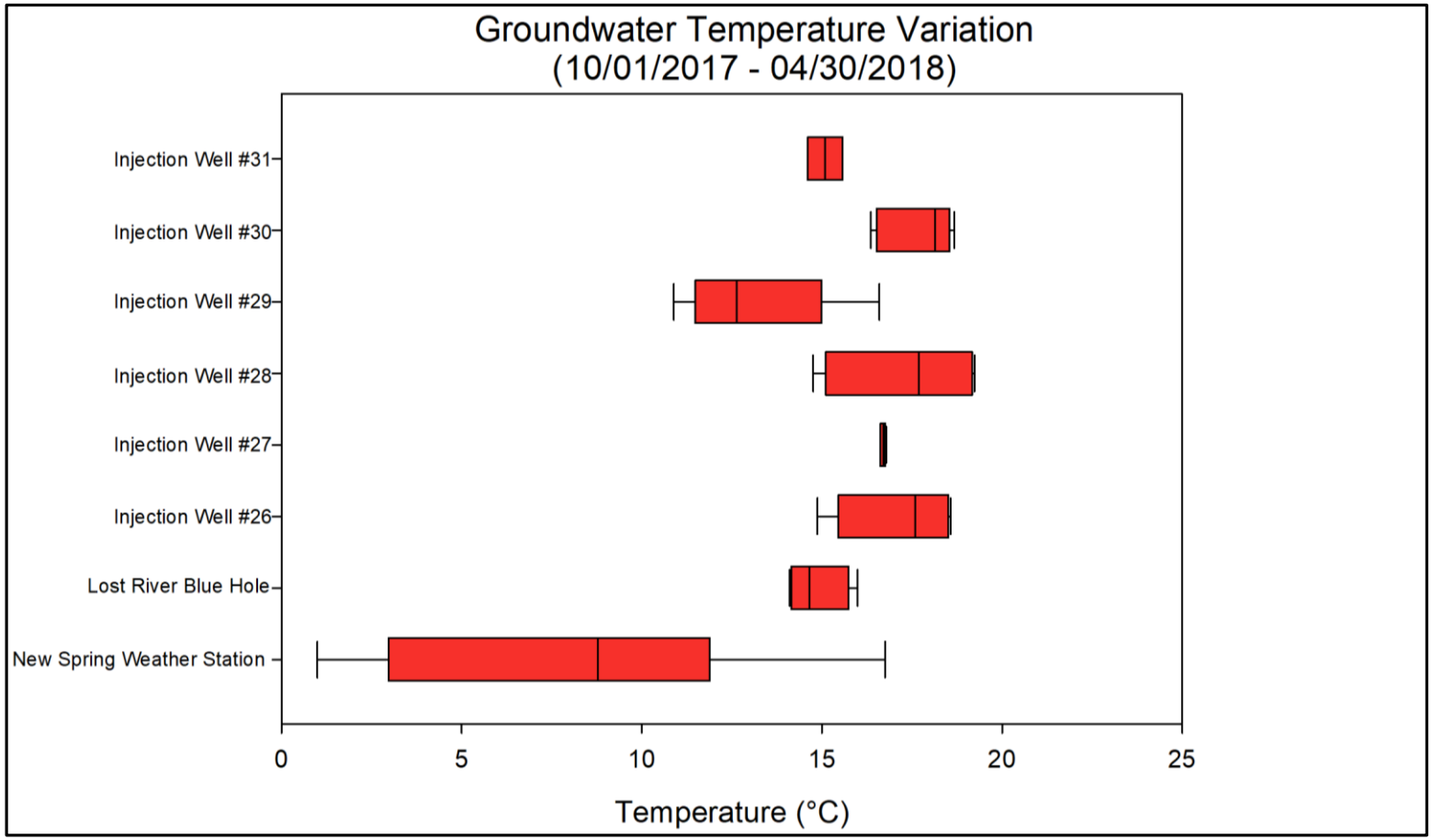

Figure 5.15: Groundwater Temperature Variation for Injection Wells 11-15 (10/01/2017 – 4/30/2018) (Created by Author).

On average, IW-27's recession rate is approximately 4.77 ft/day ± 1.02 ft/day (1.45 m/day ± 0.31 m/day); however, under smaller events preceded by unsaturated antecedent conditions, the Well's recession rate can increase as much as 212 percent. The drastic increase up to 10 percentage points might be attributed to the lack of competition from upgradient Wells. Moreover, when the primary stage increase within the borehole is caused by stormwater runoff, and not inflow from intersecting bedding planes and voids, the Well functions very efficiently. Furthermore, it is imperative to note that the hydrograph analysis reveals that all monitored wells perform significantly better during unsaturated antecedent conditions.

Outlined above were the three primary reasons Class V Injection Wells do not perform as intended and contribute to flooding. Now, it is necessary to examine Wells that are successful under similar conditions to discuss major differences between siting, design, and maintenance. The Wells to be compared against the failure subset are 5, 26, and 29. Following the logic used above, all the Wells within the success subset were determined to be connected to the regional water table, be unobstructed, and exhibit an upward seasonal trend. The graphs and charts used to make this determination are included in the appendices. In addition, from examining the multi-slope shape of the Well hydrographs (Figures 5.16, 5.17, 5.18), it is assumed that all of success subset Wells intersect well-developed karst flow paths.

One of the major differences between the failure and success subsets is drill depth. All the Wells within the failure subset have original drill depths of 100 ft (30.48 m) or greater, whereas, the drill depths for success subset are all less than 100 ft (30.48 m). Crawford and Groves (1984) state that the majority of cavern development occurs at

or above the water table, which implies that drilling below the water table depth would significantly decrease the probability of intersecting an adequate void. Additionally, the limestone near the surface

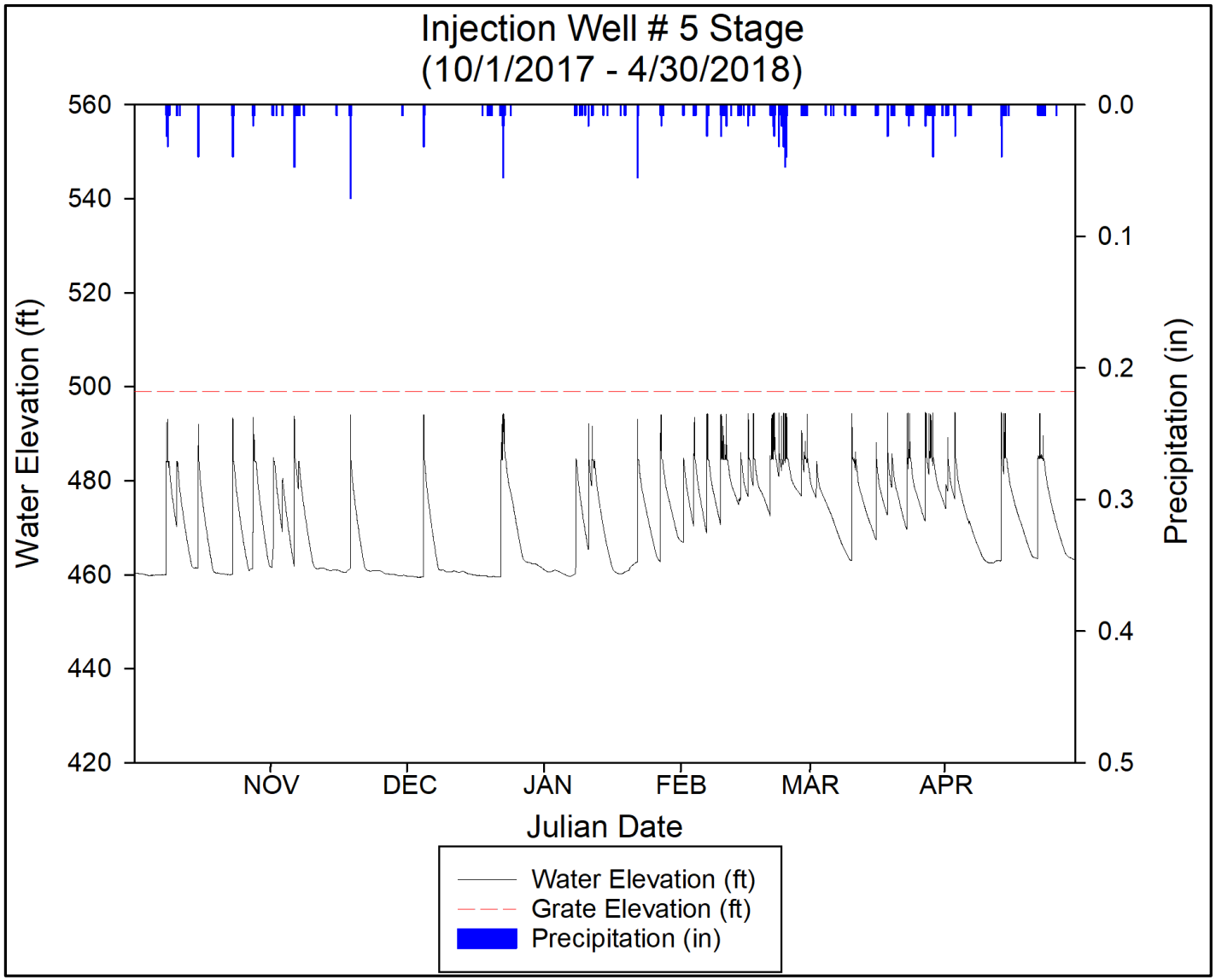

Figure 5.16: Injection Well #5 Hydrograph for the Monitoring Period (10/01/2017 – 4/30/2018) (Created by Author).

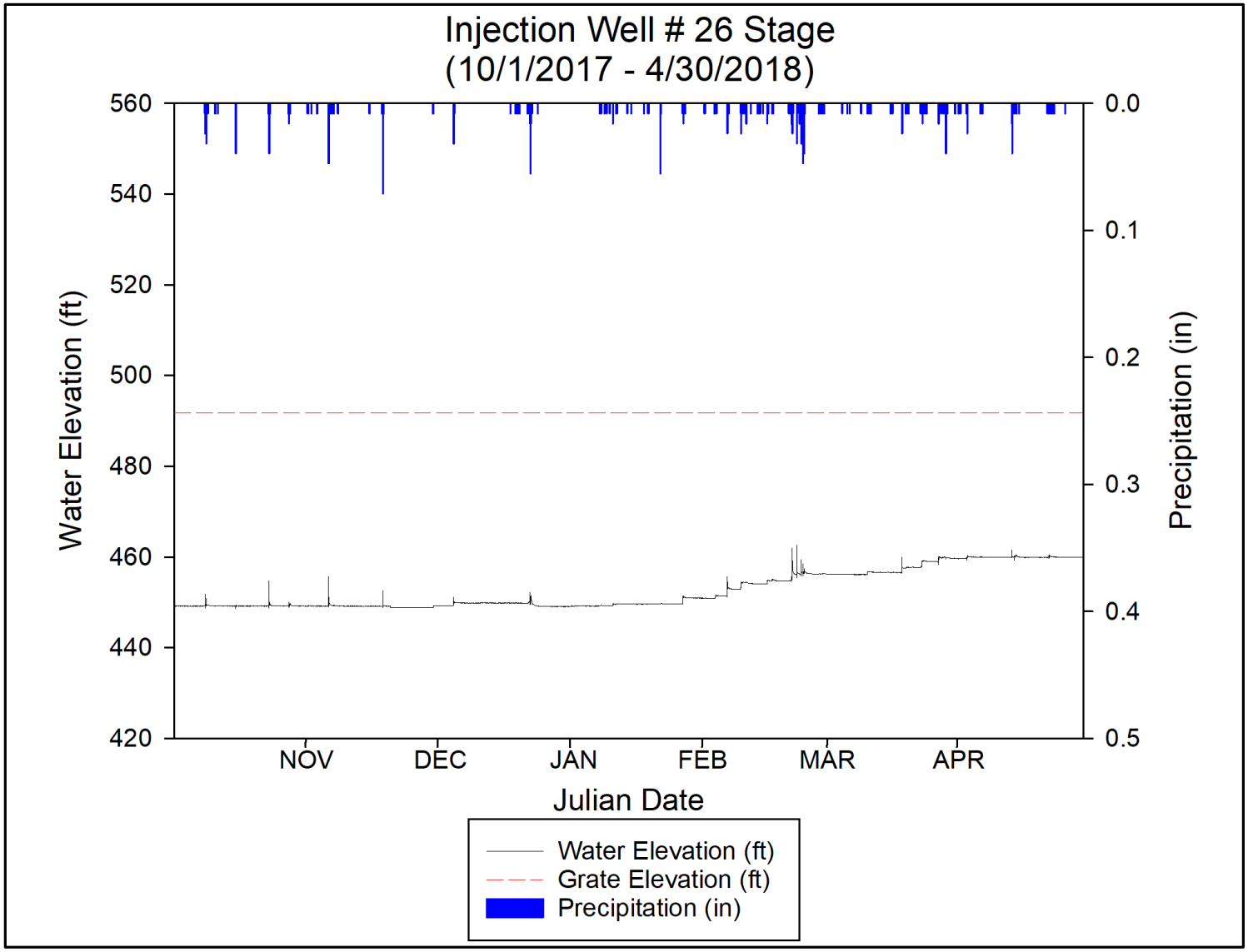

Figure 5.17: Injection Well #26 Hydrograph for the Monitoring Period (10/01/2017 – 4/30/2018) (Created by Author).

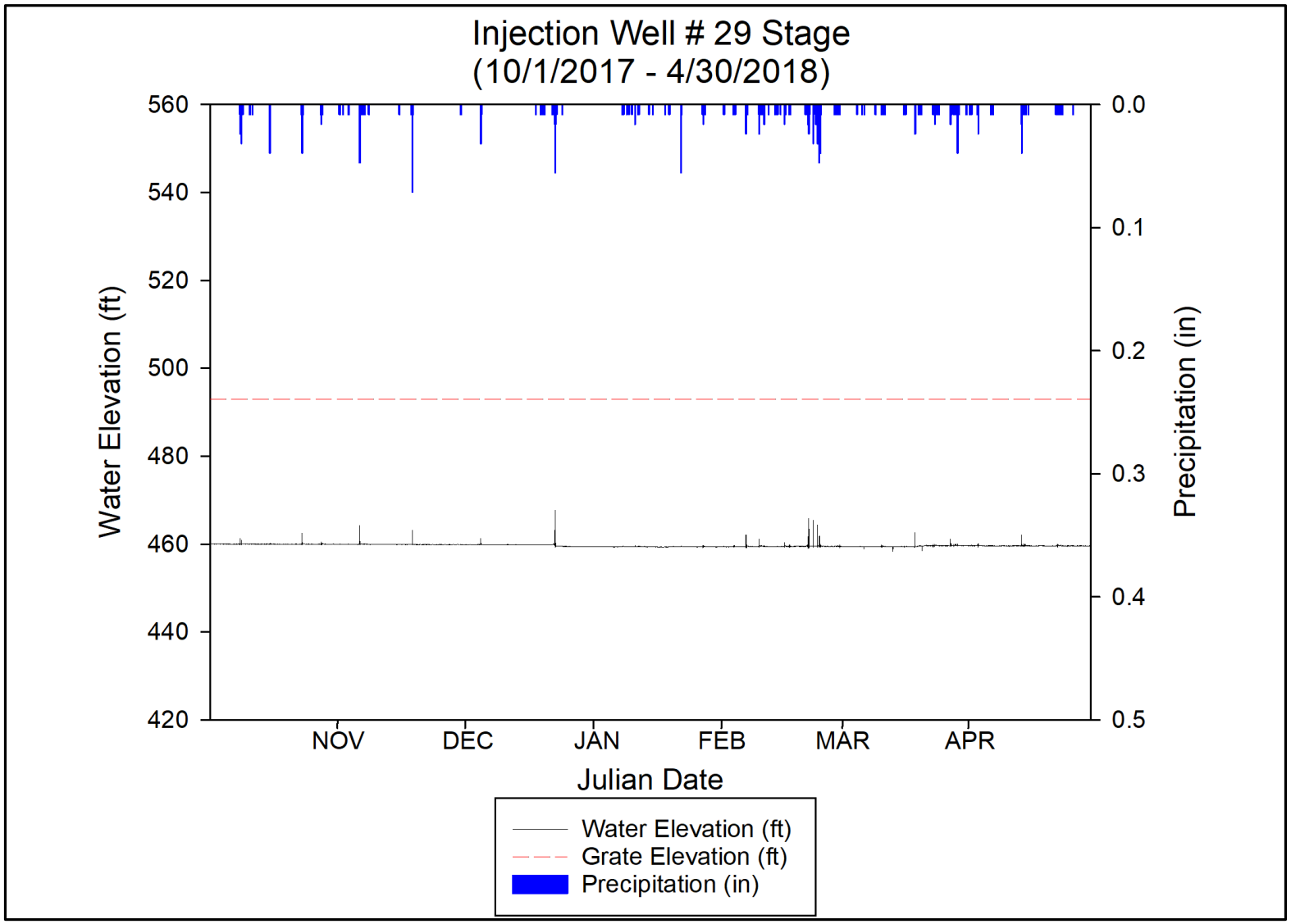

Figure 5.18: Injection Well #29 Hydrograph for the Monitoring Period (10/01/2017 – 4/30/2018) (Created by Author).

typically has more solutionally enlarged joints, bedding planes and fractures due to increased exposure to chemical weathering.

The results of the hydrograph analyses of three highest-ranking storm events in terms of cumulative precipitation and intensity are displayed below for each respective Injection Well. It is likely that the results of the analyses highlight significant differences in the hydraulic performance between the two subsets. Parameters generated in the analysis consist of free borehole volume, inflow volume, peak inflow, and recession rate (Figures 5.19, 5.20, 5.21, and 5.22).

The most deterministic factor for Injection Well drainage efficacy is recession rate. The previous statement is ostensibly intuitive, but it is not a parameter that is taken into consideration in the evaluation of the performance of an Injection Well in the CoBG. The CoBG procedure for testing the drainage capacity of Injection Well is a single slug test at the time of installation. No data are collected during the process; it is solely an observational exercise. The major issue with this procedure is the assumption that the Injection Well's recession rate is uniform under any hydrologic conditions. Unfortunately, varying antecedent conditions can significantly impact an Injection Well's drainage capacity. As an example, prior to the event on 10/05/2017, the basin received 1.37 in (3.5 cm) of rainfall and an additional 1.1 in (2.79 cm) during the event. The system was saturated, which drastically reduced the overall effectiveness of the Injection Wells. The saturated antecedent conditions caused Injection Well #29's (IW-29) average recession rate to decrease by 93 percent. Nevertheless, IW-29 did not exceed its grate elevation during the event. Another factor that contribute to the success of IW-29, as well as the other Injection Wells in the success set is a sufficient amount of free borehole

storage volume before an event; an inflow rate reduction hydrograph analysis reveals

Hydrograph Analysis (Free Borehole Volume)

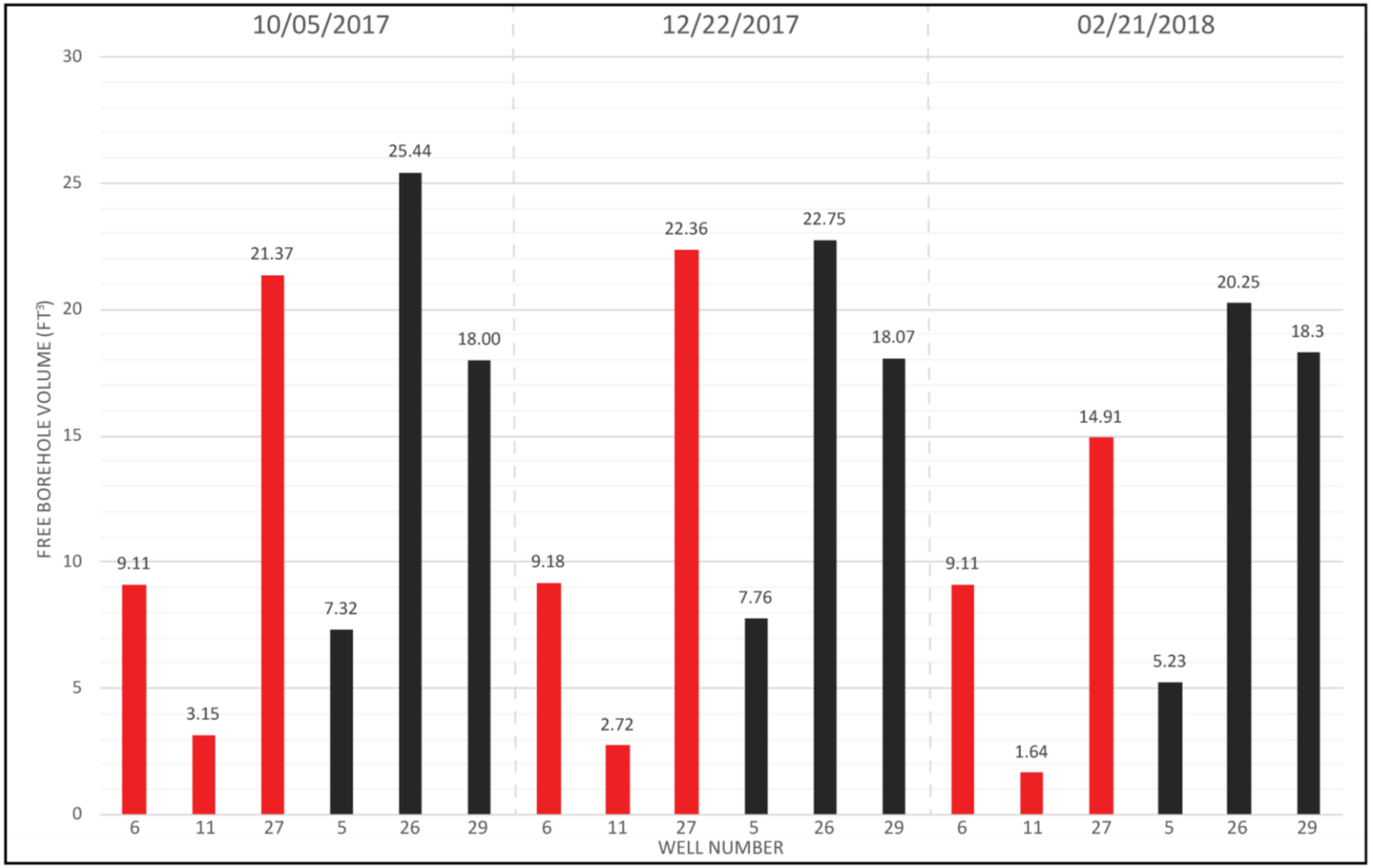

Figure 5.19: Hydrograph Analysis Results for Free Borehole Volume (Created by Author).

Hydrograph Analysis (Inflow Volume)

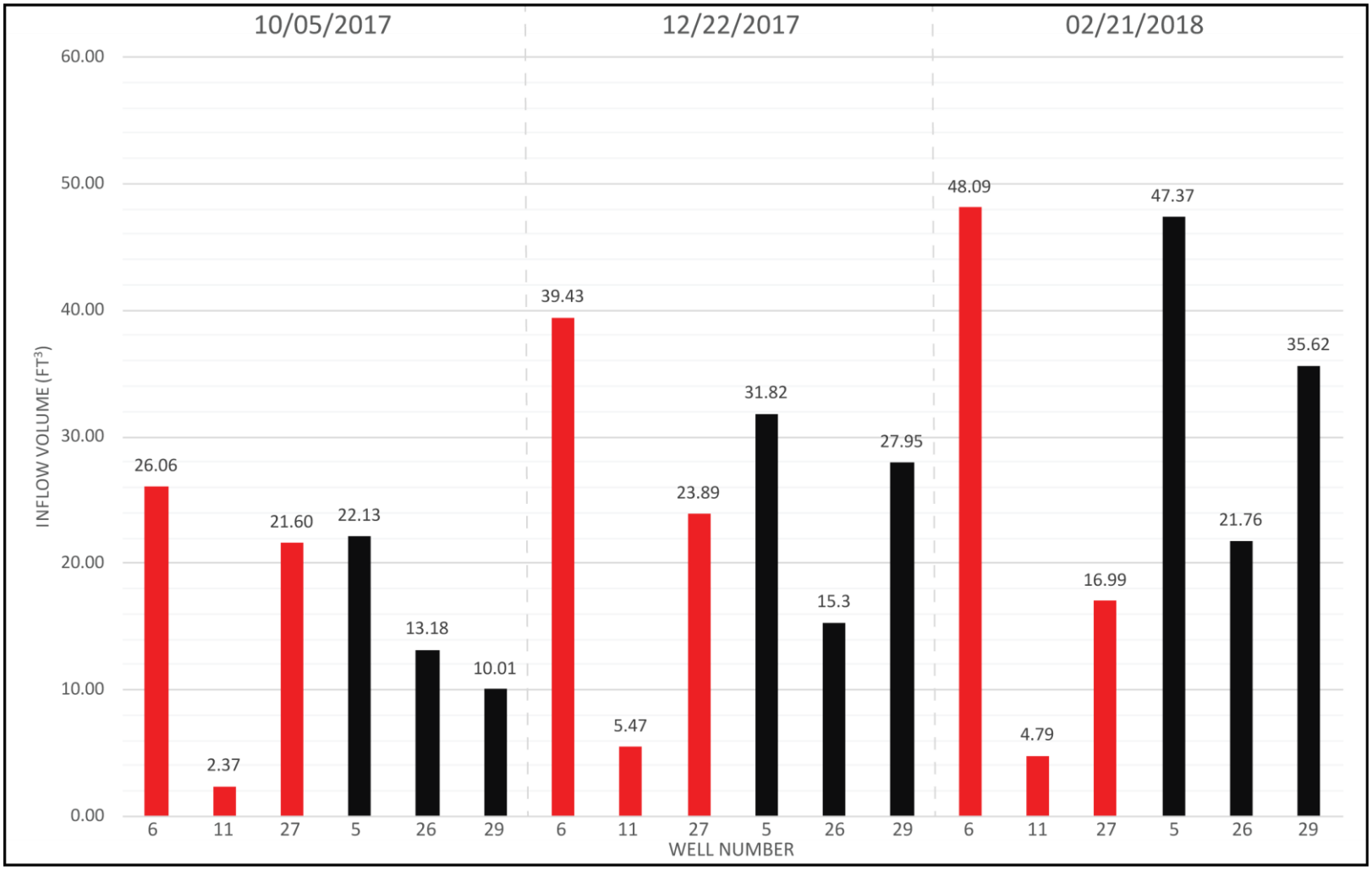

Figure 5.20: Hydrograph Analysis Results for Inflow Volume (Created by Author).

Hydrograph Analysis (Peak Inflow)

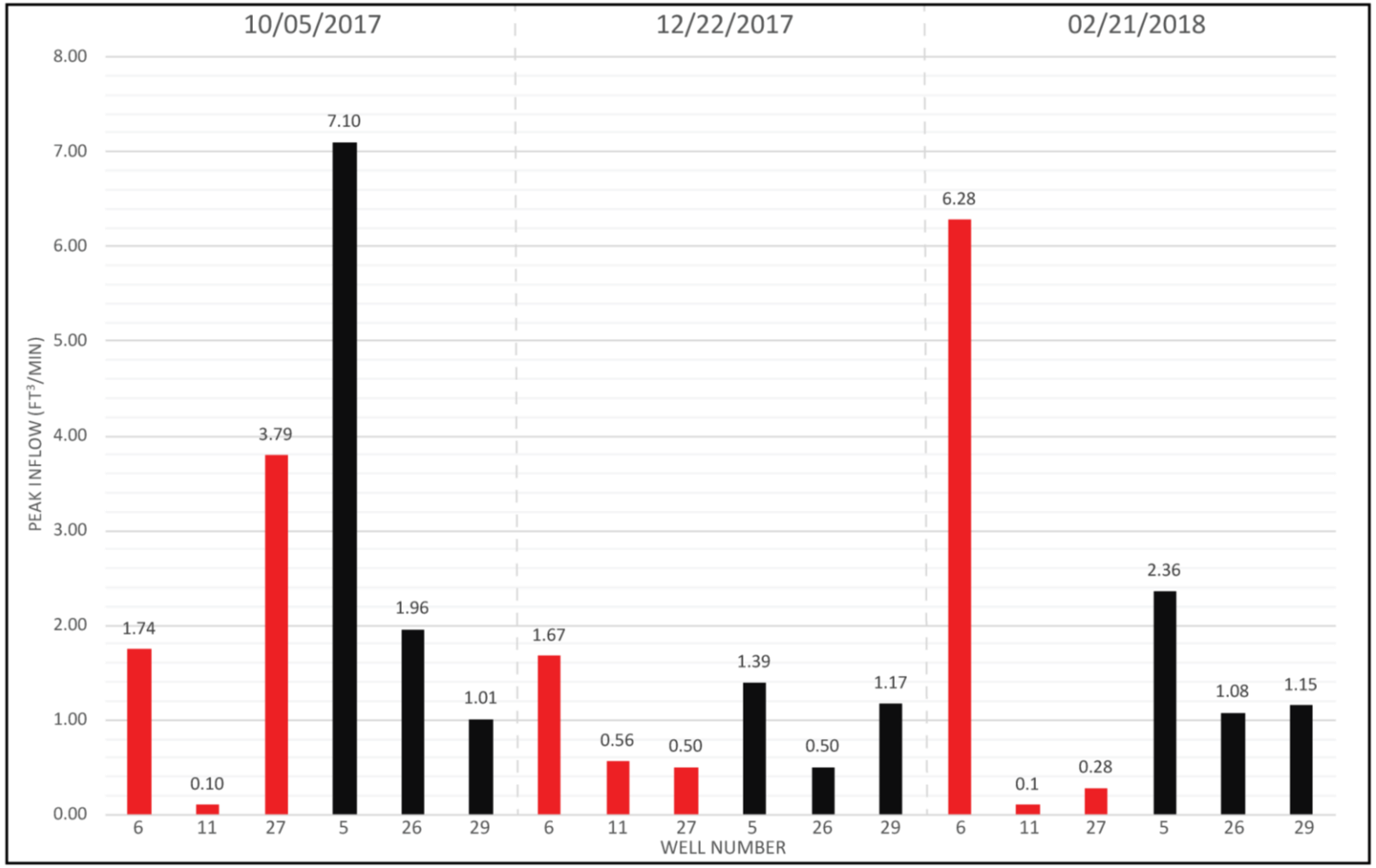

Figure 5.21: Hydrograph Analysis Results for Peak Inflow (Created by Author).

Hydrograph Analysis (Recession Rate)

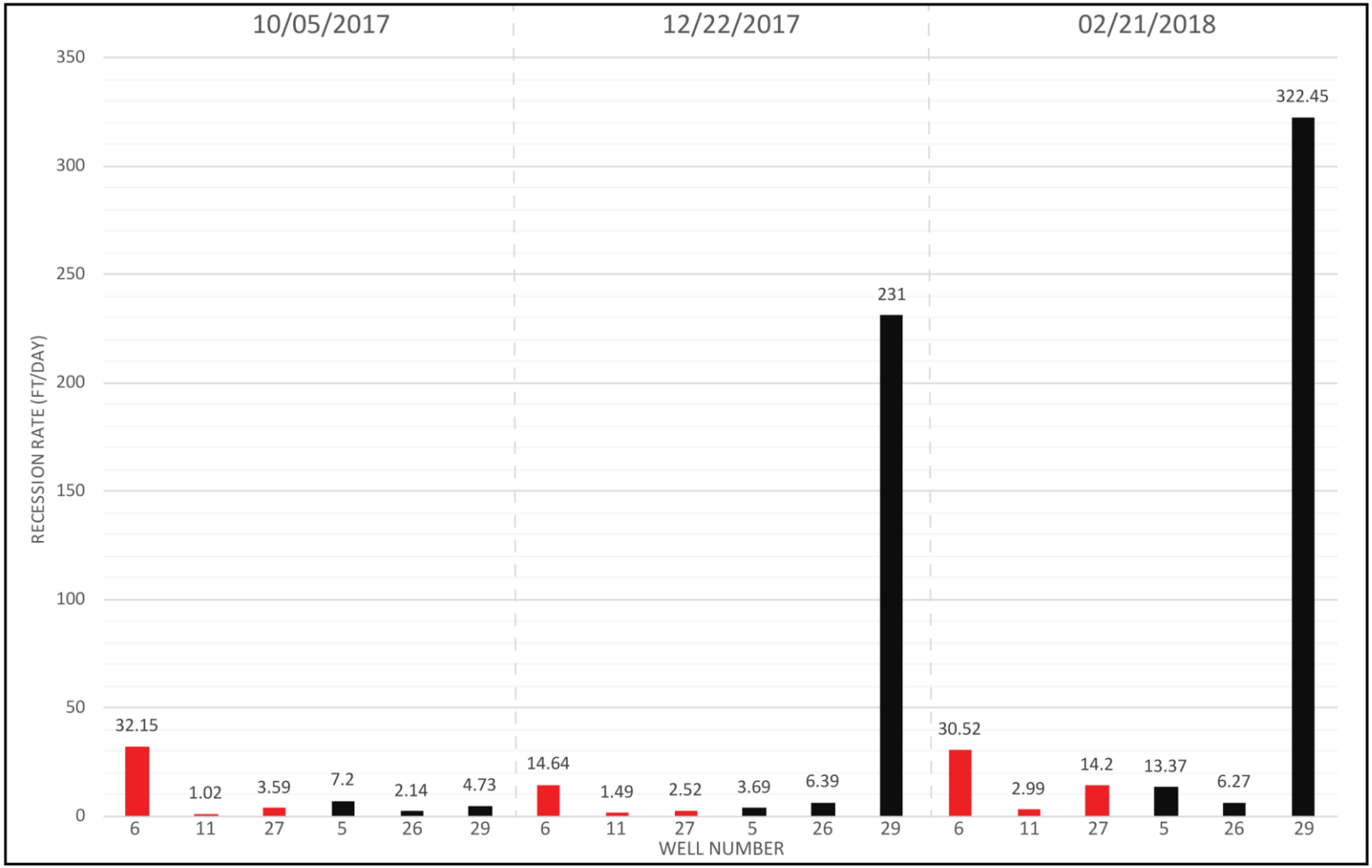

Figure 5.22: Hydrograph Analysis Results for Recession Rate (Created by Author)..

that the total inflow volume is of lesser importance than the peak inflow rate. For instance, the majority of the exceedances that occurred with IW-6 are under peak flow conditions. In a few minutes, the stage within the borehole can increase as much as 30 feet (9.144 m), however, if the inflow rate was slowed through the use of a BMP, it is reasonable to assume that IW-6 would not fail under the most probabilistic conditions. Unfortunately, some of the exceedances may be difficult to prevent without significant hydrogeological investigations.

Hydrologic Interconnectivity

Many of the monitored wells are influenced by the hydraulic connectivity of upgradient Injection Wells. As noted earlier, this is the primary contributor to the failures of IW-27. In the case of IW-27, it is difficult to trace the competing inflow sources, but, with other Wells, it is more noticeable. Figure 5.23 demonstrates the interconnectivity between Wells. In Figure 5.23, a small storm event occurs on 10/15/2017 and causes Injection Well #1 and #3 (IW-1, IW-3), to respond. Three days later, without any precipitation, an abnormal increase occurs in IW-1 hydrograph. The sudden three ft (0.91 m) increase corresponds to the tail end of IW-3's recession. It is not necessary to perform an additional trend test to determine the direction of the trends, because it is evident from the hydrograph. It is important to note this is not an isolated incident, as it occurred multiple times over the monitoring period; however, dye tracing is necessary to confirm a direct connection. The two sites are situated about 0.16 mi (0.25 km) away from each other. The surface elevation for IW-3 is at approximately 597.45 ft (182.10 m), whereas, the elevation for IW-1 is around 502.89 ft (153.28 m), which is a significant elevation drop. Over this period, some minor perturbations occurred in some of the other Injection

Wells, but not anything as substantial as IW-1. The occurrence of interconnectivity is problematic for several reasons. Firstly, interconnectivity diminishes the drainage capacity of the downgradient Well. Depending on the time of concentration between the interconnected Wells, if water backups in the downgradient Well, it could potentially cause surcharging in the upgradient Well. Likewise, if the transfer time is slow, it may cause surcharging in downgradient Wells under stable hydrologic conditions.

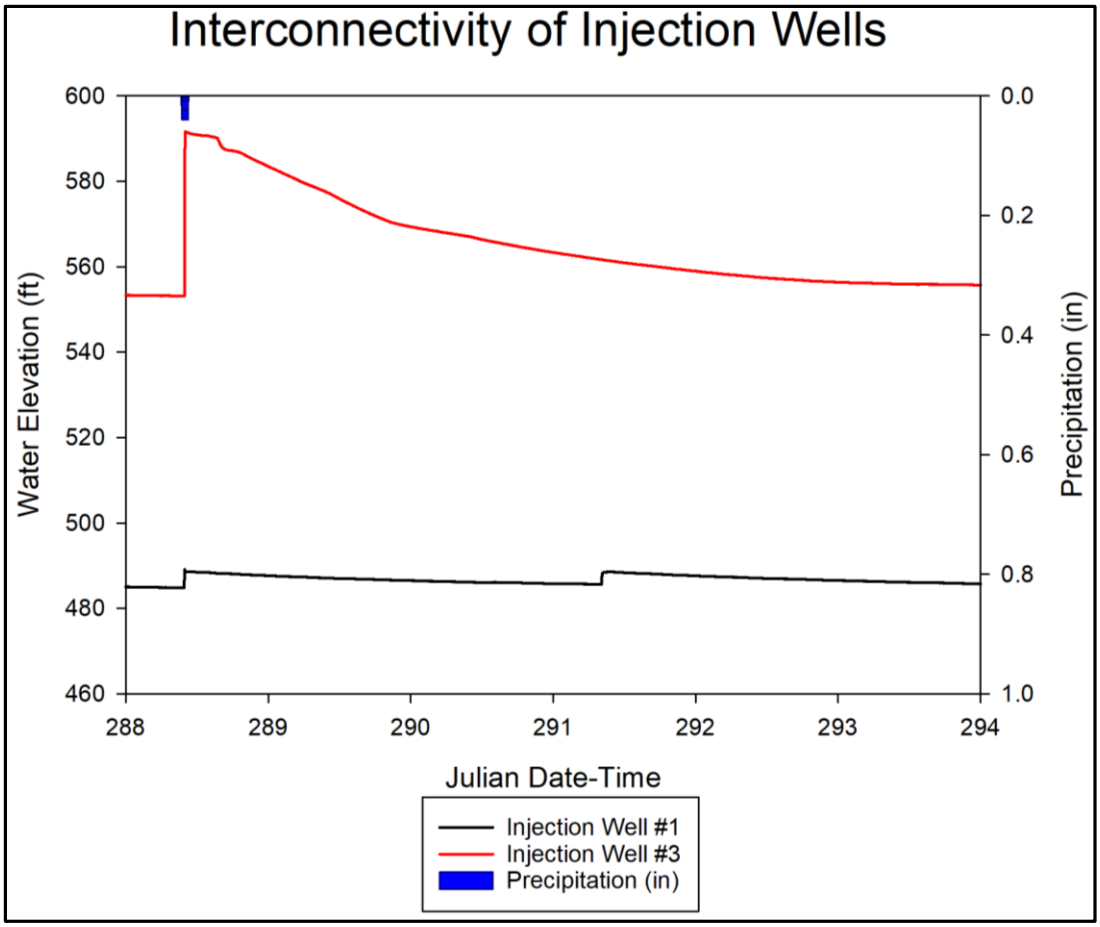

Figure 5.23: Hydrograph Showing the Interconnectivity between Injection Well #1, and #3 (Created by Author).

Class V Injection Well BMP Recommendations

The purpose of this section is to provide recommendations for new BMP's and guidelines for injection well siting, design, and maintenance. Class V Injection Wells can

be a sustainable and effective stormwater management tool in UKA's if proper BMP's are established and followed. From a scientist's perspective, the Injection Wells serve as excellent research sites that allow the researcher to better understand the dynamic nature of karst flow regimes and flooding. This study has revealed that the CoBG cannot continue to develop sustainably, without adapting strategies to combat the siting, design, and maintenance issues discussed in the preceding sections. Moreover, it is believed that the current conditions regarding stormwater infrastructure within the City contribute to water quality issues, well surcharging, and flash flooding during short duration high-intensity events, due to poor siting criterion, lack of pretreatment sediment controls, and lack of maintenance.

Throughout the study, numerous Injection Well siting, maintenance, and design issues were discovered. Unfortunately, the CoBG is now in a reactive position of having over 2,000 Injection Wells within a relatively small area (Figure 5.24); therefore, the primary concern should be formally identifying all public and private Injection Wells within the City, because it is impossible to address an issue if the causal components are not known fully. Figure 5.24 displays the disparity between the number of wells that have been mapped and those in the historical record. As an initial step, the ongoing city-wide Injection Well inventory should continue, as significant progress is being made (Shelley 2017). Out of the 801 mapped Wells, 683 wells have been assessed and necessary inventory information collected. After the completion of the inventory, a multi-basin hydrologic assessment should be conducted to determine Wells that have poor drainage capacities as well as those that contribute to flooding. During this process, obstructed Wells should be cleared then evaluated. Out of the 683 Wells that were ground-truthed,

156 were marked as obstructed. The number was reported to the city and they immediately initiated a maintenance program (Shelley 2017).

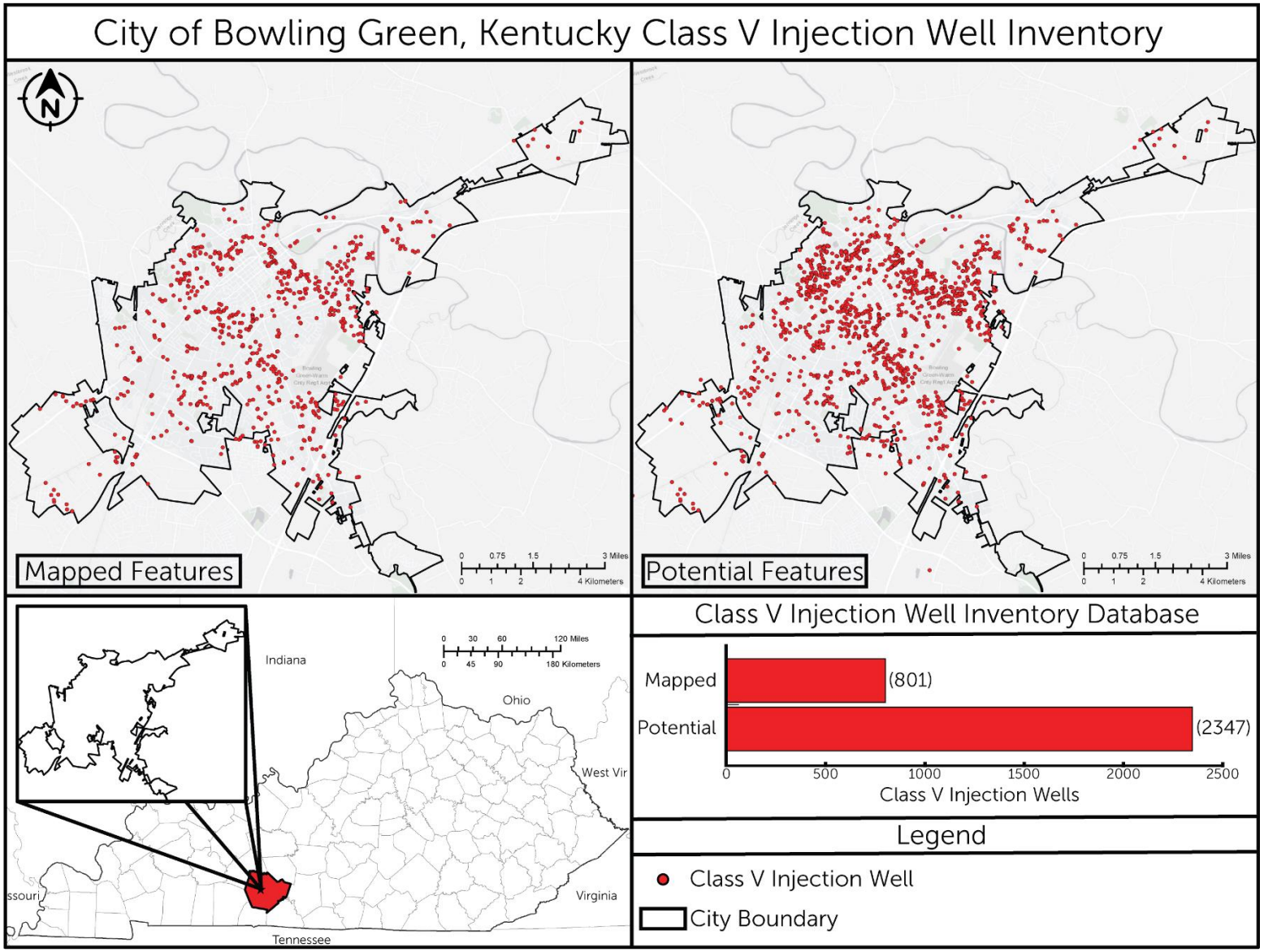

Figure 5.24: Map of the Injection Well Inventory Discrepancies between the CoBG's GIS Database and Historical Records (Created by Author).

After the maintenance program has concluded, a monitoring process should begin. The monitoring program would follow the same procedures used in this research. A HOBO data logger would be installed in each well within the basin and monitored until the catchment received three qualifying precipitation events that exceeded one-inch cumulative depth, or a rainfall intensity that charted on newly constructed IDF-curves. If the well flooded under the conditions outlined above, the EPA closure procedure would be initiated. If a Well closure occurred, the ponding stormwater should be routed to the nearest sinkhole or stormwater retention basin, while a replacement well is sited and tested. The Well testing criterion will differ from Well to Well, but the primary methods used should be monitored capacity tests, downhole video, and dye tracing.

Once an Injection Well Site has been selected, the well should be drilled to a depth of 20 feet (6.09 m). The drill depth selection is based on the data collected in this study and research conducted by Reeder (1989). Reeder (1989) determined that aquifer transmission is most efficient when wells intersect solutional features that are thicker than 0.49 ft (0.15 m). Additionally, Reeder (1989) notes that solutionally enlarged bedding planes, fractures, and joints are not transmissive and have low hydraulic conductivities. The most effective of the monitored Wells in regards to drainage have drilled depths at 30 ft (9.14) or less. A shallow drill depth also reduces the chances that the well be compromised by competing sources, as well as saving money by preventing unnecessary drill time. Furthermore, Wells should not be drilled deeper than 98.42 ft (30 meters), because the probability of hitting developed karst features decreasing substantially beyond this depth (Williams 1983; Crawford and Groves 1984; Reeder 1989).

Once a new Well is installed, a downhole camera should be sent down the

borehole to determine if sufficient voids exist. If not, the process above should be repeated until adequate voids are intersected. If the Well does not intersect any well-developed karst features by the 98.42 ft (30 m), a new site should be selected. When a plausible Well site has been found, a capacity test should be conducted. The current procedure used by the CoBG is to inject a known volume of water (66.84 ft^3 (1.89 m^3)) over a fixed amount of time, and if the Well does not flood it is considered passable. The procedure above is fraught with many incorrect assumptions. The capacity test should not be standardized. As an alternative, capacity tests should be performed multiple time times within a 72-hour window to ensure the Well has effective drainage under differing antecedent conditions. Before conducting a capacity test, a pressure transducer should be installed. The pressure transducer should be set to a delayed start that corresponds to the predetermined test start time and the logger should be set to one-second resolution for data collection.

Before each test, a well level should be measured, and a downhole camera assessment should be performed to ensure that the conditions within the borehole have not changed. After the slug has been injected the Well level should be periodically reassessed to determine if the recession is complete. Once the recession has been completed, the absolute pressure sensor should be pulled so that the recorded data can be analyzed. It may be necessary to install multiple sensors in a Well because at the one-second resolution the logger can only record data for 7.5 hours. Consequently, the start times for the additional loggers should be offset 7.5 hours from each other. If the Well functions successfully during all the tests, and has an effective recession rate, the next portion of the procedure should be initiated.

During the next phase of methodology, dye receptors should be placed in all the downgradient Wells within a 2,500 ft^2 (232.25 m^2) buffer. Once all Wells have been identified and background dye analysis has been conducted, the dye trace can begin. If the Well shows direct connectivity to numerous down gradient Wells it may be necessary to do additional groundwater monitoring to confirm that the new Well does not compromise their drainage capacities. Groundwater monitoring is recommended for the newly installed Well to see how it functions under real conditions. The monitoring process should match the procedure mentioned earlier for the existing Wells. If the Well is determined to be a successful Well, then the necessary inventory information should be recorded and logged in a GIS Database. Finally, all the recorded documentation should be sent to the EPA UIC office.

Siting is extremely important, but the overall longevity of an Injection Well hinges on the design and maintenance. Class V Injection Wells are notorious for contributing to water quality issues in UKA's (Crawford 1984; Zhou 2007). A Well's contribution to poor water quality is primarily related to the lack of pretreatment controls. Since Injection Wells are not required to support water quality BMP's, they are not typically designed with the capability (Nedvidek 2014). Not incorporating a mechanism for detention, or other forms of pretreatment, is an inherent design flaw that contributes to the failure of Injection Wells. The current design employed by the CoBG allows stormwater that contains a high sediment load, as well as trash and debris, to enter the borehole freely. The rapid infiltration of untreated rainwater allows the voids to and solutionally enlarged karst features intersected by the borehole to become clogged. Once the features develop blockages, it is impossible to remediate, and drainage is permanently

altered. After a Well becomes completely impaired, the only option available is to drill the Well again or cap it.

A significant redesign is necessary to improve the durability of Injection Wells. Some possible solution to these issues could be removing all flat horizontal grates, improving energy dissipation, and increasing storage and detention time. The flat grates become clogged easily and allow debris to flow through, thus, contributing to ponding. It is believed that switching the flat grates out for hemispherical grates would lessen the likelihood of blockages from trash and debris. Adding structural BMP's to slow stormwater down prior to entering the feature would allow infiltration to occur and cause a reduction in peak inflow rate, which would significantly decrease the probability of failure. Finally, if the drainage structure around the Injection Feature was designed in a way that it could capture most of the inflow and allow the suspended sediment to settle prior being infiltrated, the Wells would be much more successful. Given that most of the sediment build-up in the borehole is the result of the cumulative effects of the more probable storm events, the amount stormwater storage required would be around 50 ft^3 (1.41 m^3). The number suggested above is rounded from the average inflow volume received for the monitored Injection Wells. It would be a simple task to alter the structure design to include additional storage below the Well casing. Furthermore, by extending the concrete structure much further below the surface, it also lessens the erosion and soil piping that occurs around the stormwater control.

Another design flaw that poses a detriment to the functionality of an Injection Well is the casing length. In most cases, the Injection Well Casing does not extend into the bedrock contact. Not extending the casing into the bedrock allows mud to enter the

borehole from adjacent voids above the bedrock. Crawford (1989) points out that extending the casing below the bedrock-regolith contact and sealing the casing in with concrete would reduce clogging and collapse near the Well. It is important to note that the design elements suggested, provide a proactive approach for new Wells, but the fact remains that the existing Wells need to be addressed. It is not realistic to propose significant design alterations for these Wells, due to the prohibitive cost; however, regular maintenance would be beneficial, thus, prolonging the life of the existing Injection Wells. It is essential that the Wells are consistently maintained, because drainage and performance alterations resulting in improper upkeep easily prevented. Moreover, if the conditions within the system change, then the foundation for understanding system function becomes inaccurate.

Modeling System Behavior

Over the monitoring period, numerous storm events occurred, and several resulted in localized flooding. As aforementioned, a critical takeaway from the monitoring process was the speed of the response of the aquifer. If a lower monitoring resolution were chosen, the subsequent models constructed would mischaracterize the flood extent and aquifer response. Figure 5.25 illustrates the major variances between different monitoring resolutions. It is evident from the graphs below that a lower monitoring resolution would have resulted in data loss and misinterpretation of peak levels and recession rates. An increased data resolution is also beneficial when examining the meteorological input. The hourly resolution data presented in Figure 5.25 would result in much different storm intensity than displayed in the ten or one-minute resolution data. Moreover, if the initial assumptions and conceptions are inaccurate, then the error will be

propagated to the interpretation. One-minute resolution does produce significant noise, but data reduction techniques make the noise produced a non-issue.

Due to the lack of variability in storm events, it was determined that producing flood maps for the storms observed would not be useful; however, numerous potentiometric surface maps were produced to see how accurately the geostatistical technique reproduced observed conditions. Figure 5.26 displays a 3-D potentiometric surface map that was created for a storm event that occurred on 2/22/2018. Regrettably, survey data were not collected for flood extents for validation, but observational evidence was collected to confirm that flooding did occur in the projected locations. Despite being unable to determine the numerical accuracy of the flood simulation, it is believed that with additional monitoring and calibration that the process would become a reliable method for accessing flood risk in UKA's. The potentiometric maps could be used to create localized urban flood contours, as well as to provide a way to visualize aquifer response quickly. It is hoped that the techniques used in this study can be coupled with computing systems, such as ANNs, for predictive purposes.

Typically, when constructing a hydrological model, it is necessary to have a large and diverse dataset. Although variability in storm events was a limiting factor in this study, an attempt was made to create a predictive model for New Spring stage. Originally, this project sought to develop a distributed physical model to predict groundwater response to precipitation events, but due to time constraints and lack of essential data, the model development was postponed. It is believed that using an ANN model would be more cost-effective and accurate at forecasting groundwater levels than a physically based model because of the flexibility and ease of the model architecture.

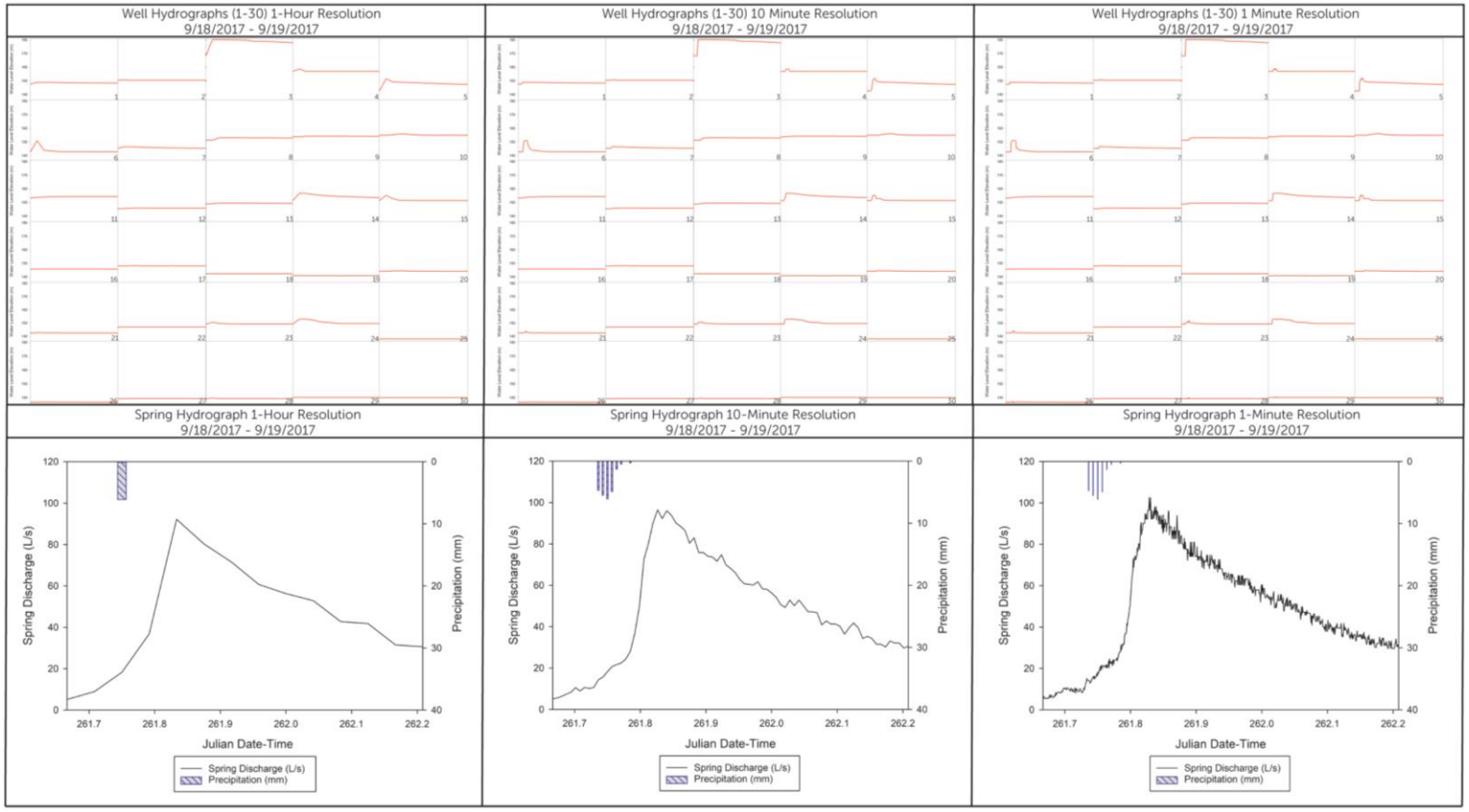

Figure 5.25: New Spring Groundwater Basin: Hydrographs at Multiple Resolutions (9/18/2017-9/19/2017) (Created by Author).

New Spring Groundwater Basin 3-D Potentiometric Response (2/22/2018)

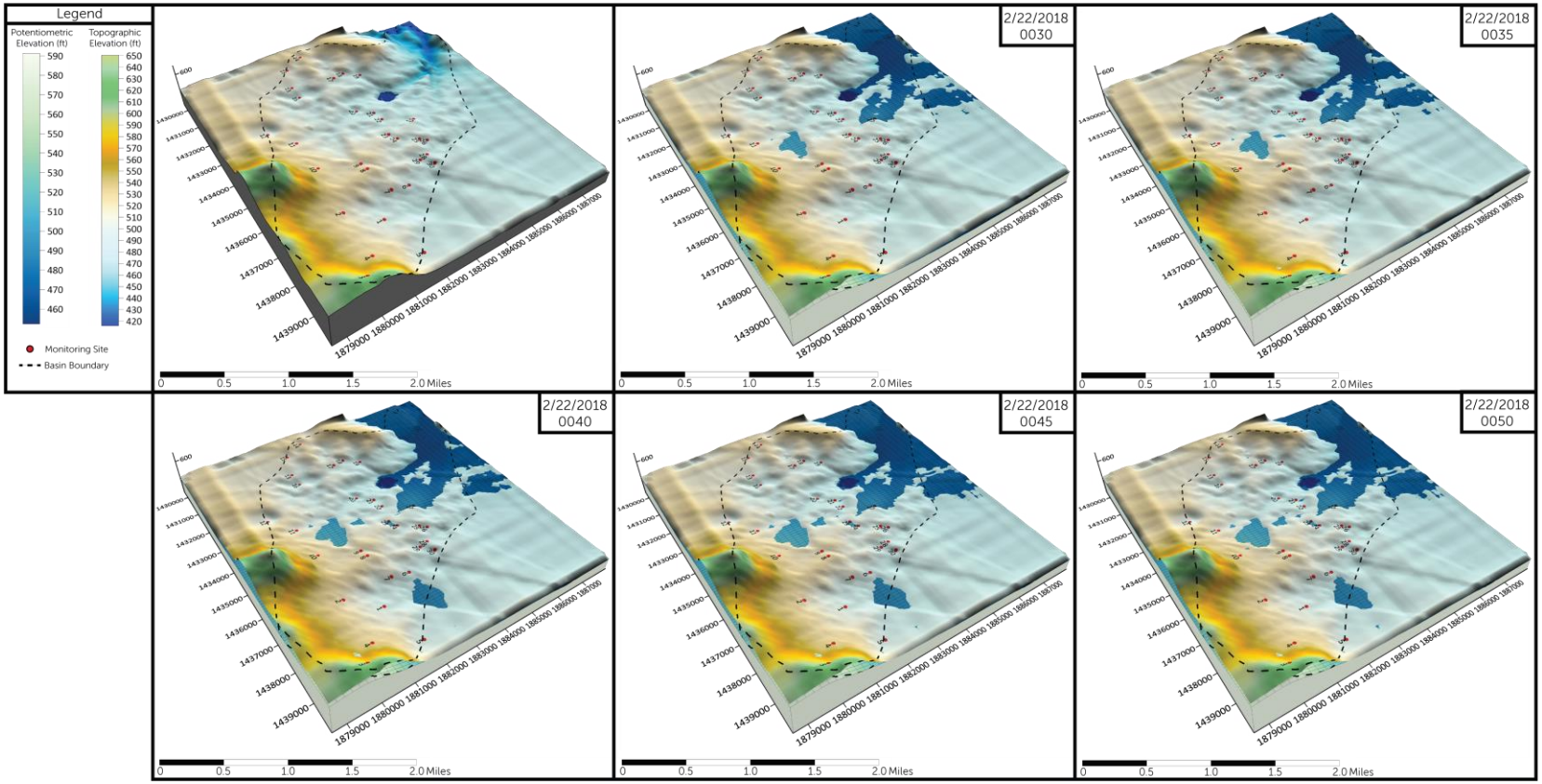

Figure 5.26: New Spring Groundwater Basin Potentiometric Response During Storm Event (2/22/2018) (Created by Author).

ANNs are well-suited for modeling the dynamic and non-linear karst systems, mainly because it does not require the user to formulate explicit mathematical expressions for the underlying processes (Sahoo and Jha 2013). Prior to creating the MLP model for New Spring stage, a cross-correlational analysis was performed to determine which correlates would be the best inputs for the model. The test parameters that were selected for analysis were those that were believed to act as a hydrologic control on the New Spring Stage. Refer to Table 5.1 for the results for the cross-correlation analysis results. Input neurons not included in Table 5.1 are precipitation and IW-27 water elevation. The selection of the optimal number of hidden nodes and activation functions used in the MLP model was determined through a trial-error approach (Eberhart and Dobbins 1990). All models were trained using the LM training algorithm. Five different model configurations were tested, and sensitivity analysis revealed that model 3 (M-3) performed the best in training and the simulation test. M-3 utilized the Logistic Sigmoid Activation Function.

The resultant MLP-LM model was used to simulate New Spring's storm response using inputs from an observed event (Figure 5.27). Sensitivity analyses were conducted on the simulation and training results (Figure 5.28). Form the analysis the simulation produced minimal error values with a RSME of 0.0154 and a MAPE of 0.000002, which indicates that the MLP-LM models can accurately predict New Spring stage. It is thought that the techniques used above are reliable enough to be applied to the Injection Well Dataset to predict well fluctuations during storm events. Furthermore, if an ANN model was constructed for each Injection Well, it would be possible to generate potentiometric surface maps for the basin for rare return periods; however, more investigation is needed

to achieve the lofty goal above due to the extreme difficulty of determining which inputs act as hydrologic controls on other wells. As an example, the control exhibited on IW-1by IW-3 is a reasonable assumption, but it is not so obvious with other wells. Moreover, further monitoring and hydrologic investigations are necessary to ensure that correlates share a physical relationship. Another factor that makes input determination increasingly difficult is the inconsistent lag time between variables in karst areas. Nevertheless, the "black box" label on karst aquifers becomes increasingly transparent as more data are collected

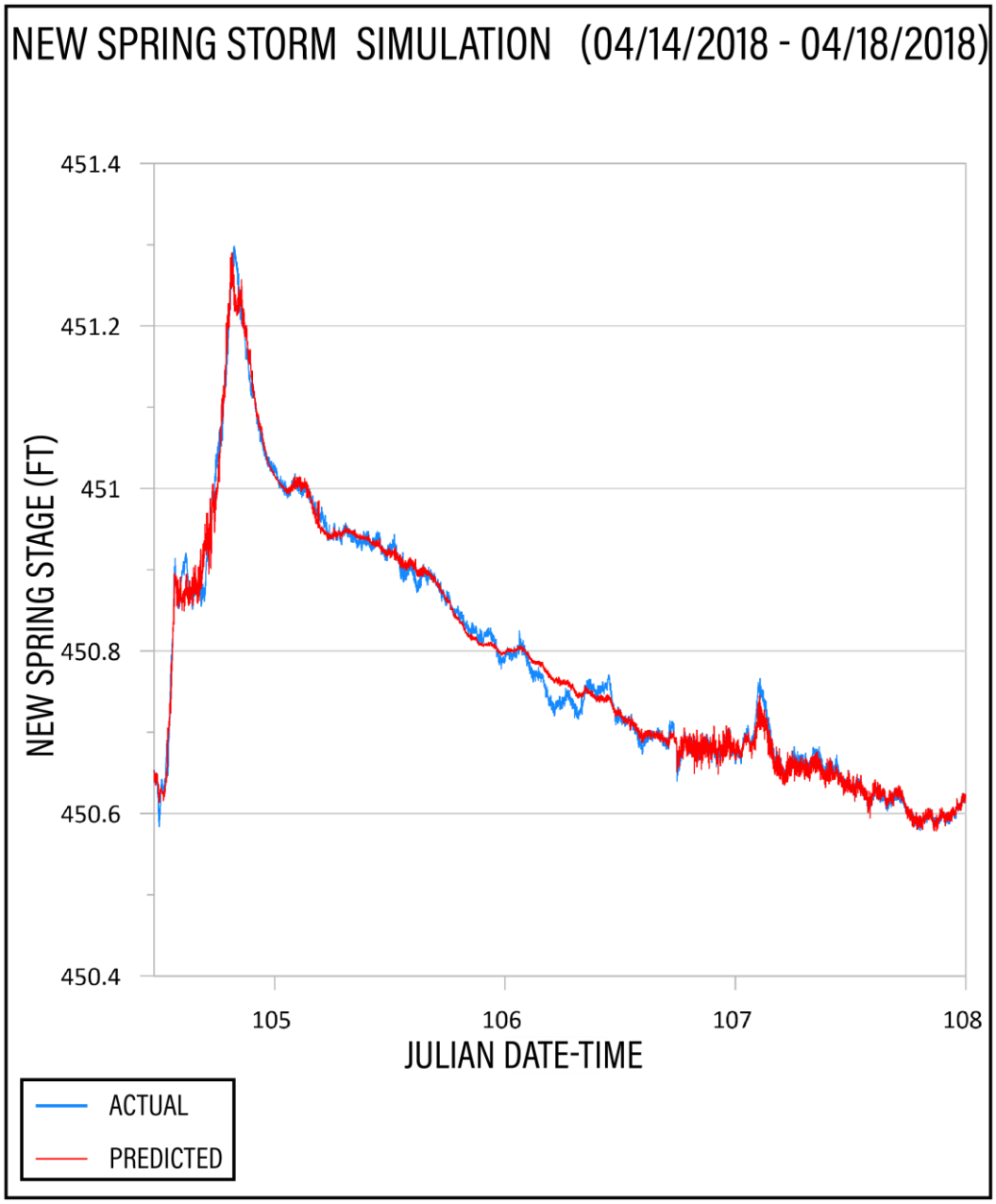

Figure 5.27: New Spring Stage ANN Model Simulation (04/14/2018-04/18/2018) (Created by Author).

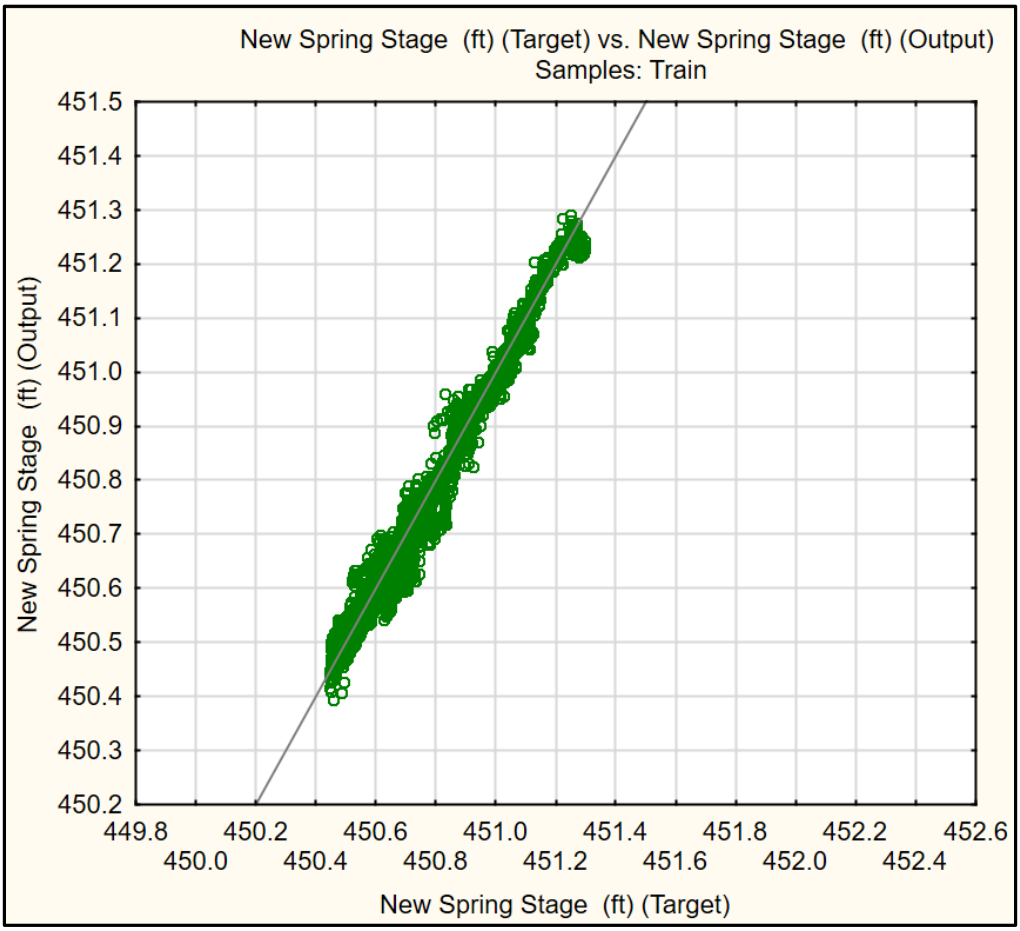

Figure 5.28: New Spring Stage ANN Model Training Results (Created by Author).

Chapter 6: Conclusions

The study led to many important discoveries surrounding the hydraulic and hydrologic functioning of Class V Injection Wells. Notably, one of the most critical findings of this study is the rate at which the karst aquifer and Injection Wells respond to storm events. The rate of increase was much quicker than expected, with some wells increasing as much as 40 feet (12.192 meters) minutes after peak rainfall, which validated the choice of a one-minute sampling resolution. A lower monitoring resolution would have resulted in data loss and misinterpretation of peak levels and recession rates. Another critical finding resulted from hydrograph analysis in combination with water budget calculations. This combination approach revealed that most of the monitored Injection Wells exceed their grate elevation under low-intensity storm conditions and have a low contribution to the overall recharge for the basin. Additionally, analysis of well and spring hydrographs indicate that the Injection Well flooding is primarily controlled by storm intensity, rather than volume; moreover, high-intensity, short duration events result in flooding more often than low-intensity, long duration events. It should be noted that aquifer response to Injection Well recharge is highly variable and almost entirely dependent on antecedent conditions. Differences in Well responses may be attributable to karst aquifer heterogeneity. Another important finding that can be shown empirically, and validated statistically, is that many of the monitored wells are influenced by the hydraulic connectivity of upgradient Injection Wells; the interconnectivity of wells is prevalent across the basin.

Most of the issues surrounding Class V Injection Wells could be ameliorated

through the adoption of practical strategies. Throughout the study, numerous Injection Well maintenance and siting issues were discovered. A significant number of Injection Wells in Bowling Green are obstructed with sediment and debris. Proper BMP's, drainage design modifications, and regular maintenance could improve longevity and reduce flooding. Also, to improve siting, the City should implement a system that utilizes high-volume capacity testing under variable hydrologic conditions and geophysical site investigations to eliminate the siting of low capacity Injection Wells. The groundwater exceedances observed during the monitoring period can be attributed to poorly sited Injection Wells that have limited connectivity to the aquifer and, thereby, only support borehole storage. It is evident from the data that the current strategies for siting, design, and maintaining the Injection Wells are not effective at mitigating the more probabilistic storm events. It should be noted that a different monitoring approach may have led to inaccurate results, due to an incomplete hydrological snapshot and, therefore, produced faulty conclusions. Furthermore, it is imperative that guidelines and regulations for the siting, design, and maintenance of Class V Injection Wells are established to prevent flooding as the City continues to expand.

Outlined below is a summary of recommendations for sustainable stormwater management strategies for UKAs that utilize Class V Injection Wells as a stormwater BMP, as well as some ideas for future work in this area:

Injection Well BMPs

- **Consult Injection Well GIS database and Karst Feature Inventory prior to drilling a New Injection Well** – this will decrease chances of installing a well in high density areas, whilst increasing the probability that the new site will intersect

a sufficient void/cave system.

- **Avoid installing Injection Wells in retention basins** – the purpose of a retention basin is to retain water and allow suspended material in the storm water to settle out. The CoBG places Injection Wells in retention basins to prevent stagnant ponding water in order to minimize health and safety risks; however, the stormwater routed to the retention basin is heavily concentrated with pollutants and sediment. This research has shown that because of a lack of sediment BMPs, Injection Wells become obstructed easily and often cannot be remediated; therefore, the Well placed in the basin will more likely cause the very thing that is trying to be prevented. Also, given the low elevation of Wells in basins it is likely that the phenomena of interconnectivity may cause surcharging which would diminish storage, as well as drainage.
- **Include energy dissipation strategies and onsite detention in the overall design of an Injection Well site** – adding structural BMP's to slow stormwater down prior to entering the feature would allow infiltration to occur and cause a reduction in peak inflow rate, which would significantly decrease the probability of failure. Finally, if the drainage structure around the Injection Feature was designed in a way that it could capture most of the inflow and allow the suspended sediment to settle prior to being infiltrated, the Wells would be much more successful. Given that most of the sediment build-up in the borehole is the result of the cumulative effects of the more probable storm events, the amount stormwater storage required would be around 50 ft^3 (1.41 m^3). The number suggested above is rounded from the average inflow volume received for the

monitored Injection Wells. It would be a simple task to alter the structure design to include additional storage below the Well casing.

- **Avoid drilling Injection Wells to unnecessary depths –** initial Well depths should start around a depth of 20 feet (6.09 m). The drill depth selection is based on the data collected in this study and research conducted by Reeder (1989). Reeder (1989) determined that aquifer transmission is most efficient when wells intersect solutional features that are thicker than 0.49 ft (0.15 m). Additionally, Reeder (1989) notes that solutionally enlarged bedding planes, fractures, and joints are not transmissive and have low hydraulic conductivities. The most effective of the monitored Wells in regards to drainage have drilled depths at 30 ft (9.14) or less. A shallow drill depth also reduces the chances that the well be compromised by competing sources, as well as saving money by preventing unnecessary drill time. Furthermore, Wells should not be drilled deeper than 98.42 ft (30 meters), because the probability of hitting developed karst features decreasing substantially beyond this depth (Williams 1983; Crawford and Groves 1984; Reeder 1989).
- **Newly Installed Injection Wells should be monitored, and capacity tested under differing hydrological conditions –** varying antecedent conditions can significantly impact an Injection Well's drainage capacity. As an example, prior to the event on 10/05/2017, the basin received 1.37 in (3.5 cm) of rainfall and an additional 1.1 in (2.79 cm) during the event. The system was saturated, which drastically reduced the overall effectiveness of the Injection Wells. The saturated antecedent conditions caused Injection Well #29's (IW-29) average recession rate

to decrease by 93 percent.

- **Hold Injection Wells to the same standard as other stormwater BMPs –** the CoBG primarily uses Class V Injection Wells as a means of flood control; thus, the design of these systems is exclusively focused on water quantity. The lack of pretreatment in Class V Injection Wells has left the karst system receiving the stormwater discharges extremely susceptible to contamination. Moreover, if the KPDES MS4 program were left to regulate the water quality of Class V Injection Well discharges, it would prove to be costly for the CoBG and other UKA's under the permitting authority. The aforementioned scenario also poses a difficult problem for stormwater managers in the CoBG. Due to a large number of Class V Injection Wells within the city, stormwater managers are left with the decision of well closure or the infeasible task of retrofitting each well, which is essentially a choice between flood control and water quality; however, it should be noted that it is possible to reconcile water quantity and quality, through improved siting and design of Class V Injection Well systems. Furthermore, by removing the regulatory overlap between the MS4 program and UIC, it may be possible to clarify "gray areas" of the regulation and eliminate legal loopholes that limit the protection of the karst system.
- **Implement an Inventory and Maintenance Program –** without proper maintenance Injection Wells and the intersecting karst feature become clogged and obstructed (Crawford 1984; Zhou 2006). Furthermore, without an accurate inventory, it is impossible to maintain all the features within an area.

In closing, Class V Injection Wells can be effective at mitigating localized

flooding in UKAs if properly sited, designed, and maintained. Additional policy amendments are necessary to ensure that proper BMPs for Class V Injection Wells are implemented. Currently, UIC regulations do not include siting and design criterion for Class V Injection Wells. The lax stance of the current regulation makes it possible for anyone to install an Injection Well, which is problematic because the use of the appropriate BMPs is not enforced or incentivized; however, if the strategies listed above are incorporated into the regulation, it may be possible to extend Injection Well design life and minimize water quality risks to groundwater. This study has shown that the Class V Injection Wells in the CoBG are not effective at minimizing localized flooding and contribute to Well sedimentation and, thereby, contaminant transport. Using the data above as a foundation, the CoBG could easily create a pilot program to determine the BMPs best suited for UKAs in order to inform UIC policy and improve conditions within the City and beyond.

Additional monitoring is needed to better understand the hydrologic influence of Class V Injection Wells on urban karst hydrology. Moreover, this study did not receive the hydrologic conditions necessary to evaluate Injection behavior during true peak flood conditions. Regardless, it is believed that accurate localized urban karst inundation mapping would be possible using the methods above. If an ANN model were constructed for each Injection Well within a catchment, it would be possible to generate potentiometric surface maps for a groundwater basin for rare return periods; however, more investigation is needed to achieve the lofty goal above, due to the extreme difficulty of determining which inputs act as hydrologic controls on other wells. Furthermore, through the adoption of the strategies outlined above, it would be

possible to reduce flooding, minimize flood risk, and eliminate water quality issues resulting from Class V Injection Wells in UKAs.

References

Adamowski, J., Karapataki, C., 2010. Comparison of multivariate regression and artificial neural networks for peak urban water-demand forecasting: Evaluation of different ANN learning algorithms. *Journal of Hydrologic Engineering*, 15(10), 729–743.

Atkinson, T.C., 1977. Diffuse flow and conduit flow in limestone terrain in the Mendip Hills. *Journal of Hydrology* 35(1-2), 93-110.

Bailly-Comte, V., Jourde, H., Roesch, A., Pistre, S., Batiot-Guilhe, C., 2008. Time series analyses for Karst/River interactions assessment: Case of the Coulazou river (southern France). *Journal of Hydrology*, 349(1), 98–114.

Bailly-Comte, V., Borrell-Estupina, V., Jourde, H., Pistre, S., 2012. A conceptual semi-distributed model of the Coulazou River as a tool for assessing surface water–karst groundwater interactions during flood in Mediterranean ephemeral rivers. *Water Resources Research 48*(9), 1-14.

Barfield, B.J., Felton, G.K., Stevens, E.W., McCann, M., 2004. A simple model of karst spring flow using modified NRCS procedures. *Journal of Hydrology* 287(1), 34-48.

Barner, W.L., 1999. Comparison of stormwater management in a karst terrane in Springfield, Missouri—case histories. *Engineering Geology 52*(1), 105-112.

Bonacci, O., Ljubenkov, I., Roje-Bonacci, T., 2006. Karst flash floods: an example from the Dinaric karst (Croatia). *Natural Hazards and Earth System Science 6*(2), 195-203.

Bonacci, O., 2015. Karst hydrogeology/hydrology of Dinaric chain and isles. *Environmental Earth Sciences 74*(1), 37-55.

Booker and Associates, INC., 1978. *Study of Sinkhole Flooding, Bowling Green and Warren County, Kentucky.* Bowling Green, Kentucky.

Brasier, F.M., Kobelski, B., 1996. Injection of industrial wastes in the United States. Deep injection of disposal of hazardous industrial waste. *Academic Press*, 1-8.

Brummett, Travis S, 2016. Vertical Implementation of Cloud for Education (V.I.C.E.). . M.S. Computer Science Thesis, Department of Computer Science, Western Kentucky University, Bowling Green, Kentucky. Available online at: https://digitalcommons.wku.edu/theses/1643/

Butler Jr., J.J., 1997. *The design, performance, and analysis of slug tests*. Boca Raton, Florida: CRC Press.

Campbell, W., 2005. Stormwater Injection Well Performance Water Quality and Quantity, and Maintenance. Unpublished.

Campbell, C.W., 2005. Complexities of flood mapping in a sinkhole area. *Sinkholes and the Engineering and Environmental Impacts of Karst*, 470-478.

Chen, C.L., 1983. Rainfall intensity-duration-frequency formulas. *Journal of Hydraulic Engineering 109*(12), 1603-1621.

City of Bowling Green, Public Works Department, 2009. *Stormwater Drainage Wells.* Available Online at: http://12 .180.242.211/publicworks/planning design/stormwater /pdf/SWdrainwellbrochure8.pdf

City of Knoxville, 2004. *Municode Library*. Available online at: https://www.municode.com/library/tn/knoxville/codes/code_of_ordinances?nodeId=APXBZORE

Clark, J.E., Bonura, D.K., Van Voorhees, R.F., 2005. An overview of injection well history in the United States of America. *Developments in Water Science 52,* 3-12.

Clean Water Act, 1972. Available online at: https://www3.epa.gov/npdes/pubs/cwatxt.txt.

Cooper, H.H., Bredehoeft, J.D., Papadopulos, I.S., 1967. Response of a finite- diameter well to an instantaneous charge of water. *Water Resources Research 3*(1), 263-269.

Cox, W.E. 1997. Evolution of the Safe Drinking Water Act: A search for effective quality assurance strategies and workable concepts of federalism. *William & Mary Environmental Law & Policy Review 21*, 69.

Crawford, N., 1981. *Karst Hydrology and Environmental Problems in the Bowling Green Area.* Bowling Green, Kentucky: The Center for Cave and Karst Studies, Western Kentucky University, 1-21.

Crawford, N.C., 1982. *Hydrogeologic problems resulting from development upon karst terrain, Bowling Green, KY*. Bowling Green, Kentucky: United States Environmental Protection Agency, 1-33.

Crawford, N.C., Groves, C., 1984. *Storm water drainage wells in the karst areas of Kentucky and Tennessee*. Bowling Green, Kentucky: United States Environmental Protection Agency & Center for Cave and Karst Studies.

Crawford, N.C., Groves, C.G., Feeney, T.P., Keller, B.J., 1987. *Hydrogeology of the Lost River karst groundwater basin, Warren County, Kentucky*. Bowling Green, Kentucky: Kentucky Division of Water and Barren River Area Development District, 1-124.

Crawford, N.C., Hoffman, W., 1989. *The karst landscape of Warren County*. Bowling Green, Kentucky: City-County Planning Commission of Warren County, 1-204.

Crawford, N.C., 2001. Field trip guide, part 1: environmental problems associated with urban development upon karst, Bowling Green, Kentucky. In *Proceedings of the 8th multidisciplinary conference on sinkholes & karst.* Beck, BF & Herring, JG. (eds.) Louisville, Kentucky, 397-424.

Cronshey, R.G., Roberts, R.T., Miller, N., 1985. Urban hydrology for small watersheds (TR-55 Rev.). *Hydraulics and Hydrology in the Small Computer Age*, 1268-1273.

Currens, J.C., 2012. Model ordinance for development on karst terrain: Kentucky, USA. *Carbonates and Evaporites 27*(2), 133-136.

Daugherty D., 1976. Storm Water Management Seminar. *City-County Planning Commission of Warren County*. Unpublished.

Delbart, C., Valdés, D., Barbecote, F., Tognelli, A., Couchoux, L., 2016. Spatial organization of the impulse response in a karst aquifer. *Journal of Hydrology* 537, 18–26.

De Rooij, R., Perrochet, P., Graham, W., 2013. From rainfall to spring discharge: Coupling conduit flow, subsurface matrix flow and surface flow in karst systems using a discrete–continuum model. *Advances in Water Resources, 61*, 29-41.

Dinger, J.S.,Rebmann, J.R., 1986. Ordinance for the Control of Urban Development in Sinkhole Areas in the Bluegrass Karst Region, Lexington, Kentucky. In Environmental Problems in Karst Terranes and Their Solutions. *National Water Well Association*, 1-16

Dinger, J.S., Zourarakis, D.P., Currens, J.C., 2007. Spectral enhancement and automated extraction of potential sinkhole features from NAIP imagery—initial investigations. *Journal of Environmental Informatics 10*(1), 22-29.

Doummar, J., Sauter, M., Geyer, T., 2012. Simulation of flow processes in a large scale karst system with an integrated catchment model (Mike She)–Identification of relevant parameters influencing spring discharge. *Journal of Hydrology 426*, 112-123.

Downer, C.W., Ogden, F.L., 2006. *Gridded Surface Subsur face Hydrologic Analysis (GSSHA) (Version 1.43) for Watershed Modeling System 6.1*. Vicksburg, Mississippi: Engineer Research and Development Center.

Durkee, J.D., Campbell, L., Berry, K., Jordan, D., Goodrich, G., Mahmood, R., Foster, S., 2012. A synoptic perspective of the record 1-2 May 2010 mid-South heavy precipitation event'. *Bulletin of the American Meteorological Society 93*(5), 611-620.

Dymond, J.R., Christian, R., 1982. Accuracy of discharge determined from a rating curve'. *Hydrological Sciences Journal 27*(4), 493-504.

Eberhart, R.C., Dobbins, R.W., 1990. Early neural network development history: the age of Camelot. *Engineering in Medicine and Biology Magazine*, IEEE, 9(3), 15–18.

Elrod, M.N., 1899. The geologic relation of some St. Louis group caves and sinkholes. *Proceedings of the Indiana Academy of Science for 1898*, 258–267.

Environmental Protection Agency, 1999. *The Class V Underground Injection Control Study Volume 3: Storm Water Drainage Wells*. Washington, D.C.: Office of Ground Water and Drinking Water.

Environmental Protection Agency, 2003. *Introduction to the Underground Injection Control Program*. Drinking Water Academy.

Environmental Protection Agency, 2016. *Protecting Underground Sources of Drinking Water from Underground Injection*. Available online at: <https://www.epa.gov/uic> [Accessed 11/20/2016]

Faust, C.R., Mercer, J.W., 1980. Ground-water modeling: recent developments. *Ground Water 18*(6), 569-577.

Federal Emergency Management Agency, 2016. *Things You Can Do To Mitigate Against Flooding*. Available online at: <https://www.fema.gov/blog/2012-03-14/things-you-can-do-mitigate-against-flooding> [Accessed 11/25/2016].

Federal Emergency Management Agency, 1993. *Flood Insurance Study: Warren County, Kentucky and Incorporated Areas*. Washington D.C.: National Flood Insurance Program.

Federal Emergency Management Agency, 2006. *Flood Insurance Study: Warren County, Kentucky and Incorporated Areas*. Washington D.C.: National Flood Insurance Program.

Fischer, J.A., 1999. Limestone ordinances of New Jersey and Pennsylvania: a practitioner's experiences. *Engineering Geology 52*(1), 61-66.

Fisher, J.C., 2013. Optimization of Water-Level Monitoring Networks in the Eastern Snake River Plain Aquifer Using a Kriging-Based Genetic Algorithm Method. *AGU Fall Meeting Abstracts.*

Fleury, S., 2009. *Land use policy and practice on karst terrains: Living on limestone*. St. Petersburg, Florida: Springer Science & Business Media.

Fleury, P., Maréchal, J.C., Ladouche, B., 2013. Karst flash-flood forecasting in the city of Nîmes (southern France). *Engineering Geology 164*, 26-35.

Ford, D.C., Williams, P., 2007. *Karst Hydrology and Geomorphology*. Hoboken, New Jersey: John Wiley and Sons Ltd.

Ford, D., Williams, P.D., 2013. *Karst hydrogeology and geomorphology*. Hoboken, New Jersey: John Wiley & Sons.

Ghasemizadeh, R., Hellweger, F., Butscher, C., Padilla, I., Vesper, D., Field, M., Alshawabkeh, A., 2012. Review: Groundwater flow and transport modeling of karst aquifers, with particular reference to the North Coast Limestone aquifer system of Puerto Rico. *Hydrogeology Journal 20*(8), 1441-1461.

Goldscheider, N., Drew, D., 2007. *Methods in Karst Hydrogeology: IAH: International Contributions to Hydrogeology, 26*. AK Leiden, The Netherlands: CRC Press.

Goldstrand, P.M., Shevenell, L.A., 1997. Geologic controls on porosity development in the Maynardville Limestone, Oak Ridge, Tennessee. *Environmental Geology 31*(3-4), 248-258.

Grant , D.M., Dawson, B.D., 1997. *ISCO Open Channel Flow Measurement Handbook.* (5th edition). Lincoln, Nebraska: ISCO.

G.R.W. Engineers, Inc., Daugherty and Trautwein, Inc., 1980. *Glendale, a Storm Drainage Study, Bowling Green, Kentucky.* Louisville, Kentucky.

Gutiérrez, F., Parise, M., De Waele, J., Jourde, H., 2014. A review on natural and human-induced geohazards and impacts in karst. *Earth-Science Reviews 138*, 61-88.

Gupta, R. J., 1995. *Hydrology and Hydraulic Systems*. Prospect Heights, Illinois: Waveland Press.

Hao, Y., Yeh, T.C.J., Wang, Y., Zhao, Y., 2007. Analysis of karst aquifer spring flows with a gray system decomposition model. *Ground Water 45*(1), 46-52.

Hart, E.A., 2006. Land use change and sinkhole flooding in Cookeville Tennessee. *Southeastern Geographer* 46(1), 35-50.

Haan, C.T., Barfield, B.J.,Hayes, J.C., 1994. *Design hydrology and sedimentology for small catchments.* San Diego, California: Elsevier.

Herschy, R., 1993. The velocity-area method. *Flow measurement and instrumentation 4*(1), 7-10.

Hjelmfelt Jr., A.T., 1991. Investigation of curve number procedure. *Journal of Hydraulic Engineering 117*(6), 725-737.

Jeannin, P.Y., Groves, C., Häuselaman, P., 2007. Speleological investigations in Methods in Karst Hydrogeology' In Goldscheider, N., Drew D. (ed.), *Methods in Karst Hydrogeology: IAH: International Contributions to Hydrogeology*, (26th Series). AK Leiden, The Netherlands: CRC Press, 25-44.

Jenkins, G.M., Watts, Donald G, 1968. *Spectral analysis and its applications*, San Francisco: Holden-Day.

Jenkins, R.N., 2006. *The uses of GSSHA to model groundwater-surface water interaction*. M.S. Civil Engineering Thesis, Department of Civil Engineering, Brigham Young University, Provo, Utah.

Kambesis, P, Crawford, N., Groves, C., 2010. Urban Development on Karst: Lessons learned…or not? A case study in Bowling Green Kentucky USA. *Geological Society of America* 42(5), 448.

Karanovic, M., Tonkin, M., Wilson, D., 2009. KT3D_H2O: A program for kriging water level data using hydrologic drift terms. *Ground Water* 47(4), 580-586.

Kemmerly, P., 1981. The need for recognition and implementation of a sinkhole floodplain hazard designation in urban karst terrains. *Environmental Geology* 3(5), 281-292.

Kemmerly, P.R., 1993. Sinkhole hazards and risk assessment in a planning context. *Journal of the American Planning Association 59*(2), 221-229.

Király, L., 2002. Karstification and Groundwater Flow. *Proceedings of the Conference on Evolution of Karst: From Prekarst to Cessation. Postojna-Ljubljana*, 155–190.

Kong-A-Siou., L., Johannet, A., Borrell, V., Pistre, S., 2011. Complexity selection of a neural network model for karst flood forecasting: The case of the Lez Basin (southern France). *Journal of Hydrology*, 403(34), 367–380.

Kong-A-Siou, L., Fleury, P., Johanneta, A., Borrell-Estupina, V., Pistre, S., Dörfligerd,

N., 2014. Performance and complementarity of two systemic models (reservoir and neural networks) used to simulate spring discharge and piezometry for a karst aquifer. *Journal of Hydrology*, 519(PD), 3178–3192.

Kong-A-Siou, L., Borrell-Estupina, V., Johannet, A., Pistre, S., 2015. Neural Networks for karst spring management. Case of the Lez spring (Southern France). *Hydrogeological and Environmental Investigations in Karst Systems*, 361-369.

Kovács, A., Sauter, M., 2007. Modelling Karst Hydrodynamics. In Goldscheider, N., Drew D. (Ed.), *Methods in Karst Hydrogeology: IAH: International Contributions to Hydrogeology,* (26th Series). AK Leiden, The Netherlands: CRC Press, 201-220.

Kovács, A., Perrochet, P., 2014. Well Hydrograph Analysis for the Estimation of Hydraulic and Geometric Parameters of Karst and Connected Water Systems. *H2Karst Research in Limestone Hydrogeology*, 97-114.

Kovács, A., Perrochet, P., Darabos, E., Lénárt, L., Szűcs, P., 2015. Well hydrograph analysis for the characterisation of flow dynamics and conduit network geometry in a karst aquifer, Bükk Mountains, Hungary. *Journal of Hydrology 530*, 484-499.

Krčmář, D., Sracek, O., 2014. MODFLOW-USG: the new possibilities in mine hydrogeology modelling (or what is not written in the manuals). *Mine Water and the Environment*, *33*(4), 376-383.

Kresic, N., 2007. Hydraulic methods. In Goldscheider, N., Drew D. (ed.), *Methods in Karst Hydrogeology: IAH: International Contributions to Hydrogeology*, (26th Series). AK Leiden, The Netherlands: CRC Press, 65-91.

Lacobellis, V., Castorani, A., Di Santo, A.R., Gioia, A., 2015. Rationale for flood prediction in karst endorheic areas. *Journal of Arid Environments 112*, 98-108.

Kumar, V., 2006. Kriging of groundwater levels–a case study. *Journal of Spatial Hydrology 6*(1) 1-12.

Lawhon, N., 2014. *Investigating Telogenetic Karst Aquifer Processes and Evolution in South-Central Kentucky, US, Using High-Resolution Storm Hydrology and Geochemistry Monitoring.* M.S. Geoscience Thesis, Department of Geography and Geology, Western Kentucky University, Bowling Green, KY. Available online at: http://digitalcommons.wku.edu/theses/1324/

Liu, Y.B., Batelaan, O., Smedt, F.D., Huong, N.T., Tam, V.T., 2005. Test of a distributed modelling approach to predict flood flows in the karst Suoimuoi catchment in Vietnam. *Environmental Geology 48*(7), 931-940.

Machiwal, D., Jha, M.K., 2012. Exploring Trends in Climatological Time Series of Orissa, India Using Nonparametric Trend Tests. In *Hydrologic Time Series Analysis: Theory and Practice*. Dordrecht: Springer Netherlands, 222–248.

Maréchal, J.C., Ladouche, B., Dörfliger, N., 2008. Karst flash flooding in a Mediterranean karst, the example of Fontaine de Nîmes. *Engineering Geology 99*(3), 138-146.

Milanović, P., 2014. Hydraulic properties of Karst Groundwater and its impacts on large structures. *H2Karst Research in Limestone Hydrogeology*, 19-48.

Mohanty, S., Madan, K., Ashwani, J., Kumar, K., Sudheer, P., 2010. Artificial Neural Network Modeling for Groundwater Level Forecasting in a River Island of Eastern India. *Water Resources Management*, 24(9), pp.1845–1865.

National Weather Service, Weather.gov., 2010. *LMK Climate - Bowling Green*. Retrieved from: http://www.weather.gov/lmk/clibwg

Nedvidek, D.C., 2014. *Evaluating the Effectiveness of Regulatory Stormwater Monitoring Protocols on Groundwater Quality in Urbanized Karst Regions.* M.S. Geoscience Thesis, Department of Geography and Geology, Western Kentucky University, Bowling Green, Kentucky. Available online at: http://digitalcommons.wku.edu/theses/1407/

National Flood Insurance Program, 2016. *Flooding History*. Available online at: <https://www.floodsmart.gov/floodsmart/pages/media_resources/fact_floodfacts.jsp>

National Oceanic Atmospheric Agency, 2016. *PFDS: Contiguous US*. Available online at: http://hdsc.nws.noaa.gov/hdsc/pfds/pfds_map_cont.html?bkmrk=ky

United States Department of Agriculture, 2009. *Hydrology National Engineering Handbook*. Washington, D.C.: National Resource Conservation Service.

United States Environmental Protection Agency, 1986. *The Enforcement Management System: National Pollutant Discharge Elimination System (Clean Water Act)*. Washington, D.C.: Office of Water.

Olsen, C.T., 2015. *A Decade of Lessons Learned: The Local Implementation of Stormwater Programs in Tennessee.* M.S. Geography Thesis, Department of Geography, University of Tennessee, Knoxville, Tennessee. Available online at: http://trace.tennessee.edu/utk_gradthes/3398/

Osterhoudt, L.L., 2014. *Impacts of Carbonate Mineral Weathering on Hydrochemistry of the Upper Green River Basin, Kentucky*. M.S. Geoscience Thesis, Department of Geography and Geology, Western Kentucky University, Bowling Green, Kentucky. Available online at: http://digitalcommons.wku.edu/theses/1337/

Palmer, A., Palmer, M., Sasowsky, I. (eds)., 1999. *Karst modeling* (5th Volume). Charles Town, West Virginia: Karst Waters Institute.

Palmer, A.N., 2007. *Cave Geology*. Dayton, Ohio: Cave Books.

Pardo-Igúzquiza, E., Durán, J.J., Robledo-Ardila, P.A., 2015. A Three-Dimensional Karst Aquifer Model: The Sierra de Las Nieves Case (Málaga, Spain). In *Hydrogeological and Environmental Investigations in Karst Systems*, 285-291.

Parise, M., 2003. Flood history in the karst environment of Castellana-Grotte (Apulia, southern Italy). *Natural Hazards and Earth System Science*, *3*(6), 593-604.

Parise, M., Gunn, J., 2007. *Natural and anthropogenic hazards in karst areas: recognition, analysis and mitigation.* London: The Geological Society.

Pielke, R.A., Pitman, A., Niyogi, D., Mahmood, R., McAlpine, C., Hossain, F., Goldewijk, K.K., Nair, U., Betts, R., Fall, S., Reichstein, M., 2011. Land use/land cover changes and climate: modeling analysis and observational evidence. *Wiley Interdisciplinary Reviews: Climate Change 2*(6), 828-850.

Piotrowski, A., Napiórkowski, J., Kiczko, A., 2012. Corrigendum to: "Differential evolution algorithm with separated groups for multi-dimensional optimization problems." *European Journal of Operational Research* 219(2), 488.

Powers, J.G., Shevenell, L., 2000. Transmissivity estimates from well hydrographs in karst and fractured aquifers. *Ground Water 38*(3), 361-369.

Price, M., Low, R.G., McCann, C., 2000. Mechanisms of water storage and flow in the unsaturated zone of the Chalk aquifer. *Journal Hydrology* 233(1-4), 54-71.

Quinlan, J.F., Smart, P.L., Schindel, G.M., Alexander, E.C., Edwards, A.J., Smith, A.R., 1991. Recommended administrative/regulatory definition of karst aquifer, principles for classification of carbonate aquifers, practical evaluation of vulnerability of karst aquifers, and determination of optimum sampling frequency at springs. *National Ground Water Association,* 573-635.

Reeder, P.P., 1989. *Effectiveness of Storm Water Drainage Wells in Reducing Sinkhole Flooding in Bowling Green, Kentucky.* M.S. Geoscience Thesis, Department of Geography and Geology, Western Kentucky University, Bowling Green, Kentucky.

Ritter, D.F., Kochel, R.C.,Miller, J.R., 2006. *Process geomorphology* (4th edition). Long Grove, Illinois: Waveland Press.

Ross, A. H., 2009. *Modeling Stormwater Pollutant Transport in a Karst Region—Bowling Green Kentucky*. M.S. Geoscience Thesis, Department of Geography and Geology, Western Kentucky University, Bowling Green, Kentucky. Available online at: http://digitalcommons.wku.edu/theses/105/

Safe Drinking Water Act, 1974. Available online at: https://www.epa.gov/sdwa.

Sahoo, S.K., Jha, M.K., 2013. Prédiction du niveau de la nappe par les techniques de régression linéaire multiple et de kréseau neuronal artificiel: Évaluation comparative. *Hydrogeology Journal*, 21(8), 1865–1887.

Salzman, J., Thompson, B.H., 2003. *Environmental Law and Policy*. New York: Foundation Press.

Schiff, K., 2014. Was the Clean Water Act Effective? *Marine Pollution Bulletin* 81(1), 1-2.

Shevenell, L., 1999. Analysis of well hydrographs in a karst aquifer: estimates of specific yields and continuum transmissivities. *Journal of Hydrology 174*(3), 331-355.

Sharif, H.O., Sparks, L., Hassan, A.A., Zeitler, J., Xie, H., 2010. Application of a distributed hydrologic model to the November 17, 2004, flood of Bull Creek watershed, Austin, Texas. *Journal of Hydrologic engineering* 15(8), 651-657.

Shanmuganathan, S., Samarasinghe, S., 2016. *Artificial Neural Network Modelling*, Cham: Springer International Publishing.

Shi, P., Ge, Y., Yuan, Y., Guo, W., 2005. Integrated risk management of flood disasters in metropolitan areas of China. *Water Resources Development 21*(4), 613-627.

Singh, R.N., Reed, S.M., 1988. Mathematical modelling for estimation of minewater inflow to a surface mining operation. *International Journal of Mine Water 7*(3), 1-33.

Slattery, T., 2012. Personal Communication, Bowling Green, KY, City Hydrologist (D. Nedvidek, Interviewer).

Stephenson, J.B., Zhou, W.F., Beck, B.F., Green, T.S., 1999. Highway stormwater runoff in karst areas—preliminary results of baseline monitoring and design of a treatment system for a sinkhole in Knoxville, Tennessee. *Engineering Geology 52*(1), 51-59.

Stevanović, Z., 2015. *Karst Aquifers—Characterization and Engineering*. Dordrecht,

London: Springer International Publishing.

Strassberg, G., Norman, J. L., Maidment, D. R., 2011. *Arc Hydro Groundwater-GIS for Hydrogeology*. Redlands, California: ESRI Press.

Toran, L., Herman, E.K.,White, W.B., 2007. Comparison of flowpaths to a well and spring in a karst aquifer. *Ground Water 45*(3), 281-287.

Toran, L., Gross, K.,Yang, Y., 2009. Effects of restricted recharge in an urban karst system. *Environmental Geology 58*(1), 131-139.

Tramblay, Y., Bouvier, C., Martin, C., Didon-Lescot, J.F., Todorovik, D., Domergue, J.M. 2010. Assessment of initial soil moisture conditions for event-based rainfall–runoff modelling. *Journal of Hydrology 387*(3), 176-187.

Trichakis, I.C., Nikolos, K., Karatzas, G.P., 2011. Artificial neural network (ANN) based modeling for karstic groundwater level simulation. *Water Resources Management*, 25(4), 1143–1152.

United States Department of Agriculture, 2004. *Soil Survey of Warren County Kentucky*. Warren County, Kentucky: National Resources Conservation Service

University of Kentucky, 2012. *Sinkhole Flooding*. Available Online at: <https://www.uky.edu/ KGS/ water/ general/karst/sinkhole_flooding.htm>

Underground Injection Control Program, 40 C.F.R. § 144, 2016.

United States Geological Survey, 2016. *USGS Current Conditions for USGS 03314500 BARREN RIVER AT BOWLING GREEN, KY*. Available online at: <http://waterdata.usgs.gov/ky/nwis/uv?site_no=03314500>

United States Census Bureau, 2015. *Population estimates, July 1, 2015, (V2015).* Available online at: <http://www.census.gov/quickfacts/table/PST0452 15/2108902>

Varouchakis, E.A., Hristopulos, D.T., Karatzas, G.P., 2012. Improving kriging of groundwater level data using nonlinear normalizing transformations—a field application. *Hydrological Sciences Journal* 57(7), 1404-1419.

Veni, G., 2002. Revising the karst map of the United States. *Journal of Cave and Karst Studies*, 64(1), 45-50.

Virdee, T.S.,Kottegoda, N.T., 1984. A brief review of kriging and its application to optimal interpolation and observation well selection. *Hydrological Sciences Journal*, 29(4), 367-387.

Woodson, F.J., 1981. Lithologic and structural controls on karst landforms of the Mitchell Plain, Indiana, and Pennroyal Plateau, Kentucky. Indiana State University: Terre Haute, Indiana.

Worthington, S.R., 1999. A comprehensive strategy for understanding flow in carbonate aquifers. *Karst modeling: special publication* 5, 30-37.

White, S.S., Boswell, M.R., 2006. Planning for water quality: implementation of the NPDES phase II stormwater program in California and Kansas. *Journal of environmental planning and management* 49(1), 141-160.

White, S.S., Boswell, M.R., 2007. Stormwater quality and local government innovation. *Journal of the American Planning Association* 73(2), 185-193.

White, W.B., 1989. *Introduction to the karst hydrology of the Mammoth Cave area.* New York, New York: Springer Science + Business Media, LLC.

White, W.B., Culver, D.C., Herman, J.S., Kane, T.C., Mylroie, J.E., 1995. Karst lands. *American Scientist 83*(5), 450-459.

White, W.B., 1999. Conceptual models for karstic aquifers. *Karst Modeling Special Publication.* 5, 11–16.

White, W.B., 2002. Karst hydrology: recent developments and open questions. *Engineering Geology 65*(2), 85-105.

Williams, P.W., 1993. *Karst terrains: Environmental Changes and Human Impact* (25th Volume). Cremlingen, Germany: Catena Verlag.

Williams, P. W., 1983. The role of the subcutaneous zone in karst hydrology. *Journal Hydrology* 61, 45-67.

Xmswiki.com, 2016. *WMS:Storage Capacity Curves - XMS Wiki.* Available online at: http://www.xmswiki.com/wiki/WMS:Storage_Capacity_Curves

Yang, L., Smith, J.A., Baeck, M.L., Zhang, Y., 2016. Flash flooding in small urban watersheds: Storm event hydrologic response. *Water Resources Research* 52(6), 4571-4589.

Zheng, Z.,Qi, S., 2011. Potential flood hazard due to urban expansion in the karst mountainous region of North China. *Regional Environmental Change* 11(3), 439-440.

Zhou, W., 2007. Drainage and flooding in karst terranes. *Environmental Geology* 51(6), 963-973.

Appendix A

Well Hydrographs

This appendix contains the hydrographs for the monitored Injection Well (10/1/2017 – 04/30/2018) that were not featured above.

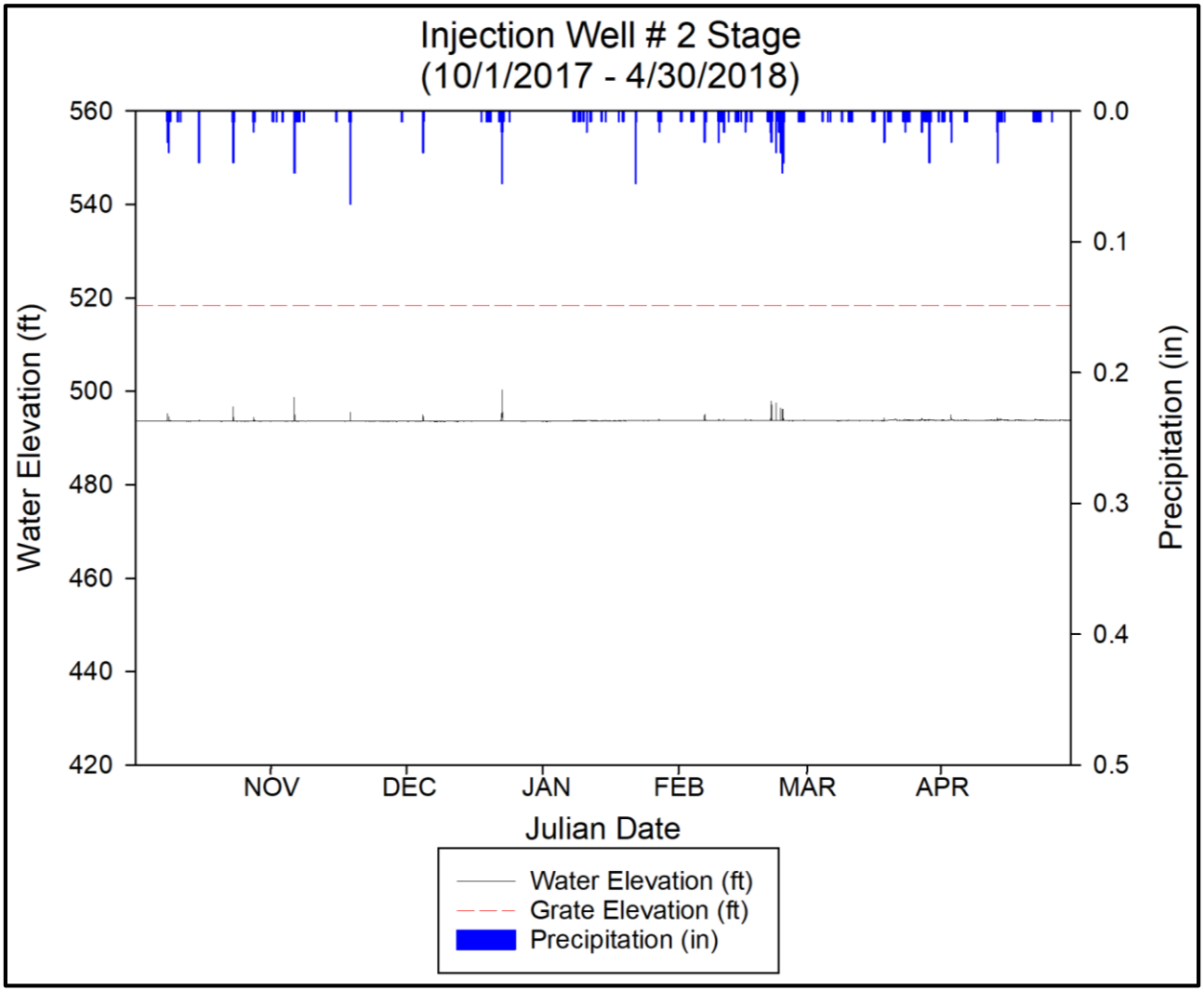

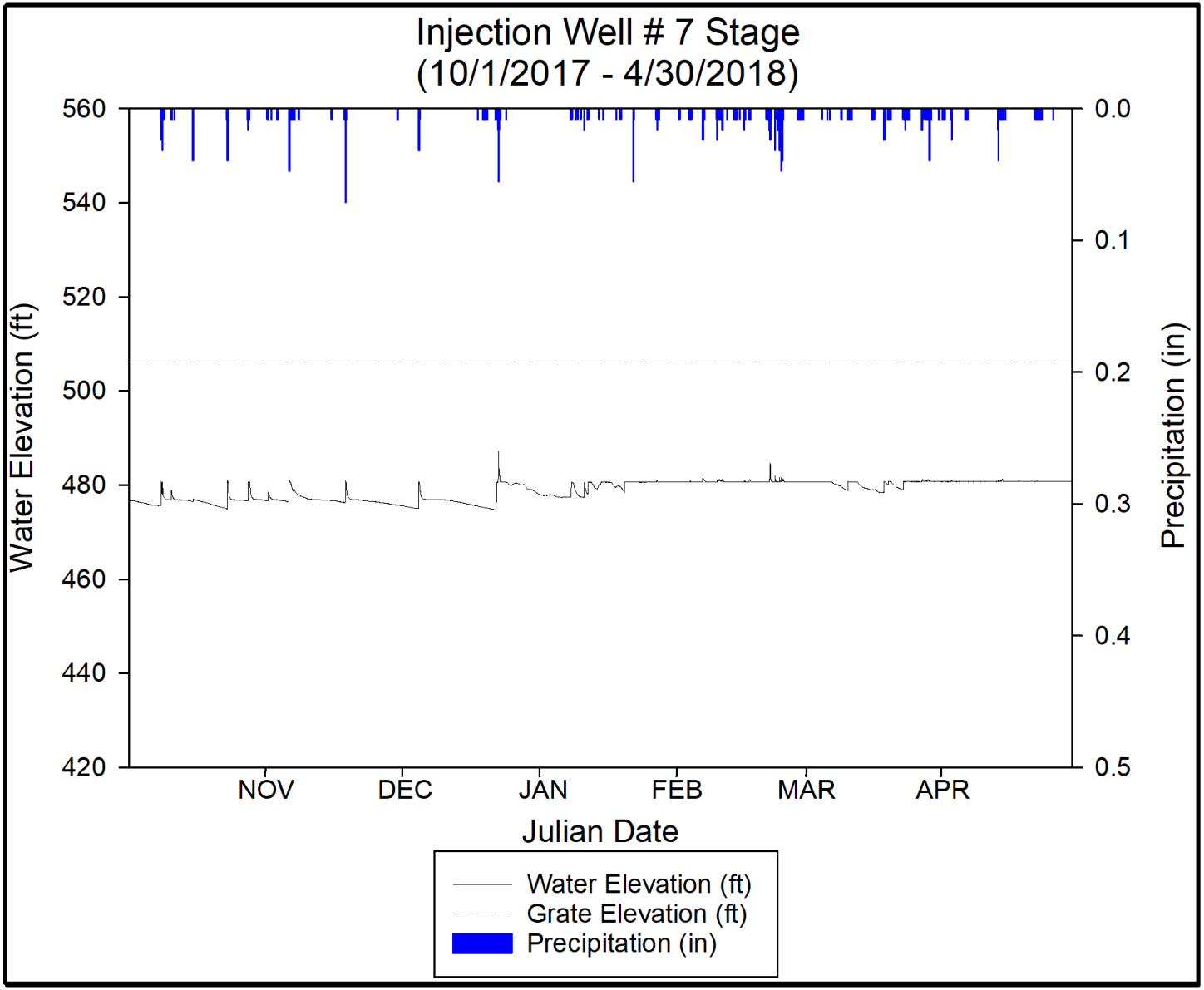
Injection Well # 7 Stage
(10/1/2017 - 4/30/2018)
Water Elevation (ft)
Precipitation (in)
560
540
520
500
480
460
440
420
0.0
0.1
0.2
0.3
0.4
0.5
NOV
DEC
JAN
FEB
MAR
APR
Julian Date
Water Elevation (ft)
Grate Elevation (ft)
Precipitation (in)

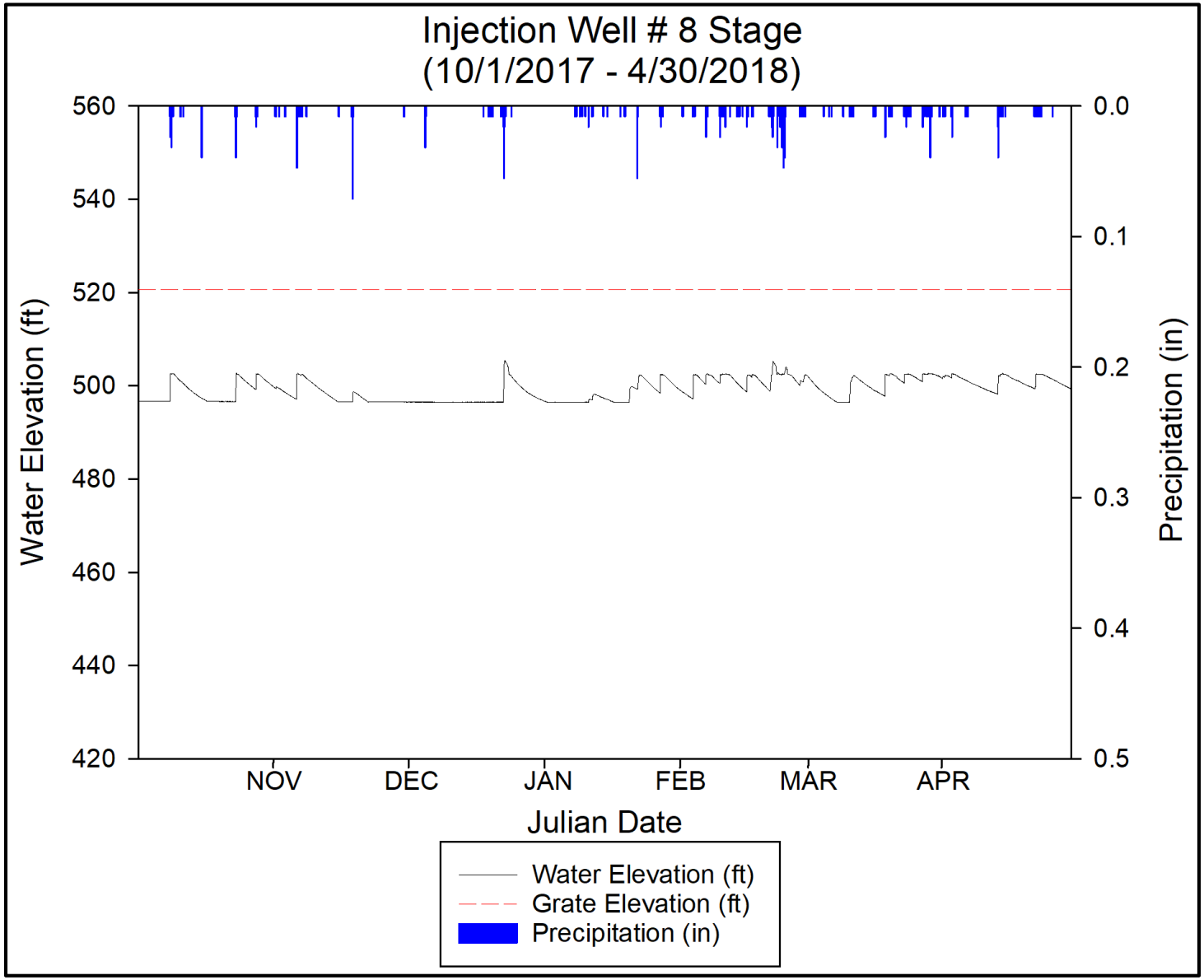
Injection Well # 8 Stage
(10/1/2017 - 4/30/2018)
Water Elevation (ft)
560
540
520
500
480
460
440
420
0.0
0.1
0.2
0.3
0.4
0.5
Precipitation (in)
NOV
DEC
JAN
FEB
MAR
APR
Julian Date
Water Elevation (ft)
Grate Elevation (ft)
Precipitation (in)

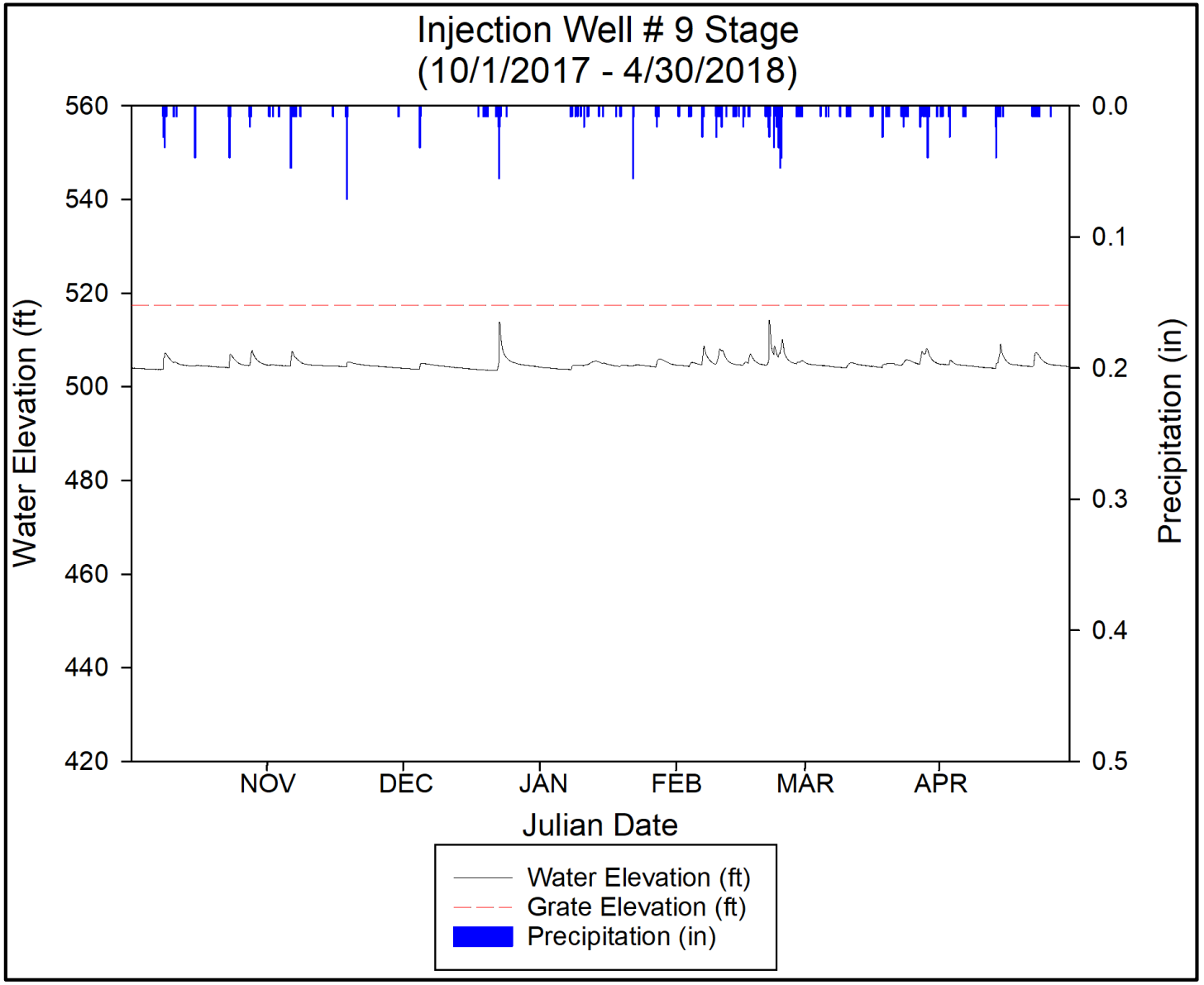
Injection Well # 9 Stage
(10/1/2017 - 4/30/2018)
Water Elevation (ft)
560
540
520
500
480
460
440
420
0.0
0.1
0.2
0.3
0.4
0.5
Precipitation (in)
NOV
DEC
JAN
FEB
MAR
APR
Julian Date
Water Elevation (ft)
Grate Elevation (ft)
Precipitation (in)

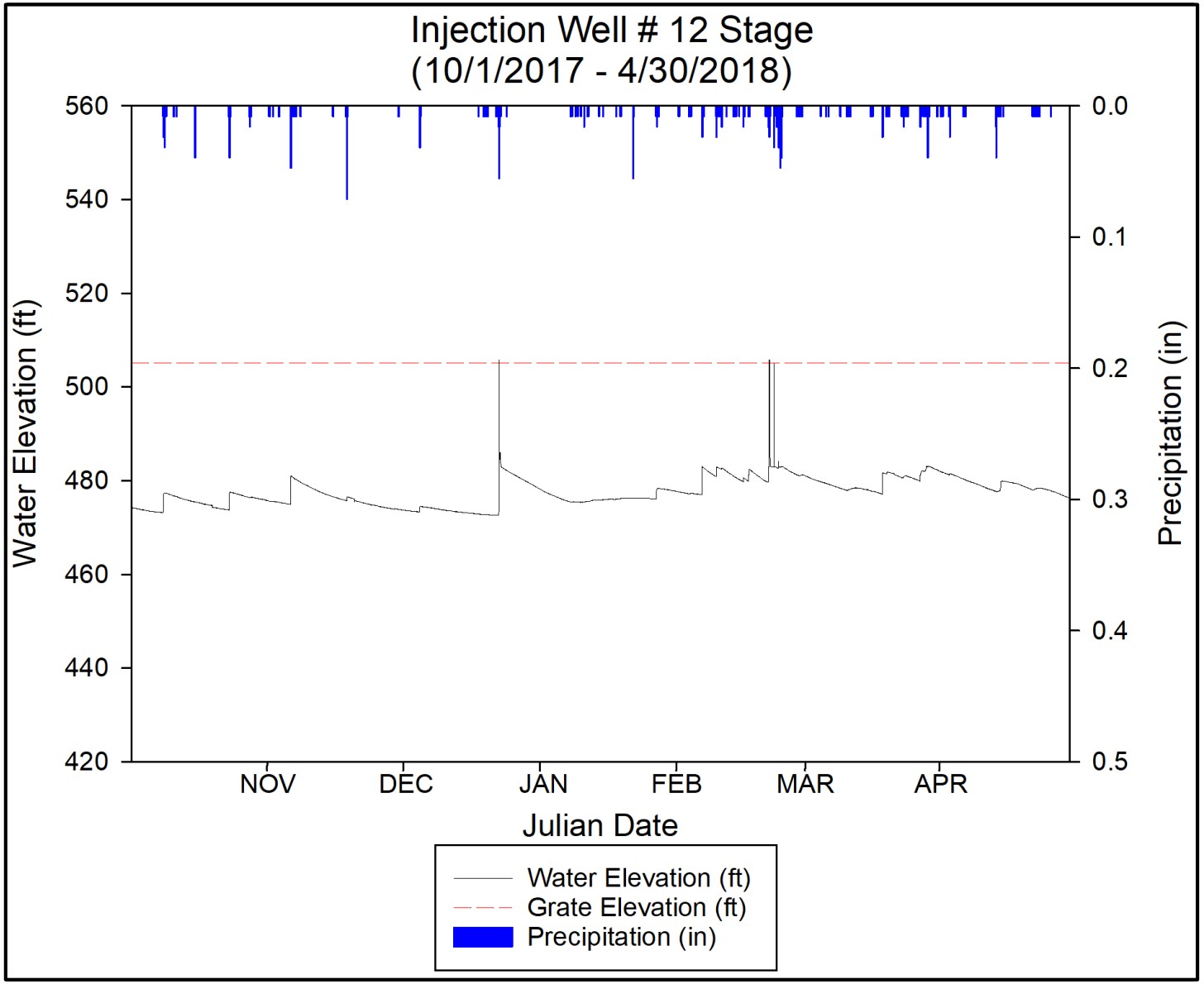
Injection Well # 12 Stage
(10/1/2017 - 4/30/2018)
Water Elevation (ft)
560
540
520
500
480
460
440
420
0.0
0.1
0.2
0.3
0.4
0.5
Precipitation (in)
NOV
DEC
JAN
FEB
MAR
APR
Julian Date
Water Elevation (ft)
Grate Elevation (ft)
Precipitation (in)

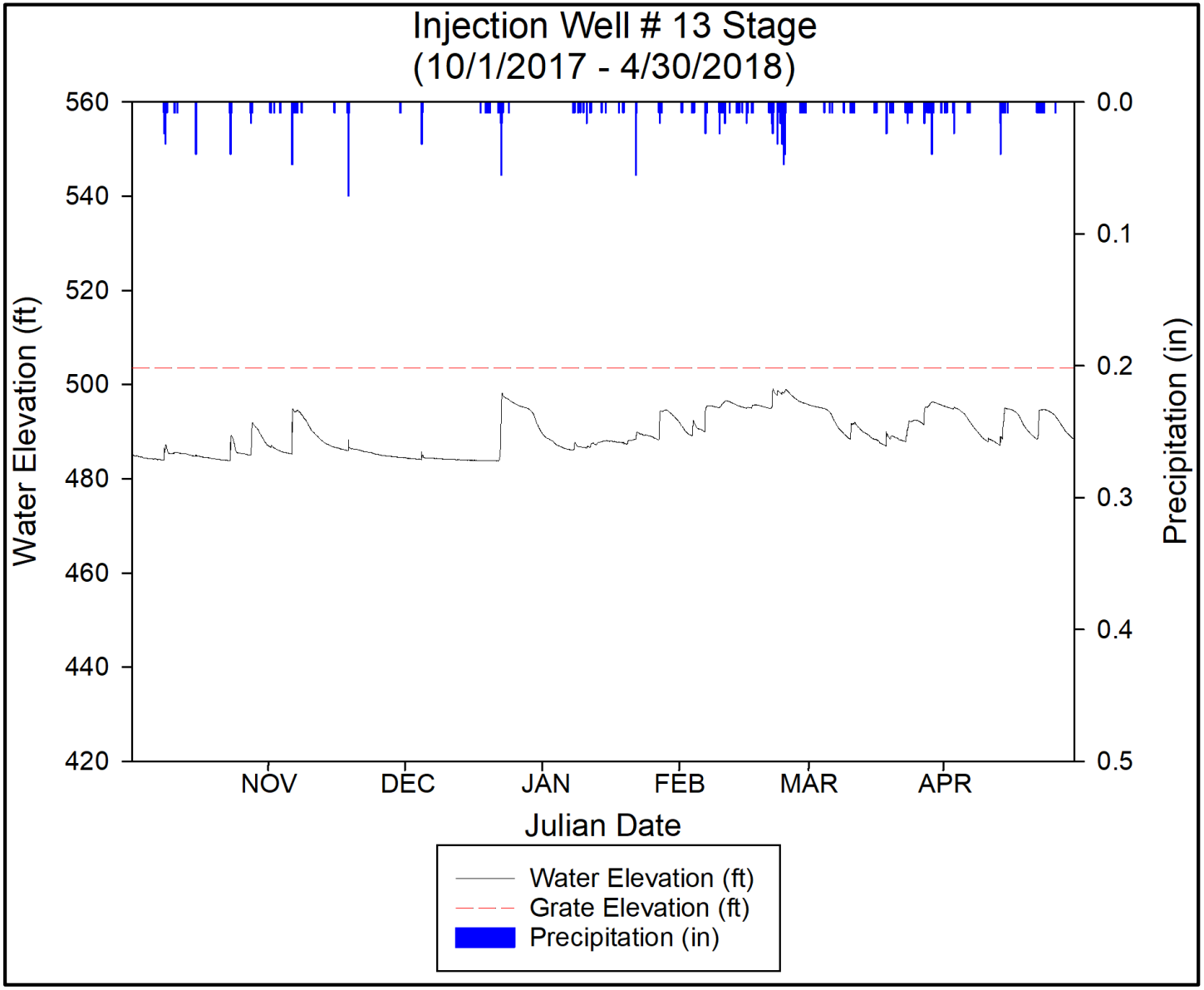
Injection Well # 13 Stage
(10/1/2017 - 4/30/2018)
Water Elevation (ft)
Precipitation (in)
560
540
520
500
480
460
440
420
0.0
0.1
0.2
0.3
0.4
0.5
NOV
DEC
JAN
FEB
MAR
APR
Julian Date
Water Elevation (ft)
Grate Elevation (ft)
Precipitation (in)

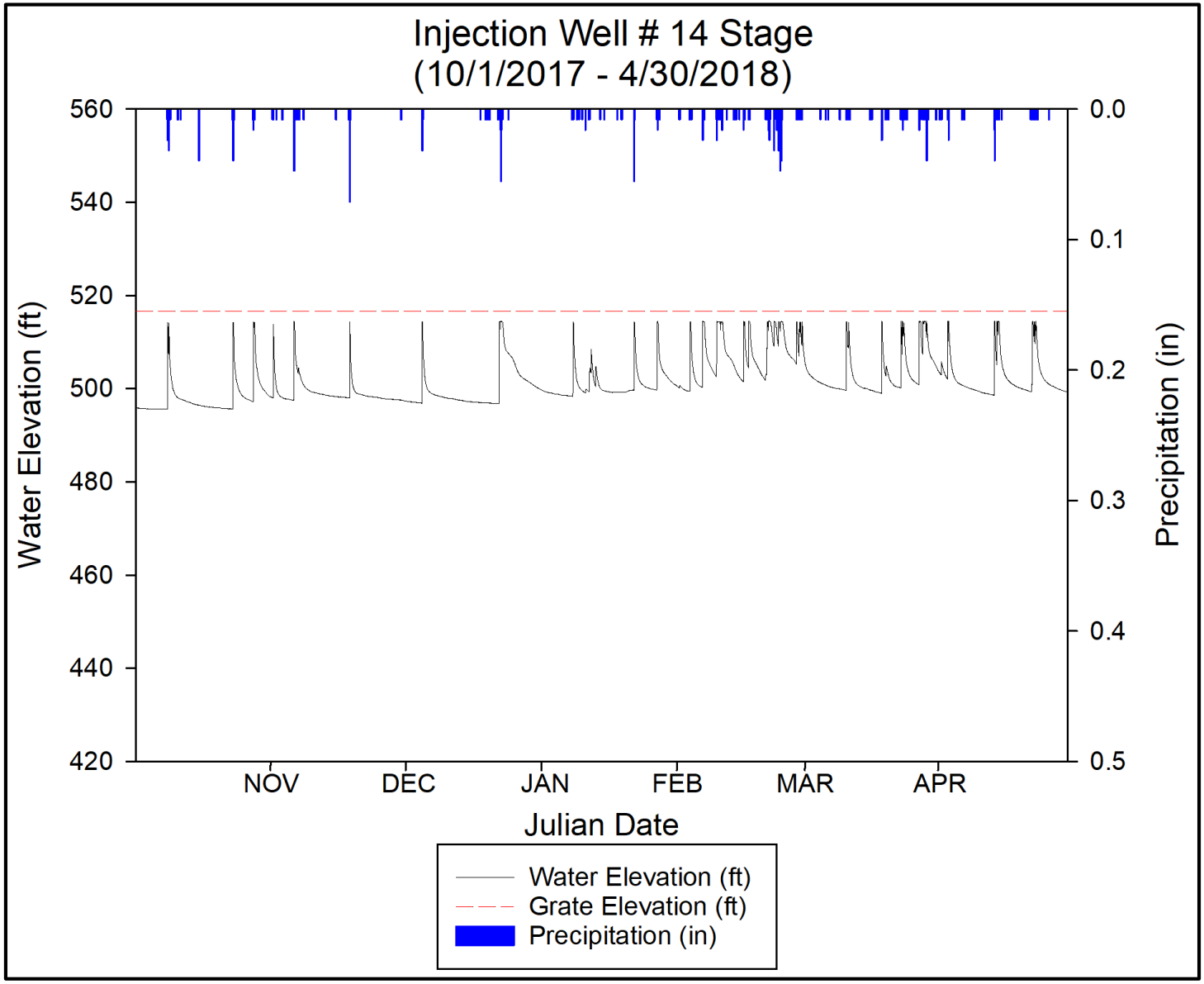
Injection Well # 14 Stage
(10/1/2017 - 4/30/2018)
Water Elevation (ft)
Precipitation (in)
560
540
520
500
480
460
440
420
0.0
0.1
0.2
0.3
0.4
0.5
NOV
DEC
JAN
FEB
MAR
APR
Julian Date
Water Elevation (ft)
Grate Elevation (ft)
Precipitation (in)

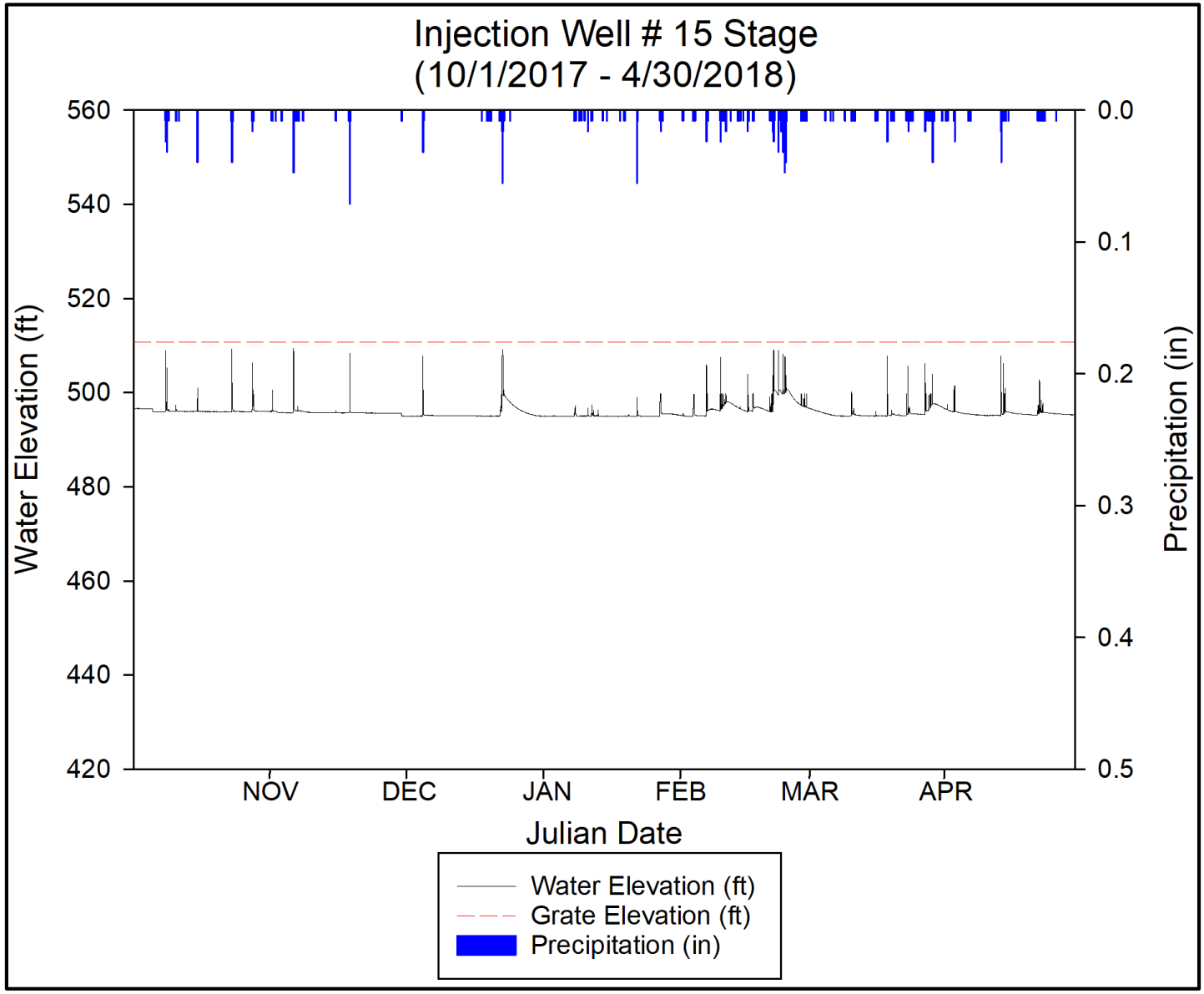
Injection Well # 15 Stage
(10/1/2017 - 4/30/2018)
Water Elevation (ft)
560
540
520
500
480
460
440
420
0.0
0.1
0.2
0.3
0.4
0.5
Precipitation (in)
NOV
DEC
JAN
FEB
MAR
APR
Julian Date
Water Elevation (ft)
Grate Elevation (ft)
Precipitation (in)

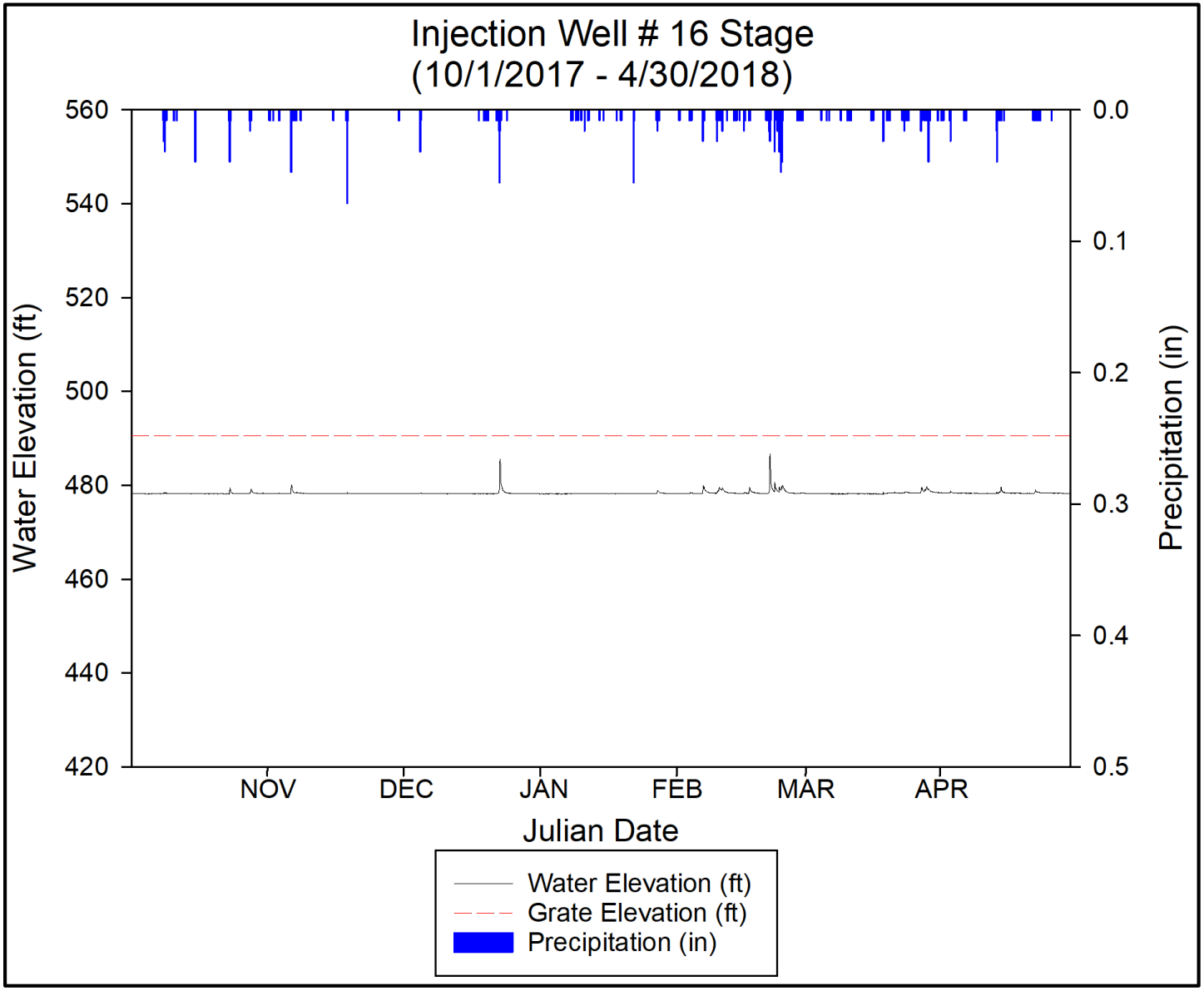
Injection Well # 16 Stage
(10/1/2017 - 4/30/2018)
Water Elevation (ft)
Precipitation (in)
560
540
520
500
480
460
440
420
0.0
0.1
0.2
0.3
0.4
0.5
NOV
DEC
JAN
FEB
MAR
APR
Julian Date
Water Elevation (ft)
Grate Elevation (ft)
Precipitation (in)

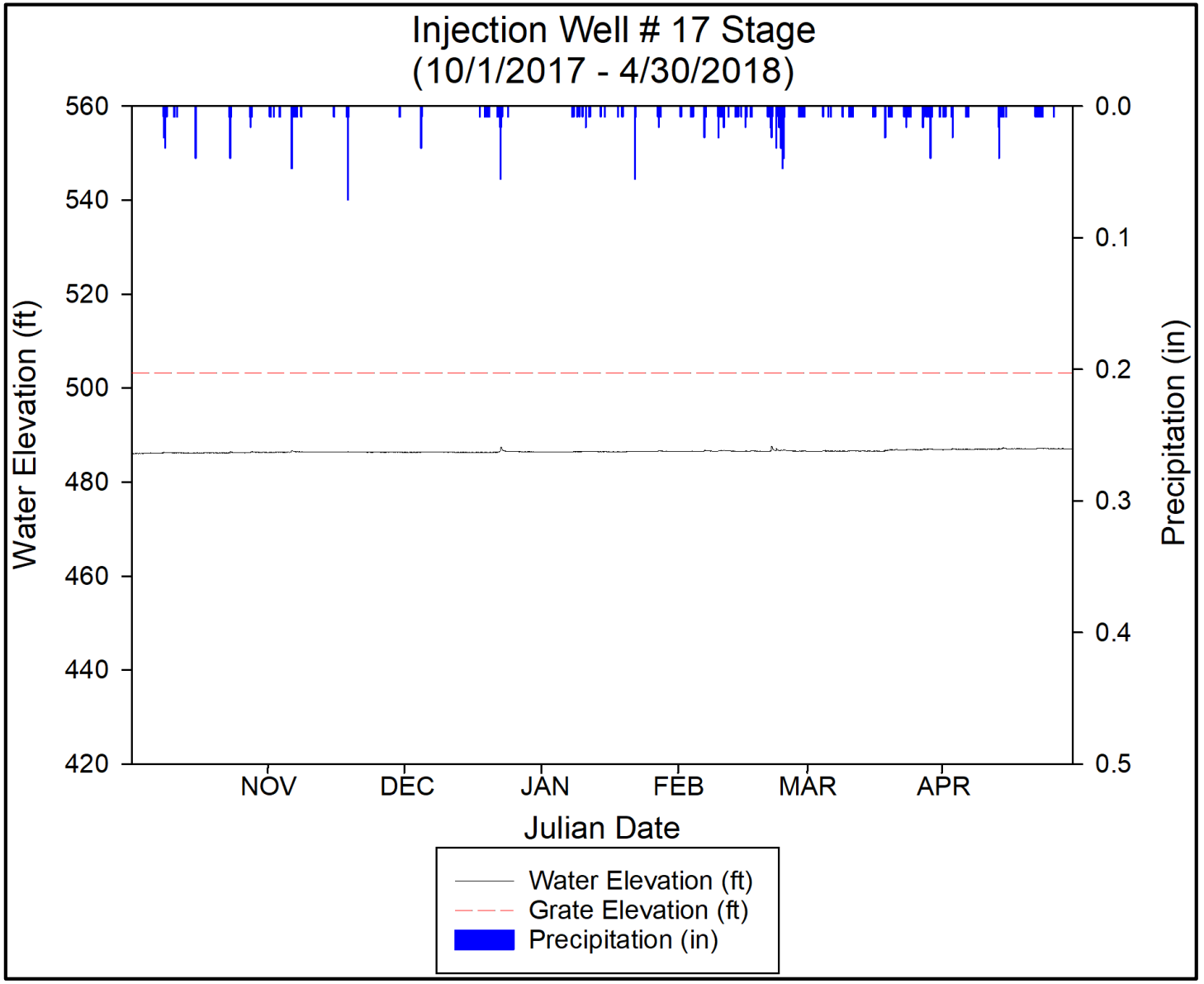
Injection Well # 17 Stage
(10/1/2017 - 4/30/2018)
Water Elevation (ft)
560
540
520
500
480
460
440
420
0.0
0.1
0.2
0.3
0.4
0.5
Precipitation (in)
NOV
DEC
JAN
FEB
MAR
APR
Julian Date
Water Elevation (ft)
Grate Elevation (ft)
Precipitation (in)

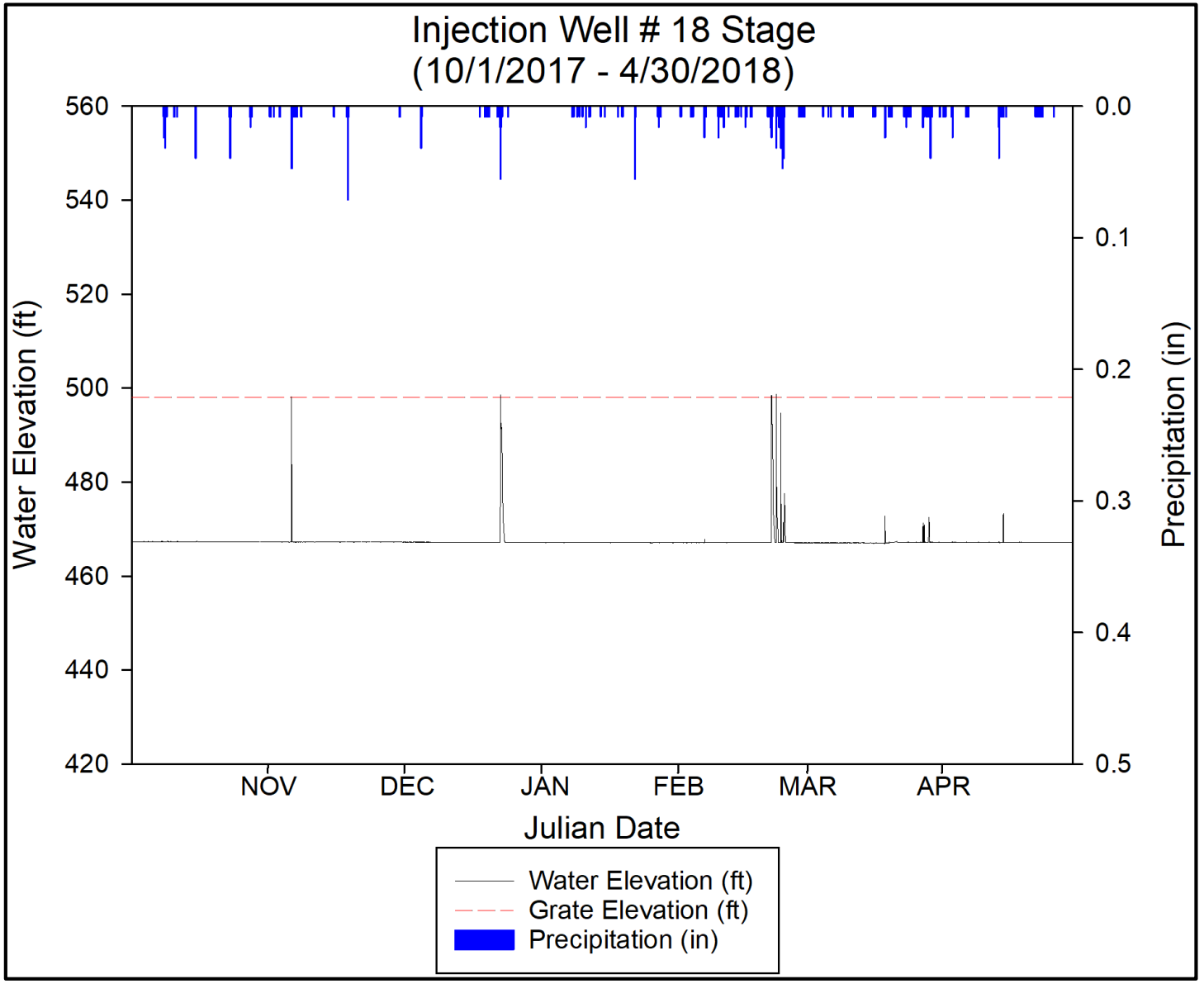
Injection Well # 18 Stage
(10/1/2017 - 4/30/2018)
Water Elevation (ft)
Precipitation (in)
560
540
520
500
480
460
440
420
0.0
0.1
0.2
0.3
0.4
0.5
NOV
DEC
JAN
FEB
MAR
APR
Julian Date
Water Elevation (ft)
Grate Elevation (ft)
Precipitation (in)

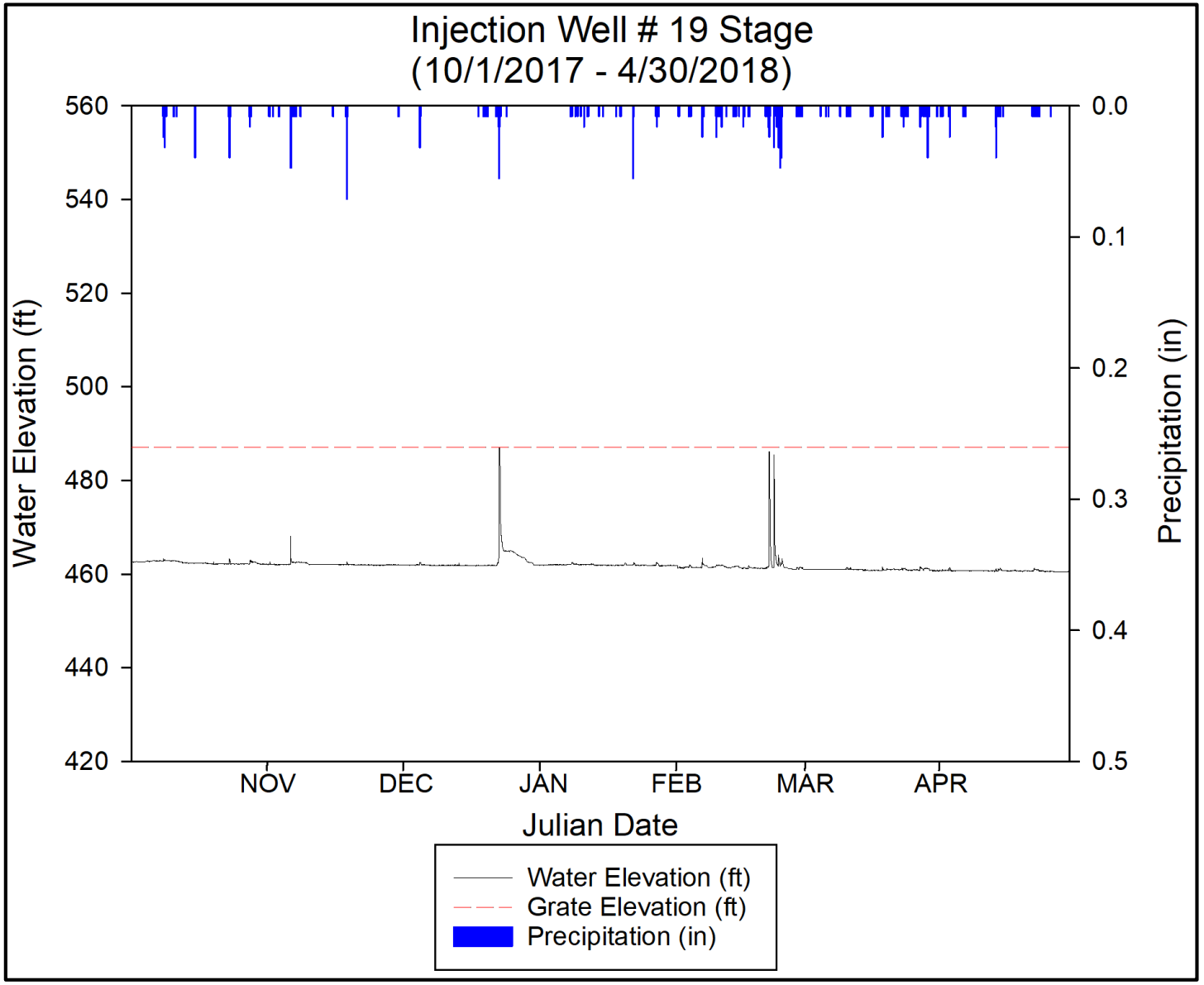
Injection Well # 19 Stage
(10/1/2017 - 4/30/2018)
Water Elevation (ft)
560
540
520
500
480
460
440
420
0.0
0.1
0.2
0.3
0.4
0.5
Precipitation (in)
NOV
DEC
JAN
FEB
MAR
APR
Julian Date
Water Elevation (ft)
Grate Elevation (ft)
Precipitation (in)

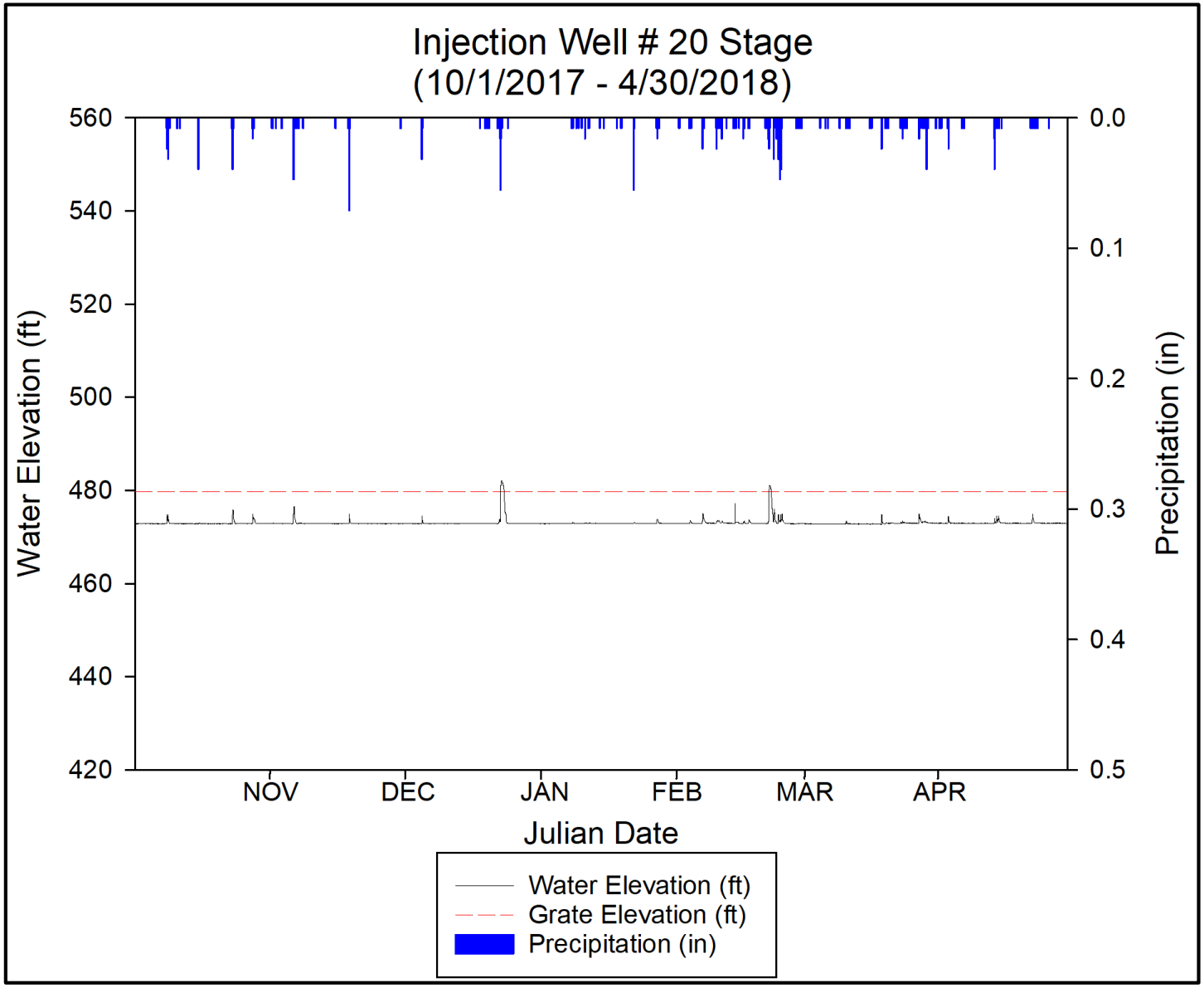
Injection Well # 20 Stage
(10/1/2017 - 4/30/2018)
Water Elevation (ft)
Precipitation (in)
560
540
520
500
480
460
440
420
0.0
0.1
0.2
0.3
0.4
0.5
NOV
DEC
JAN
FEB
MAR
APR
Julian Date
Water Elevation (ft)
Grate Elevation (ft)
Precipitation (in)

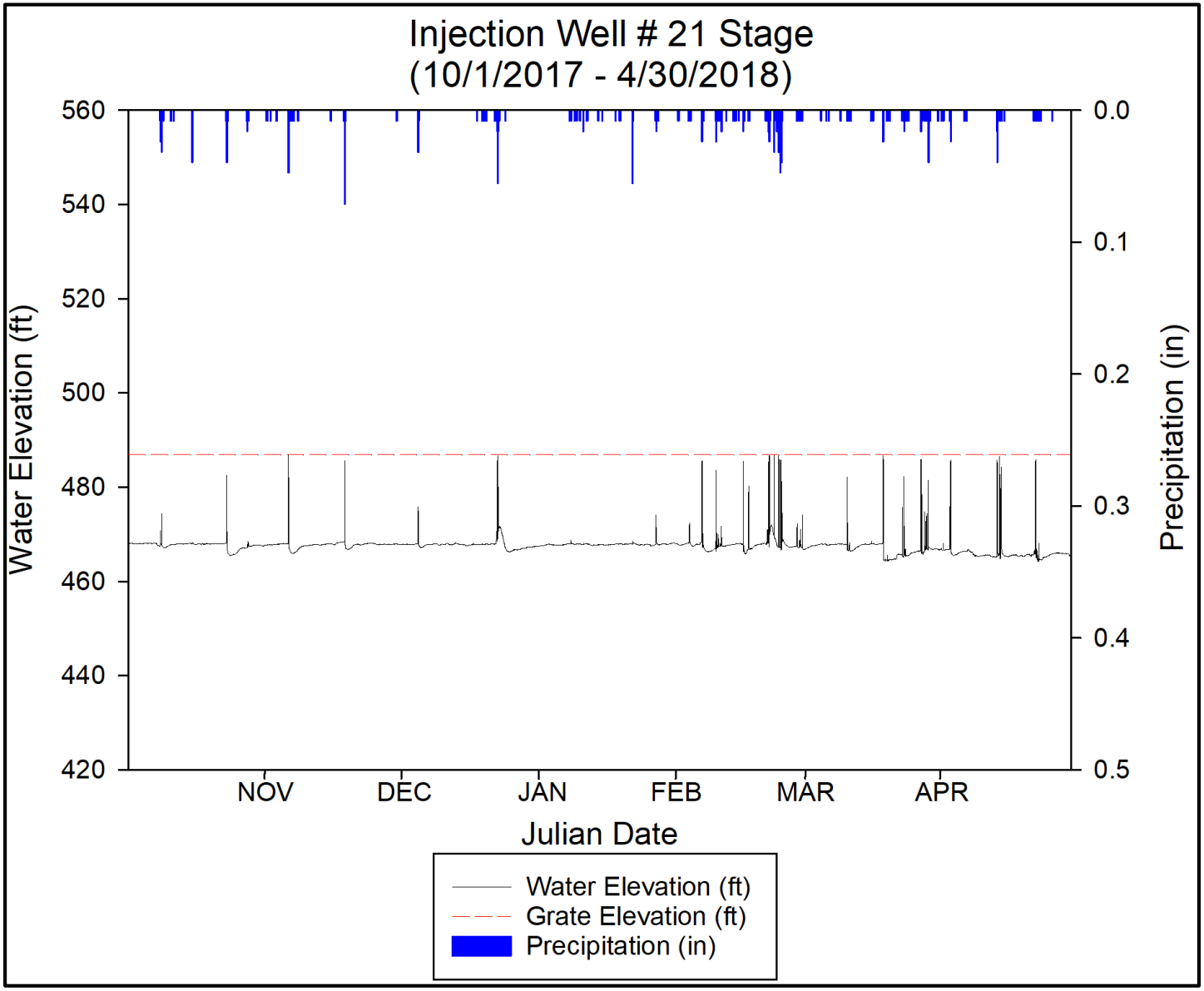
Injection Well # 21 Stage
(10/1/2017 - 4/30/2018)
Water Elevation (ft)
Precipitation (in)
560
540
520
500
480
460
440
420
0.0
0.1
0.2
0.3
0.4
0.5
NOV
DEC
JAN
FEB
MAR
APR
Julian Date
Water Elevation (ft)
Grate Elevation (ft)
Precipitation (in)

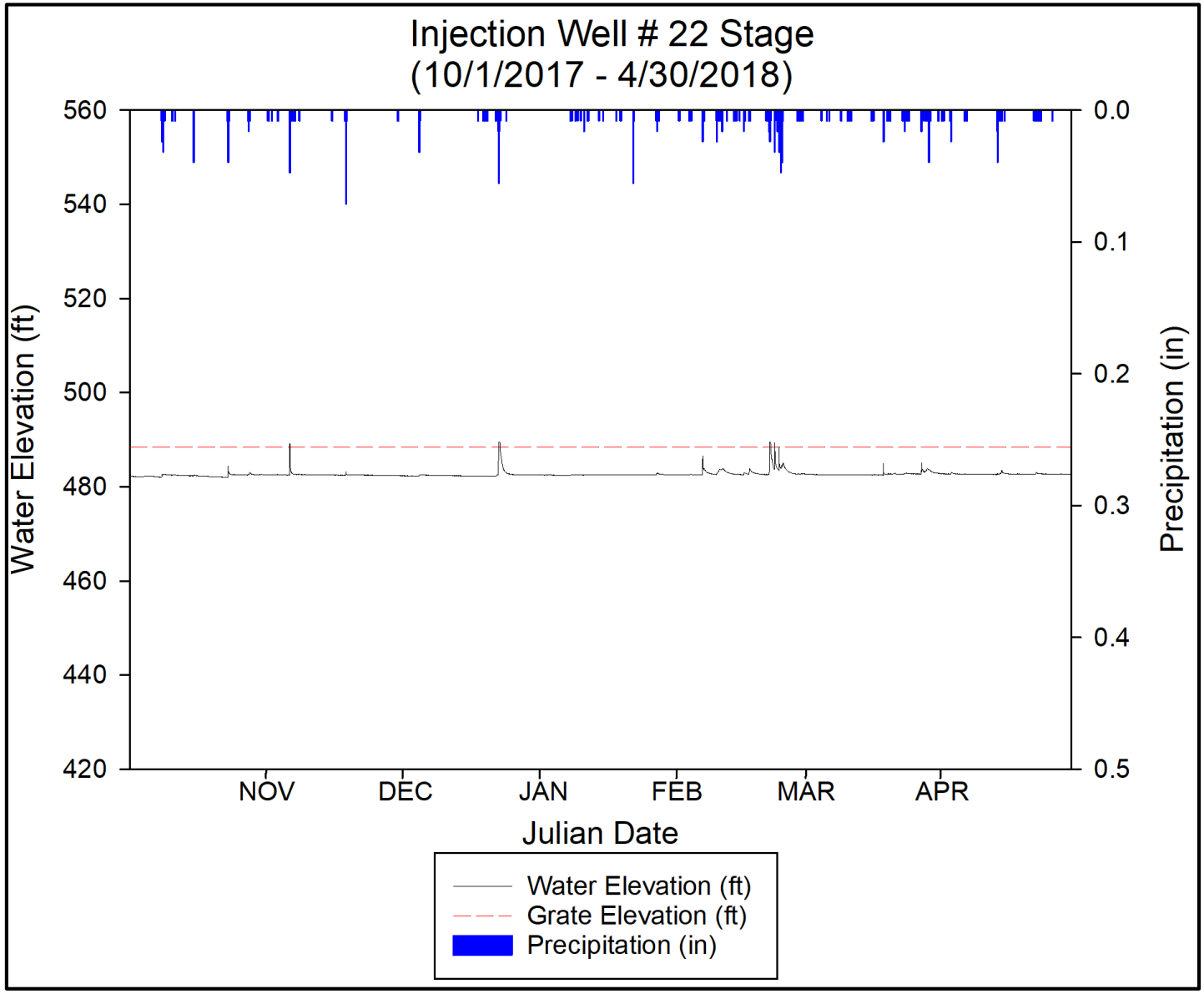
Injection Well # 22 Stage
(10/1/2017 - 4/30/2018)
Water Elevation (ft)
Precipitation (in)
560
540
520
500
480
460
440
420
0.0
0.1
0.2
0.3
0.4
0.5
NOV
DEC
JAN
FEB
MAR
APR
Julian Date
Water Elevation (ft)
Grate Elevation (ft)
Precipitation (in)

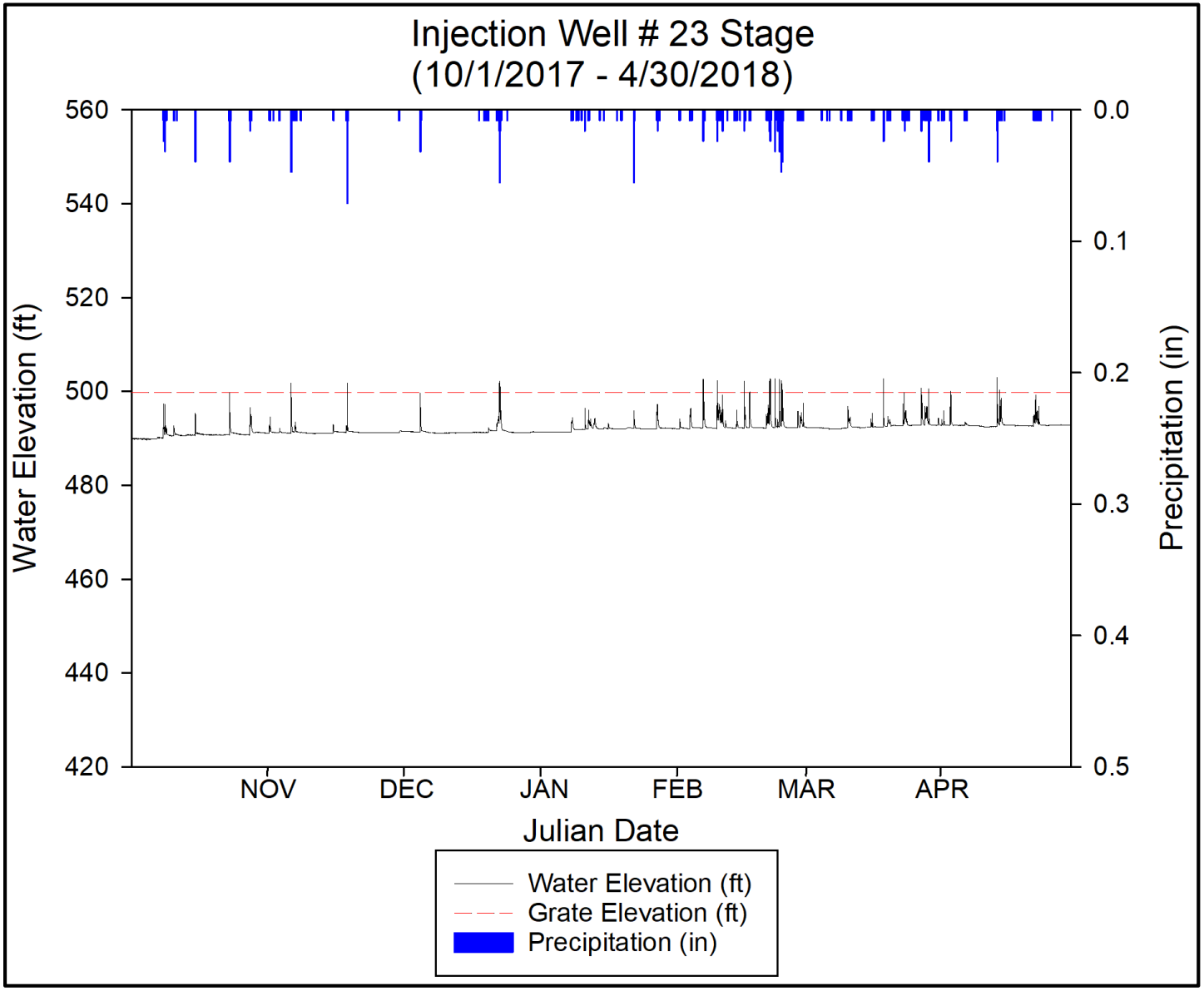
Injection Well # 23 Stage
(10/1/2017 - 4/30/2018)
Water Elevation (ft)
Precipitation (in)
560
540
520
500
480
460
440
420
0.0
0.1
0.2
0.3
0.4
0.5
NOV
DEC
JAN
FEB
MAR
APR
Julian Date
Water Elevation (ft)
Grate Elevation (ft)
Precipitation (in)

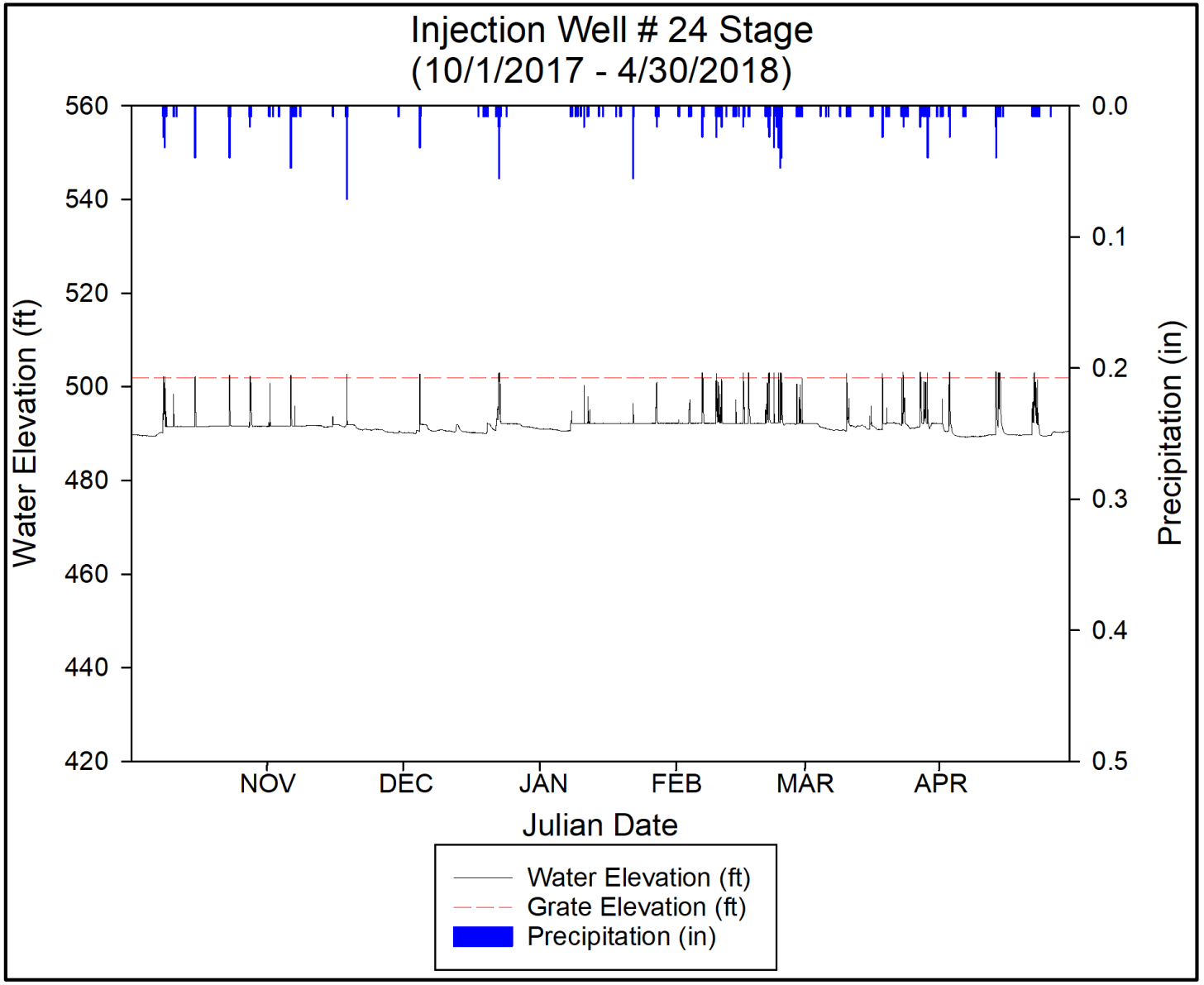
Injection Well # 24 Stage
(10/1/2017 - 4/30/2018)
Water Elevation (ft)
Precipitation (in)
560
540
520
500
480
460
440
420
0.0
0.1
0.2
0.3
0.4
0.5
NOV
DEC
JAN
FEB
MAR
APR
Julian Date
Water Elevation (ft)
Grate Elevation (ft)
Precipitation (in)

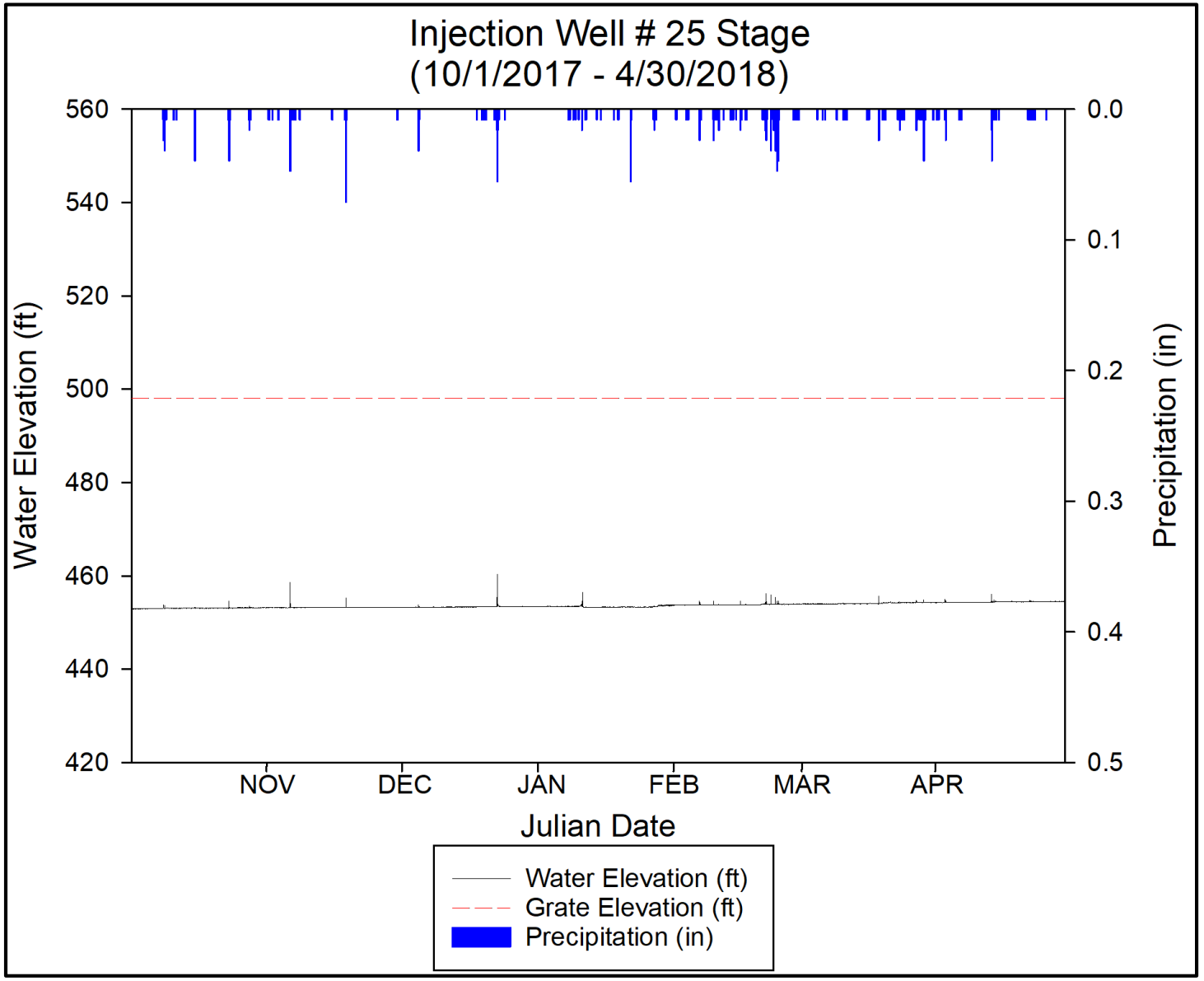
Injection Well # 25 Stage
(10/1/2017 - 4/30/2018)
Water Elevation (ft)
Precipitation (in)
560
540
520
500
480
460
440
420
0.0
0.1
0.2
0.3
0.4
0.5
NOV
DEC
JAN
FEB
MAR
APR
Julian Date
Water Elevation (ft)
Grate Elevation (ft)
Precipitation (in)

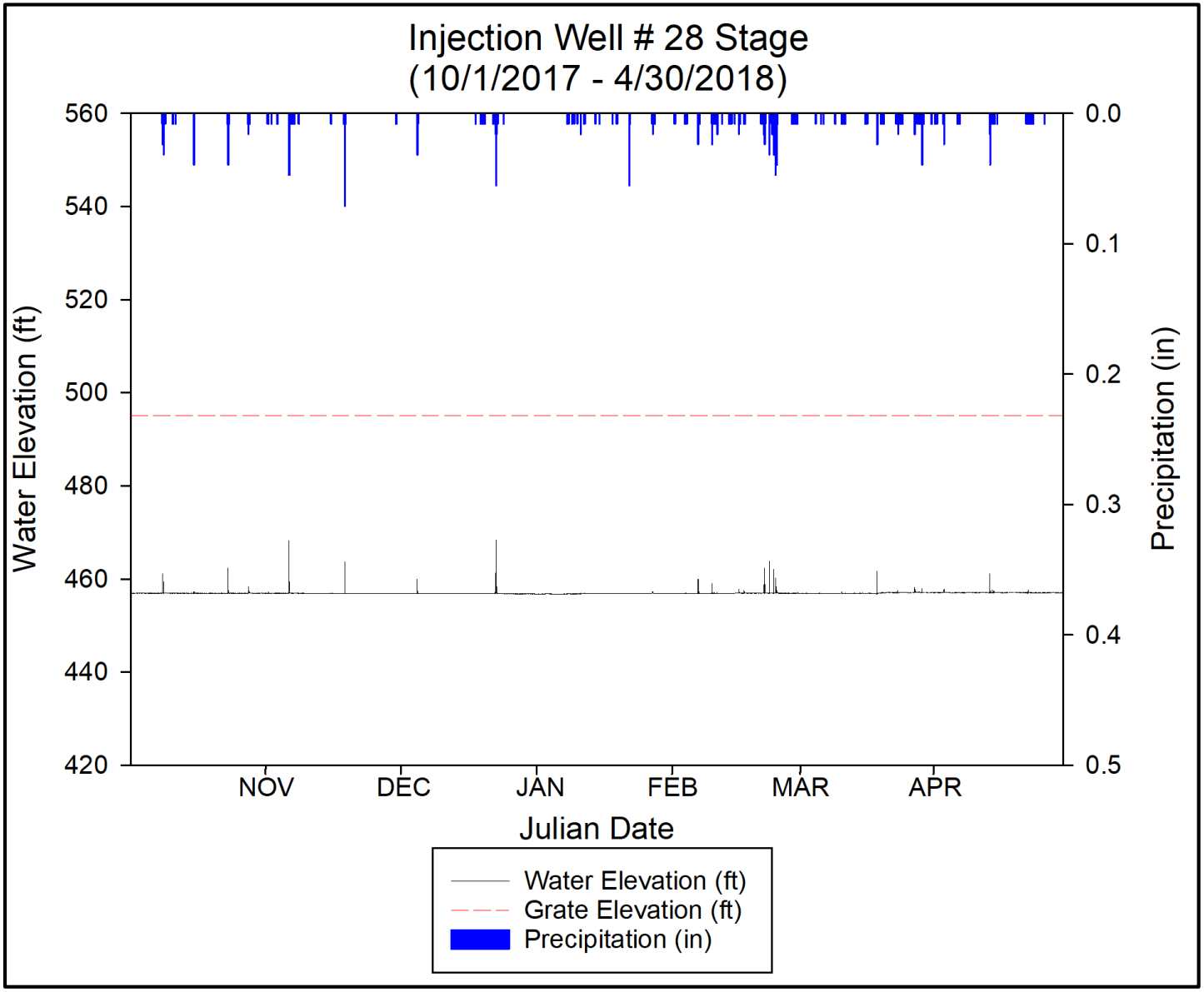
Injection Well # 28 Stage
(10/1/2017 - 4/30/2018)
Water Elevation (ft)
Precipitation (in)
560
540
520
500
480
460
440
420
0.0
0.1
0.2
0.3
0.4
0.5
NOV
DEC
JAN
FEB
MAR
APR
Julian Date
Water Elevation (ft)
Grate Elevation (ft)
Precipitation (in)

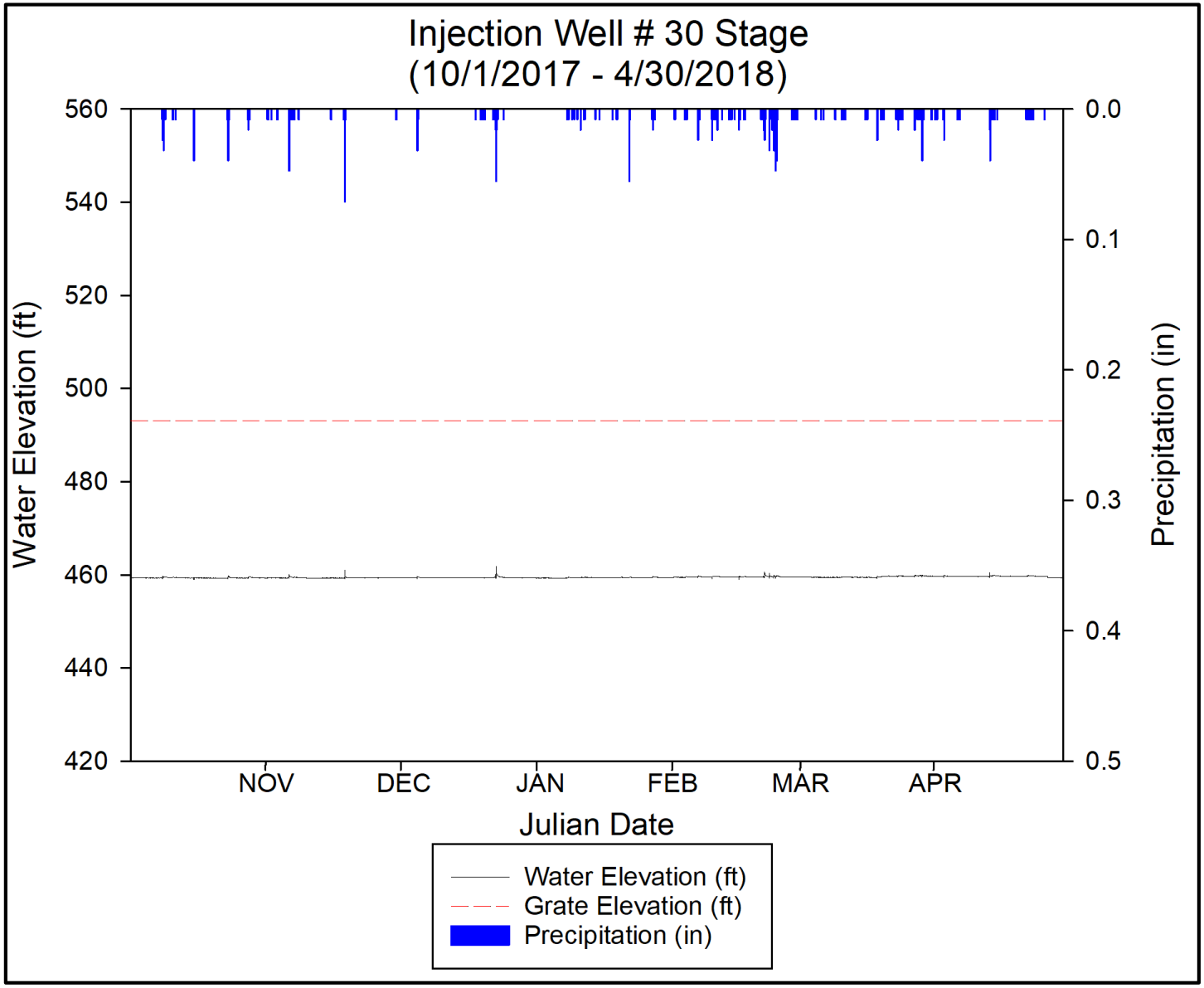
Injection Well # 30 Stage
(10/1/2017 - 4/30/2018)
Water Elevation (ft)
Precipitation (in)
560
540
520
500
480
460
440
420
0.0
0.1
0.2
0.3
0.4
0.5
NOV
DEC
JAN
FEB
MAR
APR
Julian Date
Water Elevation (ft)
Grate Elevation (ft)
Precipitation (in)

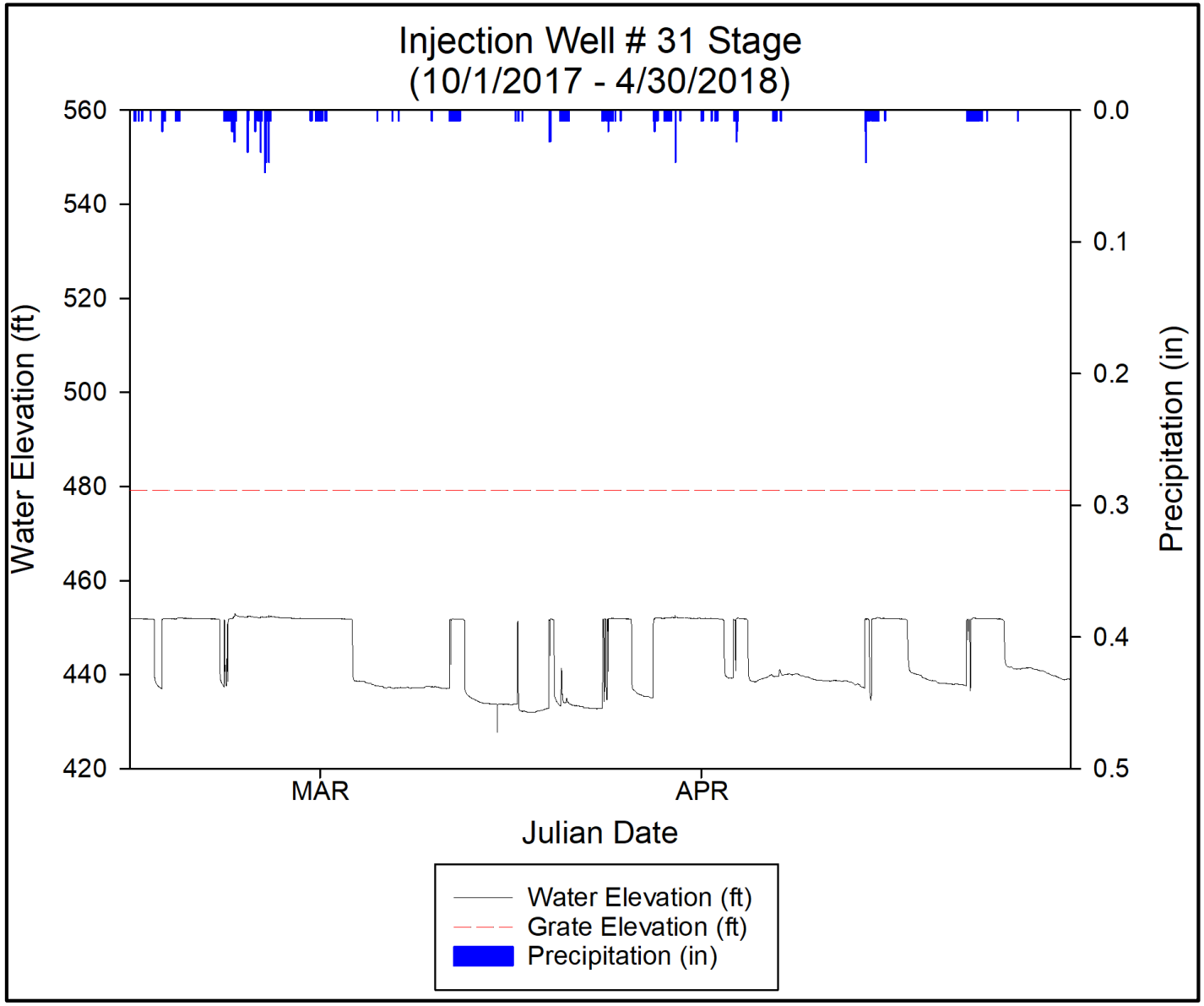
Injection Well # 31 Stage
(10/1/2017 - 4/30/2018)
Water Elevation (ft)
560
540
520
500
480
460
440
420
Precipitation (in)
0.0
0.1
0.2
0.3
0.4
0.5
MAR
APR
Julian Date
Water Elevation (ft)
Grate Elevation (ft)
Precipitation (in)

Appendix B

Recession Rate Boxplots

This appendix contains the Recession Rate Boxplots for the monitored Injection Wells (10/1/2017 – 04/30/2018).

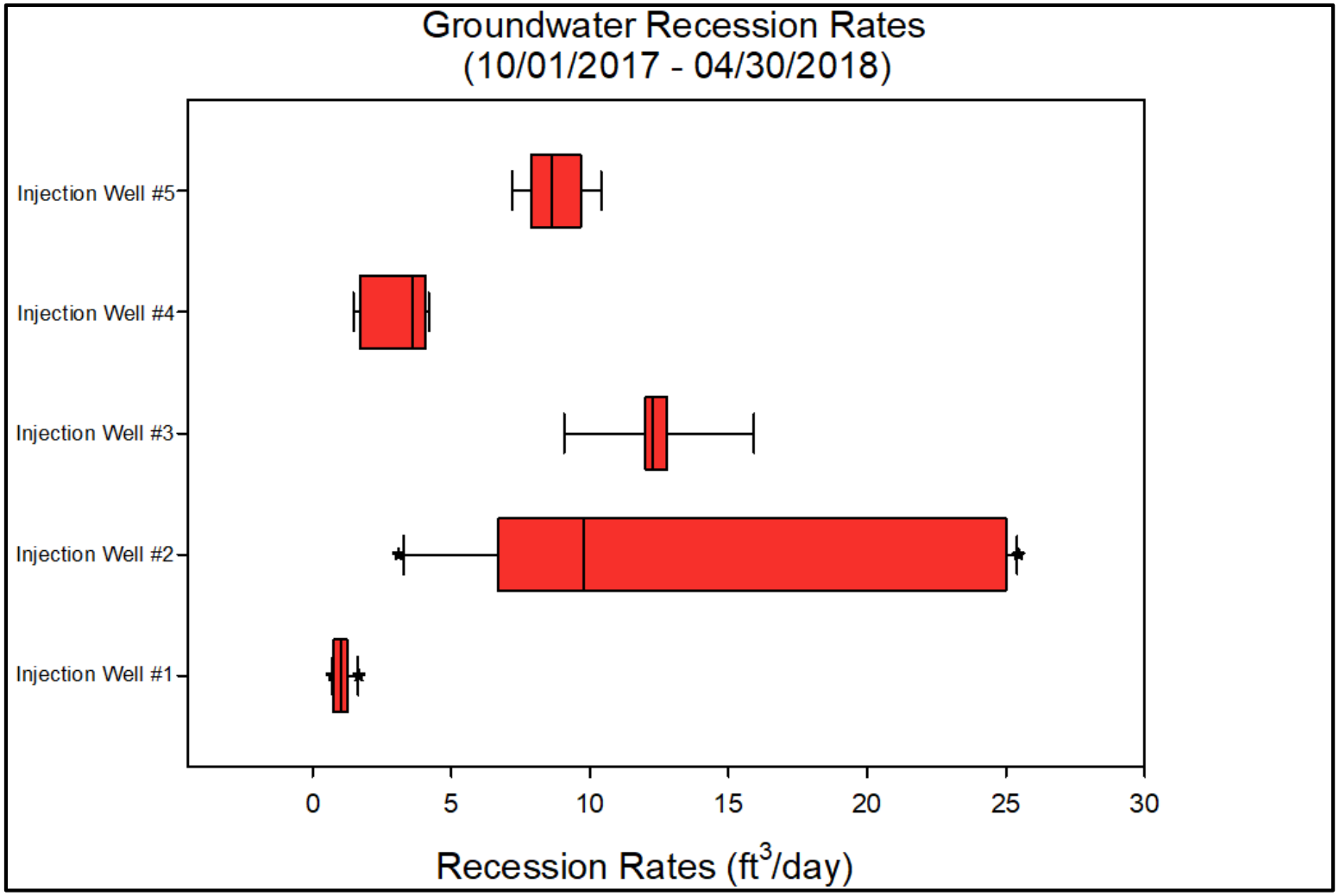

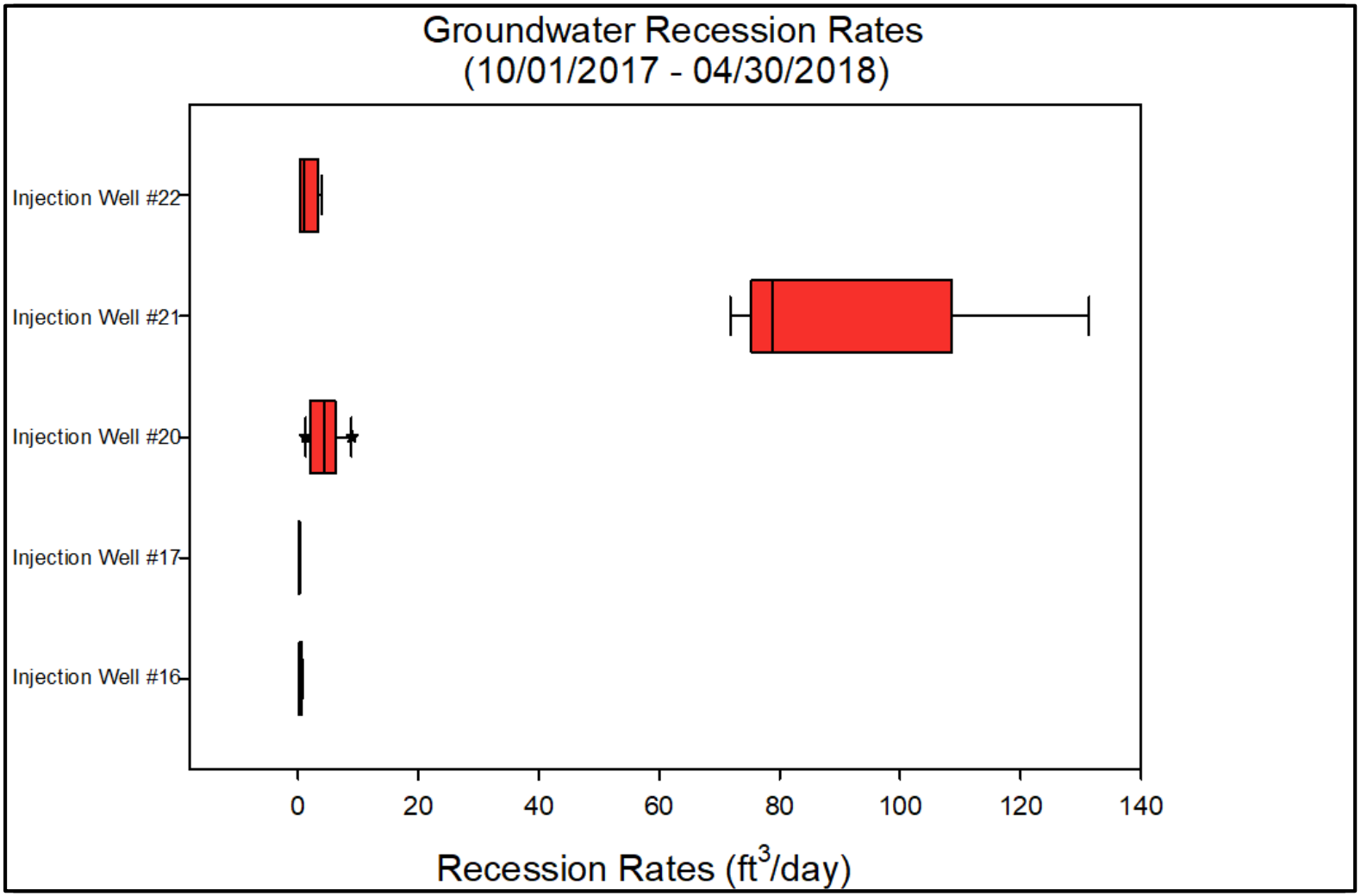
Groundwater Recession Rates
(10/01/2017 - 04/30/2018)
Injection Well #22
Injection Well #21
Injection Well #20
Injection Well #17
Injection Well #16
0
20
40
60
80
100
120
140
Recession Rates (ft3/day)

Appendix C

Groundwater Temperature Boxplots

This appendix contains the groundwater temperature boxplots for the monitored Injection Wells (10/1/2017 – 04/30/2018).

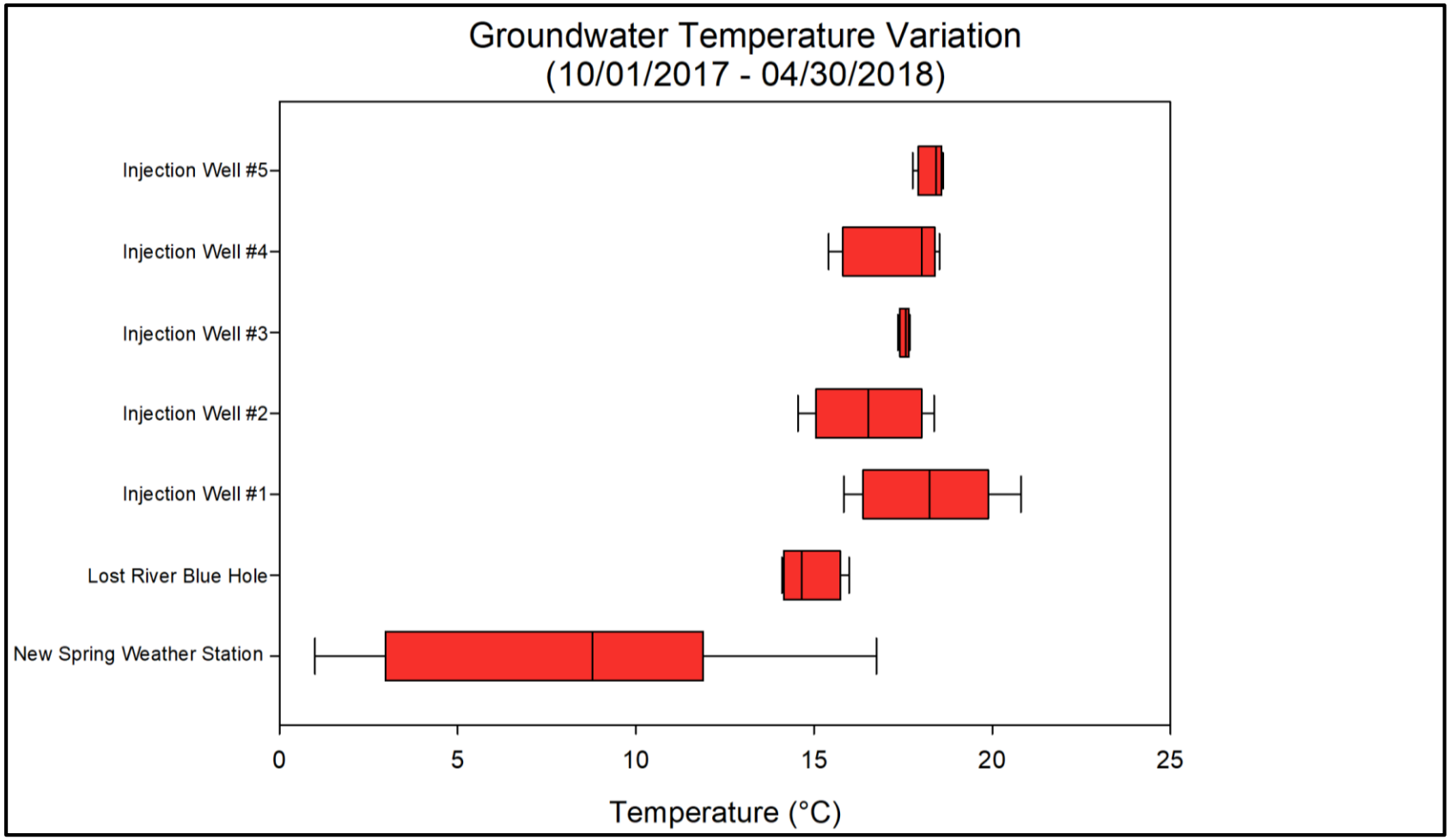

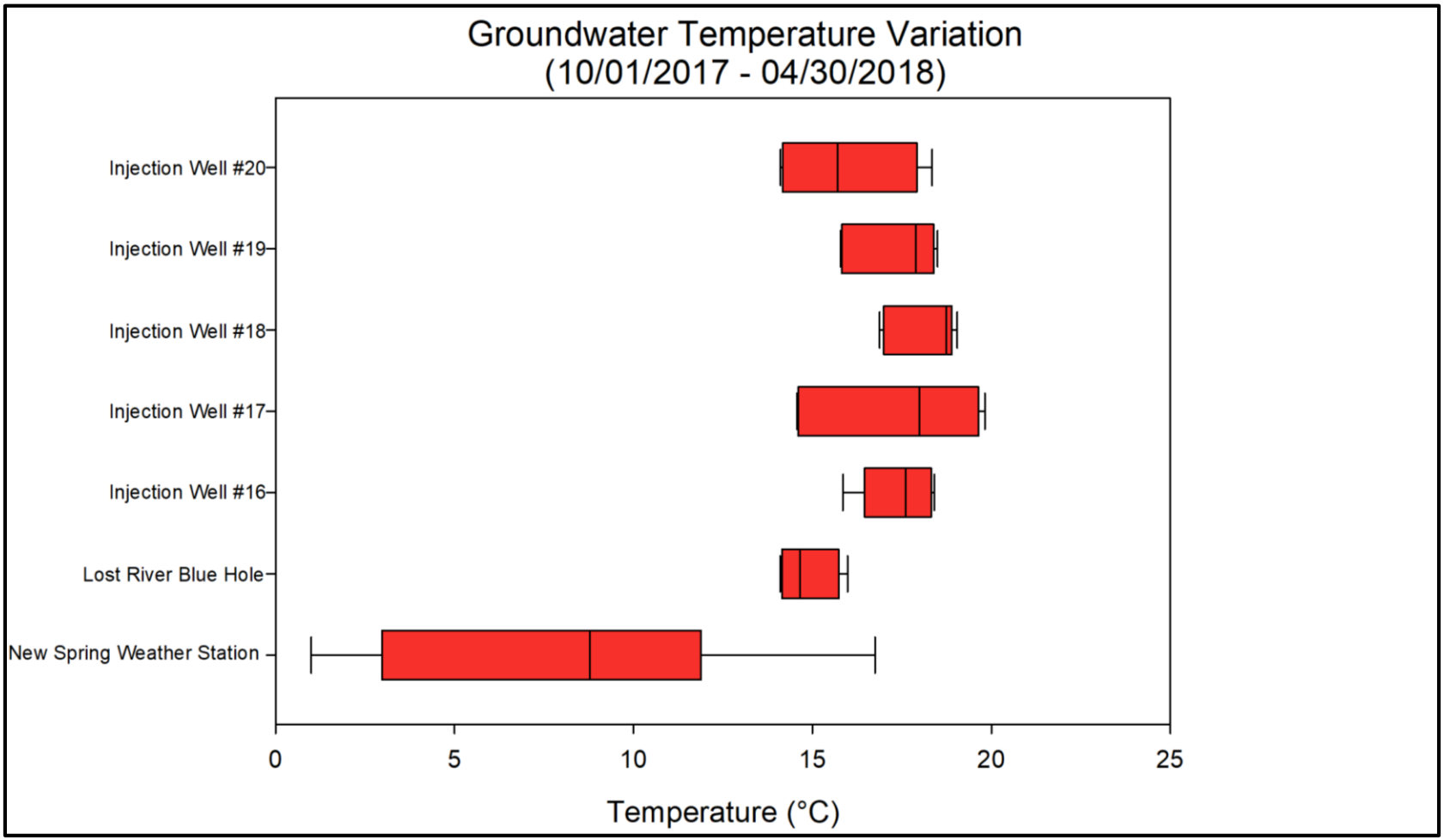
Groundwater Temperature Variation
(10/01/2017 - 04/30/2018)
Injection Well #20
Injection Well #19
Injection Well #18
Injection Well #17
Injection Well #16
Lost River Blue Hole
New Spring Weather Station
0
5
10
15
20
25
Temperature (°C)

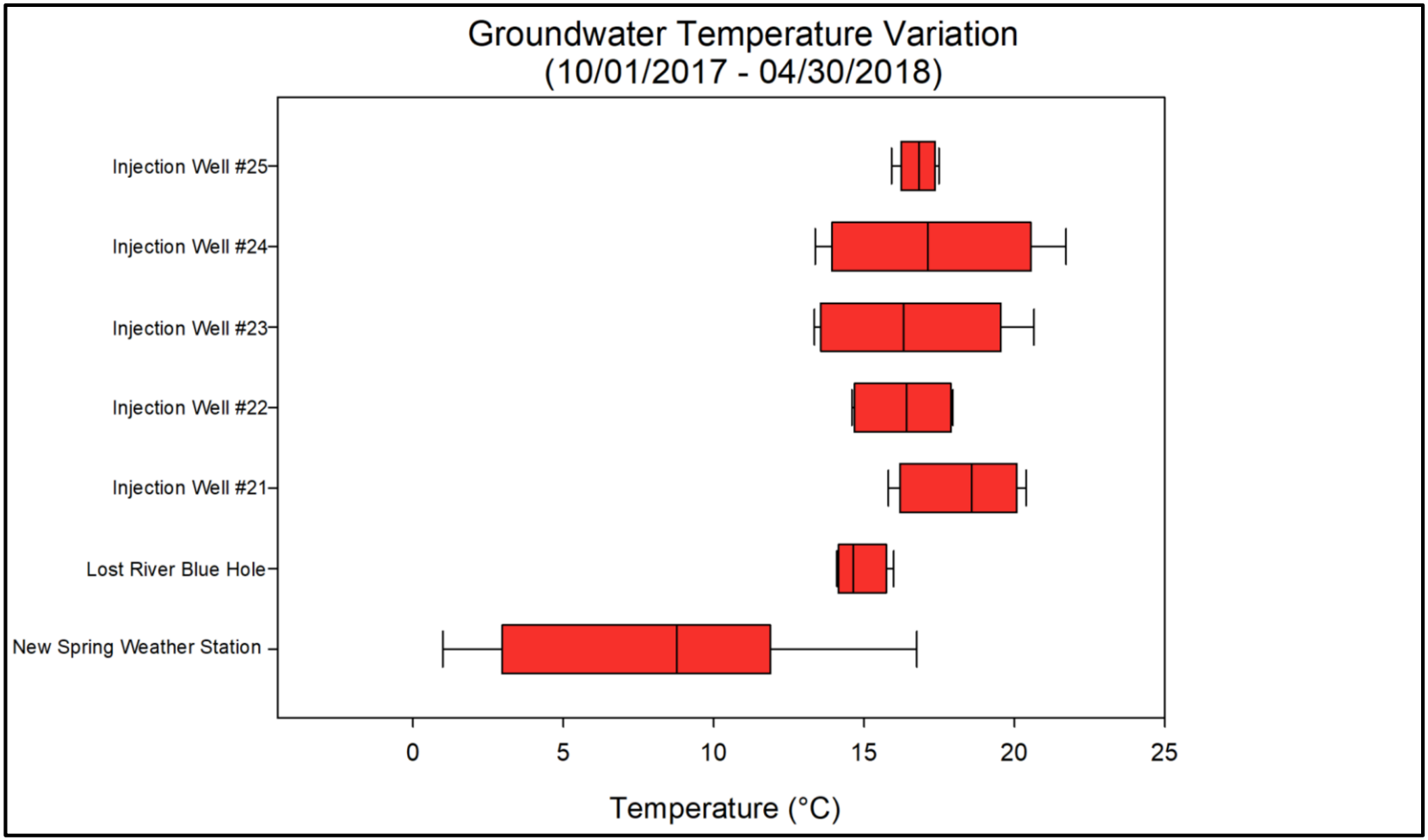
Groundwater Temperature Variation
(10/01/2017 - 04/30/2018)
Injection Well #25
Injection Well #24
Injection Well #23
Injection Well #22
Injection Well #21
Lost River Blue Hole
New Spring Weather Station
0
5
10
15
20
25
Temperature (°C)

Appendix D

Injection Well Descriptive Statistics

This appendix contains the Injection Well Descriptive Statistics (10/1/2017 – 04/30/2018).

Injection Well Descriptive Statistics												
	N	Range	Minimum	Maximum	Mean		Std. Deviation	Variance	Skewness		Kurtosis	
	Statistic	Statistic	Statistic	Statistic	Statistic	Std. Error	Statistic	Statistic	Statistic	Std. Error	Statistic	Std. Error
Well No. 1 Water Level (ft)	305280	8.347	-20.415	-12.068	-17.18158	0.003587	1.982095	3.929	-0.093	0.004	-1.056	0.009
Well No. 1 Water Elevation (ft)	305280	8.347	482.478	490.825	485.71109	0.003587	1.982076	3.929	-0.093	0.004	-1.056	0.009
Well No. 2 Water Level (ft)	305280	6.845	-25.411	-18.566	-25.23181	0.000248	0.136827	0.019	12.636	0.004	362.820	0.009
Well No. 2 Water Elevation (ft)	305280	6.845	493.542	500.387	493.72109	0.000248	0.136827	0.019	12.636	0.004	362.820	0.009
Well No.3 Water Level (ft)	305280	43.177	-48.159	-4.982	-38.53339	0.024781	13.692219	187.477	1.362	0.004	0.394	0.009
Well No. 3 Water Elevation (ft)	305280	43.177	549.295	592.472	558.92021	0.024781	13.692219	187.477	1.362	0.004	0.394	0.009
Well No.4 Water Level (ft)	305280	7.036	-21.504	-14.468	-20.81284	0.002004	1.107282	1.226	3.186	0.004	10.268	0.009
Well No. 4 Water Elevation (ft)	305280	7.036	514.670	521.706	515.36096	0.002004	1.107282	1.226	3.186	0.004	10.268	0.009
Well No. 5 Water Level (ft)	305280	35.221	-39.608	-4.387	-28.58041	0.016551	9.144975	83.631	0.372	0.004	-1.120	0.009
Well No. 5 Water Elevation (ft)	305280	35.221	459.421	494.642	470.44839	0.016551	9.144975	83.631	0.372	0.004	-1.120	0.009
Well No. 6 Water Level (ft)	305280	28.836	-26.438	2.398	-25.73929	0.004064	2.245460	5.042	9.884	0.004	106.744	0.009
Well No. 6 Water Elevation (ft)	305280	28.836	468.217	497.053	468.91522	0.004064	2.245459	5.042	9.884	0.004	106.744	0.009
Well No. 7 Water Level (ft)	305280	12.518	-31.553	-19.035	-27.40705	0.003691	2.039495	4.160	-0.374	0.004	-1.494	0.009
Well No. 7 Water Elevation (ft)	305280	12.518	474.693	487.211	478.83855	0.003691	2.039495	4.160	-0.374	0.004	-1.494	0.009
Well No. 8 Water Level (ft)	305280	9.017	-24.284	-15.267	-21.45737	0.004241	2.343261	5.491	0.167	0.004	-1.415	0.009
Well No. 8 Water Elevation (ft)	305280	9.017	496.416	505.433	499.24213	0.004241	2.343261	5.491	0.167	0.004	-1.415	0.009
Well No. 9 Water Level (ft)	305280	10.837	-13.959	-3.122	-12.55676	0.001886	1.042187	1.086	3.102	0.004	16.465	0.009
Well No. 9 Water Elevation (ft)	305280	10.837	503.481	514.318	504.88274	0.001886	1.042187	1.086	3.102	0.004	16.465	0.009
Well No. 10 Water Level (ft)	305280	21.441	-21.304	0.137	-20.71146	0.003647	2.015306	4.061	7.244	0.004	55.046	0.009
Well No. 10 Water Elevation (ft)	305280	21.441	508.256	529.697	508.84834	0.003647	2.015306	4.061	7.244	0.004	55.046	0.009
Well No. 11 Water Level (ft)	305280	11.138	-9.119	2.019	-6.12451	0.004092	2.261182	5.113	0.453	0.004	-0.741	0.009
Well No. 11 Water Elevation (ft)	305280	25.059	502.691	527.750	507.83884	0.011593	6.405615	41.032	1.877	0.004	2.361	0.009
Well No. 12 Water Level (ft)	305280	33.265	-32.615	0.650	-27.60247	0.005276	2.915128	8.498	0.614	0.004	3.016	0.009
Well No. 12 Water Elevation (ft)	305280	33.265	472.569	505.834	477.58103	0.005276	2.915128	8.498	0.614	0.004	3.016	0.009
Well No. 13 Water Level (ft)	305280	15.370	-19.669	-4.299	-13.93404	0.007807	4.313794	18.609	0.347	0.004	-1.210	0.009
Well No. 13 Water Elevation (ft)	305280	15.370	483.827	499.197	489.56176	0.007807	4.313794	18.609	0.347	0.004	-1.210	0.009
Well No. 14 Water Level (ft)	305280	19.065	-21.035	-1.970	-15.17719	0.008556	4.727214	22.347	1.340	0.004	1.136	0.009
Well No. 14 Water Elevation (ft)	305280	19.065	495.590	514.655	501.44781	0.008556	4.727214	22.347	1.340	0.004	1.136	0.009
Well No. 15 Water Level (ft)	305280	14.566	-15.802	-1.236	-14.82109	0.002216	1.224254	1.499	4.060	0.004	27.726	0.009
Well No. 15 Water Elevation (ft)	305280	14.566	494.915	509.481	495.89611	0.002216	1.224254	1.499	4.060	0.004	27.726	0.009
Well No. 16 Water Level (ft)	305280	8.782	-12.572	-3.790	-12.23703	0.000711	0.392828	0.154	11.469	0.004	181.814	0.009
Well No. 16 Water Elevation (ft)	305280	8.782	477.988	486.770	478.32307	0.000711	0.392828	0.154	11.469	0.004	181.814	0.009
Well No. 17 Water Level (ft)	305280	1.697	-17.206	-15.509	-16.66723	0.000501	0.276874	0.077	0.792	0.004	-0.179	0.009
Well No. 17 Water Elevation (ft)	305280	1.697	486.042	487.739	486.58117	0.000501	0.276874	0.077	0.792	0.004	-0.179	0.009
Well No. 18 Water Level (ft)	305280	31.865	-31.257	0.608	-30.76673	0.003048	1.684213	2.837	13.204	0.004	188.060	0.009
Well No. 18 Water Elevation (ft)	305280	31.865	466.840	498.705	467.33067	0.003048	1.684213	2.837	13.204	0.004	188.060	0.009
Well No. 19 Water Level (ft)	305280	26.605	-26.758	-0.153	-25.34051	0.002673	1.476986	2.181	10.545	0.004	158.176	0.009
Well No. 19 Water Elevation (ft)	305280	26.605	460.388	486.993	461.80569	0.002673	1.476986	2.181	10.545	0.004	158.176	0.009
Well No. 20 Water Level (ft)	305280	9.528	-7.123	2.405	-6.69557	0.001339	0.739770	0.547	9.461	0.004	97.907	0.009
Well No. 20 Water Elevation (ft)	305280	9.528	472.574	482.102	473.00103	0.001339	0.739770	0.547	9.461	0.004	97.907	0.009

Well No. 21 Water Level (ft)	305280	22.653	-22.670	-0.017	-19.43763	0.002975	1.643492	2.701	5.651	0.004	57.070	0.009
Well No. 21 Water Elevation (ft	305280	22.653	464.222	486.875	467.45477	0.002975	1.643492	2.701	5.651	0.004	57.070	0.009
Well No. 22 Water Level (ft)	305280	7.656	-6.443	1.213	-5.71979	0.001024	0.565727	0.320	7.241	0.004	71.650	0.009
Well No. 22 Water Elevation (ft	305280	7.656	481.941	489.597	482.66391	0.001024	0.565727	0.320	7.241	0.004	71.650	0.009
Well No. 23 Water Level (ft)	305280	13.355	-10.189	3.166	-7.82939	0.002112	1.166710	1.361	2.216	0.004	12.255	0.009
Well No. 23 Water Elevation (ft	305280	13.355	489.676	503.031	492.03591	0.002112	1.166710	1.361	2.216	0.004	12.255	0.009
Well No. 24 Water Level (ft)	305274	14.004	-12.646	1.358	-10.22046	0.003431	1.895647	3.593	3.346	0.004	15.513	0.009
Well No. 24 Water Elevation (ft	305280	14.004	489.269	503.273	491.69474	0.003432	1.896170	3.595	3.346	0.004	15.507	0.009
Well No. 25 Water Level (ft)	305280	7.500	-45.227	-37.727	-44.48884	0.000848	0.468803	0.220	0.570	0.004	-0.500	0.009
Well No. 25 Water Elevation (ft	305280	7.500	452.879	460.379	453.61676	0.000848	0.468803	0.220	0.570	0.004	-0.500	0.009
Well No. 26 Water Level (ft)	305280	14.093	-43.275	-29.182	-39.16790	0.007663	4.233718	17.924	0.710	0.004	-1.182	0.009
Well No. 26 Water Elevation (ft	305280	14.093	448.544	462.637	452.65090	0.007663	4.233718	17.924	0.710	0.004	-1.182	0.009
Well No. 27 Water Level (ft)	305280	41.669	-41.167	0.502	-31.39256	0.016441	9.084078	82.520	1.107	0.004	0.625	0.009
Well No. 27 Water Elevation (ft)	305280	41.669	455.910	497.579	465.68464	0.016441	9.084078	82.520	1.107	0.004	0.625	0.009
Well No. 28 Water Level (ft)	305280	11.632	-38.486	-26.854	-38.28119	0.000274	0.151407	0.023	23.502	0.004	1126.491	0.009
Well No. 28 Water Elevation (ft	305280	11.632	456.714	468.346	456.91861	0.000274	0.151407	0.023	23.502	0.004	1126.491	0.009
Well No. 29 Water Level (ft)	305280	9.437	-34.743	-25.306	-33.32864	0.000468	0.258593	0.067	2.077	0.004	34.952	0.009
Well No. 29 Water Elevation (ft	305280	9.437	458.236	467.673	459.65066	0.000468	0.258593	0.067	2.077	0.004	34.952	0.009
Well No. 30 Water Level (ft)	305280	2.853	-34.222	-31.369	-33.72169	0.000261	0.144468	0.021	1.189	0.004	1.416	0.009
Well No. 30 Water Elevation (ft	305280	2.853	458.961	461.814	459.46161	0.000261	0.144468	0.021	1.189	0.004	1.416	0.009
Well No. 31 Water Level (ft)	109946	25.262	-51.471	-26.209	-35.35647	0.022574	7.485258	56.029	0.007	0.007	-1.713	0.015
Well No. 31 Water Elevation (ft)	109951	25.262	427.729	452.991	443.84389	0.022574	7.485287	56.030	0.007	0.007	-1.713	0.015

Appendix E

Surface Sites Descriptive Statistics

This appendix contains the descriptive statistics for the surface sites (10/1/2017 – 04/30/2018).

Surface Sites Descriptive Statistics												
	N	Range	Minimum	Maximum	Mean		Std. Deviation	Variance	Skewness		Kurtosis	
	Statistic	Statistic	Statistic	Statistic	Statistic	Std. Error	Statistic	Statistic	Statistic	Std. Error	Statistic	Std. Error
New Spring Stage (ft)	305280	2.155	0.250	2.405	0.67508	0.000505	0.278748	0.078	0.996	0.004	1.731	0.009
New Spring Elevation (ft)	305280	2.155	450.053	452.208	450.47808	0.000505	0.278748	0.078	0.996	0.004	1.731	0.009
Limestone Lake stage (ft)	249560	2.479	1.877	4.356	2.32686	0.000946	0.472378	0.223	2.411	0.005	5.527	0.010
New Spring Elevation (ft)	249560	2.479	463.819	466.298	464.26916	0.000946	0.472378	0.223	2.411	0.005	5.527	0.010
Barren River Stage (ft)	82680	11.462	6.130	17.592	10.25235	0.005367	1.543317	2.382	1.453	0.009	5.731	0.017
Barren River Elevation (ft)	82680	11.462	422.045	433.507	426.16770	0.005367	1.543318	2.382	1.453	0.009	5.731	0.017
Jenning's Creek Stage (ft)	24780	6.401	0.000	6.401	3.22541	0.007433	1.170117	1.369	-0.321	0.016	1.702	0.031
Jennings Creek Elevation (ft)	24780	6.401	416.298	422.699	419.52321	0.007433	1.170117	1.369	-0.321	0.016	1.702	0.031

Appendix F

Synthetic Mass Curves

This appendix contains the Synthetic Mass Precipitation Frequency Curves for the CoBG (10/1/2017 – 04/30/2018).

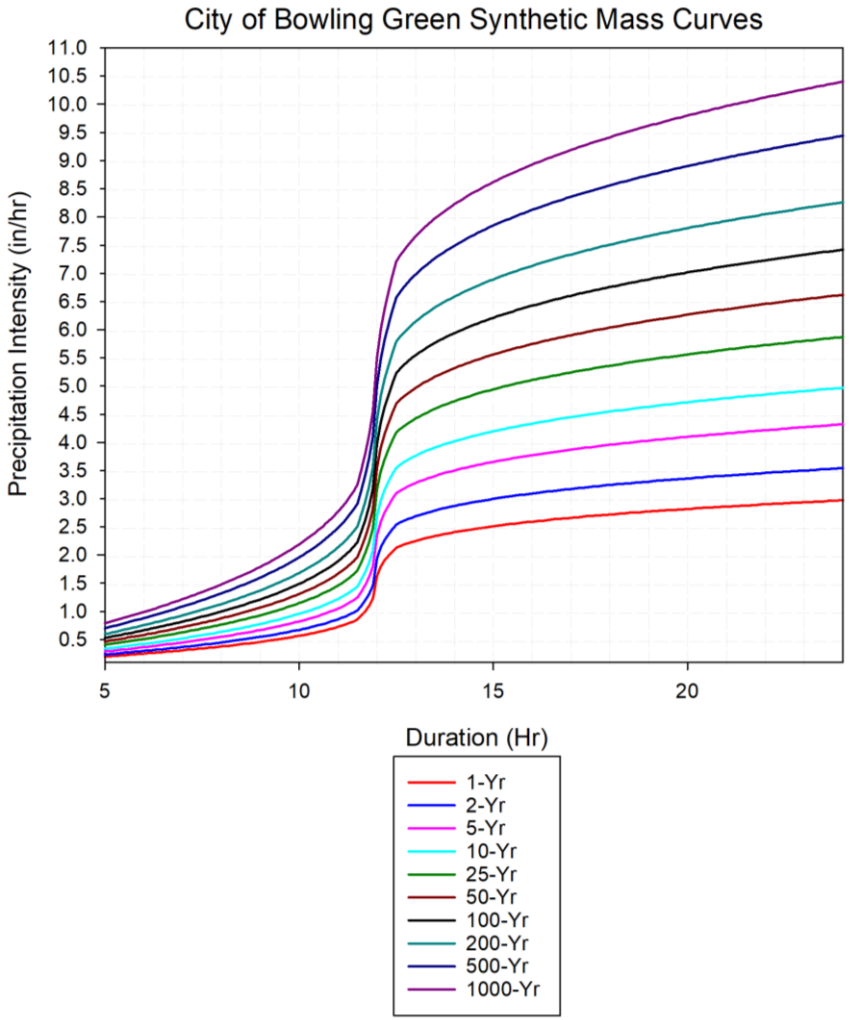

Appendix G

Injection Well Drainage Design

This appendix contains an axonometric diagram for a new Injection Well drainage design.

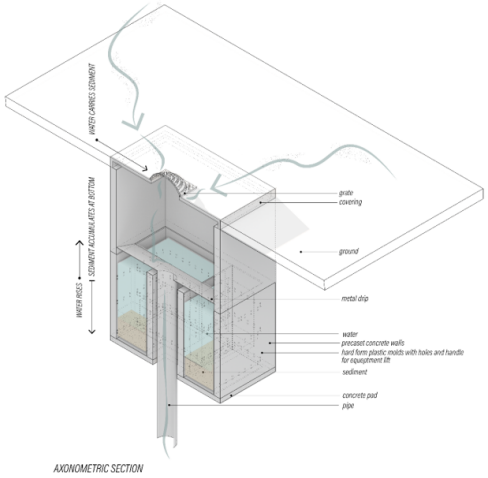

AXONOMETRIC SECTION

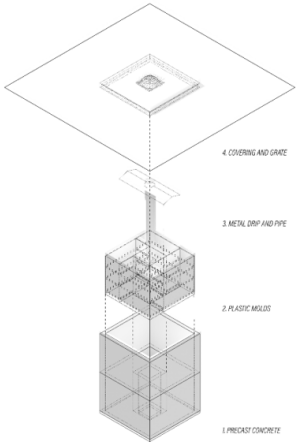

AXONOMETRIC SECTION

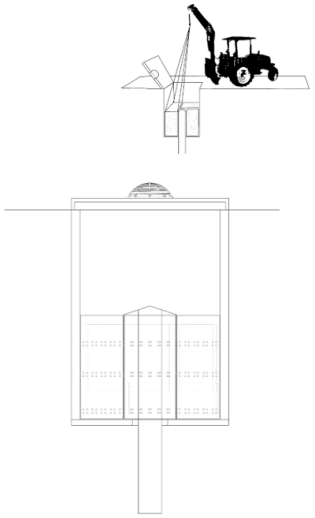

SECTION - size may vary

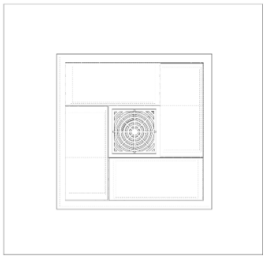

PLAN - size may vary